Transactions

of the

A.S.M.E.

NOVEMBER, 1945

VOL. 67, NO. 8

Transactions

of The American Society of Mechanical Engineers

Published on the tenth of every month, except March, June, September, and December

---

Published monthly by The American Society of Mechanical Engineers. Publication office at 20th and Northampton Streets, Easton, Pa. The editorial department is located at the headquarters of the Society, 29 West Thirty-Ninth Street, New York 18, N. Y. Cable address, "Dynamic," New York. Price $1.50 a copy, $12.00 a year; to members and affiliates, $1.00 a copy, $7.50 a year. Changes of address must be received at Society headquarters two weeks before they are to be effective on the mailing list. Please send old as well as new address. . . . By-Law: The Society shall not be responsible for statements or opinions advanced in papers or . . . printed in its publications (B13, Par. 4). . . . Entered as second-class matter March 2, 1928, at the Post Office at Easton, Pa., under the act of August 24, 1912, . . .

Heat Transfer From a Baffled-Finned Cylinder to Air

By A. W. LEMMON, JR.,[1] A. P. COLBURN,[2] and H. B. NOTTAGE[3]

Air-cooled aircraft-engine cylinders utilize extensive finned surface to permit maintenance of proper metal temperatures with high rates of heat transfer occurring at high engine power outputs. The process of heat transfer to the flowing air stream differs from that of usual finned tubes not only in size of the cylinder but also because baffles are utilized which force all the air to pass through the fin spaces. Because of this latter difference, data on finned tubes in general do not apply. Therefore, special tests have been carried out to establish the mechanism of heat transfer in this case and to provide a generalization of the data useful for design. The work was carried out at the University of Delaware in conjunction with a Pratt & Whitney Aircraft heat-transfer research program. The experiments were conducted on a typical section of an aluminum finned cylinder barrel. The cylinder was heated by an internal electrical heater. Temperatures were measured not only of the entrance and exit air stream but also at eight points, equally spaced circumferentially, in the base metal. The results were interpreted by comparison with heat-transfer relations for flow inside conduits. The maximum heat-transfer rates were in close agreement with these relations although the average rates were lower owing to the decreased cooling-air velocities over the front and rear fin surfaces outside of the baffled portion of the cylinder. The over-all pressure drop is shown to be about double the estimated frictional resistance; the inlet and exit losses provide an explanation.

Nomenclature

THE following nomenclature is used in the paper:

A_b = cylinder fin-base area (based on outside diameter of base), sq ft
A_{cs} = cross-sectional area for flow in cylinder fin spaces, sq ft
A_f = total external heat-transfer surface of cylinder, sq ft
C = heat capacity of humid air mixture, Btu/(lb)(deg F)
D_{eq} = equivalent diameter of fin space, ft
E_{hp} = pumping horsepower
G = mass velocity, lb/(hr)(sq ft)
g_c = dimensional constant, 4.169×10^8 ft/hr^2
h = mean surface conductance per unit of A_f, Btu/(hr)(sq ft)(deg F)
h_x = "local" surface conductance per unit of A_f, Btu/(hr)(sq ft)(deg F)
P_T = total power loss per unit of A_f, ft-lb/(hr)(sq ft)
ΔP_{Bi} = baffle pressure drop, in. H_2O (ΔP_{BP} = lb/sq ft)
t_{avg} = average air temperature across cylinder, deg F
t_b = average fin-base temperature, deg F
t_{max} = maximum (rear) fin-base temperature, deg F
t_1, t_2, etc. = observed fin-base temperatures, deg F
Δt_m = arithmetic-mean temperature difference, average fin-base temperature to average air-stream temperature, deg F
Δt_0 = reference mean temperature difference, deg F (Δt_0 = 100)
Δt_r = mean temperature difference ratio, $\Delta t_m / \Delta t_0$
U = over-all heat-transfer conductance per unit of A_b, Btu/(hr)(sq ft)(deg F)
U_x = "local" value of U
W = air flow rate, lb per hr
ρ = air density, pcf
ρ_{avg} = air density at average temperature and pressure across cylinder, pcf
ρ_0 = density of air at 70 F, and 30 in. Hg, pcf ($\rho_0 = 0.0753$)
ϕ = over-all pressure loss coefficient, Equation [5]
μ = viscosity of air at average air temperature across cylinder, lb/(hr)(ft)
N_{Pr} = Prandtl number, $C\mu/k$
N_{Re} = Reynolds number, $D_{eq}G/\mu$
N_{St} = Stanton number, h/CG

Introduction

Problems of designing a fin-and-baffle system to be fitted to cylindrical sections of the size employed as air-cooled aircraft-engine cylinders have recently become of critical importance. Adequate design requires a foundation of fundamental and generalized data from which any desired performance requirements may be met.

Since the publication of earlier preliminary work (2, 4, 7, 8)[4] along these lines, the general conception of the nature of the processes and problems prevailing in an extended fin-and-baffle system has considerably advanced, and improvements in experimental equipment and techniques have been made. On both of these counts, further experimental studies to permit extending the accuracy and range of the available design data have been needed, together with a broadened fundamental basis for generalizing the behavior of this type of heat-transfer system. Preliminary studies of the problem have suggested that the processes within the fin flow passages, where effectively all of the heat transfer takes place, can be treated most satisfactorily and comprehensively in terms of their relation to the established data on heat transfer in straight tubes or passages; all with due allowance for the effects of the extended-surface boundaries of the passages and the particular nature of the flow system both within the baffle section and at the front and rear points where the stream enters and leaves.

[1] Research Fellow in Chemical Engineering, University of Delaware, Newark, Del. Present address, National Defense Research Committee, Washington, D. C.

[2] Professor of Chemical Engineering, University of Delaware. Mem. A.S.M.E.

[3] Project Engineer, Pratt and Whitney Aircraft, East Hartford, Conn. Jun. A.S.M.E.

Contributed by the Heat Transfer Division and presented at the Annual Meeting, New York, N. Y., Nov. 27–Dec. 1, 1944, of The American Society of Mechanical Engineers.

[4] Numbers in parentheses refer to the Bibliography at the end of the paper.

In this paper are presented the results of experimental study and analysis for an actual aluminum-finned section of an aircraft-engine cylinder barrel, fitted with representative baffles and tested under controlled conditions of uniform internal electrical heating and smooth approaching air flow, as well as of visual-flow observations which aid in understanding local effects. These results have been given fundamental study and interpretation, with particular emphasis upon the role and importance of local point-to-point conditions in the heat-transfer and flow processes.

Description of Experimental Arrangement

Requirements for the experimental system were based on the need for a flexible assembly yielding reproducible results with a simple operating control. General features decided upon were the following:

1 A once-through air-duct system, arranged with a free room-air intake to the test cylinder.

2 A test section to contain the cylinder and baffle assembly being studied, arranged for simple removal and adjustment, and with effective heat insulation.

3 An electrical heating element to fit snugly within the test cylinder and permit ease of heating control.

4 Measurement of the temperature, pressure, and moisture content of the intake air.

5 Measurement of the static pressure drop and temperature rise of the air passing across the test cylinder, which latter requires a downstream mixing section to obtain the mixed-mean air temperature, and the use of effective over-all heat insulation.

6 Measurement of the temperature pattern about the base of the test cylinder by means of thermocouples installed within the base metal, with the junctions and adjacent sections of leads in isothermal zones.

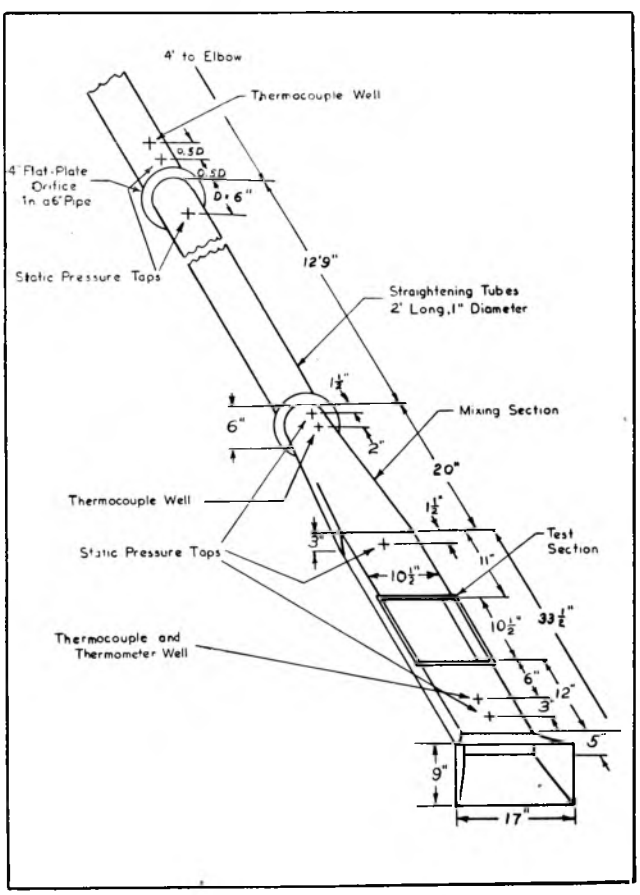

Fig. 1 Dimensioned Sketch of Test Apparatus

An over-all dimensioned sketch of the duct system constructed, showing the points of static pressure and temperature measurement for the air stream, is given in Fig. 1.

Cylinder and Heater Assembly. Plan dimensions of the finned-cylinder and baffle installations are given in Fig. 2. The baffle was made of sheet metal, held in place by wooden blocks. Detailed dimensions of the finned test cylinder are given in Table 1. The fins on the test cylinder were lathe-turned from a forged blank of Alcoa A51S-T aluminum, having a nominal thermal conductivity of 99.2 Btu/(hr)(ft)(deg F) at 100 deg C. The alumi-

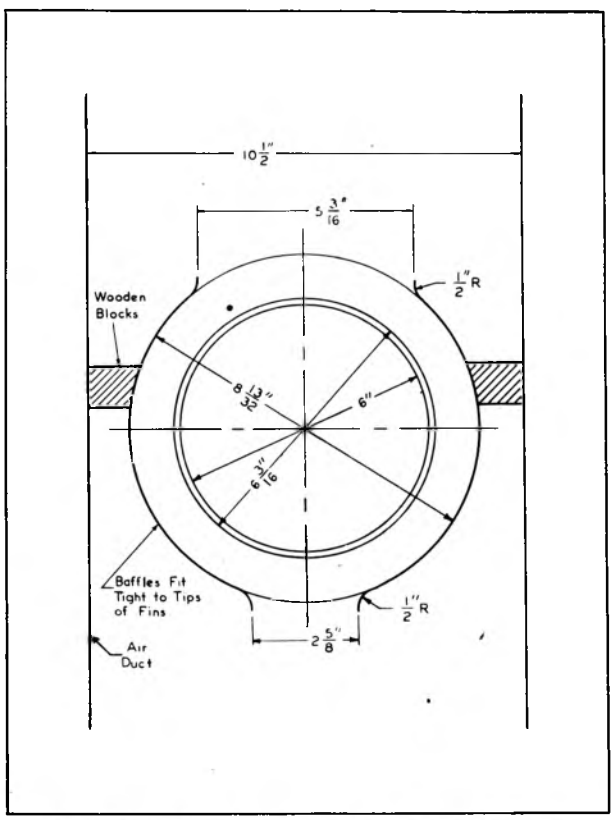

Fig. 2 Plan View of Fin-and-Baffle Arrangement

TABLE 1 GEOMETRICAL DATA ON FINNED TEST CYLINDER

Axial length of test cylinder at fin base, in.	2⅝
Outside diameter of fins, in.	8 13/32
Root diameter of fins, in.	6 3/16
Radial width of fins, in.	1 7/64
Thickness of cylindrical fin base, in.	3/32
Fin thickness at tip, in.	0.02
Fin thickness at root, in.	0.04
Center-line spacing of fins, in.	0.141
Number of fins	18
Base area of fin-root cylindrical surface (A_b), sq ft	0.349
Total fin side-surface area (A_f), sq ft	6.67
Cross-sectional area of flow stream between fins, measured on diameter with tight baffles (A_{cs}) sq ft	0.0308
Equivalent diameter of fin passages (D_{eq}), in.	0.202
Equivalent diameter of fin passages (D_{eq}), ft	0.01683

TABLE 2 SPECIFICATIONS OF HEATER

Type of wire	Chromel "A"
Wire gage	B. & S. 18
Number of coils	2
Length of wire in each coil, ft	55
Length of each close-wound coil, in.	61
Length of each stretched coil, in.	87
Resistance of each coil (cold), ohms	22.4
Resistance of each coil (400 F), ohms	23.0
Amperage of each coil at 250-v rating, amp	9.2
Total heat-release rate from heater at maximum output, w	4600

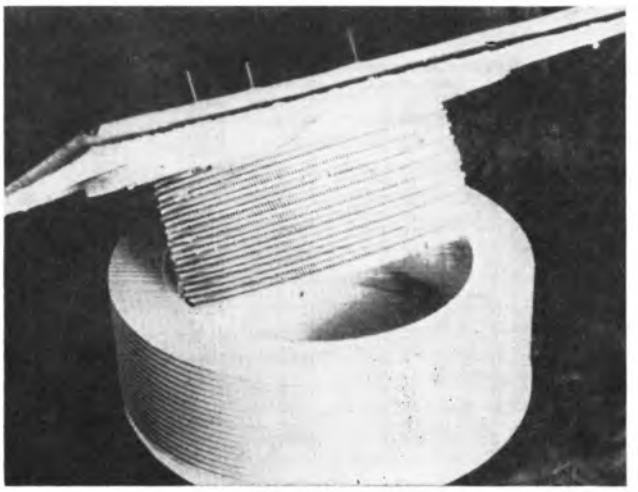

FIG. 3 TEST SECTION SHOWING HEATER AND TEST CYLINDER

num machined surface was given a protective anodizing treatment before testing. The baffles were installed in contact with the fin tips.

The method of arranging the heater in the test cylinder is shown in Fig. 3. The heater consisted of two coils of chromel wire, each rated at 2 kw for 250 v. These coils were wound spirally on a core which was built up from $^1/_2$-in. sheets of transite. Larger end disks of transite were attached to this core and fitted tightly to the base section of the test cylinder, so that the uppermost and lowermost fin-side surfaces were exposed to an air stream of slightly less than one half of the cross section between normal consecutive fins. Power for the heater was furnished by two 125-v 3-kw motor generator sets. The generator voltage was controlled through variable-field rheostats. The transite end disks on the heater assembly serve as an effective initial barrier to endwise heat leakage. The entire assembly was completely wrapped in a blanket of 4-in-thick glass wool before testing.

Mixing Unit. The mixing unit was located in the transition duct between the test and metering sections. This consisted of a three-piece disk-and-doughnut section with the disk in the middle, each piece spaced 6 in. from the next. The disk and the holes were each 4 in. diam.

Metering Section. Fig. 1 shows the over-all dimensions of the metering section. The 4-in. orifice in the 6-in. pipe, carefully installed according to the Fluid Meters Report (1) with so-called vena-contracta taps, was considered to have a flow coefficient of 0.684 (including velocity of approach factor) without supplementary calibration.

Instrumentation. The heater power input was determined by a direct-current voltmeter (0–150 v) and ammeter (0–25 amp), both instruments being accurate to 0.5 per cent of full scale deflection. The voltage taps were connected directly to the heater terminals.

The static pressure drop from the room to the tap just before the test section, and the static gage pressure at the metering orifice were read to 0.1 in. on vertical U-tube water manometers. The static pressure drops across both the baffled and sealed-in test cylinder and the metering orifice were obtained with Type-B Uehling draft gages, graduated to 0.01 in., in the range below 1 in. H_2O; and for the higher range, U-tube water manometers were employed, graduated to 0.1 in.

All thermocouples were made from Leeds and Northrup selected, 28-gage iron-constantan duplex-insulated wire. The thermocouple emf's were read on a Leeds and Northrup portable precision potentiometer, Type 8662. Single thermocouples were employed to measure the air temperature in three locations: (*a*) Directly beside the intake-air thermometer, as a check thereon; (*b*) close behind the last "doughnut" of the mixer, with provision for traversing, to determine the mixed-mean heated-air temperature; and (*c*) in the discharge stream from the metering orifice, to establish the air temperature for calculating the flow rate. Measurements of the metal temperatures in the cylindrical base section of the finned test specimen were accomplished by the use of thermocouples, the junctions of which were installed in the bottom of small holes drilled in axially to the mid-section of the cylinder base from one end. Eight of these thermocouples were installed around the muff, spaced every 45 deg.

EXPERIMENTAL PROCEDURE

Thorough precautions were taken when assembling the heater and finned cylinder to insure a tight fit and seal against all possible air leaks. Room drafts were not allowed during a test, in order to insure constancy of the air source and the surroundings.

Each point required the setting of a heater power and an air-flow rate. Once this was done, conditions were held constant until a steady state was assured. A normal test then consisted of four sets of readings, taken at 5-min intervals, of the inlet and heated-air temperatures, the orifice-air temperature, and of the heater power; and one set of readings of the other variables. The readings taken only once included the metal temperatures, the pressures, and the wet- and dry-bulb temperatures of the inlet air. When making calculations, the readings which were taken four times were averaged for purposes of analysis.

No test point was accepted until its heat balance had been judged satisfactory. All data retained were within the maximum limit of 10 per cent difference between the rate of energy reception by the air stream and the heater power input.

METHODS OF CALCULATION

Air-Flow Correlations. Mass flow rates and Reynolds numbers were calculated from the following relations

$$G = W/A_{cs} \text{ and } N_{Re} = D_{eq}G/\mu$$

The values of μ were taken at the average air temperature across the muff; these values were obtained from the Fluid Meters Report (1).

Pumping horsepower, the total power required to pump air through the muff with negligible kinetic-energy and density changes, is calculated from the relation

$$E_{hp} = \frac{W\,\Delta P_{BP}}{33{,}000 \times 60\ \rho_{avg}} \quad \ldots\ldots\ldots\ldots [1]$$

and since

$$\Delta P_{BP} = 62.3\,\Delta P_{Bi}/_{12}$$

$$E_{hp} = 2.62 \times 10^{-6} W\,\Delta P_{Bi}/\rho_{avg} \quad \ldots\ldots\ldots [2]$$

For purposes of correlation in order to present E_{hp} as a function independent of density, this term is multiplied by the factor $(\rho_{avg}/\rho_0)^2$.

Over-all power loss per unit surface area, also multiplied by $(\rho_{avg}/\rho_0)^2$, is calculated as follows

$$P_T(\rho_{avg}/\rho_0)^2 = \frac{62.3 W\,\Delta P_{Bi}\,\rho_{avg}}{12\rho_0^2 A_f} \quad \ldots\ldots\ldots [3]$$

The over-all pressure-loss coefficient is evaluated by an expression similar to that for the friction factor in smooth pipes. Since in this study it was not possible to measure the pressure drop

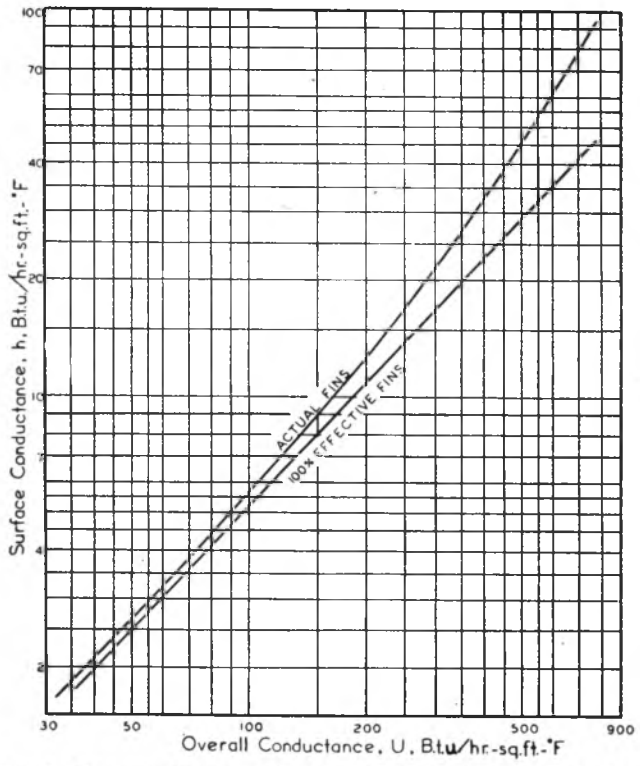

FIG. 4 RELATION BETWEEN SURFACE CONDUCTANCE AND OVER-ALL CONDUCTANCE

due to friction alone, the over-all static pressure drop has been employed for the purpose of obtaining an index of the over-all flow loss which could be compared to the friction factor for flow inside conduits, the friction factor as usual being defined as

$$f/2 = \frac{g\rho_{avg} A_{cs} \Delta P}{G^2 A_f} \quad \ldots\ldots\ldots\ldots\ldots\ldots [4]$$

where ΔP = frictional pressure drop. In this case where only the over-all pressure drop is known, the pressure-loss coefficient is calculated by the analogous equation

$$\phi/2 = \frac{g_c \rho_{avg} A_{cs} \Delta P_{BP}}{G^2 A_f} = 9.95 \times 10^6 \rho_{avg} \Delta P_{Bi}/G^2 \ldots\ldots [5]$$

Heat-Transfer Coefficients. The mean temperature difference used in calculation of the heat-transfer coefficients in this study has been taken as that prevailing between the arithmetic-average metal temperature indicated by the thermocouples in the base of the muff and the average air temperature. The over-all unit heat-transfer conductance U is then calculated by the relation

$$U = Q_c/A_b \Delta t_m \ldots\ldots\ldots\ldots [6]$$

Magnitudes of the mean unit surface conductance h are obtained from the over-all conductance according to the method of Harper and Brown (5) for tapered annular fins. Fig. 4 shows the relation between U and h calculated for the dimensions of the test cylinder.

TABLE 3 HEAT-BALANCE DATA

Run no.	Air flow, lb per hr	Air temp rise, deg F	Heat Rates, Btu per Hr — Electrical input	To air stream	Heat lost	Per cent heat lost
1	1390	19.6	6714	6617	97	1.45
2	1404	23.5	8568	8028	540	6.30
3	1418	14.5	4936	5000	—64	—1.31
4	1433	8.7	3190	3031	159	4.96
7	1116	15.1	4298	4097	201	4.69
8	990.0	16.0	4097	3852	245	5.98
9	723.6	23.1	4439	4064	375	8.44
10	561.6	13.2	1764	1789	—25	—1.43
11	558.0	19.3	2722	2614	108	3.97
12	547.2	35.2	4856	4684	172	3.56
13	540.0	51.5	6840	6728	112	1.63
14	532.8	68.5	8978	8834	144	1.60
17	1019	7.1	1742	1760	—18	—1.03
18	756.0	9.5	1728	1746	—18	—1.04
19	565.2	12.5	1732	1717	15	2.91
20	392.4	16.1	1681	1526	155	9.20
21	993.6	6.4	1667	1544	123	7.35
22	554.4	12.4	1696	1670	26	1.48
23	381.6	17.6	1678	1786	—108	—6.44
24	982.8	17.7	4532	4230	302	6.67
25	302.0	61.3	4655	4464	191	4.10
26	174.2	102.7	4630	4309	321	6.93

TABLE 4 FIN-BASE TEMPERATURES

Run no.	Fin-base temperature, deg F — 0°*	45°	90°	135°	180°	225°	270°	315°
1	124.0	120.6	116.1	125.6	159.3	142.0	135.0	124.0
2	133.3	129.1	124.6	136.1	178.6	153.5	144.0	133.4
3	104.6	102.1	98.9	106.5	133.2	120.6	116.5	106.3
4	91.6	89.2	86.4	90.2	110.2	103.6	100.2	92.0
7	111.4	108.8	106.6	113.5	137.4	125.9	120.5	110.6
8	113.8	111.8	110.4	117.1	139.7	128.1	122.3	114.8
9	121.4	119.3	118.8	128.7	153.6	138.8	129.9	122.4
10	95.4	94.6	94.7	99.4	110.9	105.4	101.6	97.0
11	107.8	107.1	108.0	115.0	131.7	122.1	115.0	109.4
12	137.3	136.0	137.3	150.7	180.3	160.2	146.0	139.2
13	164.1	162.1	164.4	183.6	225.7	195.7	173.9	165.4
14	190.2	188.2	192.3	217.6	271.6	231.8	202.6	192.0
17	90.2	88.9	87.4	90.1	102.3	98.8	96.3	91.2
18	92.8	91.7	91.6	95.2	106.8	102.1	98.9	94.1
19	99.1	98.2	99.2	103.8	115.1	109.0	104.8	100.5
20	97.2	97.0	98.8	104.1	115.8	109.1	103.4	99.1
21	87.4	85.9	84.6	87.3	99.2	95.9	93.3	88.6
22	92.3	91.6	92.3	96.7	108.2	102.3	98.1	93.5
23	95.5	95.0	97.3	103.0	115.0	107.3	101.2	96.5
24	113.9	111.5	110.5	118.1	143.6	130.1	122.4	115.0
25	146.0	146.3	155.4	175.1	209.6	183.8	160.1	148.4
26	170.9	172.5	192.7	220.8	256.9	227.0	193.3	172.2

* At upstream center of test cylinder; other angles clockwise from this point.

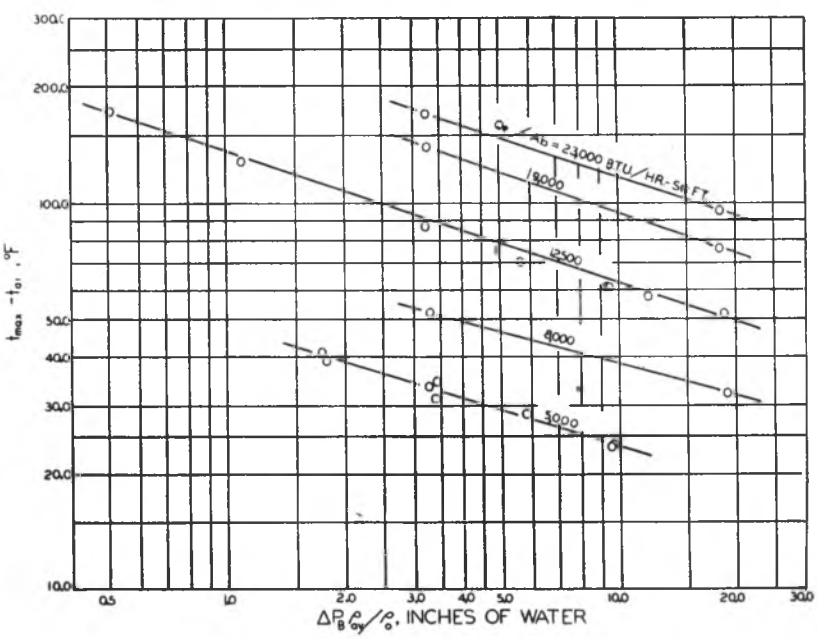

FIG. 5 RELATION OF MAXIMUM METAL TEMPERATURE, BAFFLE PRESSURE DROP, AND HEAT FLUX

TABLE 5 CORRELATION DATA

Run no.	Pressure drop, in. H_2O	Average density, pcf	Air-flow rate, lb per hr	Mass velocity, lb/(hr) (sq ft)	Reynolds number	$\Delta P_B \rho_{avg}/\rho_s$ in. H_2O	$P_T(\rho_{avg}/\rho_s)^2$ ft-lb/(hr) (sq ft)	$\phi/2$
1	19.43	0.0706	1390	45100	16860	18.29	261662	0.00669
2	19.43	0.0710	1404	45600	17150	18.34	265795	0.00670
3	19.60	0.0714	1418	46050	17420	18.65	272320	0.00655
4	19.68	0.0729	1433	46500	17700	19.00	282129	0.00658
7	12.56	0.0713	1116	35200	13610	11.93	137149	0.00718
8	10.04	0.0712	990.0	32150	12020	9.55	97118	0.00687
9	5.96	0.0714	723.6	23500	8750	5.69	42256	0.00765
10	3.51	0.0727	561.6	18210	6890	3.40	19666	0.00764
11	3.45	0.0716	558.0	18100	6775	3.30	18915	0.00748
12	3.45	0.0723	547.2	17780	6550	3.24	18731	0.00783
13	3.39	0.0695	540.0	17520	6410	3.14	17459	0.00762
14	3.41	0.0687	532.8	17280	6280	3.13	17129	0.00779
17	10.23	0.0728	1019	33050	12500	9.96	104143	0.00677
18	5.92	0.0711	756.0	24600	9260	5.78	43668	0.00690
19	3.54	0.0704	565.2	18370	6880	3.44	19330	0.00733
20	1.84	0.0712	392.4	12710	4760	1.80	7055	0.00805
21	9.80	0.0729	993.6	32200	12200	9.56	97412	0.00684
22	3.36	0.0734	554.4	18000	6810	3.28	18763	0.00756
23	1.79	0.0729	381.6	12390	4680	1.75	6833	0.00844
24	9.82	0.0696	982.8	31900	11980	9.47	92180	0.00669
25	1.24	0.0701	302.0	9790	3590	1.11	3602	0.00900
26	0.57	0.0676	174.2	5650	2020	0.51	921	0.01198

TABLE 5 (*Continued*) CORRELATION DATA

Run no.	Inlet air, deg F	Heat flux (Q_s/A_b), $\frac{\text{Btu}}{(\text{hr})(\text{sq ft})}$	Δt_m, deg F	U, Over-all coefficient	h, Surface coefficient	$U(\Delta t_r)^{0.18}$	$\frac{h}{CG}(N_{Pr})^{2/3}(\Delta t_r)^{0.18}$	$\frac{h}{C}(\Delta t_r)^{0.18}$
1	80.6	19210	42.9	449	38.3	413	0.00249	137.60
2	75.4	24560	54.4	451	38.3	424	0.00257	142.9
3	74.0	14120	29.8	474	41.8	420	0.00252	141.74
4	73.3	9110	17.7	516	48.1	434	0.00264	150.04
7	80.6	12290	28.6	429	36.6	378	0.00286	123.28
8	82.6	11720	29.2	400	32.3	354	0.00277	109.12
9	81.3	12710	36.2	350	26.4	316	0.00321	92.34
10	79.0	5040	15.0	337	24.9	279	0.00341	75.93
11	80.0	7800	24.4	320	20.6	278	0.00306	67.64
12	82.4	13900	48.4	287	20.0	267	0.00337	73.25
13	81.1	19570	72.5	269	18.3	260	0.00335	71.84
14	78.6	25680	97.9	262	17.4	261	0.00339	71.66
17	78.4	4990	11.2	445	38.0	358	0.00272	110.09
18	78.6	4940	13.3	372	28.9	304	0.00286	86.11
19	82.2	4950	15.2	325	23.9	269	0.00324	72.78
20	77.9	4810	17.1	281	19.4	235	0.00389	60.44
21	76.6	4770	10.5	455	38.4	363	0.00279	110.14
22	75.6	4850	15.1	321	23.5	266	0.00324	71.47
23	74.5	4850	18.1	265	17.9	223	0.00370	56.06
24	79.9	12970	31.8	408	33.3	370	0.00292	114.01
25	72.9	13300	62.0	215	13.2	205	0.00424	50.74
26	71.6	13230	78.0	170	10.1	166	0.00583	40.27

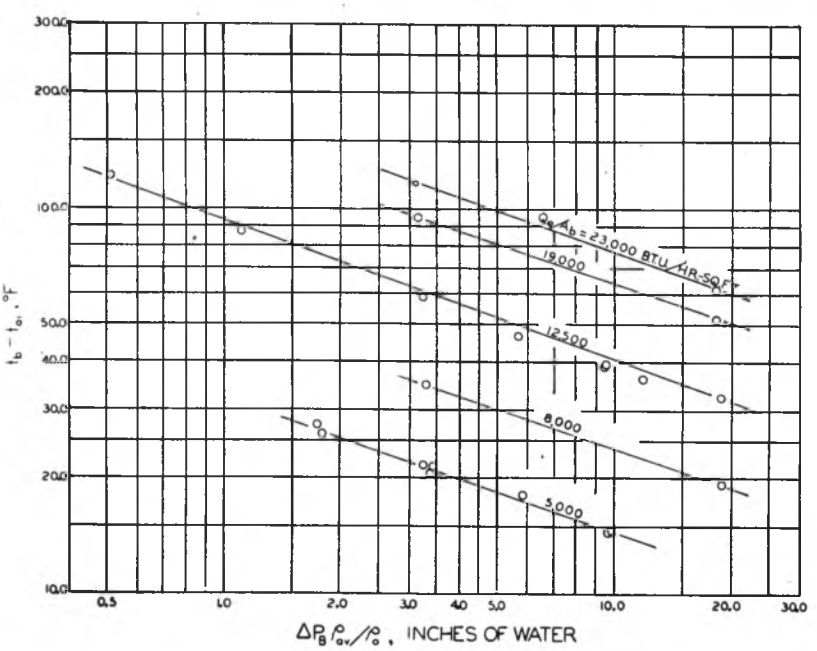

FIG. 6 RELATION OF AVERAGE METAL TEMPERATURE, BAFFLE PRESSURE DROP, AND HEAT FLUX

The so-called "local" values of the unit over-all conductance U_x were calculated on the basis of an assumed uniform heat flux to all sectors of the cylinder and the actual measured fin-base temperature distribution. These local values apply at the various angular positions. Assuming a linear temperature rise of the air through the fin passages, these data then allow the local fin-root-to-air temperature difference to be established, from which the local U_x follows. Fig. 4 then yields the corresponding value of h_x. The values of h_x are average values across the radius of the fin for various angular positions.

The remaining calculations need no further explanation. Complete details are summarized in Tables 3, 4, and 5.

OBSERVED RESULTS

Maximum and Average Base Temperatures. The variation of the maximum (rearmost in these tests) and average temperatures of the fin-base cylindrical section is represented in Figs. 5 and 6, as a function of the over-all static pressure drop across the test section, with the base heat flux as a parameter. The state of

the inlet air is, in this instance, taken into account through the definition of the co-ordinates, that is, the metal temperatures are represented as differences with respect to the initial air temperature, and the air density is included in the adjustment of the pressure drop to standard density by means of the ratio of the average density to the "standard" value chosen. The points as plotted are adjusted to "smoothed" values of heat flux according to the assumption that temperature difference is proportional to heat flux. These curves illustrate the familiar condition of decreasing return, in the form of metal-temperature reduction, as the air-flow rate is increased with the heat-dissipation rate remaining fixed.

Demonstration of Effect of Baffles on Temperature Distribution. In order to illustrate the need for baffles around a finned cylinder of the dimensions tested, if the temperature distribution is to be kept within bounds, reference is made to Fig. 8. Comparative base-temperature distributions are presented for baffled and unbaffled cylinders for a fixed air-inlet temperature and with the over-all heat-dissipation rate being nearly the same. These patterns demonstrate that the air simply will not flow properly around and in-between the relatively deep fins on the rear of the test cylinder without the guiding influence of baffles.

Relation Between Air-Flow Rate and Over-All Static Pressure Drop. While it is the mass flow of air which accomplishes the transfer of heat, it is the over-all total pressure drop which represents the flow-energy "potential" which must exist in order to cause the flow of air. For these tests the total and static pressure drops are essentially the same. The relation between the flow rate and the static pressure drop thus becomes an important step in establishing or predicting performance. Fig. 7 presents these data on an over-all basis for the test system. The mass velocity through the fin passages is also included because of its fundamental role in characterizing the heat-transfer and flow processes in the fluid stream.

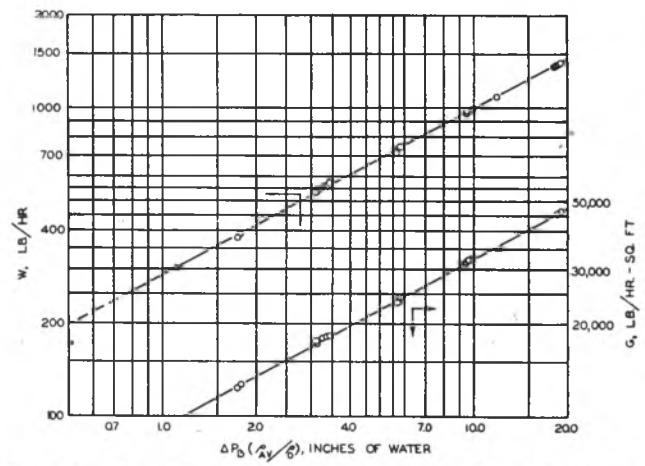

FIG. 7 RELATION BETWEEN AIR-FLOW RATE AND BAFFLE PRESSURE DROP

This treatment of the data implies an effective constant density for the air stream at the average temperature and pressure across the test cylinder. It is fully recognized that this approximation has a limited range of validity, and that density variations and component flow losses entering, through, and leaving the fin passages need to be considered in this problem.

Visual Flow Pattern. Before taking up the fundamental correlations, it will be helpful to consider the behavior of the flow stream with respect to the flow problems relating to the temperature patterns presented.

Figs. 9 and 10 present typical flow patterns obtained in a special visual apparatus with a full-scale installation of a section of the test cylinder. A slurry of aluminum powder in water is employed as the photogenic flow medium. Similarity to the air-flow case is characterized by maintaining comparable magnitudes of the Reynolds number in the fin flow passages.

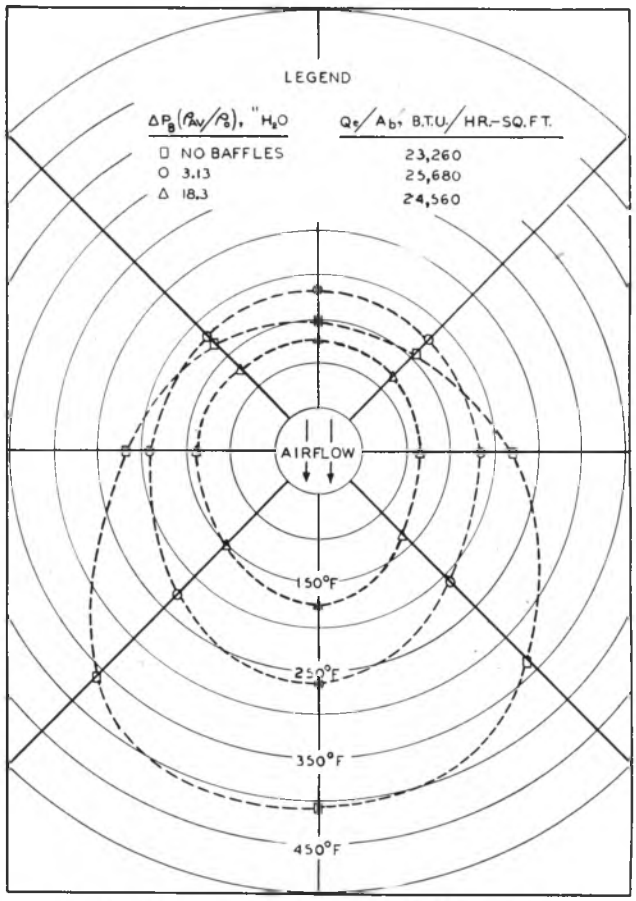

FIG. 8 EFFECT OF BAFFLES ON METAL TEMPERATURES

By comparing the two illustrations, representative of high and low flow rates, it may be observed that no noticeable discontinuities of flow behavior need be expected within the range covered. The difference between water, behaving as an incompressible

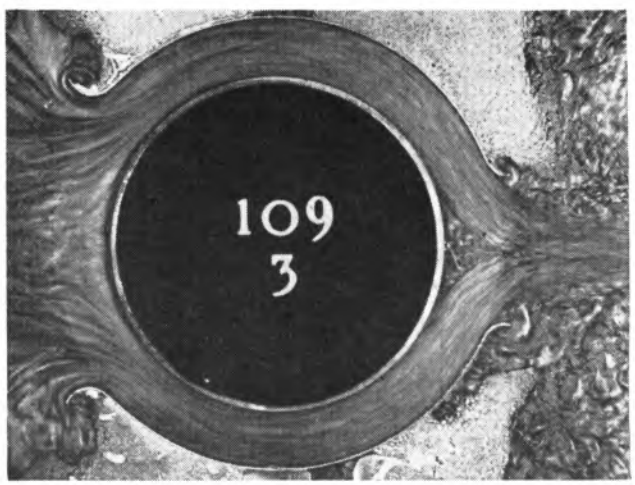

FIG. 9 VISUAL-FLOW PATTERN, REYNOLDS NUMBER OF 3550

fluid, and air, a compressible fluid, is recognized; but this is no handicap for qualitative purposes in the range of air tests covered.

A careful study of the flow pattern will show up such details of interest as: (*a*) Flow around the entrance lip of the baffle with some separation to be noted; (*b*) partial stagnation and turning of the flow approaching the cylinder "head-on;" (*c*) traces of the secondary radial-flow component as the flow develops within the curved passage covered by the baffle; (*d*) abrupt separation of the flow from the base cylinder near the end of the baffle coverage; (*e*) the large eddy-stagnant area over the rear of the fins; (*f*) interaction of the two jets behind the cylinder; and (*g*) eddy dissipation in the section of abrupt fluid shear as the jet passes through the downstream region of "still" fluid to lose eventually its excess of directed kinetic energy.

Since an effective transfer of heat from a surface by a fluid stream requires a clean and rapid "sweeping" of the surface at all points, the nature of these visual flow patterns would indicate that the finned surfaces of the test cylinder are subjected to particularly unfavorable heat-transfer conditions within the eddy-separation zone over the rear, and to a lesser extent in the stagnation region over the front. These unfavorable conditions are accompanied by related undesirable distortions of the temperature distribution.

Fundamental Heat-Transfer and Flow Correlations

Mean Unit Over-All Conductance and Its Variation With Air-Flow Rate and Heat Flux. The mean unit over-all conductance, as calculated in these studies, covers many component influences of local conditions. The approach employed here need not be accepted as final, particularly in regard to the definition of the effective over-all mean temperature difference which has been invoked. The over-all arithmetic mean implies that the cylinder-base temperature is either constant or of linear variation from front to rear, that the rate of heat gain by the cooling air stream is the same for each unit of the circumference swept over from front to rear, that the fin effectiveness has the same value at all points about the cylinder, and that there is no radial variation of air temperature at any point around the cylinder. It is to be recognized that these conditions may be met only to various degrees of approximation in the actual cylinder assembly.

Without more detailed experimentation, it is possible to establish the effect of these approximations only indirectly through calculations and cross-checks of the data correlations. To begin with, under the idealizing postulates the mean over-all conductance would be desired to be a function of the air-flow rate and fluid properties only. This thought was investigated through the checking of data obtained at constant heat dissipation and varying air flow by cross-runs at constant air flow and varying heat dissipation. It was determined in this way that the mean over-all conductance, as defined, was a function of both the air-flow and heat-dissipation rates, the fluid properties remaining essentially constant.

Fig. 10 Visual-Flow Pattern, Reynolds Number of 13,820

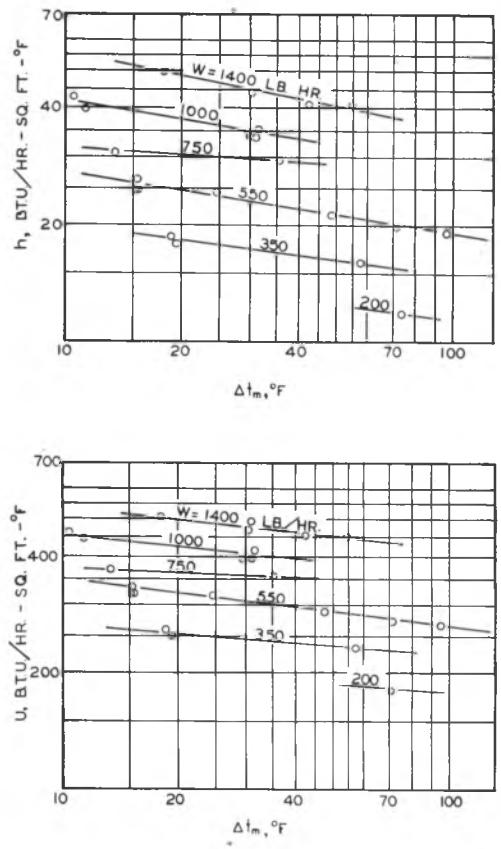

Fig. 11 Variation of Heat-Transfer Coefficient With Mean Temperature Difference

Fortunately, the influence of the heat-transfer rate on the over-all conductance was found to be small. It was decided to represent this influence empirically as a correcting function of the mean temperature difference raised to some power, which was found to be —0.10 for these tests. Fig. 11 shows the data on which this observation is based. Thus in all correlations involving the over-all conductance as a function of the air-flow rate, it is necessary to remove the scatter occasioned by different heat-dissipation rates by plotting not the conductance U, alone, but the product $U(\Delta t_m/\Delta t_0)^{0.10}$. The factor Δt_0 is an arbitrary constant reference temperature difference, taken as 100 F. Fig. 12 shows the corrected mean unit over-all conductance represented as a function of the mass velocity in the fin spaces for the test conditions. This unusual effect of temperature difference in turbulent flow points to new factors involved in this type of apparatus. These are believed to include the effects of non-uniformity of flow and temperature in the fin spaces.

Calculated Mean Unit Surface Conductance and Its Variation With Air Flow and Heat Flux. Next, turning to the mean unit surface conductance h, it is expected that similar approximations apply, particularly since the surface conductance is calculated analytically from the over-all conductance. But since the relation between the mean over-all and surface conductance is not one of direct proportionality, the resultant effect would be of a

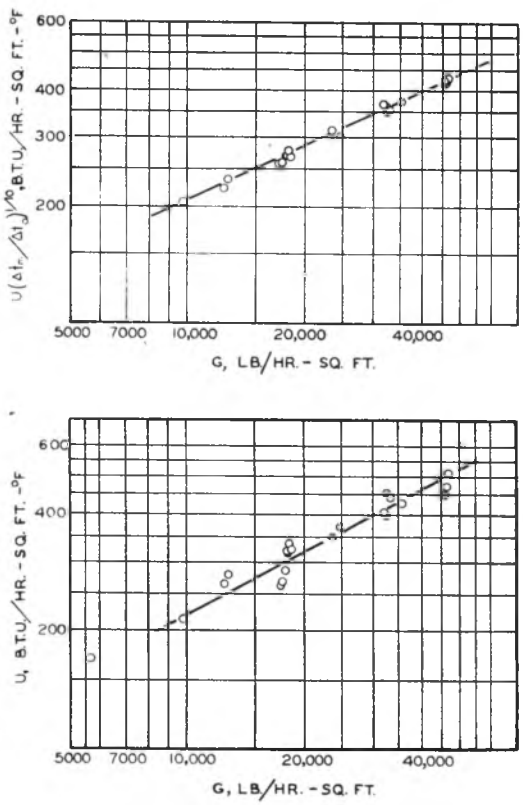

FIG. 12 OVER-ALL HEAT-TRANSFER COEFFICIENT VERSUS MASS VELOCITY

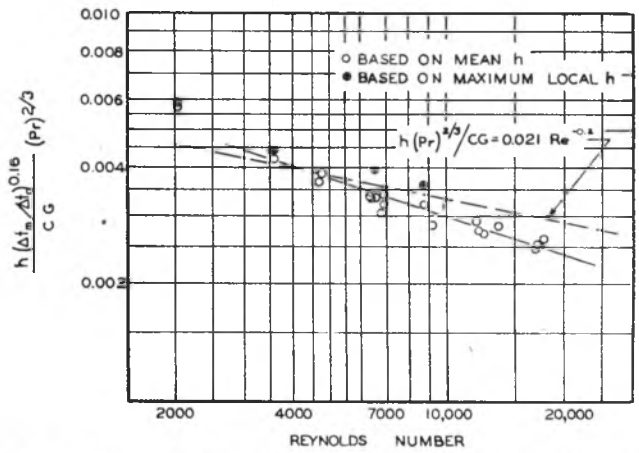

FIG. 13 HEAT TRANSFER FROM A BAFFLED-FINNED CYLINDER COMPARED WITH FLOW INSIDE TUBES

slightly different magnitude in the two cases. In Fig. 11 the same empirical approach is shown, establishing the mean unit surface conductance to be proportional to the —0.16 power of the over-all mean temperature difference employed.

Before discussing the correlation of this calculated conductance, it may be well to consider more closely the method and inherent limitations of its determination. The Harper and Brown (5) procedure is judged to be the most satisfactory analytical means currently available for relating the over-all and surface conductances. But the present data have the limitation of dealing only with mean values. Mean values offer difficulties of generalized extrapolation for systems which are not dominated by fully developed flow and thermal fields. The finned-and-baffled-cylinder studies have flow and thermal fields which are strongly influenced by upstream and entrance-flow conditions, passage curvature, variations in fin-surface temperature, flow separation, and stream interaction at the exit. Large variations locally in the unit surface conductance would be expected under these conditions, so that any mean value would be unfair to the best local performance and overly favorable to the poorest local performance. Preliminary results of analyses dealing with the calculation of local radius-mean conductances will be reported in this paper to support the fundamental inadequacy of over-all mean data.

The mean unit surface conductances inferred from the over-all data, and corrected for the effect of heat flux, are presented in Fig. 13 as a correlation of $N_{St}N_{Pr}^{2/3}(\Delta t_m/\Delta t_0)^{0.16}$ versus N_{Re}. The choice of $\Delta t_0 = 100$ F is seen to make the data correspond with the accepted function for straight passages at a Reynolds number of approximately 4000. Since experimental values of Δt_m varied from 10 F to 98 F, this empirical correction has had the effect of lowering very slightly the test points from the uncorrected level.

These data serve to demonstrate that the mean heat-transfer characteristic of the fin passages is similar to that of straight passages, but that at the same time there are differences which are too apparent to be overlooked. An effort was made to explore the possible effect of employing a local surface conductance instead of the over-all mean. Through a procedure to be indicated subsequently, the maximum local surface conductance was estimated for the four representative points shown in Fig. 13. It is seen that these maximum points are more in line with the accepted data for straight passages, so the trend shown by the mean values may be partially explained in terms of the unit surface-conductance distribution being variable with flow conditions.

Relation Between Maximum Unit Surface Conductance and Over-All Power Loss per Unit of Surface Area. Fig. 14 shows the calculated maximum unit surface heat-transfer conductance which occurs at point about halfway through the baffles, as a function of the over-all unit power loss. The comparison of these data with data for heat transfer for flow inside tubes is favorable, which indicates that on the basis of heat transfer from the finned surfaces inside the baffles, no great improvement of the maximum transfer can be expected from subsequent design changes unless some special effects are invoked.

Since the mean-temperature difference is evaluated as a radial mean and is not the over-all circumferential mean, there is not believed to be necessity for the temperature-difference correction which has been shown necessary for the over-all case.

Over-All Pressure-Loss Coefficient. A measure of the extent to which over-all flow losses in the assembly tested were found to exceed those which would occur for isothermal flow through straight tubes (6) is indicated in Fig. 15. As indicated previously, in Equations [4] and [5], the over-all static pressure-drop data have been reduced by an equation equivalent to that defining the friction factor, to establish the "over-all pressure-loss coefficient." By comparing these magnitudes with the accepted friction-factor data for tubes, it becomes immediately apparent that the effects of entrance, internal curvature-induced, frictional, eddying, and separation losses, and the poor flow conditions at the exit are of considerable magnitude.

It may generally be remarked at this juncture that test runs with the fin-passage Reynolds number extending down to about 1000 showed no tendency in the over-all loss to pass through the "dip" region of the friction factor in the transition between laminar and turbulent flow. This indicates that the fin-passage flow is too far under the influence of entrance, exit, and curvature conditions to allow the normal development of true laminar-flow behavior in this test range.

Calculated Local Magnitudes of Unit Surface Conductance. The

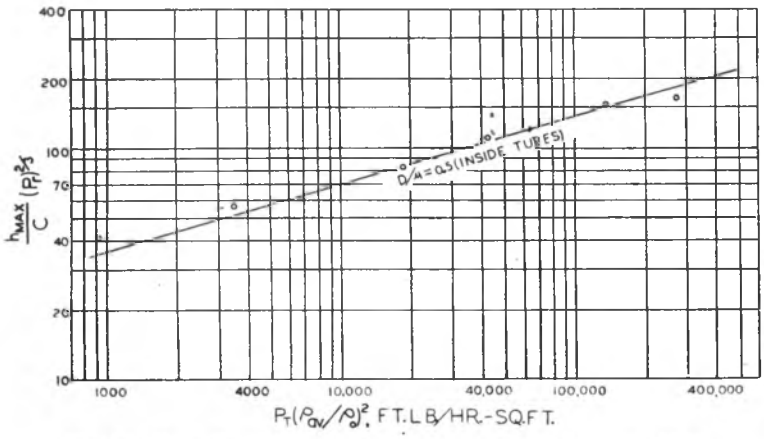

FIG. 14 HEAT TRANSFER AS A FUNCTION OF POWER LOSS PER UNIT SURFACE AREA; COMPARISON OF A BAFFLED-FINNED CYLINDER WITH FLOW INSIDE TUBES

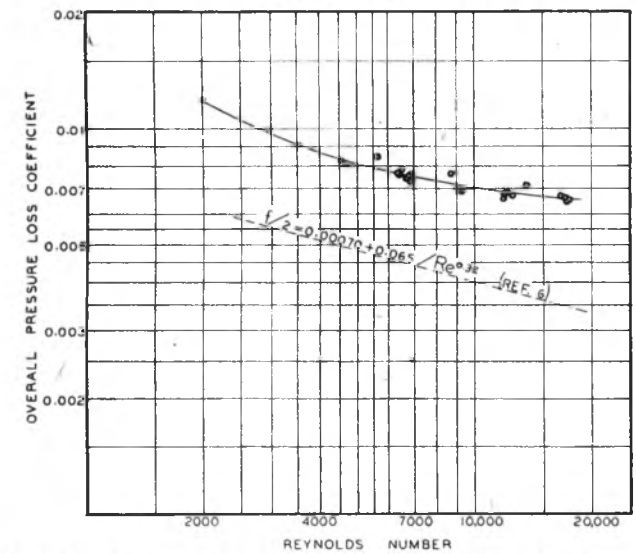

FIG. 15 OVER-ALL PRESSURE-LOSS COEFFICIENT; COMPARISON WITH FRICTION FACTOR FOR FLOW INSIDE TUBES

uniform nature of the electrical heating employed in these tests permits calculations to be made of the local surface conductance for the fins, under the assumption that the rate of heat transfer per unit of circumferential angle is constant around the cylinder. This calls for a linear variation of mean cooling-air temperature from the front to the rear of the cylinder. Then, having the fin-base temperature from direct experimental data, local unit over-all conductances U may be calculated for different positions around the cylinder. From the pattern of these over-all conductances around the cylinder the corresponding local unit surface conductances may be determined according to procedure established for relating U and h, indicated in Fig. 4. The surface conductance thus established is a mean over a radial sector of the fins.

For precise results calculation of circumferential heat conduction would have to be considered. Preliminary estimations indicate that the proportion of such heat flow is small. Consideration of such conduction would result in even lower values of h at the rear of the cylinder.

An example of the air and fin-root metal-temperature distributions for a representative run is shown in Fig. 16. The metal temperatures represent averages from both sides of the cylinder. Fig. 17 presents the distribution of unit over-all conductances for four values of the fin-passage Reynolds number, where the

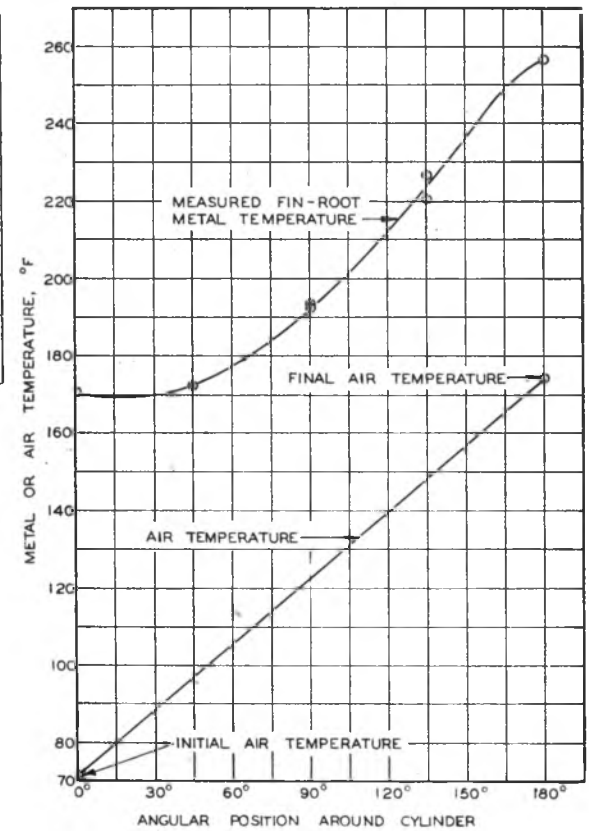

FIG. 16 POINT-TO-POINT TEMPERATURE DISTRIBUTION, RUN 26, $N_{Re} = 2020$

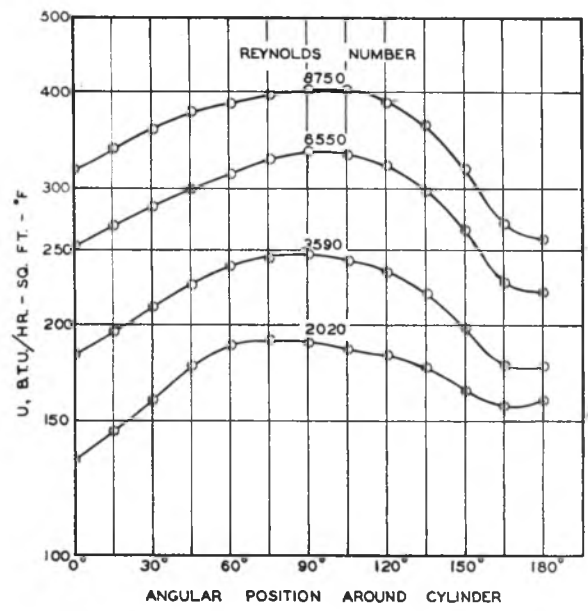

FIG. 17 LOCAL OVER-ALL HEAT-TRANSFER COEFFICIENTS, RUNS 9, 12, 25, AND 26

maximum conductances are observed to range from 30 to 50 per cent above the minimum values. The nature of these variations is quite in accord with the pattern of the flow stream about the cylinder. Corresponding magnitudes of the unit surface conductance are shown in Fig. 18.

In due fairness to the performance of the fin surfaces it is again to be pointed out that the conductances are quite favorably

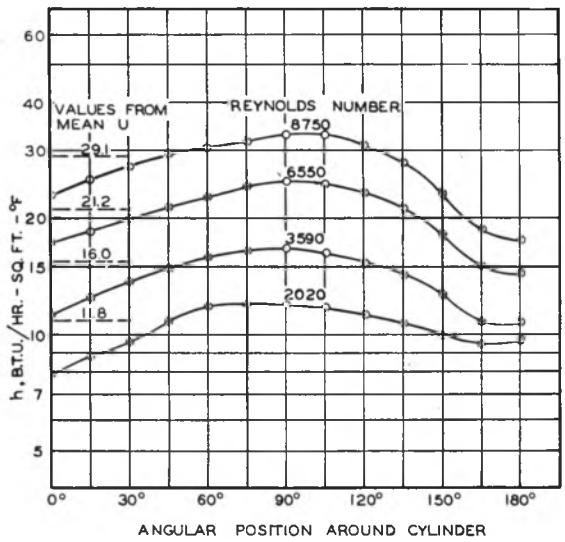

FIG. 18 LOCAL SURFACE HEAT-TRANSFER COEFFICIENTS

high where the flow stream is enclosed by the baffles; and that where the conductances are shown to be low over the unbaffled portions, then the effective Reynolds number for the flow stream in these regions is also low, due to the fact that here the full stream is not passing circumferentially between the fins. A complete adjustment of the data in terms of actual local conditions can be made only with the aid of properly detailed point-to-point experimental studies.

The mean unit surface conductances as previously calculated from the mean unit over-all conductances are also shown in Fig. 18 for reference. The maximum conductances from these curves are those representing the four corresponding points in the general correlation of Fig. 13. These maximum points have been previously noted as representing slightly better performance than the accepted data for straight tubes. It is observed that the angular position of the maximum conductance increases with increasing flow rate, presumably serving as an indication of the influence of the entrance- and exit-flow effects upon the development of the flow within the covered passages.

CONCLUSIONS

1 Heat transfer from a finned-and-baffled cylinder of the proportions tested has been found to be generally similar to the behavior of a heat exchanger composed of a set of parallel passages.

2 The local patterns of metal temperatures and flow conditions have been emphasized as governing the resultant heat-transfer processes in the fin system.

3 The over-all rate of energy loss in the flow stream has been pointed out to be considerably higher than that for frictional dissipation in straight smooth passages, due primarily to the influence of entrance and exit conditions.

4 Possible applications of the data obtained to performance problems in engine-cylinder cooling may be developed.

BIBLIOGRAPHY

1 "Fluid Meters, Their Theory and Application," by A.S.M.E. Special Research Committee on Fluid Meters, fourth edition, parts 1 and 3, 1937.

2 "Heat Transfer From Finned Metal Cylinders in an Air Stream," by Arnold E. Biermann and Benjamin Pinkel, N.A.C.A. Technical Report No. 488, 1934.

3 "Heat Transfer by Natural and Forced Convection," by Allan P. Colburn, Purdue University, vol. 26, January, 1942, p. 50.

4 "Surface Heat-Transfer Coefficients of Finned Cylinders," by Herman H. Ellerbrock, Jr., and Arnold E. Biermann, N.A.C.A. Technical Report, No. 676, 1939.

5 "Mathematical Equations for Heat Conduction in the Fins of Air-Cooled Engines," by D. R. Harper and W. B. Brown, N.A.C.A. Technical Report No. 158, 1922.

6 "Heat Transmission," by William H. McAdams, McGraw-Hill Book Company, Inc., New York, N. Y., second edition, 1942, p. 119.

7 "Blower Cooling of Finned Cylinders," by Oscar W. Schey and Herman H. Ellerbrock, Jr., N.A.C.A. Technical Report No. 587, 1937.

8 "The Effect of Baffles on the Temperature Distribution and Heat-Transfer Coefficients of Finned Cylinders," by Oscar W. Schey and Vern G. Rollin, N.A.C.A. Technical Report No. 511, 1935.

Discussion

C. M. ASHLEY.[5] Comments have been made concerning the radial movement of elements of the stream flowing between the fins. The writer believes that this radial movement can be explained by considering the fact that the circumferential movement of the stream in the fin passage constitutes in essence, a portion of a vortex. With initially uniform pressure for all parts of the stream, the velocity of that portion of the stream flowing at the outer portion of the fin will be lower than that flowing at the inner portion with correspondingly higher static pressure. Next to the fin, however, the fluid friction slows down the circumferential velocity, thus permitting the difference of pressure between the inner and outer portions of the fin to become effective, and resulting in an inward flow of fluid along the surface of the fins. In order to balance this there must be an equal outward flow in the main portion of the stream.

G. K. BERNHARDT.[6] The authors have made a valuable contribution to those concerned with heat transfer from finned surfaces. This paper did not mention how the authors treated the radiation effects. Although these effects should be small, the writer would appreciate a discussion of how they accounted for the radiation between the fin surfaces and from the barrel portion of their muff.

F. A. MCCLINTOCK.[7] In calculating the local surface conductance, the authors assumed that "the rate of heat transfer per unit of circumferential angle is constant around the cylinder." This assumption seems valid enough for the heat flow to the inside of the muff when radiant heat is used, but if there is a circumferential flow of heat, the flow from the outside of the muff will not be constant around the cylinder. The presence of a circumferential temperature gradient indicates that there must be some circumferential heat flow. The following analysis shows that, for the authors' tests, the local surface conductances are markedly in error because the circumferential flow was neglected, and that an appreciable amount of the heat flow to the rear of the cylinder was carried away by conduction along the walls:

The cylinder height is designated by L and the other symbols are as shown in Fig. 19 of this discussion. Term q is defined as the rate of heat flow per unit area. The mean temperature of the wall T and the rate of heat flow to the inside wall $2\pi r_0 L q_{r0}$ are known. Each side of the cylinder is cooled by the flow of air $W/2$, whose specific heat C_p and initial temperature T_i are known.

For steady-state conditions, the heat efflux from any given section must equal the influx, as follows

$$q_{r1} r_1 L \Delta\theta + (q_\theta + \Delta q_\theta) t L = q_{r0}\, r_0\, L \Delta\theta + q_\theta t L \ldots\ldots [7]$$

By rearranging

[5] Director of Development, Carrier Corporation, Syracuse, N. Y.

[6] Experimental Test Engineer, Pratt & Whitney Aircraft, East Hartford, Conn. Jun. A.S.M.E.

[7] Research Division, United Aircraft Corporation, East Hartford, Conn. Jun. A.S.M.E.

$$\frac{q_{r1}r_1}{q_{r0}r_0} = 1 - \frac{\Delta q_\theta t}{\Delta\theta} \quad \ldots\ldots [7a]$$

The rate of circumferential flow per unit area q_θ is equal to the negative of the thermal conductivity of the wall times the temperature gradient

$$q_\theta = -k\frac{dT}{rd\theta} \quad \text{and} \quad \Delta q_\theta = -k\Delta\frac{dT}{rd\theta} \quad \ldots\ldots [8]$$

If the temperature gradient is constant from r_0 to r_1, Equations [7a] and [8] can be combined as follows

$$\frac{q_{r1}r_1}{q_{r0}r_0} = 1 + \frac{kt}{q_{r0}r_0r_m}\frac{\Delta}{\Delta\theta}\left(\frac{dT}{d\theta}\right) \quad \ldots\ldots [9]$$

where r_m is the log mean radius of a radial section.

As $\Delta\theta$ approaches zero, Equation [9] becomes

$$\frac{q_{r1}r_1}{q_{r0}r_0} = 1 + \frac{kt}{q_{r0}r_0r_m}\frac{d^2T}{d\theta^2} \quad \ldots\ldots [9a]$$

The term $\frac{q_{r1}r_1}{q_{r0}r_0}$ is unity when the heat flow to the inner wall is equal to that from the outer wall. Therefore the term $\frac{kt}{q_{r0}r_0r_m}\frac{d^2T}{d\theta^2}$ denotes the ratio of net circumferential flow to radial inflow at any section.

Exact evaluation of the terms is difficult for two reasons: (*a*) The second derivative of temperature with respect to angular position $\frac{d^2T}{d\theta^2}$, depends to a large extent on how the temperature-angle curve is faired. (*b*) The temperatures and hence the circumferential gradients in the fins are less than those in the base metal, so that if the thickness t includes the fins, the estimated circumferential flow is too high.

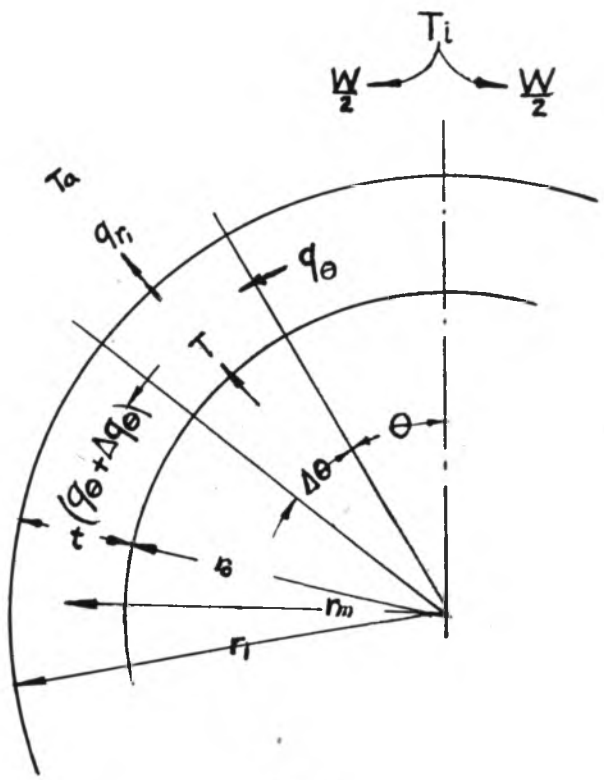

FIG. 19

The run plotted in the authors' Fig. 16, and shown as R_e = 2020 in Figs. 17 and 18, is taken as an example. A trigonometric series was fitted to the mean temperatures at the five points, with the condition that the slope was zero at the front and rear of the cylinder. This condition must be satisfied if the second derivative is to be finite at those points. The resulting second derivative was —151 deg F/radian². A power series fitting the same points and conditions gave a second derivative of —464 deg F/radian². If a curve is chosen so that the second derivative is constant between the 135-deg point and the rear of the cylinder, the second derivative has the least possible magnitude, which turns out to be —108 deg F/radian². The trigonometric series is used here because it seems to give the most reasonable result, namely, —151 deg F/radian². The full cross-sectional area of the fins was used in calculating the thickness t, and the log-mean radius r_m. The following values are used in solving Equation [3a] for the circumferential flow:

k = 100 Btu hr^{-1} ft^{-1} deg F^{-1} $\quad r_1$ = 0.2578 ft
q_{r0} = 13,460 Btu hr^{-1} ft^{-2} $\quad r_m$ = 0.283 ft
r_0 = 0.250 ft $\quad t$ = 0.0275 ft

$$\text{Hence } \frac{\text{Circumferential flow}}{\text{Inflow}} = \frac{kt}{q_{r0}r_0r_m}\frac{d^2T}{d\theta^2} = 0.44$$

Because of the assumptions, the ratio may be less, but it is almost certainly over 20 per cent. At other locations on the muff it is even harder to estimate the second derivative accurately, but it may be as much as one third of that at the rear, with resulting circumferential flows of 5 to 10 per cent. Therefore the plot of local surface conductance, Fig. 18 of the paper, may be significantly distorted, especially at the rear of the cylinder. More data would be necessary to determine the actual shape of the surface-conductance plot to see if the surface conductance may be practically constant in the baffled region. In cylinder heads, where the wall thickness is greater, metal conduction may well account for the major part of the cooling.

Circumferential heat flow also makes the air-temperature rise deviate somewhat from a straight line. The air temperature can be calculated as follows

$$T_a = T_i + \int_0^\theta \frac{q_{r1}r_1Ld\theta}{W/2\ C_p} \quad \ldots\ldots [10]$$

Substituting for $q_{r1}r_1$ from Equation [9a]

$$T_a = T_i + \frac{q_{r0}r_0L\theta}{W/2\ C_p} + \frac{ktL}{W/2\ C_pr_m}\frac{dT}{d\theta} \quad \ldots\ldots [11]$$

The last term gives the deviation from a straight-line function, which in this case does not exceed 5 deg F.

R. G. VANDERWEIL.[8] The illustrations showing the flow characteristics through the baffled fins were taken from water-flow patterns. Were any provisions made to guarantee that this water pattern is actually the same as the pattern resulting by the use of air? If such provisions were made, how did the Reynolds number of the water flow compare with the Reynolds number of the actual air flow?

W. R. WYKOFF.[9] The authors deserve credit for attempting to break these data down into local heat-transfer functions. It is apparent to those who have attempted to predict cooling performance with data for the type of finned cylinders involved, that over-all data are very restricted as to extrapolation to other

[8] Office of Consulting Engineer, Chase Brass & Copper Co., Waterbury, Conn.

[9] Experimental Test Engineer, Pratt & Whitney Aircraft, East Hartford, Conn. Jun. A.S.M.E.

than the original test conditions. It appears necessary to expand approximate point variable analyses of this type, including both component pressure-loss and heat-transfer functions, in order to predict effectively the performance of fin passages over the maximum attained operating range.

The authors have pointed out that over the unbaffled portions at the front and rear of the muff, the full air stream does not pass circumferentially between the fins. Also, they have used the mean stream temperature for computing local heat-transfer coefficients in these front and rear regions, as well as in the baffled section. It would appear from observation of the flow patterns, that a rather large radial-temperature gradient exists in the air stream over the unbaffled fins. Thus it is felt that the local coefficients over these exposed sections are only equivalent functions and should be so designated by broken lines in Fig. 18.

In Fig. 14 the authors have plotted a local heat-transfer factor against an over-all power loss. In order to rate fairly the heat-transfer surfaces a local power loss should be used. In the calculations reported, baffle entrance and exit losses, which make up an appreciable component of the over-all loss, are included. If these losses were removed, the experimental points shown would fall slightly above the "tube" line. This can be explained perhaps as an effect of the radial "sweeping" component of flow in the fin passages, as noted by the authors.

Furthermore, in regard to the "mean-temperature difference effect" in Fig. 11, what is the interpretation of this? Presumably, any quantity which is properly designated as a "conductance" should be independent of the potential acting.

Authors' Closure

Even beyond the clarification of incidental details in this paper, the authors are appreciative of the opportunity given by the discussers' comments to speak further concerning the basic interpretation of the results released for publication.

Mr. Ashley's comments on the flow behavior in the fin passages are in accord with the expected effects which were observed in the visual study. Still further evidence has been gained from an enlarged scale model, where pressure and velocity distributions could be obtained.

As to Mr. Bernhardt's question on radiation, no analysis of this has been attempted as yet. Radiation would have a small effect on the fin surface-temperature pattern within the fin spaces, and radiant exchange with the surroundings would enter as a small term in the heat balance. Quantitative investigation remains for the future.

Mr. McClintock has brought forth the question of heat conduction in the circumferential direction, which has been skipped over in the published discussion. For purposes of practical judgment, it is unfortunate that run 26, as analyzed in Fig. 16 according to the approximate method adopted by the authors, was the one at the very lowest air-flow rate. At higher rates of air flow and heat transfer Mr. McClintock's Equation [9*a*] will yield much lower proportions of circumferential conduction.

There exists some question of how closely the idealized cylindrical-shell system of Fig. 19 may be taken as representing a cooling-fin system. While the discussers' comments mention some uncertainty, indeed, it has been the authors' preference to adopt somewhat different analytical procedures for a quantitative study of how much error is introduced through adoption of the simplest one-dimensional concepts for preliminary and entirely practical purposes. The actual system is three-dimensional in its behavior at any point. An initial experimental study of fin and air temperatures over all radial and circumferential-angle positions has shown very interesting temperature patterns, which at once demonstrate the weakness of one-dimensional simplifications. Analytical studies in two-dimensional co-ordinates (radial and circumferential) lead to a system of partial-differential equations which are basically significant but solvable only by tedious methods. Some preliminary calculations, however, have demonstrated the fundamental importance of the circumferential conduction component over the unbaffled portions of the finned cylinder; but, contrary to the implications of Mr. McClintock's numerical results, these calculations have shown that designs of engine-cylinder fins may generally be made to an accuracy compatible with production and assembly tolerances without allowing for the presence of circumferential conduction. Thus for the time being, such refinements will be developed slowly rather than adopted immediately.

The whole broad question of developing basic design procedures with fin-base circumferential temperature distribution as one of the variables remains for future consideration.

In replying to Mr. Vanderweil, the fin-passage Reynolds numbers, based on the mean velocity, were kept within the same range for the air and water tests. Lampblack patterns have been obtained on the fin surfaces with air flow, and these appear to be the same as for the water tests. The greatest inadequacy of the visual pictures in comparison to the actual system lies in another point. This point is that the fin passage in which the photographs were taken was formed by substituting a sheet of plate glass for a fin. This substitution changed the entrance contraction, the cross-sectional form, and the exit contraction of the topmost passage as compared to the others. Justification resides in the fact that the visual studies were employed for qualitative purposes only.

Mr. Wykoff's comments concerning Fig. 18 are appreciated and agreed with. He is also correct in regard to Fig. 14. Data from other tests have allowed independent determination of the frictional loss within the baffle-enclosed passages, which has been shown to be roughly two thirds of the over-all loss.

Then the "mean-temperature-difference effect" of Fig. 11 comes up for further explanation. The authors offer this as nothing more than an empirical result, obtained from the particular test installation, instrumentation, and procedures of data analysis which were employed in these tests. The so-called "conductances" reported are not to be employed for calculations outside of the range of the test results. These preliminary tests simply did not include sufficient internal measurements within the test specimen to allow a more satisfactory analysis of the data. The demonstrated weaknesses of the over-all treatment may serve as an excellent example of how real systems do not usually behave in accord with simple idealizing postulates. The interpretation of Fig. 11 is therefore that the over-all-mean procedure, as applied to the temperature difference and the conductance U, is basically inadequate. This has been known for several years, but the practical slant follows the reply to Mr. McClintock.

Readers will also recognize that the conductance h has been calculated and not directly measured. This leads to the possibility of a small error in the magnitudes reported; but this is no worse than the use of an over-all mean.

By way of further interest to those concerned with applications to design problems, it is hoped that the eventual removal of wartime restrictions will allow release of the very considerable amount of additional data which have been obtained in other more comprehensive studies. The flow-system design problems, in particular, have been entirely neglected in this paper. Yet in some respects, and particularly for low-density air, the flow-loss design requirements may be more critical than those for the over-all heat transfer.

The combined challenges of obtaining improved basic data and extending application design methods to meet all problems encountered in practice are, however, goals within the grasp of continued effort.

Local Coefficients of Heat Transfer for Air Flowing Around a Finned Cylinder

By W. H. McADAMS,[1] R. E. DREXEL,[2] and R. H. GOLDEY[3]

This paper describes an apparatus for measuring local coefficients of heat transfer, hitherto never obtained for a jacketed or baffled-finned cylinder. The inner surface of the vertical cylinder was divided into narrow vertical segments to collect steam condensate, a measure of the local flux. Since the over-all heat balances agreed within a few per cent, local heat balances were used to calculate local air temperatures. Wall temperatures of the base of each segment were measured by calibrated thermocouples, and local coefficients of heat transfer were determined at 11 stations around one half of the cylinder. The results were easily duplicated and the condensate from the undivided side agreed closely with that from the divided side. Average surface coefficients from fins to air agreed satisfactorily with published data. For a given Reynolds number, temperature difference had no effect on the Stanton number.

Nomenclature

The following nomenclature is used in the paper:

A = area of total air-cooled heat-transfer surface, 12.6 sq ft
A_b = area at base of fins, 0.686 sq ft
A_x = local area at base of fins for 1 segment, 0.0312 sq ft
a = dimensional term $\sqrt{2h/(kx_m)}$, reciprocal feet, in equation for effectiveness
C = correction factor in Equation [1] for effectiveness, dimensionless
C_C = for curvature, Fig. 9
C_T = for taper, Fig. 9
c_p = specific heat of air, 0.24 Btu per lb per deg F
D_e = equivalent diameter of gas passage arbitrarily taken as $D_e = 4sw/2(s + w)$, ft
e = base of natural logarithms
f' = over-all friction factor, dimensionless, in Fanning equation:

$$\Delta p = \frac{4f'LG^2}{2g_cD_e\rho}$$

G = mass velocity, lb air/(hr)(sq ft of cross-sectional area of gas passage 90 deg from front of cylinder)
h = surface coefficient of heat transfer, from surface of fins to air, Btu/(hr)(sq ft)(deg F difference in temperature), from U and Equation [2]
h_a = based on arithmetic mean Δt
h_x = based on local Δt
h_m = based on logarithmic mean Δt
k = thermal conductivity of fins, Btu/(hr)(sq ft) (deg F/ft)
L = nominal length of air travel, arbitrarily taken as $\pi(R_b + 0.5w)$, ft
q = rate of heat transfer for entire finned cylinder, Btu/hr
q_x = rate for 1 segment having base area A_x
R = radius, ft
R_b = radius at base of fins, ft
s = mean spacing of adjacent fins, ft
s_b = fin spacing at base of fins, ft
s_t = fin spacing at tips of fins, ft
t = local air temperature, deg F
t_1 = temperature of entering air, deg F
t_2 = temperature of exit air, deg F
t_b = local temperature of base of fins, deg F
t_{bm} = length-mean temperature
U = apparent coefficient of heat transfer, $U = q/A(t_b - t)$, Btu/(hr)(sq ft of base area) (deg F, base to air)
U_m = mean value, from Equations [4] and [5]
U_x = local value, from Equation [3]
w = width (radial length) of fin, ft
w' = $w + 0.5x_t$, ft
x = thickness of fin, ft
x_m = mean thickness of fin, ft
x_t = fin thickness at tip, ft
Δt = temperature difference, deg F
Δt_a = arithmetic-mean temperature difference
Δt_m = logarithmic-mean temperature difference
η = effectiveness of tapered radial fin, dimensionless, from Equation [1]
η' = approximate effectiveness, $\tanh aw'/aw'$
μ = viscosity of air at mean bulk temperature, lb/(hr)(ft), equal to 2.42 × centipoises
ρ = density of air at mean bulk temperature, pounds/cu ft
D_eG/μ = Reynolds number
h_m/c_pG = Stanton number

Introduction

The finned cylinders of air-cooled engines are provided with external baffles which jacket a portion of each cylinder and cause the air to flow between the fins. It is known that the cooling of the cylinder may be profoundly influenced by factors such as the extent to which the baffles cover the cylinder, the clearance between the baffles and the tips of the fins, and the shape of the baffle at the air entrance and exit. For the important case where the air velocity through the passages between the fins is known, average coefficients of heat transfer for the entire finned cylinder are reported in the literature, but local coefficients are not available.

The purpose of the present study was to develop an apparatus for measuring the local coefficients of heat transfer around a jacketed or baffled-finned cylinder.

[1] Department of Chemical Engineering, Massachusetts Institute of Technology, Cambridge, Mass.
[2] Department of Chemical Engineering, Massachusetts Institute of Technology. Present address, E. I. du Pont de Nemours & Company, Wilmington, Del.
[3] Department of Chemical Engineering, Massachusetts Institute of Technology. Present address, Hotel Miramar, Miami, Fla.

Contributed by the Heat Transfer Division and presented at the Annual Meeting, New York, N. Y., Nov. 27–Dec. 1, 1944, of The American Society of Mechanical Engineers.

Apparatus Developed in Investigation

The apparatus developed in this investigation consisted of a special finned heat-transfer surface constructed so that local heat flux could be measured, a blower to draw air through the test section, a boiler to supply steam, and standard orifices. Fig. 1 is a diagrammatic sketch of the apparatus. The cooling air passed through an entrance fairing and then across the baffled-finned cylinder into a mixer after which the air temperature was

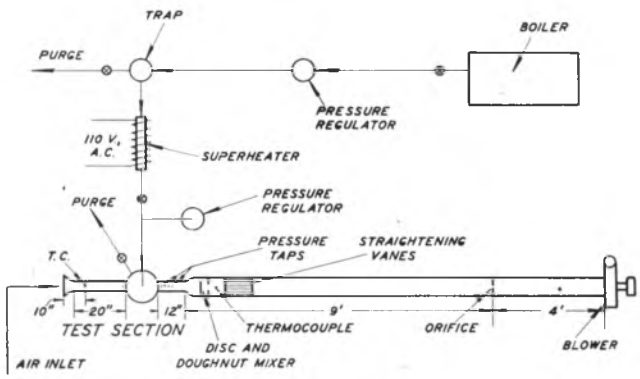

Fig. 1 Diagrammatic Plan of Apparatus
(Entrance fairing always starts 20 in. from leading edge of fin.)

measured. The ducting between the test section and the mixing section was insulated with hair felt 1 in. thick. After flowing through straightening vanes, the air was metered by a standard orifice and passed to the blower and out to the room. The blower was driven by a 5-hp variable-speed motor.

Steam free from impurities, which would cause dropwise condensation, was generated in a gas-fired boiler at a gage pressure of 15 psi; the pressure was reduced by passing the steam through a regulator. Moisture was removed from the steam in a trap, and the steam was superheated as it passed through an electrically heated section of pipe before entering the test section.

The heat-transfer surface consisted of two aluminum-alloy muffs from an air-cooled airplane engine. The fins of nonuniform width were machined off and the remainder of the muffs,[4] Fig. 2, were shrunk onto a vertical steel barrel having the same outside diameter (6.015 in.) as an actual engine cylinder. One side of the barrel was divided into eleven vertical segments, Fig. 3, which collected steam condensate (1).[5] The equally spaced segments were formed by steel strips silver-soldered into slits cut entirely through the barrel on a milling machine, provided with a dividing head.[6] A machined ring, Fig. 4, silver-soldered to the division strips and cylinder, collected the condensate which flowed out of the apparatus into 100-cc graduates through $^1/_8$-in. copper tubes and U-bends of glass tubing which served as liquid seals.

A cross section of the test section is shown in Fig. 5 and indicates the methods used to prevent heat losses by conduction from both ends of the test section and the precaution taken to collect only the condensate resulting from heat transfer from the finned surface. To prevent heat loss from the top of the test section, the top of the nonfinned portion of the barrel was kept at steam temperature by the steam in the upper chamber made of 8-in. steel pipe. The horizontal glass plate supported by pegs prevented condensate from the top cover from dripping into the collector ring. In the lower steam chamber the condensate lines were bathed in steam to prevent heat losses. The condensate level was kept constant in the drain lines by adjusting the pressure inside the apparatus by means of a needle valve in the inlet steam line and by adjusting the water level in a water seal used as a final pressure regulator. To make certain that conden-

[4] Each muff had an inside diameter of 5.995 in. and a diameter of 6.188 in. at the base of the fins. Each fin had a width (radial length) of 1.11 in., and the thickness decreased uniformly from 0.040 in. at the base to 0.020 in. at the tip. The center-to-center spacing of fins was 0.141 in.; since the average thickness of each fin was 0.03 in., the average clearance was 0.111 in. The total cross section between the fins was 0.0616 sq ft. The two muffs contained 36 such fins and the total air-cooled surface was 12.6 sq ft. The height of the two muffs was 5.09 in., and the total area at the base of the fins was 0.686 sq ft. Since each segment represents $^1/_{22}$ of the total base area, A_x was 0.0312 sq ft.

[5] Numbers in parentheses refer to the Bibliography at the end of the paper.

[6] Drew and Ryan (1) first used this method of measuring local flux and applied it to a bare vertical cylinder placed in the center of a wind tunnel.

Fig. 2 Aluminum-Alloy Muffs

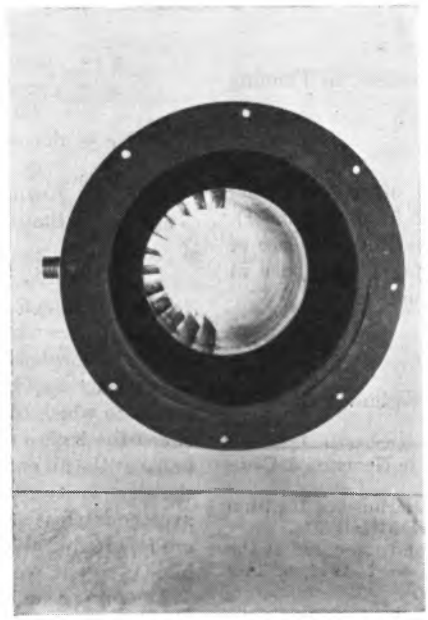

Fig. 3 Steel Barrel and Division Strips

Fig. 4 Collector and Drains

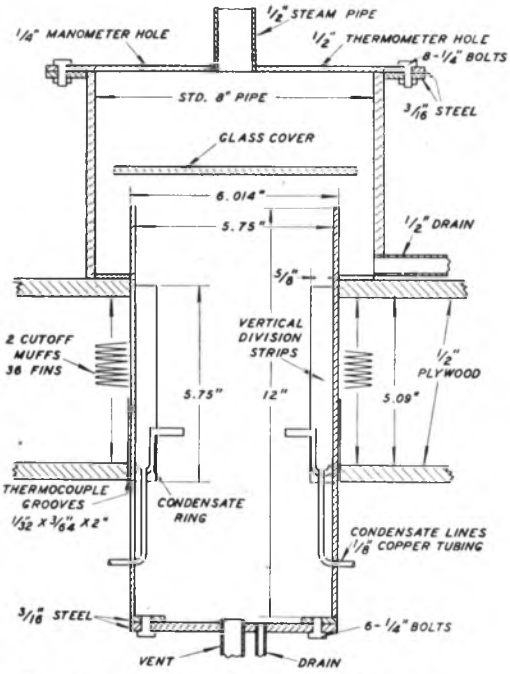

FIG. 5 SECTIONAL ELEVATION OF TEST SECTION

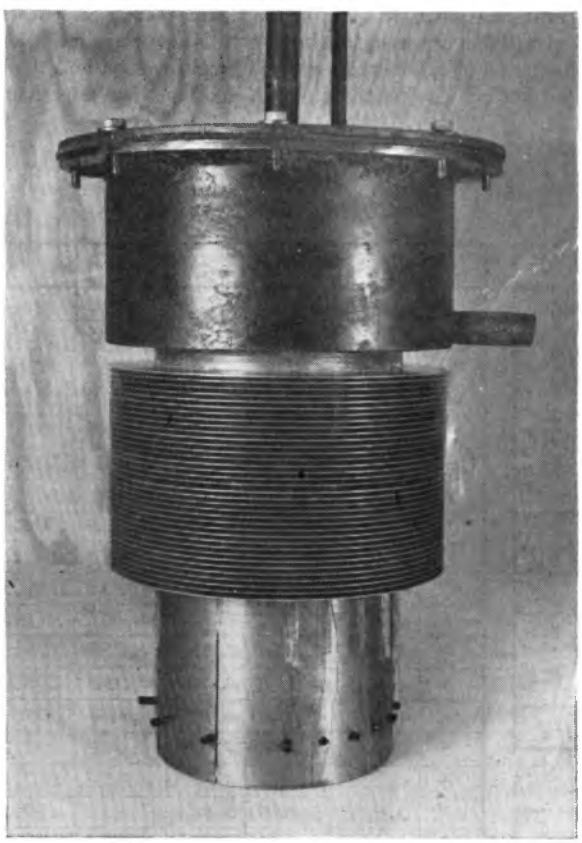

FIG. 6 TEST SECTION WITHOUT JACKET OR BAFFLE
(Air-cooled surface is 12.6 sq ft.)

sate was not overflowing from the collector ring, sight glasses were installed in the top cover of the test section so that frequent observation of the interior of the apparatus could be made; film-type condensation was always obtained. Steam was vented

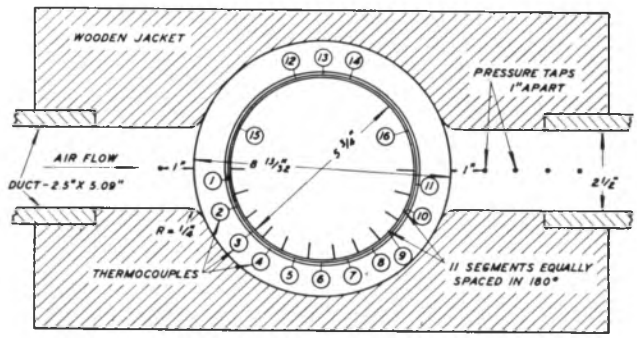

FIG. 7 PLAN VIEW OF TEST SECTION WITH JACKET
(All thermocouples are 2 in. from bottom of lower muff, except No. 12, which is 1/2 in., and No. 14, which is 1 in. Jacket touches tips of fins, and cross-sectional area for air flow is 0.0616 sq ft. Entrance fairing is 5.25 in. long and reduces from a rectangle 7.50 in. wide × 10 in. high to a rectangle 2.50 in. wide × 5.09 in. high.)

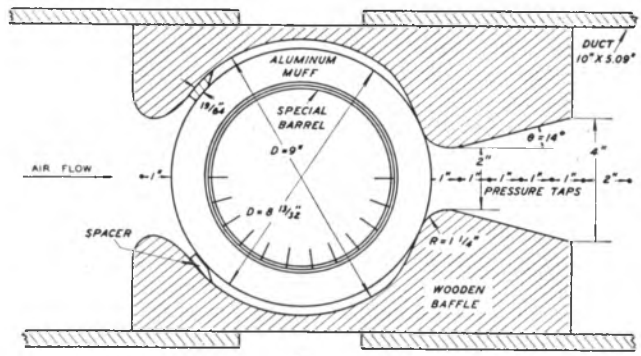

FIG. 8 PLAN VIEW OF TEST SECTION WITH BAFFLE REPLACING JACKET
(Mass velocity of air was arbitrarily based upon total cross-sectional area, 0.0816 sq ft of air passage, 90 deg from front of cylinder. The entrance fairing is 7 in. long and reduces from a rectangle 16 in. wide × 11.0 in. high to a rectangle 10 in. wide × 5.09 in. long.)

from both the upper and lower chambers, to remove noncondensable gases. Fig. 6 shows the test section.

Calibrated thermocouples (No. 30 copper-constantan) were inserted in slots in the base of the bottom muff and cemented in place with "Insalute" cement prior to heating the muffs and shrinking them onto the steel barrel. The thermocouples were connected to a cold junction immersed in an ice bath, and a Leeds and Northrup portable precision potentiometer (Serial No. 347007) by means of a selector switch. A couple was located at the center of each segment 2 in. from the bottom of the lower muff. Thermocouples were also placed in the steel barrel and at different depths in the muff on the undivided side. The locations of thermocouples 1–16 are shown in Fig. 7. Air temperatures were measured by a shielded thermocouple (No. 19) in the inlet stream, by a shielded couple (No. 17) 1 in. behind the trailing edge of the muff, and by a thermocouple (No. 18) after the mixer. Temperatures of the air at the orifice, of the inlet steam, and of the vent steam from the bottom of the apparatus were taken with thermometers.

Static pressures were measured before the test section and before the orifice. Pressure drops across the test section were measured from the pressure tap 1 in. in front of the leading edge of the muff to pressure taps 1, 2, 3, 4, 5, and 7 in., respectively, from the trailing edge of the muff. The pressure drop across the orifice was also measured.

Tests were made with a jacket, Fig. 7, and with a baffle, Fig. 8. To determine whether temperature difference had any effect on the heat-transfer coefficients, the inlet air was preheated in some runs (Series B); heating steam was available at a gage

pressure of 40 psi. In these runs the entrance fairing was replaced by a special section consisting of an air heater, a disk-and-doughnut mixer, and straightening vanes.

Procedure Followed in Tests

When the test section had become heated, the blower was started and the speed adjusted to give the desired air-flow rate. The steam valve was again adjusted to maintain the steam-chamber pressure at 7 cm of water gage. Water was then forced back into the apparatus through all the drain lines to remove air bubbles. The apparatus was then allowed to run for about $^1/_2$ hr, until steady-state operation was secured.

The run was started when consistent readings of several thermocouples indicated that a steady state had been reached. Eleven 100-cc graduates were simultaneously placed under the condensate outlets from the divided side of the cylinder; a beaker was placed under the condensate outlets from the undivided side of the cylinder; and the timer was started. Condensate was collected during three consecutive intervals of equal duration. Constancy of the amount of condensate from a given segment during each interval was a confirmation of steady-state operation. All the readings of the thermocouples, thermometers, and manometers were recorded during each interval. Runs lasted from 30 to 90 min, depending upon the air-flow rate.

The consistency of the data taken in the three different parts of a run is a test of the reproducibility of the data. Table 1 gives the complete data for run 6-J. The volumes of condensate in different portions of a run usually checked within 1 cc; since the smallest volume ever collected from any segment was 20 cc, the maximum error so introduced was 5 per cent. Upon repeating a run 1 month later, using a different observer, it was found that the maximum deviation in a local coefficient was only 2 per cent from the mean value. The pressure-drop data agree within the possible error in reading the manometers.

The close agreement between the condensates from the two halves of the cylinder verified the assumption that the air flow divided equally around the cylinder. In the worst case (run 2A), the condensate rates on the two sides disagreed by 6 per cent.

The heat balances range from 1.5 to —8.4 per cent; as an average the steam condensate indicates 4 per cent less heat transfer than that calculated from the air rate and the measured temperature rise.

The areas of the segments were accurate within 1 per cent. The local air temperature was calculated from the measured total temperature rise (accurate within 0.5 deg F) and the ratio of condensate up to this point to the total condensate. It was felt that the condensate ratios are accurate within 2 per cent. The local temperature difference was evaluated from the calculated local air temperature and the observed wall temperature; the thermocouples are accurate within 0.2 deg F, and these readings varied but little.

Method of Calculation

On air-cooled cylinders the average temperature of the surface of the fins is of secondary interest. The purpose of cooling and finning is to reduce the temperature at the base of the fins. Since this temperature is of primary interest, a correlation of surface heat-transfer coefficients should involve the fin-base temperature. This temperature and a mathematical effectiveness of the fins are used herein to calculate surface coefficients. In the design of cylinders the procedure is reversed and the calculated surface coefficients and the mathematical effectiveness

TABLE 1 COMPLETE DATA FOR RUN 6-J

CONDENSATE (C.C.)

POSITION	A	B	C
1	97	98	97
2	100	101	100
3	77	78	77
4	70	71	71
5	64	64	65
6	53	53	54
7	50	51	50
8	36	36	36
9	33	34	33
10	24	25	24
11	19	19	18
TOTAL	623	630	625
OTHER SIDE	624	628	628
GRAND TOTAL	1247	1258	1253
TIME MIN.	30	30	30

PRESSURE (CM. WATER)

	A	B	C
2" ORIFICE Δp	2.1	2.1	2.1
UPSTREAM STATIC AT ORIFICE	1.1	1.1	1.1
UPSTREAM STATIC AT TEST SECTION	0.2	0.2	0.2
Δp_1	0.9	1.1	1.0
Δp_2	1.0	1.1	1.1
Δp_3	1.0	1.0	1.0
Δp_4	0.9	1.0	1.0
STEAM CHEST	7.5	7.5	7.5
BAROMETER- 760.2 MM. Hg			

THERMOMETERS, °C.

	A	B	C
AIR IN	24.3	24.3	24.3
AIR OUT	85.6	85.2	86.0
ORIFICE	67.2	67.2	67.0
STEAM IN	107.0	107.5	108.2
STEAM OUT	101.5	100.5	100.5

TEMPERATURE (THERMOCOUPLE . M. V.)

NO.	A	B	C	AVE.	°F.
1	3.928	3.926	3.923	3.926	198.3
2	4.028	4.024	4.022	4.025	202.1
3	4.047	4.047	4.044	4.046	203.0
4	4.082	4.080	4.078	4.080	204.3
5	4.112	4.108	4.105	4.108	205.4
6	4.112	4.110	4.122	4.115	205.7
7	4.148	4.137	4.132	4.139	206.6
8	4.132	—	4.125	4.128	206.1
9	4.207	4.203	4.200	4.203	209.0
10	4.237	4.233	4.230	4.233	210.1
11	4.267	4.262	4.257	4.262	211.3
12	4.062	4.054	4.052	4.056	203.3
13	4.103	4.098	4.094	4.098	205.0
14	4.111	4.102	4.100	4.104	205.2
15	4.050	4.041	4.037	4.042	202.9
16	4.256	4.253	4.248	4.252	210.9
17	3.872	3.850	3.845	3.856	195.5
18	3.687	3.672	3.665	3.673	188.4
19	0.982	0.980	0.962	0.973	76.2

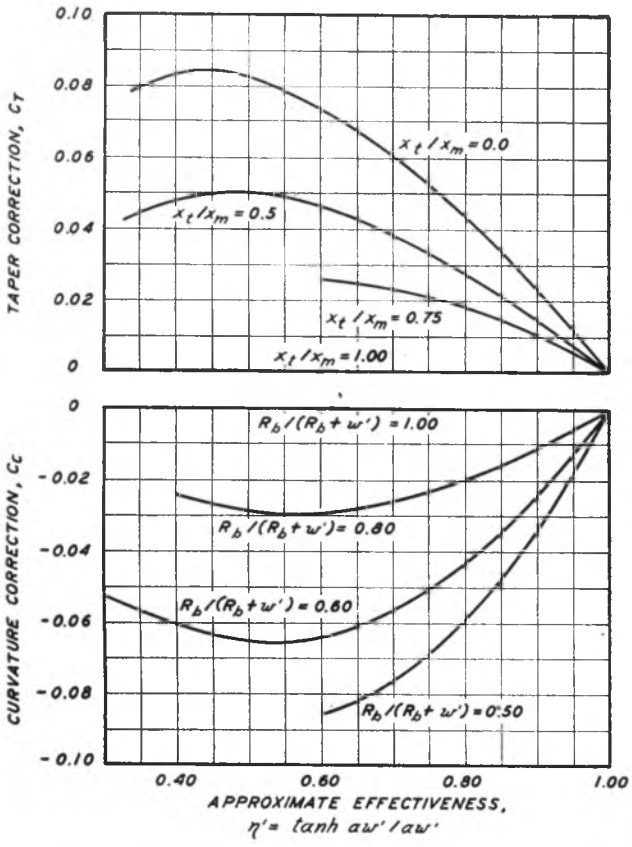

FIG. 9 TAPER AND CURVATURE CORRECTIONS TO BE ADDED TO APPROXIMATE EFFECTIVENESS η' IN OBTAINING TRUE EFFECTIVENESS (Taken from Harper and Brown, reference 3, by courtesy of National Advisory Committee for Aeronautics.)

are combined to give the fin-base temperature. Furthermore, it is known that average surface coefficients, based upon the measured mean temperature of the surface of the fins, often differ from those based upon measured base temperatures and a calculated effectiveness. Consequently, both the correlation of test data and the design procedure based thereon should involve base temperatures and calculated effectiveness, so that any errors due to differences between measured and calculated effectiveness are not involved.

The effectiveness η is defined as the mean temperature difference between the surface of the fins and the air, divided by the temperature difference between the base of the fins and the air, and is given by the following equation for tapered radial fins

$$\eta = \frac{\tanh aw'}{aw'} + C_T + C_C = \eta' + C_T + C_C \quad [1]$$

in which a equals $\sqrt{2h/kx_m}$ and C_T and C_C are corrections for taper and curvature, respectively, taken from Harper and Brown (3) and shown in Fig. 9. It is seen that the effectiveness depends upon the surface coefficient, assumed constant along the radius of the fin, and the dimensions and thermal conductivity of the fin.

The surface coefficient is obtained from the following new equation for tapered radial fins

$$U = \frac{h}{(s + x_m)}\left[\left(2w' + \frac{ww'}{R_b} + \frac{wx_t}{2R_b}\right)\eta + s_b\right] \quad [2][7]$$

[7] See footnote 7 at bottom of next column.

For a given fin η', C_T, C_C, and consequently η and U are unique functions of h, and hence a plot of U can be constructed by assuming values of h. The local apparent coefficient U is first calculated from the data by the simple relation

$$U_x = \frac{q_x/A_x}{t_b - t} \quad [3]$$

and values of h_x are then read directly from the curve of U_x versus h_x, thus avoiding trial-and-error calculations.

RESULTS OF TESTS

All the data for the muff with the jacket or baffle are given in Table 2. Table 3 summarizes calculated values, including average surface coefficients h_m, calculated from

$$U_m = \frac{q/A}{\Delta t_m} \quad [4]$$

based upon the logarithmic-mean apparent temperature difference

$$\Delta t_m = \frac{(t_{bm} - t_1) - (t_{bm} - t_2)}{\ln_e \dfrac{t_{bm} - t_1}{t_{bm} - t_2}} \quad [5]$$

LOCAL SURFACE COEFFICIENTS h_x

Runs (Series J) were made at various air-flow rates with the jacket shown in Fig. 7, and similar runs (Series A) were made with the baffle shown in Fig. 8. The results are summarized in Figs. 10 and 11, plotted in terms of local surface coefficients h_x versus the position of the segment; position 0 is at the front and 11 is at the rear. For a given Reynolds number $D_e G/\mu$, for both the jacket and the baffle, the curves of h_x go through a maximum roughly half-way around the cylinder; as the Reynolds number increases, the maximum shifts somewhat nearer the front of the cylinder. For these runs, it is noted that the local surface coefficient of heat transfer from muff to air was always found to be lower in the rear than at the front.[8]

From Figs. 10 and 11 it appears that the local surface coefficients of heat transfer are unduly high for segment 2 (position 1–2) and low for segment 8 (position 7–8). Data for the jacketed cylinder are shown plotted versus location of segment in Fig. 12, which suggests that the contact between the steel barrel and the muff was unusually close in segment 2 and less close in segment 8, which doubtless was caused by high spots on the cement in the grooves on the inner wall of the muff. At segment 8, where the muff temperature and local condensation rate were abnormally low, heat flows circumferentially by conduction in the muff from adjacent segments 7 and 9. If this effect were allowed for, the local coefficients for segments 7 and 9 would decrease and that for 8 would increase, tending to eliminate the dip in the curve of h_x at segment 8.

Tests (Series B) were run on the baffled cylinder to determine the effect of temperature difference on the mean surface coefficient of heat transfer, h_m. The temperature difference was varied by changing the temperature of the inlet air at substantially constant Reynolds number. The data are plotted in Fig.

[7] Equations [1] and [2] will reduce to the usual approximate equation of reference (4) for a bar fin of constant cross section

$$U = \frac{h}{(s + x_m)}\left[\frac{2}{a}\left(1 + \frac{w}{2R_b}\right)\tanh aw' + s_b\right] \quad [2a]$$

if the sum C_T and C_C is assumed zero and the term $wx_t/2R_b$ is neglected. Although in some cases Equation [2a] will give a result not differing seriously from that obtained from the more rigorous Equations [1] and [2], the latter were used herein.

[8] In order to simplify Figs. 10 and 11, runs are shown only for alternate Reynolds numbers; intermediate Reynolds numbers (not shown) gave curves of the same shape as those shown.

TABLE 2 DATA FOR TESTS

	6-J	5-J	4-J	3-J	2-J	1-J	7-J	8-J	5-A	3-A	4-A	1-A	2-A	4-B	2-B	5-B	1-B	3-B
Run number	6-J	5-J	4-J	3-J	2-J	1-J	7-J	8-J	5-A	3-A	4-A	1-A	2-A	4-B	2-B	5-B	1-B	3-B
Air rate, lb/hr	208	288	396	533	728	980	1390	1620	355	431	1040	1220	1790	1040	1040	1040	1040	1040
Temp exit air, deg F	188.4	179.0	168.4	162.2	153.7	145.0	134.0	129.7	160.4	153.7	132.5	127.1	119.3	184.6	176.5	163.6	131.4	131.5
Temp inlet air, deg F	76.2	75.7	75.0	78.3	80.8	79.7	76.2	80.6	77.0	74.0	76.0	75.6	75.9	165.8	152.6	128.6	75.0	74.6
Divided side, cc cond/30 min	624	817	1018	1202	1464	1707	2101	2287	813	897	1534	1772	2091	557	698	973	1554	1588
Undivided, cc cond/30 min	627	826	1014	1204	1449	1695	2118	2285	833	919	1578	1762	2175	570	736	1016	1619	1600
Length of run, min	90	75	59	80	60	62.5	60	30	75	90	45	45	39	90	60	60	45	45
Δp_4, cm water	1.0	1.6	2.5	4.2	6.95	11.1	20.2	26.7	1.6	2.1	8.9	11.5	220	9.6	9.6	9.2	8.8	8.8
Δp_7, cm water	.....	.....	.....	.....	.....	.....	.....	.....	1.7	2.2	8.9	11.8	22.3	9.7	9.6	9.3	8.8	8.9
t_{bm}, deg F	205.6	203.2	201.0	198.4	195.5	192.0	186.5	182.9	203.3	200.5	192.2	191.8	184.4	206.1	203.6	200.1	190.7	190.8

TABLE 3 RESULTS OF TESTS

q(air), Btu/hr	5620	7140	8880	10700	12700	15300	19300	19100	7130	8300	14100	15100	18700	4700	5980	8750	14100	14200
q(steam), Btu/hr	5300	6950	8580	10200	12300	14400	17800	19300	6970	7670	13200	14900	18100	4770	6060	8410	13400	13500
q(air)/q(steam)	1.060	1.027	1.035	1.049	1.032	1.062.	1.084	0.990	1.023	1.082	1.068	1.013	1.033	0.985	0.987	1.040	1.052	1.052
D_eG/μ	1230	1710	2370	3150	4300	5800	8230	9580	1590	1959	4730	5660	8290	4370	4390	4480	4730	4730
h_m	8.94	10.5	12.1	15.1	18.3	22.4	29.4	30.6	8.07	9.21	16.9	17.5	24.9	16.2	16.3	16.5	16.1	16.2
h_m/C_pG	0.0110	0.0093	0.0078	0.0073	0.0064	0.0058	0.0054	0.0049	0.0078	0.0074	0.0055	0.0060	0.0048	0.0053*	0.0054*	0.0054*	0.0053*	0.0053*
$f^1/_2$	0.0220	0.0180	0.0155	0.0143	0.0128	0.0113	0.0102	0.0099	0.0240	0.0210	0.0147	0.0144	0.0126	0.0143	0.0143	0.0144	0.0145	0.0148
$(h_m/C_pG) \div f^1/_2$	0.50	0.52	0.50	0.51	0.50	0.51	0.53	0.50	0.32	0.35	0.37	0.35	0.38	0.37	0.38	0.37	0.37	0.36

* Adjusted to D_eG/μ of 4730.

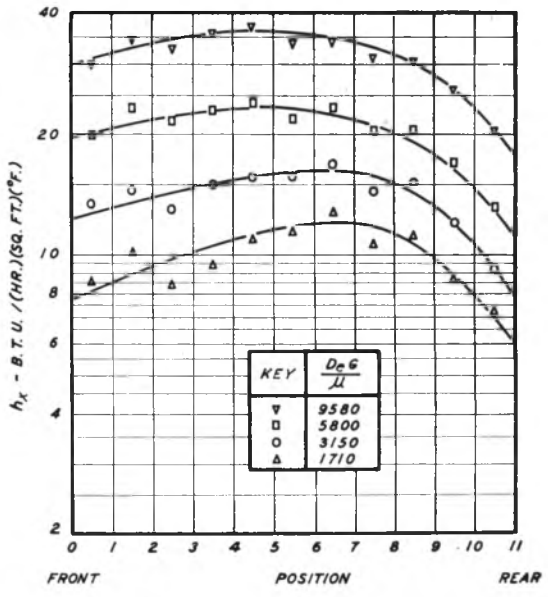

FIG. 10 LOCAL SURFACE COEFFICIENTS h_x VERSUS POSITION FOR JACKETED MUFF, FOR SEVERAL REYNOLDS NUMBERS

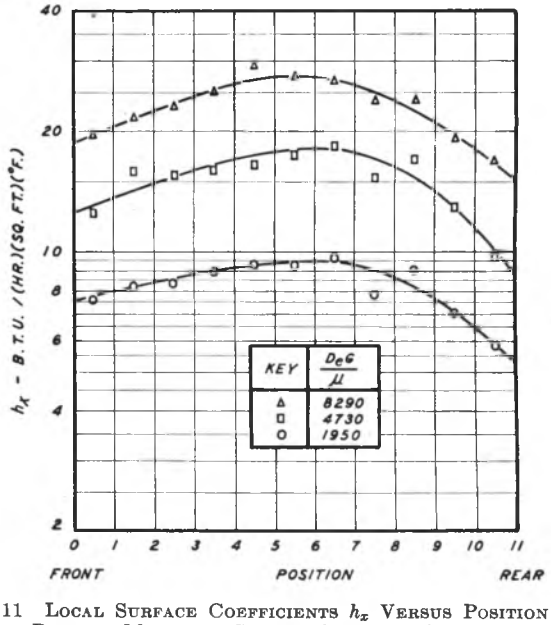

FIG. 11 LOCAL SURFACE COEFFICIENTS h_x VERSUS POSITION FOR BAFFLED MUFF, FOR SEVERAL REYNOLDS NUMBERS

13 and show that h_m/c_pG is independent of Δt_m. Heat balances agreed within a maximum deviation of 7.7 per cent and an average deviation of 3.4 per cent.

Fig. 14 shows the present data for both the jacketed and baffled cylinders, plotted as Stanton numbers, h_m/c_pG versus the Reynolds number, D_eG/μ based upon the equivalent diameter of the passages between the fins. It is seen that the results with the jacket are higher than those for the baffle, for the same Reynolds number; this would still be the case if the definition of D_e had been based upon the total air passage instead of that between the fins.

The data of reference (2) for an electrically heated muff with a jacket were recalculated by means of Equations [1] and [2] as an approximation, obtaining h_m from U_m based upon an arithmetic-mean temperature difference

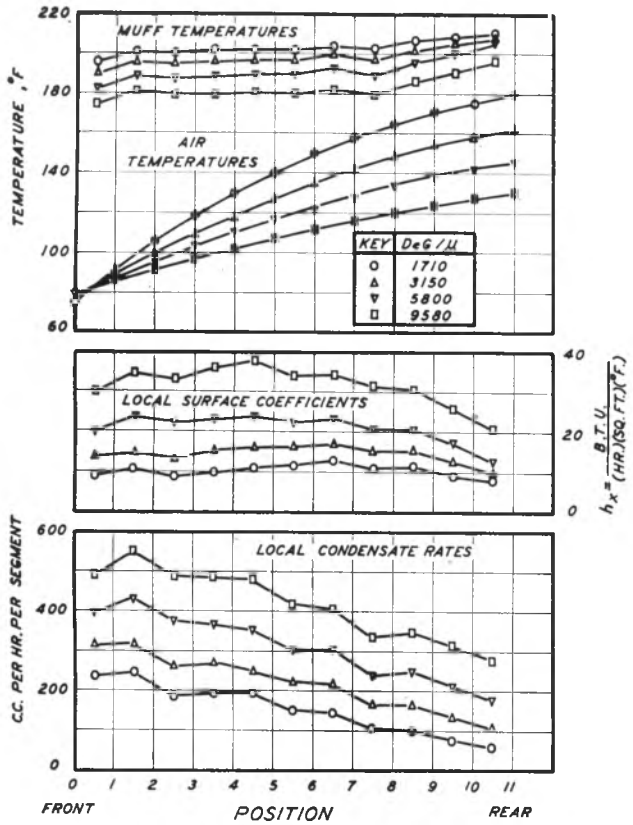

FIG. 12 PLOT OF DATA FOR JACKETED MUFF VERSUS POSITION
(Plot shows minor but systematic irregularities of muff temperatures, condensate rates, and local surface coefficients.)

$$\Delta t_a = \frac{(t_{bm} - t_1) + (t_{bm} - t_2)}{2} \quad \ldots\ldots\ldots\ldots [6]$$

which is a fair type of mean to use with these data obtained with electric heat. The results are plotted in Fig. 14 and average but little below the present data for a jacketed muff. The present data lie on or above the usual equation for turbulent flow of air in long straight tubes

$$\frac{h_m}{c_p G} = \frac{0.023/(0.74)^{2/3}}{(D_e G/\mu)^{0.2}} \quad \ldots\ldots\ldots\ldots [7]$$

given in reference (5); the data of reference (2) shown in Fig. 14 fall on both sides of this equation.

The over-all pressure drops across the test section are reported in the tables, along with the corresponding over-all Fanning friction factors calculated from the data by taking the length of air travel arbitrarily as one half the mean perimeter of a fin. The ratio of the mean Stanton number, h_m/c_pG, to one half the over-all friction factor $f'/2$ was found to average 0.51 with the jacket and 0.36 for the baffle, as compared with a value of 1.0 predicted by the Reynolds analogy and 1.22 by the Colburn analogy (5) for turbulent flow of air in long straight tubes.

The jacket gave 20 to 30 per cent greater surface coefficients h_m than the baffle for the same over-all pressure drop, and 22 to 40 per cent greater coefficients for the same power loss per square foot of finned surface.

By measuring local coefficients for each portion of the baffled-finned cylinder it is possible to determine the faults in location and design of baffles, and improvements in baffles can be worked out more readily and on a sounder basis than when measuring only the usual average coefficients of heat transfer for the entire finned cylinder. Data for other designs and arrangements of baffles have been obtained and may be released in a subsequent paper.

CONCLUSIONS

This study established the following points:

1 The data were reproducible.

2 Good heat balances were obtained.

3 The condensate rates from the divided and undivided halves of the cylinder agreed within 6 per cent.

4 In every run with the baffle or jacket tested, the local coefficient of heat transfer from fins to air was low in front, high roughly halfway around the cylinder, and lowest in the rear.

5 For a given Reynolds number, the baffle gives a somewhat lower Stanton number than the jacket.

6 In terms of average surface coefficients of heat transfer, the data for the jacketed muff of the present study agree well with those of other investigators who determined only average coefficients.

7 For a given Reynolds number, temperature difference was varied from 30 to 85 deg F in tests on the baffled cylinder and had no effect on the Stanton number, expressed in terms of the average surface coefficient of heat transfer for the entire cylinder.

ACKNOWLEDGMENT

It is desired to acknowledge the co-operation of the Pratt and Whitney Division of United Aircraft, in donating the muffs.

BIBLIOGRAPHY

1 "The Mechanism of Heat Transmission—Distribution of Heat

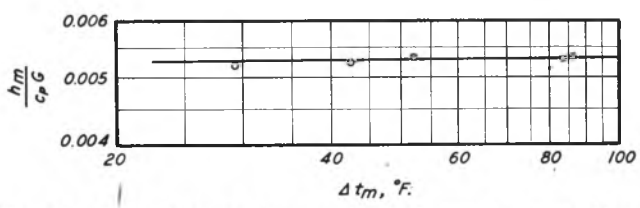

FIG. 13 MEAN STANTON NUMBERS (h_m/c_pG) FOR REYNOLDS NUMBER OF 4730, PLOTTED VERSUS TEMPERATURE DIFFERENCE FROM BASE OF FINS TO AIR

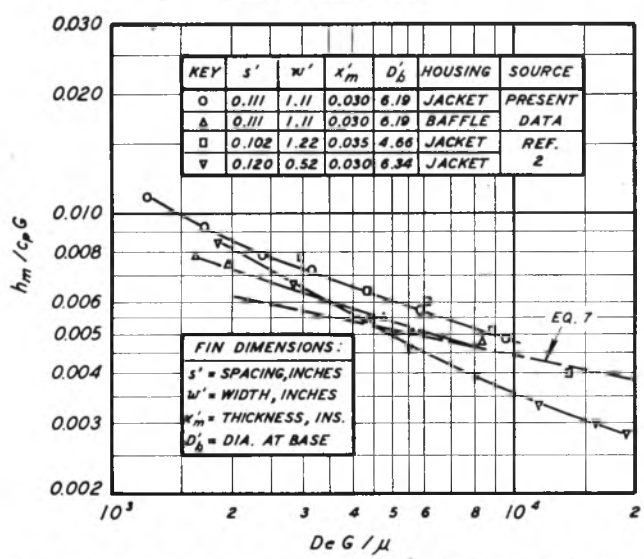

FIG. 14 MEAN STANTON NUMBERS (h_m/c_pG) PLOTTED VERSUS REYNOLDS NUMBER (D_eG/μ) FOR PRESENT DATA AND THOSE OF REFERENCE (2) FOR SIMILAR MUFFS
(Primes are for dimensions in inches.)

Flow About the Circumference of a Pipe in a Stream of Fluid," by T. B. Drew and W. P. Ryan, Trans. A.I.Ch.E., vol. 26, 1931, pp. 118–147; see also "Heat Transmission About a Cylindrical Pipe at Right Angles to Forced Air Flow," by W. J. Paltz and C. E. Starr, S.B. Thesis in Chemical Engineering, Massachusetts Institute of Technology, 1931.

2 "Surface Heat-Transfer Coefficients of Finned Cylinders," by H. H. Ellerbrock, Jr., and A. E. Biermann, National Advisory Committee for Aeronautics, Report 676, 1939.

3 "Mathematical Equations for Heat Conduction in the Fins of Air-Cooled Engines," by D. R. Harper, 3rd, and W. B. Brown, National Advisory Committee for Aeronautics, Report 158, 1922.

4 "Heat Transfer From Finned Metal Cylinders in an Air Stream," by A. E. Biermann and B. Pinkel, National Advisory Committee for Aeronautics, Report 488, 1934.

5 "A Method of Correlating Forced Convection Heat Transfer Data and a Comparison With Fluid Friction," by A. P. Colburn, Trans. A.I.Ch.E., vol. 29, 1933, pp. 174–210.

Efficiency of Extended Surface

By KARL A. GARDNER,[1] NEW YORK, N. Y.

The work of previous investigators on heat flow through extended surface is briefly reviewed and literature citations are given. General equations are derived for the temperature gradient and fin efficiency in any form of extended surface to which the assumptions listed are applicable. The solution of these equations in terms of Bessel functions is shown to cover practically any form of extended surface whose thickness varies as some power of the distance measured along an axis normal to the basic surface. Curves are presented for the fin efficiency of several forms of straight fins, annular fins, and spines.

Nomenclature

The following nomenclature is used in the paper:

- A = fin surface between origin and point x
- A_f = total surface of one fin
- a = cross-sectional area of fin normal to x axis at point x
- a_b = area of fin base
- c = a constant (Equations [2] and [7])
- h, h_e = heat-transfer coefficient on finned side of extended-surface element
- h_i = heat-transfer coefficient on unfinned side of extended-surface element
- $I_n(u)$ = modified Bessel function of the first kind and order n
- $i = \sqrt{-1}$
- $K_n(u)$ = modified Bessel function of the second kind and order n
- k = thermal conductivity of fin material
- L = length of straight fins
- m = a constant (Equation [2])
- n = a constant, order of Bessel function
- p = a constant (Equation [2])
- q = rate of heat flow through section a
- q_f = total rate of heat flow through entire fin
- q_b = rate of heat flow through basic surface which would be covered by base of fin
- q_1 = rate of heat flow through total basic surface
- q_2 = rate of heat flow through basic plus extended surface
- r = function of u defined following Equation [20]
- u = function of x defined by Equation [7][2]
- $w = \pm(x_b - x_e)$ = fin height
- x = distance along axis normal to basic surface[2]
- y = half thickness of fin at point x
- y_b = half thickness of fin base
- α, β = constants
- $\eta = \phi A_f/a_b$ = fin effectiveness
- θ = temperature difference between fin and surrounding fluid at point x
- θ_b = temperature difference between fin at base and surrounding fluid
- ϕ = fin efficiency

[1] The Griscom-Russell Company.

[2] Subscripts b and e refer to conditions at base and edge, respectively.

Contributed by the Heat Transfer Division and presented at the Annual Meeting, New York, N. Y., Nov. 27–Dec. 1, 1944, of The American Society of Mechanical Engineers.

Introduction

In a conventional heat exchanger heat is transferred from one fluid to another through a metallic wall and, other things being equal, the rate of heat flow is directly proportional to the extent of the wall surface and to the temperature difference between one fluid and the adjacent surface. If thin strips of metal are attached to the basic surface, extending into one of the fluids, the total surface for heat transfer is thereby increased and it might be expected that the rate of heat flow per unit of basic surface would increase in direct proportion. However, the average surface temperature of these strips, by virtue of the temperature gradient through them, tends to approach the temperature of the surrounding fluid so the effective temperature difference is decreased and the net increase of heat flow may be considerably less than would be anticipated on the basis of surface alone.

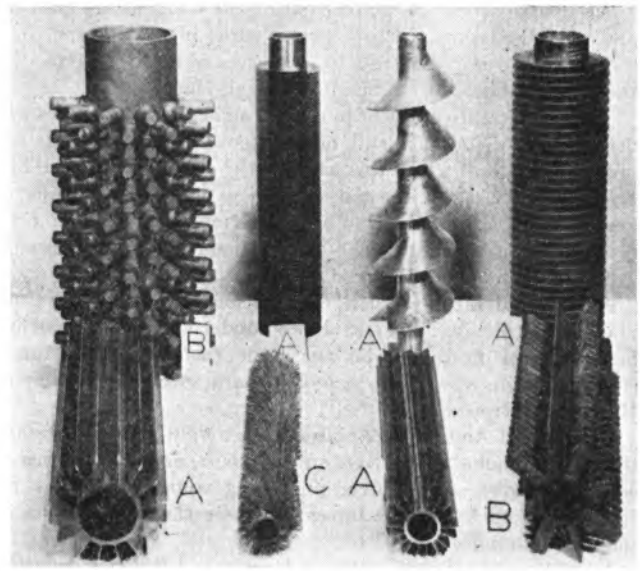

Fig. 1 Some Commercial Forms of Extended Surface
(Samples furnished through the courtesy of *A* The Griscom-Russell Company, *B* The Babcock & Wilcox Company, *C* Thermek Corporation.)

These added heat-conducting strips constitute "extended surface;" they may be of various forms, as shown in Fig. 1. The ratio of the average temperature difference over the extended surface to that over the basic surface is commonly called the "fin efficiency," "fin" being used as a concise generic term for all forms of extended surface. It is the purpose of this paper to derive a general equation for the temperature gradient in fins and to present a solution for fin efficiency which, although not perfectly general, nevertheless includes all the forms previously investigated and several others besides. A secondary purpose is the review and compilation of the significant results of previous investigators.

Literature Review

Some early measurements of the temperature distribution in long metallic rods are available in the experimental determination of the thermal conductivities of iron and copper by Stewart (1).[3]

[3] Numbers in parentheses refer to the Bibliography at the end of the paper.

The iron rod was $^3/_4$ in. sq $\times$ $4^1/_2$ ft long, and the copper rod was $^1/_2$ in. diam $\times$ 7 ft long.

Parsons and Harper (2) derived an equation for the efficiency of straight fins of constant thickness in the course of a paper on airplane-engine radiators. Harper and Brown (3), in connection with air-cooled aircraft engines, investigated straight fins of constant thickness, wedge-shaped straight fins, and annular fins of constant thickness; equations for the fin efficiency of each type were presented and the errors involved in certain of the assumptions were evaluated.

Schmidt (4) covered the same three types of fin from the standpoint of material economy. He stated that the least metal is required for given conditions if the temperature gradient is linear, and showed how the thickness of each type of fin must vary to produce this result. Finding, in general, that the calculated shapes were impractical to manufacture, he proceeded to show the optimum dimensions for straight and annular fins of constant thickness and for wedge-shaped straight fins under given operating conditions.

Murray (5) presented equations for the temperature gradient and the effectiveness of annular fins of constant thickness with a symmetrical temperature distribution around the base of the fin.

A stepwise procedure for calculating the temperature gradient and efficiency for fins whose thickness varies in any manner whatsoever was given by Hausen (6). Curves of both properties for the fins investigated by Schmidt (4) are also included.

The temperature gradient in conical and cylindrical spines was determined by Focke (7) and, independently, by the writer in unpublished work of which this paper is the outcome. Focke, like Schmidt, showed how the spine thickness must vary in order to keep the material requirement to a minimum; he, too, found the result impractical and went on to determine the optimum cylindrical- and conical-spine dimensions.

Avrami and Little (8) derived equations for the temperature gradient in thick-bar fins and showed under what conditions fins might act as insulators on the basic surface. Approximate equations were also given including, as a special case, that of Harper and Brown.

Carrier and Anderson (9) discussed straight fins of constant thickness, annular fins of constant thickness, and annular fins of constant cross-sectional area, presenting equations for the fin efficiency of each. In the latter two cases the solutions are in the form of infinite series.

A rather unusual application of Harper and Brown's equation was made by the writer (10), in considering the ligaments between holes in heat-exchanger tube sheets as fins and thereby estimating the temperature distribution in tube sheets.

The types of extended surface previously investigated, aside from those which may be approximated by Hausen's method, are as follows:

1 Straight fins of constant thickness (2, 3, 4, 6, 8, 9).
2 Wedge-shaped straight fins (3, 4, 6).
3 Annular fins of constant thickness (3, 4, 5, 6, 9).
4 Annular fins of constant cross-sectional area (9).
5 Cylindrical spines (7).
6 Conical spines (7).

Mathematical Treatment—Assumptions

The mathematical analysis is based upon the following assumptions, which are essentially those given by Murray (5), but which are common to all previous investigations except that of Avrami and Little (8):

1 The heat flow and temperature distribution throughout the fin are independent of time, i.e., the heat flow is steady.
2 The fin material is homogeneous and isotropic.
3 There are no heat sources in the fin itself.
4 The heat flow to or from the fin surface at any point is directly proportional to the temperature difference between the surface at that point and the surrounding fluid.
5 The thermal conductivity of the fin is constant.
6 The heat-transfer coefficient is the same over all the fin surface.
7 The temperature of the surrounding fluid is uniform.
8 The temperature of the base of the fin is uniform.
9 The fin thickness is so small compared to its height that temperature gradients normal to the surface may be neglected.
10 The heat transferred through the outermost edge of the fin is negligible compared to that passing through the sides.

Of these assumptions, only 6, 8, 9, and 10 are open to serious question. With some types of fin the heat-transfer coefficient undoubtedly does vary from point to point on the fin, but McAdams and Turner, in a discussion of a paper by Sage (11), show that the use of average coefficients and average conductivity in the theoretical equation for temperature gradient gives good agreement with Stewart's measurements (1). Murray's paper shows how to take account of a nonuniform temperature at the base of annular fins, although it seems reasonable that an average temperature based on the average inside-film coefficient should give sufficiently accurate results for many purposes. The question of temperature variation at the base of the fin is not apt to arise for other types.

The error involved in assumptions 9 and 10 has been investigated by Harper and Brown (3), and Avrami and Little (8), for straight fins of constant thickness; it is very small for most practical forms of extended surface.

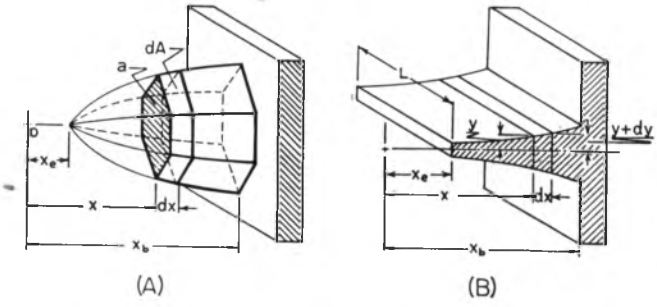

Fig. 2 Diagrams of (*A*), Generalized Element of Extended Surface; (*B*) Straight Fin
(Thicknesses are greatly exaggerated.)

Application of Bessel's Differential Equation

Temperature Gradient. The basic differential equation results from a heat balance on an element of the fin normal to the direction of heat flow, as shown in Fig. 2(*a*)

$$\frac{d^2\theta}{dx^2} + \left(\frac{1}{a}\frac{da}{dx}\right)\frac{d\theta}{dx} - \left(\frac{h}{ka}\frac{dA}{dx}\right)\theta = 0 \quad \ldots\ldots [1]$$

In this, θ represents the temperature difference between the fin and the surrounding fluid at a distance x from some reference point. Termwise comparison of this equation (after multiplication by x^2) with the general form of Bessel's equation given by Douglass (12)

$$x^2\frac{d^2\theta}{dx^2} + [(1-2m)x - 2\alpha x^2]\frac{d\theta}{dx} + [p^2c^2x^{2p} + \alpha^2x^2 + \alpha(2m-1)x + (m^2 - p^2n^2)]\theta = 0 \quad \ldots [2]$$

shows that both have the same form if

$$a = \lambda x^{1-2pn} \quad \ldots\ldots [3]$$

and

$$\frac{dA}{dx} = \mu x^{2p(1-n)-1} \quad [4]$$

where λ and μ are positive constants.

Thus if the cross-sectional area of a fin can be described by Equation [3], and its surface by Equation [4], the solution may be expressed in terms of Bessel functions. The general solution is found by application of the boundary conditions

1 When $x = x_b$, $\theta = \theta_b$

2 When $x = x_e$, $\frac{d\theta}{dx} = 0$ (from assumption 10).

For n equal to zero or an integer

$$\theta = \theta_b \left(\frac{u}{u_b}\right)^n \left[\frac{I_n(u) + \beta K_n(u)}{I_n(u_b) + \beta K_n(u_b)}\right] \quad [5]$$

where

$$\beta = \frac{I_{n-1}(u_e)}{K_{n-1}(u_e)} \quad [6]$$

For n equal to a fraction

$$\theta = \theta_b \left(\frac{u}{u_b}\right)^n \left[\frac{I_n(u) + \beta I_{-n}(u)}{I_n(u_b) + \beta I_{-n}(u_b)}\right] \quad [5a]$$

where

$$\beta = -\frac{I_{n-1}(u_e)}{I_{1-n}(u_e)} \quad [6a]$$

In these equations

$$u = -icx^p = x\sqrt{\frac{h}{ka}\frac{dA}{dx}} \quad [7]$$

and u_b and u_e are found by substituting the values of x, a, and (dA/dx) for the base or edge of the fin, respectively.

Fin Efficiency.[4] The fin efficiency of extended surface is given by

$$\phi = \frac{\int_0^{A_f} \theta dA}{\theta_b A_f} \quad [8]$$

from which, for n equal to zero or an integer

$$\phi = \frac{2(1-n)}{u_b\left[1 - \left(\frac{u_e}{u_b}\right)^{2(1-n)}\right]} \left[\frac{I_{n-1}(u_b) - \beta K_{n-1}(u_b)}{I_n(u_b) + \beta K_n(u_b)}\right] \quad [9]$$

or, for n equals a fraction,

$$\phi = \frac{2(1-n)}{u_b\left[1 - \left(\frac{u_e}{u_b}\right)^{2(1-n)}\right]} \left[\frac{I_{n-1}(u_b) + \beta I_{1-n}(u_b)}{I_n(u_b) + \beta I_{-n}(u_b)}\right] \quad [9a]$$

Fin Effectiveness.[4] Another property of extended surface which is often used is the ratio of the heat transferred through the base of a fin to that which would be transferred through the same base area if the fin were not there, *the base temperature remaining constant.* This ratio is termed the "effectiveness," and it can be simply expressed as a function of the fin efficiency

$$\left(\frac{q_f}{q_b}\right)_{\theta_b = \text{const}} = \eta = \frac{A_f}{a_b}\phi \quad [10]$$

However, in most practical cases, the addition of extended surface to a metal wall changes the base temperature to an extent depending on the heat-transfer coefficients on both sides of the wall. The effectiveness is therefore a misleading indication of the value of extended surface, as comparison with the following more accurate expression will show

$$\frac{q_f}{q_b} = \eta \frac{\left(1 + \frac{h_s}{h_t}\right)}{\left(1 + \eta\frac{h_s}{h_t}\right)} \quad [11]$$

In this, h_s and h_t are the film coefficients on the finned and bare sides of the wall, respectively. Obviously, the advantage of extended surface is greatest when h_s is small compared to h_t.

Types of Extended Surface

In the foregoing, general relations have been developed for the temperature gradient and the fin efficiency without inquiring to what types of extended surface they may be applied, other than noting that they must be described by Equations [3] and [4]. For a given fin the exponents of x in these equations are known; there are two exponents, so it is possible to eliminate p between them and to solve for the appropriate value of n.

Space does not permit detailed derivation or discussion of the equations for the various types of extended surface, so the following are submitted without proof:

Straight Fins. The thickness may vary thus

$$y = y_b\left(\frac{x}{x_b}\right)^{\frac{1-2n}{1-n}} \quad [12]$$

The value of u to be used in the temperature-difference and efficiency equations is

$$u = 2(1-n)\left(\frac{x}{x_b}\right)^{\frac{1}{2(1-n)}}\sqrt{\frac{h}{ky_b}}\cdot x_b \quad [13]$$

In these and subsequent equations it is assumed that the square of the slope of the fin sides is negligible compared to unity, which it usually is for thin fins and spines. This assumption is not necessary for $n = 1/2$ and $n = 0$. Equations and curves are given in Fig. 3. Reference to Fig. 2(*b*) will help in verifying these equations.

Spines—Circular or Regular Polygonal Section.

$$y = y_b\left(\frac{x}{x_b}\right)^{\frac{1-2n}{2-n}} \quad [14]$$

$$u = \frac{2\sqrt{2}\,(2-n)}{3}\left(\frac{x}{x_b}\right)^{\frac{3}{2(2-n)}}\sqrt{\frac{h}{ky_b}}\cdot x_b \quad [15]$$

The solution is exact for $n = 1/2$ and $n = -1$. Equations and curves are given in Fig. 4.

Annular Fins.

$$y = y_b\left(\frac{x}{x_b}\right)^{\frac{-2n}{1-n}} \quad [16]$$

$$u = (1-n)\left(\frac{x}{x_b}\right)^{\frac{1}{1-n}}\sqrt{\frac{h}{ky_b}}\cdot x_b \quad [17]$$

[4] The terms "fin efficiency" and "fin effectiveness," in the meanings adopted here have not been consistently adhered to in the English literature; the latter phrase has been used for both ϕ and η. In the German literature, ϕ is called "der Wirkungsgrad."

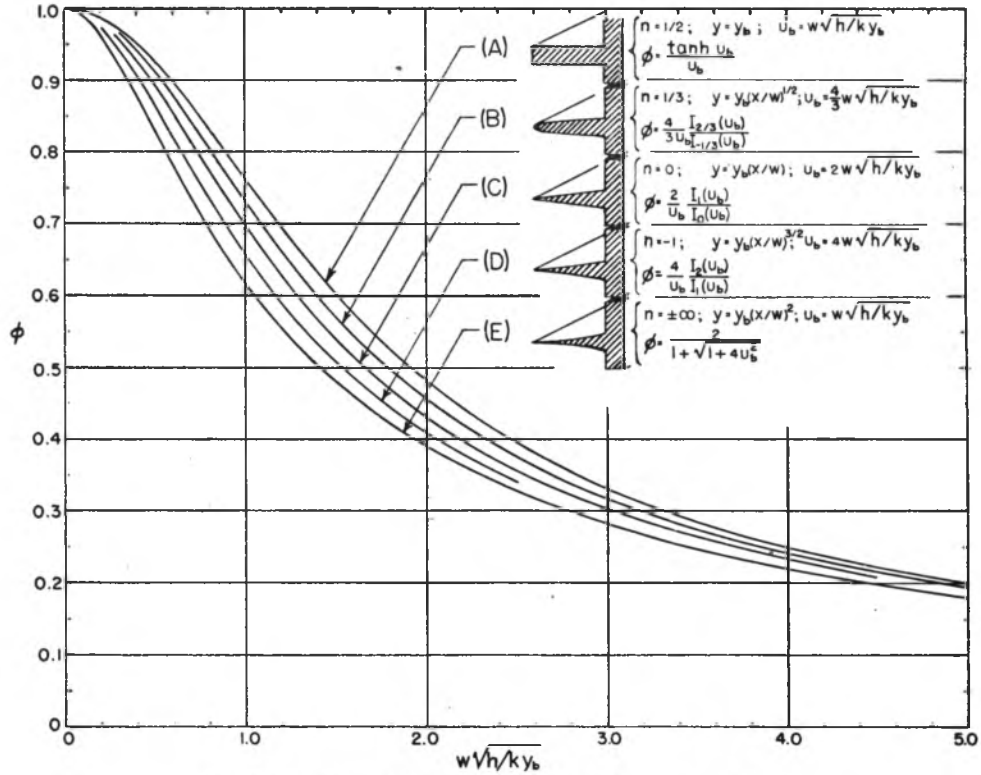

FIG. 3 FIN EFFICIENCY OF SEVERAL TYPES OF STRAIGHT FIN

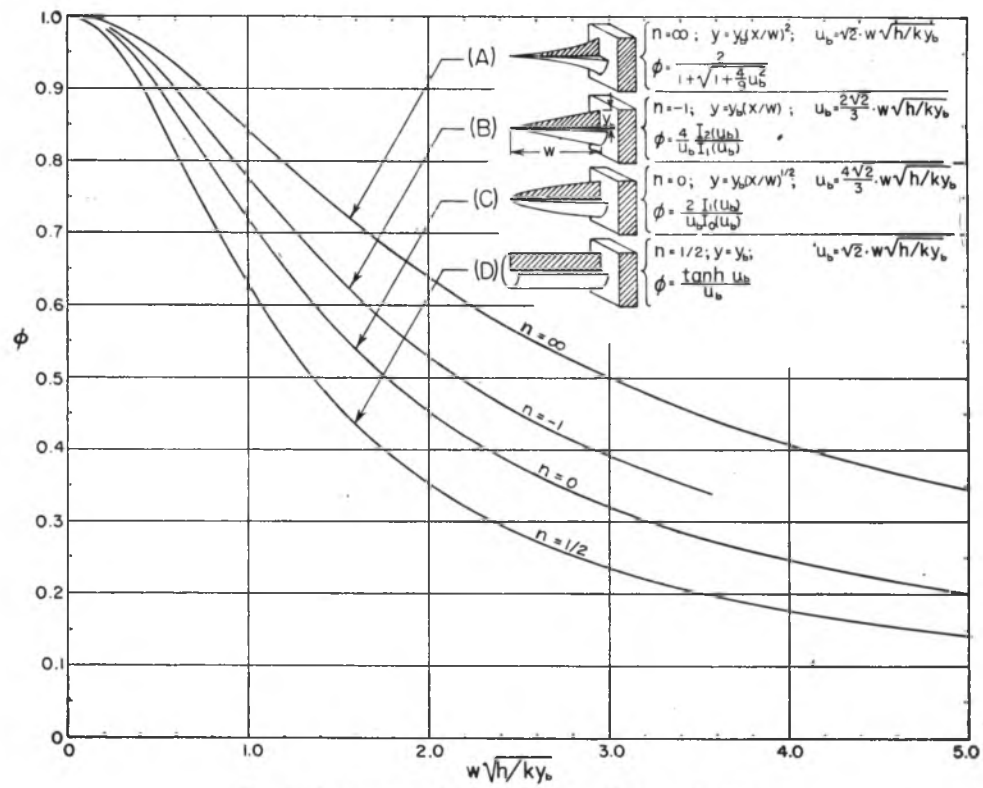

FIG. 4 EFFICIENCY CURVES FOR FOUR TYPES OF SPINE

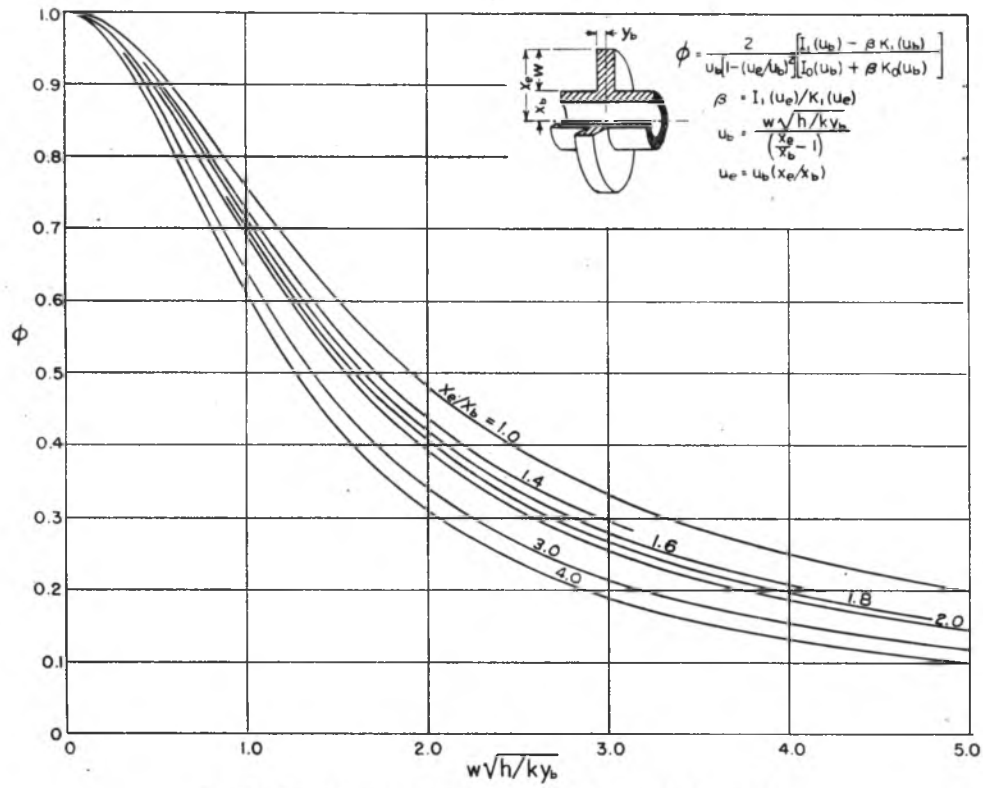

FIG. 5 EFFICIENCY OF ANNULAR FINS OF CONSTANT THICKNESS

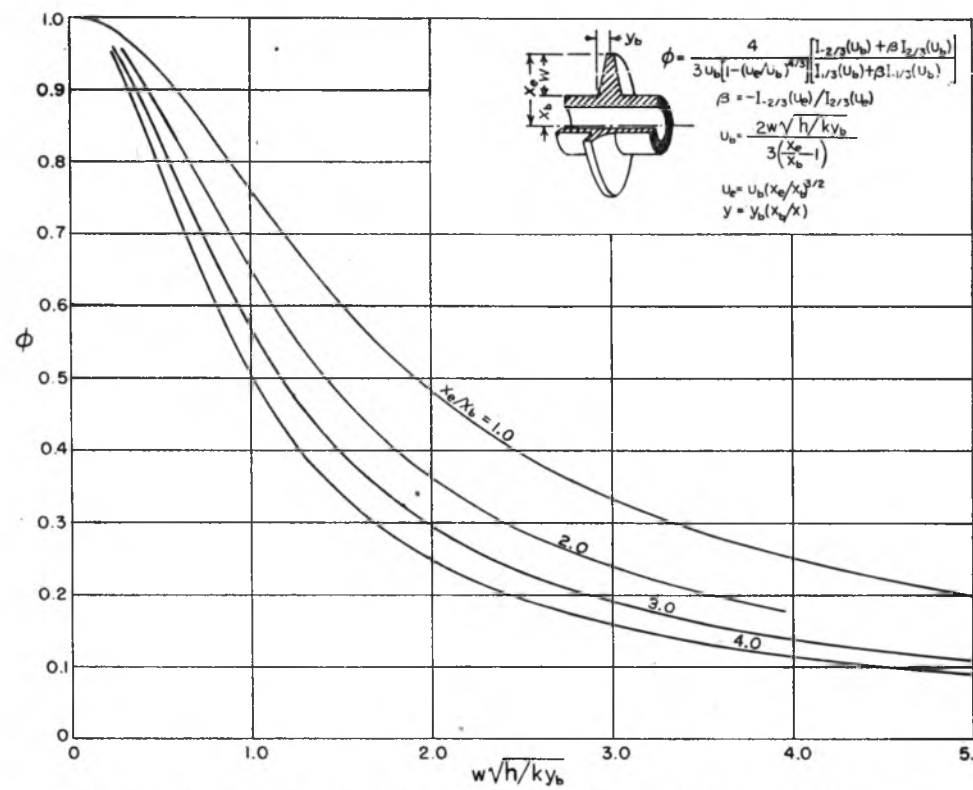

FIG. 6 EFFICIENCY OF ANNULAR FINS WITH CONSTANT METAL AREA FOR HEAT FLOW

Equations and curves are shown in Figs. 5 and 6. The solution is exact for $n = 0$.

Three general classes of extended surface have been investigated thus far; straight fins, spines, and annular fins. Other classes might be discussed but the most practical forms have already been included. It will be noted, however, that no straight fin or spine whose thickness varies as the square of the distance along it, can be described in terms of Bessel functions, since n becomes infinite and u is a constant. This case will now be treated for the sake of completeness and to reproduce the results of Schmidt (4), and Focke (7). Termwise comparison of Equation [1] with Euler's differential equation shows that the cross section and surface may vary thus

$$a = \lambda x^{1-2m} \quad [18]$$

and

$$\frac{dA}{dx} = \mu x^{-(1+2m)} \quad [18a]$$

For the case where $x_e = 0$

$$\theta = \theta_b \left(\frac{x}{x_b}\right)^r \quad [19]$$

and

$$\phi = \frac{2}{1 + \sqrt{1 + (u/m)^2}} \quad [20]$$

where

$$r = m\left[1 - \sqrt{1 + (u/m)^2}\right]$$

In these equations, u has exactly the same definition as before (Equation [7]) but for this special case, is a constant. The requirement of Schmidt (4) that the temperature gradient be linear to use the minimum material is met if r in Equation [19] equals unity, from which

$$u^2 = (1 - 2m) \quad [21]$$

For straight fins, $(1 - 2m) = 2$, and for regular spines, $(1 - 2m) = 4$, both of which correspond to a thickness varying as the square of the distance from the edge (or tip). In each case the least material is required if

$$\frac{hx_b^2}{ky_b} = 2 \quad [22]$$

Generality of Equations

The equations for temperature gradient and fin efficiency derived in this paper are obviously quite general since, by substituting the appropriate value of n, the equations of all previous investigators are readily reproduced. These may be summarized as follows:

$n = 1/2$. This corresponds to the straight fins or spines of constant thickness investigated by Harper and Brown (3), Parsons and Harper (2), Schmidt (4), Focke (7), et al. In the case of spines, the section need not be circular but may be square, triangular, elliptical, or any other shape within the limitations of the assumptions. The same value also describes annular fins whose thickness varies inversely as the square of the distance from the center, although the values of u_b and u_e are not the same as for straight fins or spines. The efficiency is

$$\phi = \frac{\tan h\,(u_b - u_e)}{(u_b - u_e)} \quad [23]$$

where the expressions for u_b and u_e are given in Figs. 3 and 4.

$n = 0$. This yields the equations for wedge-shaped straight fins and annular fins of constant thickness, as derived by Harper and Brown and Schmidt. Furthermore, the same equations apply to spines whose thickness varies as the square root of the distance from a point at or beyond the tip.

$n = -1$. This represents the conical spines investigated by Focke (7). It also covers straight fins whose thickness varies as the $3/2$ power of the distance from a point at or beyond the edge.

With these three values of n all previous expressions for fin efficiency based on assumptions 1 through 10 are reproduced. Furthermore, the general solution makes it possible to recognize the applicability of the equations for one particular type of fin to other types, e.g., only five different types of fin have been shown previously to be covered by these three values of n, yet it has just been shown that at least seven types can be included. Some other types for which special equations have been developed may also be mentioned.

$n = 1/3$. This corresponds to the annular fins with constant metal area for heat flow, for which Carrier and Anderson gave a solution in terms of infinite series (9). It could also represent straight fins whose thickness varies as the square root of x, and spines whose thickness varies as the fifth root of x.

$n = \infty$. This covers the straight fins of Schmidt (4), and the spines of Focke (7), whose thickness varies as the square of the distance from the edge or tip.

In order to bring the abscissas on all graphs to a common basis, the fin height w has been introduced into the various expressions for u_b and u_e by writing

$$w = \pm(x_b - x_e), \text{ or } w = x_b \text{ if } x_e = 0$$

Aside from this no attempt is made to compare one type of extended surface with another. Straight fins with the same height, base thickness, conductivity, and surface coefficient are comparable one with the other, and the same is true of annular fins. This is so because changing the contour of the sides of such fins has a negligible effect on the surface. Therefore, to some extent Fig. 3 gives an indication of the relative merits of various straight fins, and Figs. 5 and 6, of annular fins. Fig. 4, however, should not be considered as anything more than a means for determining fin efficiency, because the surfaces of the different spines are not the same, e.g., the thorn-shaped spine represented by the highest curve has only one third the surface of the cylindrical spine of the same height and base thickness, represented by the lowest curve in Fig. 4.

Acknowledgment

The author wishes to thank Joseph Price, Vice-President in Charge of Engineering, The Griscom-Russell Company, for permission to publish this paper. The co-operation of the Griscom-Russell Company, The Babcock and Wilcox Company, and the Thermek Corporation in furnishing samples of extended-surface tubing, and the assistance of O. W. Heimberger, Assistant Chief Engineer, the Griscom-Russell Company, and A. C. Mueller, Chemical Engineer, Technical Division, Engineering Department, E. I. du Pont de Nemours and Company, Wilmington, Del., in pointing out references to earlier work are also greatly appreciated.

BIBLIOGRAPHY

1 "The Absolute Thermal Conductivities of Iron and Copper," by R. W. Stewart, Philosophical Transactions, Royal Society of London, Eng., vol. 184, series A, 1893, p. 569.

2 "Radiators for Aircraft Engines," by S. R. Parsons and D. R. Harper, U. S. Bureau of Standards, Technical Paper no. 211, 1922, pp. 327–330.

3 "Mathematical Equations for Heat Conduction in the Fins of Air-Cooled Engines," by D. R. Harper and W. B. Brown, National Advisory Committee for Aeronautics, Report no. 158, 1922.

4 "Die Wärmeübertragung durch Rippen," by E. Schmidt, *Zeit. V.D.I.*, vol. 70, 1926, pp. 885–889, and 947–951.

5 "Heat Dissipation Through an Annular Disk or Fin of Uniform Thickness," by W. M. Murray, *Journal of Applied Mechanics*, Trans. A.S.M.E., vol. 60, 1938, p. A-78.

6 "Wärmeübertragung durch Rippenrohre," by H. Hausen, *Zeit. V.D.I.*, Beiheft 2, 1940, pp. 55–57.

7 "Die Nadel als Kühlelemente," by R. Focke, *Forschung auf dem Gebiete des Ingenieurwesens*, vol. 13, 1942, pp. 34–42.

8 "Diffusion of Heat Through a Rectangular Bar and the Cooling and Insulating Effect of Fins, I. "The Steady State," by Melvin Avrami and J. B. Little, *Journal of Applied Physics*, vol. 13, 1942, pp. 255–264.

9 "The Resistance to Heat Flow Through Finned Tubing," by W. H. Carrier and S. W. Anderson, *Heating, Piping and Air Conditioning*, vol. 10, 1944, pp. 304–320.

10 "Heat Exchanger Tube Sheet Temperatures," by K. A. Gardner, *Refiner and Natural Gasoline Manufacturer*, vol. 21, 1942, pp. 71–77.

11 "The Value of Extended Heating Surfaces," by C. S. Sage, *Journal of the American Society of Heating and Ventilating Engineers*, vol. 33, 1927, pp. 707–714, and vol. 34, 1928, pp. 385–388.

12 "Applied Mathematics in Chemical Engineering," by T. K. Sherwood and C. E. Reed, McGraw-Hill Book Company, Inc., New York, N. Y., 1939, p. 211.

13 "A Treatise on Bessel Functions and Their Applications to Physics," by A. Gray, G. B. Mathews, and T. M. MacRobert, Macmillan and Company, London, 1931.

14 "Tables of Functions," by E. Jahnke and F. Emde, B. G. Teubner, Leipzig and Berlin, 1938; also Dover Publications, New York, N. Y.

Appendix 1

Details of Derivation of Equations

The heat flowing through an element of a fin normal to the basic surface (Fig. 2*a*) is given by the Fourier equation

$$q = -ka\frac{d\theta}{dx} \quad \ldots\ldots [24]$$

The heat entering or leaving the sides of the element is

$$-dq = h\theta dA \quad \ldots\ldots [25]$$

By differentiating Equation [24] and substituting the result into Equation [25], dq is eliminated and Equation [1] is obtained.

If the second terms of Equations [1] (after multiplication through by x^2) and [2] are to be identical, then

$$\frac{x^2}{a}\frac{da}{dx} = (1-2m)x - 2\alpha x^2 \quad \ldots\ldots [26]$$

Integration gives

$$\ln a = (1-2m)\ln x - 2\alpha x + \text{const} \quad \ldots\ldots [27]$$

or

$$a = \lambda x^{1-2m}e^{-2\alpha x} \quad \ldots\ldots [27a]$$

From the third terms

$$-\frac{hx^2}{ka}\frac{dA}{dx} = [p^2c^2x^{2p} + \alpha^2x^2 + \alpha(2m-1)x + (m^2 - p^2n^2)] \quad [28]$$

Introducing a from Equation [27*a*] and rearranging

$$\frac{dA}{dx} = -\frac{k}{h}\lambda e^{-2\alpha x}x^{-(1+2m)}[p^2c^2x^{2p} + \alpha^2x^2 + \alpha(2m-1)x + (m^2 - p^2n^2)] \quad [29]$$

Since the surface variation is not a function of k or h, the terms within the brackets must either be zero or inversely proportional to (k/h); α, p, and m occur as exponents so they cannot contain (k/h). Therefore, $\alpha = 0$, and $m = pn$, leaving c^2 as the only constant involving (k/h). Substitution of these results into Equations [27*a*] and [29] gives Equations [3] and [4].

In order to integrate Equation [8] to obtain the fin efficiency, dA must be expressed in terms of u; from Equations [4] and [7]

$$dA = \nu u^{1-2n}du \quad \ldots\ldots [30]$$

where all constants have been collected in ν; then

$$\phi = \frac{\int_{u_e}^{u_b} u^{1-n}[I_n(u) + \beta K_n(u)]du}{u_b{}^n[I_n(u_b) + \beta K_n(u_b)]\int_{u_b}^{u_e} u^{1-2n}\,du} \quad \ldots\ldots [31]$$

Integration of this result to Equation [9] is easily accomplished by reference to the integral formulas of Appendix 2. Similar considerations lead to Equation [9*a*].

Appendix 2

Tables and Properties of Bessel Functions

Derivatives:

$$\frac{d}{du}[u^nI_n(u)] = u^nI_{n-1}(u) \qquad \frac{d}{du}[u^nK_n(u)] = -u^nK_{n-1}(u)$$

$$\frac{d}{du}[u^{-n}I_n(u)] = u^{-n}I_{n+1}(u) \qquad \frac{d}{du}[u^{-n}K_n(u)] = -u^{-n}K_{n+1}(u)$$

$$\frac{d}{du}[I_n(u)] = \frac{n}{u}I_n(u) + I_{n+1}(u) \qquad \frac{d}{du}[K_n(u)] = \frac{n}{u}K_n(u) - K_{n+1}(u)$$

Indefinite Integrals:

$$\int u^{n+1}I_n(u)du = u^{n+1}I_{n+1}(u)$$

$$\int \frac{I_n(u)}{u^{n-1}}\,du = \frac{I_{n-1}(u)}{u^{n-1}}$$

$$\int u^{n+1}K_n(u)du = -u^{n+1}K_{n+1}(u)$$

$$\int \frac{K_n(u)}{u^{n-1}}\,du = -\frac{K_{n-1}(u)}{u^{n-1}}$$

Identities:

$$I_{-n}(u) = I_n(u) \text{ and } K_{-n}(u) = K_n(u) \text{ if } n = \text{an integer}$$

$$\frac{2n}{u}I_n(u) = I_{n-1}(u) - I_{n+1}(u)$$

$$\frac{2n}{u}K_n(u) = K_{n+1}(u) - K_{n-1}(u)$$

$$I_{1/2}(u) = \sqrt{\frac{2}{\pi u}}\sinh u$$

$$I_{-1/2}(u) = \sqrt{\frac{2}{\pi u}}\cosh u$$

$$I_{3/2}(u) = \sqrt{\frac{2}{\pi u}}\left(\cosh u - \frac{\sinh u}{u}\right)$$

$$I_{-3/2}(u) = \sqrt{\frac{2}{\pi u}}\left(\sinh u - \frac{\cosh u}{u}\right)$$

Tables of Bessel functions are given in the Jahnke-Emde "Tables of Functions" (14), and in "Bessel Functions" by Gray, Mathews, and MacRobert (13). The latter is a treatise on the properties and application of Bessel functions; for more elementary discussion sufficient for many engineering purposes, see Sherwood and Reed (12). The nomenclature used in this paper is that used by Gray, et al. (13). If the Jahnke-Emde tables are used, it will be necessary to substitute $i^{-n}J_n(iu)$ for $I_n(u)$, and $i^{-n}H_n^{(1)}(iu)$ for $K_n(u)$ in the various equations of this paper.

Discussion

G. M. Dusinberre.[5] For all fin problems the writer recommends the "relaxation" method of Southwell. This has been outlined by Emmons.[6] There is a great advantage of ease and simplicity as compared with the solutions in Bessel functions, and there need be no sacrifice in accuracy. In fact, there may be a gain in accuracy with thick fins and short cylindrical spines, since it is not necessary to make the author's tenth assumption.

In Fig. 5, for example, if $x_e/x_b = 4$, and $w\sqrt{h/ky} = 1$, a rough calculation gives $\phi = 0.605$, neglecting the edge, and this agrees very well with the curve. But if we take account of the edge, we get $\phi = 0.583$.

This agrees with the author's references, that the error in ϕ due to assumption 10 is not large. But the point is, why introduce an error, however small, for the sake of permitting a certain mathematical treatment, when we can avoid that error by the use of a much simpler mathematical treatment?

An inexperienced person, intending to use the author's curves and noting that the edge area was neglected in computing the efficiency, might assume that this area should consequently be neglected in using the curves to estimate the over-all performance of a proposed design. But the edge area may be a considerable fraction of the lateral area. It would add to the usefulness of the paper if the author would clarify this point in his closure.

Walter Gloyer.[7] Next to the fin efficiency, the correct spacing of fins is of great importance to the designer. Though this is not within the exact scope of the paper, a few words may be said about it here.

If a maximum of heat per unit area of base surface could be transferred just by an increase in extended surface, then fins placed on close centers would be the ideal solution. Fins have to be spaced, however, in such a manner that adjoining fins do not interfere with each other. Fig. 7 of this discussion represents three adjoining straight fins, showing the so-called boundary layers on the center rib as they develop under flow condition, L being the length of a straight rib in the direction of flow or diameter of a circular rib. Before the fluid stream reaches the leading edge of the fin, its velocity is constant over the whole cross section. After entering the fin section at the leading edge, the velocity field is changed, however. The velocity of the fluid is zero at the fin surface and increases within the boundary layer to the full maximum. Blasius[8] investigated the velocity field of the boundary layer theoretically and gives for viscous flow the following equation for the thickness of the boundary layer

$$\delta = 5.83\sqrt{\frac{v \cdot L}{w}}$$

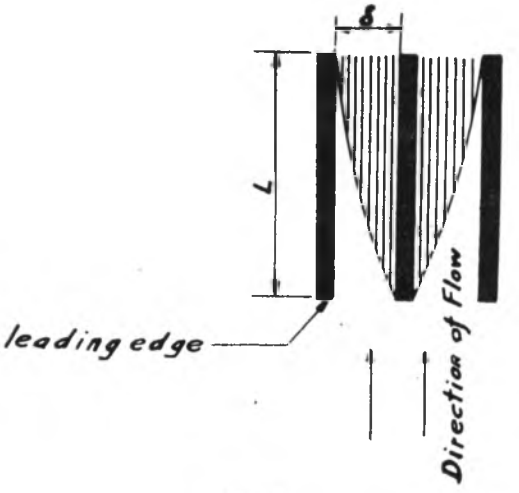

Fig. 7

For turbulent flow von Kármán[9] determined the boundary-layer thickness from theoretical considerations and gives the following equation

$$\delta = 0.37\ L^{4/5}\left(\frac{v}{w}\right)^{1/5}$$

wherein

δ = thickness of boundary layer, cm
v = kinematic viscosity, in stokes, cm² per sec
w = fluid velocity outside boundary layer, cm per sec
L = distance from leading edge, cm

If no interference between adjoining ribs would be allowable at all, the distance between them should be twice the thickness of the boundary layer as calculated from the foregoing equations. To clarify this point, Wagener[10] carried through a series of tests on straight ribs with air as the cooling medium. The ribs were of trapezoidal shape, 20 mm high and 20 cm long in the direction of flow. For the tests, the spacing of the ribs as well as the air velocities were varied. Wagener plotted, as shown in Fig. 8, heat transmitted per unit area, time and degrees temperature differential for various air velocities against the spacing of the ribs.

Each resulting curve shows, at a certain spacing, a maximum which swings with decreasing air velocities to a larger spacing. Using a formula of the von Kármán type, Wagener found the most effective spacing to be about 12 per cent larger than the thickness of the boundary layer. These results show that interference between adjoining ribs is slight in the outer regions of the boundary layer. Using his tests as a basis, Wagener recommends a minimum rib spacing of one boundary-layer thickness.

A series of tests similar to Wagener's was conducted at the Langley Memorial Aeronautical Laboratory by Oscar W. Schey and Herman H. Ellerbrock.[11] These tests were conducted on finned cylinders. All cylinders had a diameter of 4.5 in., and fins which varied in height, thickness and pitch. The tests were run with air as the cooling medium, and the air velocity was varied between 10 and 130 mph. Schey and Ellerbrock observed the same phenomena as Wagener, but presented no explanation.

[5] Department of Mechanical Engineering, Virginia Polytechnic Institute, Blacksburg, Va. Now on duty at U. S. Naval Academy, Annapolis, Md. Mem. A.S.M.E.

[6] "The Numerical Solution of Heat Conduction Problems," by H. W. Emmons, Trans. A.S.M.E., vol. 65, 1943, pp. 607–615.

[7] American Locomotive Company, New York, N. Y.

[8] "Grenzschichten in Flüssigkeiten mit Kleiner Reibung," by H. Blasius, *Zeit. für Mathematik und Physik*, vol. 56, 1908, pp. 1–37.

[9] "Über laminare und turbulente Reibung," by T. von Kármán, *Zeit. für Angew. Mathematik und Mechanik*, vol. 1, 1921, pp. 233–252.

[10] "Der Wärmeuebergang an Kühlrippen," by G. Wagener, *Beihefte zum Gesundheits Ingenieur*, Reihe 1, Heft 24, 1929.

[11] "Blower Cooling of Finned Cylinders," by O. W. Schey and H. H. Ellerbrock, Jr., U. S. National Advisory Committee for Aeronautics, Report no. 587, 1937.

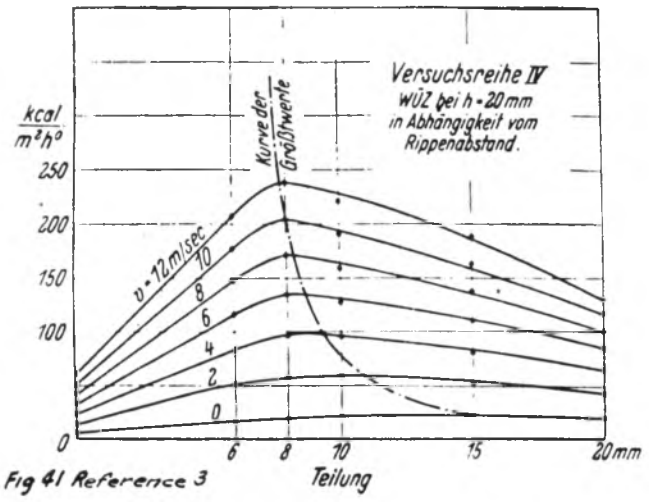

FIG. 8

MAX JAKOB.[12] The author has used an idea of R. D. Douglass to generalize the equations which describe temperature distribution, total heat output, and efficiency of various types of fins. This is presented in such a clear and simple manner as is not often found in the literature on applied mathematics. The paper bristles with Bessel functions; however, an engineer with not more than undergraduate knowledge of calculus and who may never have heard of Bessel functions should be able to operate straightaway with the formulas and one of the tables of Bessel functions referred to in the paper.

According to the outline, contained in the abstract at the beginning of the paper, some forms are excluded from the author's generalization. One of them is the annular fin requiring a minimum of metal, described in E. Schmidt's paper.[13] Using the author's nomenclature, the profile curve of that fin is represented by the equation

$$y = \frac{h}{6k}\left(2x^2 - 3x_e x + \frac{x_e^3}{x}\right)$$

or

$$a = \frac{2\pi h}{3k}\left(2x^3 - 3x_e x^2 + x_e^3\right)$$

which does not satisfy the author's Equation [3].

The differential equations of temperature distribution and heat output of annular fins with triangular or trapezoidal profile do not seem to have been solved exactly as yet, nor are they included in Gardner's generalization, except for the special case where $x \cdot y = \text{const}$.

On the other hand, Gardner's equation covers many cases not dealt with in literature so far. So the generalization in addition to its aesthetic value from a mathematical viewpoint possesses considerable practical value for engineering purposes.

C. F. KAYAN.[14] The excellent treatment of the fin problem by the author leads one to consider comparative methods of analysis by other means. Herein the validity of some of the different assumptions cited by the author and by other workers in this field might be verified, and possibly the effect of a varying heat-transfer coefficient over the fin surface could be studied. It is believed that the use of a geometrical type of electrical analog could uncover some interesting information along this line. The present paper prompts such a study, with one objective being the determination of isotherms under different conditions of fin shape and of boundary conditions.

H. B. NOTTAGE.[15] The author of this paper is to be complimented for having presented an excellent analytical summary of the extended-surface heat-transfer problem which lends itself very neatly to the treatment of different geometrical contours. With the usual idealizations and boundary conditions being invoked, it is significant to note how Bessel's equation may be employed to represent the different cases. For most practical designs, it would commonly be possible to describe the efficiency of representative fin types, which can be manufactured through ordinary procedures, either in terms of some one or another of the solutions presented or through an approximate interpolation.

Certain considerations beyond the simpler cases remain for future study, however, and it may be helpful to offer a few comments based upon recent experience in similar analyses.

The simplification introduced by the assumption that the heat transfer from the outer edge of the fin tip is negligible, which leads to the author's Equations [6] and [6a], is certainly justifiable for most ordinary problems. However, for precise analyses of large fins, such as those employed on air-cooled engine cylinders, this assumption may be undesirable. The tip-effect correction suggested by Harper and Brown[16] is believed to offer a better approximation.

It may further be worthy of mention to point out that F. D. Bennett has obtained a solution to the case of an annular fin of tapered straight-sided form, described by the sectional contour equation

$$y = y_b - \text{const}\ (x - x_b)$$

employing the author's nomenclature.

This was accomplished through attacking the difficult differential equation by Picard's method of successive approximations,[17] which is an iteration procedure. The details here are reasonable but tedious, so that there is probably little to recommend for most practical engineering purposes. Harper and Brown suggest an approximate treatment for this type of fin in terms of a taper correction derived for a straight-base fin, and this seems the best simple expedient.

Finally, it may be well to point out an aspect of the fin-design problem which has been dealt with only by inference in this and other recent papers. Fin systems in which the fins are especially wide, and where the fluid medium passes through the interfin passages for an appreciable length, offer important design problems. In these more extended systems the boundary conditions and analytical concepts become more involved than those given here. Point-to-point considerations of the unit surface conductance h, and of the velocity and temperature fields in the fluid become quite important. Compressible fluids make things still more involved.

The fin efficiency then does not remain the constant quantity at all positions along the fin which might be assumed from an application of the simpler analyses. To aid in appreciating the involved features possible, one might visualize this extension of

[12] Consultant in Heat Research, Armour Research Foundation; Research Professor of Mechanical Engineering, Illinois Institute of Technology, Chicago, Ill.; Nonresident Research Professor of Heat Transfer, Purdue University, Lafayette, Ind. Mem. A.S.M.E.

[13] Reference (4) of author's bibliography.

[14] Assistant Professor, Department of Mechanical Engineering, Columbia University, New York, N. Y. Mem. A.S.M.E.

[15] Project Engineer, Pratt & Whitney Aircraft, East Hartford, Conn. Jun. A.S.M.E.

[16] Reference (3) of author's bibliography.

[17] "The Mathematics of Physics and Chemistry," by H. Margenau and G. M. Murphy, D. Van Nostrand Co., New York, N. Y., 1943, p. 467.

the basic fin problem as a peculiar type of cross-flow heat exchanger, in which a conduction heat stream has replaced one of the fluids. It is believed that analyses of the problems involved in this connection may produce some interesting results, for instance, in the question of a design study to establish fin dimensions for a specified performance.

P. R. TRUMPLER.[18] The use of extended surface in industrial applications is rapidly increasing in scope, and often the economics of a design show great advantages to be gained with large ratios, such as 20 or 30 to 1, of extended to prime surface. Fin efficiency may be a very important factor in such cases.

The problem which the author has solved is idealized, as he has clearly pointed out. In most commercial installations the fin efficiency is 90 per cent or better, and even an appreciable error in determining its value is not serious. It is, however, pertinent to examine the assumptions to find if they are sufficiently close for other applications.

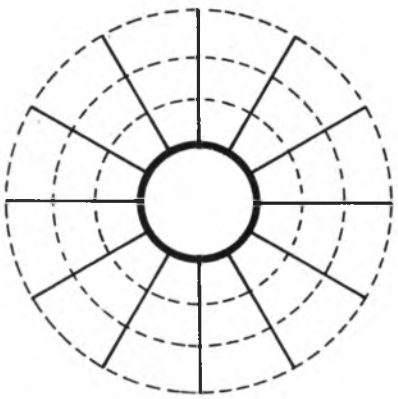

FIG. 9

Let us concern ourselves only with the author's assumptions 6 and 7. With longitudinal or spine fins on tubes, it is apparent that with transfer of sensible heat from a flowing fluid, the longer the fin the wider the variation in film coefficient and the variation in temperature of fluid surrounding the fin. For long fins, however, the efficiency is much more important than for short fins, and it is exactly the condition of long fins that stretches the assumptions.

Next, let us see if the assumptions give a conservative value of fin efficiency in the cases cited. In general, the film coefficient will be less at the base than at the tip of the fin, and the fluid temperature will be closer to the prime-surface temperature near the base than near the tip. The heat load is therefore greater at the tip, and less at the base, than the author's equation would indicate. Thus the calculated fin efficiency is higher than it should be, and we conclude that the calculated values are not conservative.

The possibility of changing assumptions 6 and 7 is not without interest. With much hesitation, the writer proposes a mechanism, as yet untried, to improve the situation for the case of flow parallel to the axis of a finned tube. The flow is channeled into a number of annular spaces separated by membranes as indicated by the dotted lines in Fig. 9 of this discussion. The film coefficients, fluid temperatures, and fin efficiency may be calculated. (The equations for an annulus of differential thickness may be readily set up if the hydraulic diameter is taken as the distance between two adjacent fins at the annular radius.) If the film coefficient at the membranes is taken as infinite, assumption 7 holds. True fluid-temperature conditions exist for membrane-film coefficients which are finite but greater than zero.

The proposed mechanism replaces assumption 6 and permits a conservative assumption in place of 7. It remains to be seen whether the mechanism can be handled mathematically.

In crossflow over finned tube an appreciable variation of film coefficient is to be expected, and the author's values of efficiency must be used with particular care.

With most finned tubes a thermal resistance of appreciable importance is added when the fin is bonded to the tube by pressure contact, solder, or welding. It may be noted that this thermal resistance, often included in the "fin efficiency" of engineering terminology, is not included in the term as used by the author.

[18] Development Engineer, M. W. Kellogg Company, New York, N. Y. Jun. A.S.M.E.

AUTHOR'S CLOSURE

It is gratifying to observe the extent of interest in this particular phase of heat transfer apparent in the comments received. Several points requiring amplification are discussed in the following.

In the preparation of this paper it was necessary, due to space limitations, to eliminate certain sections. Among these was that dealing with heat flow through the fin edge, upon which questions are raised by Mr. Nottage and Commander Dusinberre. Assumption 10 is not at all necessary to the author's treatment in terms of Bessel functions; it merely simplifies the expressions for β, Equations [6] and [6a], without introducing, in most cases, any significant error. The proper statement of boundary condition 2, following Equation [4], is

$$2(a) \text{ when } x = x_e, \frac{d\theta}{dx} = -\frac{h}{k}\theta$$

from which, for n equal to zero or an integer

$$\beta = \frac{I_{n-1}(u_e) + \frac{1}{p}\sqrt{\frac{ha_e}{k(dA/dx)_e}}\, I_n(u_e)}{K_{n-1}(u_e) - \frac{1}{p}\sqrt{\frac{ha_e}{k(dA/dx)_e}}\, K_n(u_e)} \quad \ldots\ldots [32]$$

or for n equal to a fraction

$$\beta = -\left[\frac{I_{n-1}(u_e) + \frac{1}{p}\sqrt{\frac{ha_e}{k(dA/dx)_e}}\, I_n(u_e)}{I_{1-n}(u_e) + \frac{1}{p}\sqrt{\frac{ha_e}{k(dA/dx)_e}}\, I_{-n}(u_e)}\right] \quad \ldots\ldots [32a]$$

The exact expression for ϕ is

$$\phi = \frac{a_e\theta_e + \int_0^{A_f}\theta dA}{(a_e + A_f)\theta_b} \quad \ldots\ldots [33]$$

Harper and Brown suggest that substantially the same result may be obtained by considering the fin to be of height, $w + y_e$, instead of w, and using the simpler equations. The fin surface exclusive of the edge area should be used in conjunction with the fin efficiencies presented in this paper. The gain in accuracy by taking the edge area into account may be illusory, since a fin of such dimensions as to make this area an appreciable fraction of the total will probably also violate assumption 9. Professor Kayan's electrical analog seems the simplest solution for such cases.

The variation of film coefficient and ambient temperature which is ignored by assumptions 6 and 7, is probably most appreciable for single annular fins as pointed out by Mr. Nottage. For flow across banks of annular finned tubes, the temperature change over any one film will be considerably less. Although it is

certainly desirable to know as accurately as possible each of the component parts in the resistance to heat flow through extended surfaces, it should be borne in mind that the *sum* of these resistances (reciprocal heat-transfer coefficients) is the ultimate object. Test data taken to determine film coefficients on extended surface yield an over-all resistance; the outside film resistance sought is obtained by subtracting the other known resistances, among them a metal resistance derived from the fin efficiency. Any error in ϕ due to the assumptions made is therefore reflected in the experimental values of h. However, this resistance $(1/h)$ will ordinarily be used in combination with other different internal film and metal resistances. If the latter are based on the same assumptions as used in the original analysis of the test data, much of the error is canceled out in the sum, so that the net effect on over-all heat-transfer coefficient is not so serious as a casual consideration of the points raised by Nottage and Trumpler might suggest.

The author has not had an opportunity to try either of the suggestions for avoiding assumptions 6 and 7 made by Nottage and Trumpler but will add one further suggestion for consideration. If the film coefficient h can be expressed in certain functions of x or θ, Equation [1] can still be solved in many cases, thus eliminating assumption 6.

The ease and speed with which numerical results may be obtained by Southwell's "relaxation" method as recommended by Commander Dusinberre is certainly impressive; however, its use seems to be limited to the solution of specific numerical problems. The choice between such a solution and an analytical solution appears to be comparable to a machine-shop problem: A certain operation may require one hour setup time for fifteen minutes of actual machining; by spending eight hours on making a suitable jig the setup time may be reduced to ten minutes. If less than ten parts are to be made it will not pay to make the jig; for any greater number it will. The author believes the fin efficiency curves constitute a well-justified jig for the solution of extended-surface problems.

The digest of the literature on fin spacing contained in Mr. Gloyer's comments is a welcome addition to the symposium on extended surface. So also is Dr. Jakob's inclusion of Schmidt's equations for the most economical annular fin.

Dr. Jakob's comment on annular fins with triangular or trapezoidal profile is partially answered in Mr. Nottage's remarks, although the solution obtained is not claimed to be exact. However, the author has been advised by Dr. G. E. Tate[19] that he has obtained an exact solution in terms of Mathieu or allied functions.

[19] Research Physicist, Foster-Wheeler Corporation, New York, N. Y.

Tube Spacing in Finned-Tube Banks

By S. L. JAMESON,[1] SCHENECTADY, N. Y.

One of the methods used to fulfill application requirements in the design of finned-tube gas coolers for industrial use more adequately is to vary the spacing of the tubes. In the past there has been very little information available on the effect of tube spacing on cooler performance. This paper covers the results of a series of tests made to determine the effect of tube spacing on the pressure drop and the heat-transfer coefficient of air flowing across a bank of helically finned tubes. The tests covered a wide range of tube spacings, both at right angles to air flow and between rows in the direction of air flow. All tests were made on staggered tube rows. The tests showed that tube spacing has a marked effect on air pressure drop, but a negligible effect on the air-side heat-transfer coefficient. The number of fins per linear inch of tube had a similar effect. Baffles in the spaces at the ends of short tube rows were found to be beneficial in minimizing edge effects, the improvement in heat transfer gained by their use more than compensating for the increase in air pressure drop.

Nomenclature

THE following nomenclature is used in the paper:

A = air-side tube and fin surface, sq ft per linear ft
B = projected tube perimeter, ft per linear ft
b = spacing between tube rows in direction of air flow, in.
c_p = specific heat at constant pressure, Btu/(lb)(deg F)
d = equivalent diameter of finned tube, ft = $2A/\pi B$
D = equivalent diameter of tube bundle, as defined by Equation [5], ft
f = friction factor = $\Delta P \rho g / 2G^2 N$
g = acceleration due to gravity, ft/hr²
G = mass velocity, lb/(hr)(sq ft) free area in a row of tubes
h = true air-film heat-transfer coefficient, Btu/(hr)(sq ft)(deg F)
H = fin height, ft
j = heat-transfer factor = $(h/c_p G)(c_p \mu/k)^{2/3}$
k = thermal conductivity, Btu/(hr)(sq ft)(deg F)/(ft)
N = cooler depth, rows of tubes in direction of air flow
Δp = pressure drop over tube bank, in. water
ΔP = pressure drop over tube bank, psf
r = diagonal spacing between tubes in successive rows, diameters d
R = Reynolds number
s = tube spacing across cooler face, diameters d
t = fin thickness, ft
U = over-all heat-transfer coefficient, Btu/(hr)(sq ft)(deg F)
V = water velocity in tubes, fps
y = ratio of heat-transfer rate from water to tube at any temperature to that at 90 F average water temperature
ρ = density, lb per cu ft
μ = viscosity, (lb)/(hr)(ft)
σ = spacing between fins, ft
C, n = constants

Test Method

The range of tube diameters and tube spacings tested was made possible by the use of a flexible-duct construction to set up the tube banks. The over-all size of the duct was determined from a study of the capacity of the existing fan and duct equipment, the test banks being made as large as possible in order to make the results more directly applicable to commercial air-cooler design (see Table 1).

TABLE 1 PHYSICAL DATA FOR TUBES AND TEST SECTION

Tubes:					
Diameter of bare tubes, in.	0.625		0.750	1.00	
Fins:					
Number per linear inch	8.7	7.0	9.05	8.8	7.0
Outside diameter, in.	1.121		1.463	1.737	
Thickness, in.	0.010		0.012	0.012	
Height/2 × spacing.	1.133	0.895	1.746	1.751	1.357
Surface, sq ft per ft tube	1.138	0.946	2.049	2.560	2.085
Projected area, sq in./ft tube	8.24	8.14	10.19	13.19	13.01
Projected perimeter, ft/ft tube	10.3	8.67	14.48	14.54	11.98
Equivalent diameter, ft	0.0702	0.0693	0.0901	0.1119	0.1108
Ratio gas to water-side surface	8.25	6.86	12.02	10.85	8.85
Test section:					
Width between side plates, in.			23½		
Length of tubes, in.			24		
Centers first to last tube in long row, in.	22.18		21.80	21.55	
Center outer tube to side of duct, in.	0.66		0.85	0.975	
Height of baffle in short tube rows, in.	0.40		0.44	0.44	
Tubes in long tube row	13 to 19		9 to 15	8 to 12	

The initial setup provided for making isothermal pressure-drop tests only. Three to six pressure-drop measurements were made for each tube-bank arrangement, covering about a 10-to-1 range in air flow. Most of these tests were run at room temperature. A few check tests were made at 120 to 140 F.

When it became apparent that there was considerable variation in air pressure drop with tube spacing, the test duct was altered so water could be circulated through the finned tubes and heat-transfer data obtained.

Air-pressure-drop readings were taken during all heat-transfer test runs. In these tests the air temperature drop over the tube banks varied from 10 to 100 deg F. The average air temperature was taken as the arithmetic-mean water temperature plus the log-mean temperature difference between water and air.

All pressure-drop data were corrected to an average air temperature of 120 F, and a pressure of 14.7 psia. Correction factors for test pressure and temperature were based on constant mass-air velocity, assuming that pressure drop varied as the 1.75 power of air velocity. (An error in the assumed value of this coefficient has no effect on the correction factors for pressure, and a negligible effect on the correction factor for temperature, if the factors are based on mass velocity instead of on linear velocity.) These correction factors are given in Fig. 5. There was no appreciable deviation between the results of the isothermal pressure-drop tests and those of the varying temperature tests on a given tube bank.

Heat-transfer test runs on each tube bank were made at the maximum water velocity through the tubes obtainable for each setup, usually about 4 fps, and at approximately 1 fps for each

[1] Engineer, General Electric Company. Jun. A.S.M.E.

Contributed by the Heat Transfer Division and presented at the Annual Meeting, New York, N. Y., Nov. 27–Dec. 1, 1944, of The American Society of Mechanical Engineers.

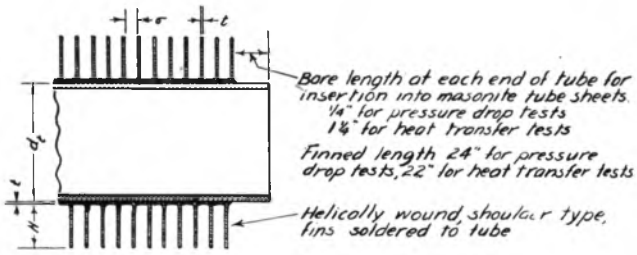

FIG. 1 SKETCH OF FINNED TUBING USED FOR TESTS

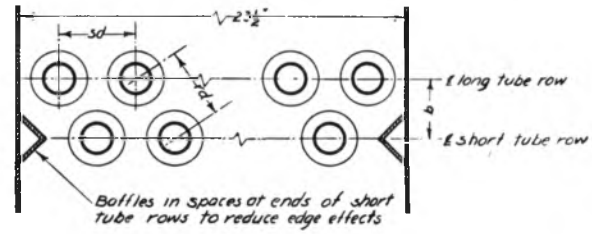

FIG. 2 SKETCH OF TUBE ARRANGEMENT

of at least two different air flows. In several cases check tests were made at about 2-fps water velocity. Special care was taken to hold the mass-air velocity constant for each set of tests at varying water velocities.

The heat-transfer test data were correlated by plotting

$$1/U \text{ versus } 1/yV^{0.8}$$

The temperature drop through the tube wall is negligible and special care was taken to keep the tubes clean, so the zero intercept of this curve is the reciprocal of the effective air-side heat-transfer coefficient. The "effectiveness factor" of the fins is readily calculated for any effective air-side heat-transfer coefficient, and the true air-side heat-transfer coefficient obtained. This correlation takes into account variations in average water temperature. Variation of average air temperature affects the heat-transfer coefficient about 1 per cent for each 25 deg F and was neglected since the average air temperature was maintained within 15 deg F of the 120 F correlating temperature.

TEST EQUIPMENT AND MEASUREMENTS

The tests were made in a duct system especially designed and constructed for air-flow testing. The general arrangement is shown in Fig. 3.

The air-circulating blower was driven by a direct-current motor with a 10:1 speed range. Fine adjustments in air flow could be obtained by adjustment of a damper in the duct ahead of the blower.

Air flow was measured by rounded-approach nozzles of spun aluminum geometrically similar to nozzles calibrated by the Bureau of Standards. In each test enough nozzles were plugged to make the pressure drop over those in use between 0.5 and 1.0 in. of water. The air pressure drop over the nozzles was measured by an Ellison inclined draft gage with 0.01-in. water scale divisions.

The air pressure drop over the test section was measured by an Ellison draft gage, calibrated in 0.01-in. scale divisions for the first inch of water and 0.1-in. divisions for the next 5 in.

The pressure tap in the inlet duct to the test section was a $^1/_{16}$-in. hole in a plate flush with the duct wall 12 in. upstream from the coil face. All other pressure taps were $^1/_4$-in. tubes with $^1/_{32}$-in. holes at intervals over a 4-in. length. These tubes were enclosed in 2 × 2 × 6-in. cages of fine-mesh screen containing a ribbon of screening wound back and forth over the tubes. Tests have shown that this arrangement reads true static pressures, even in the presence of considerable velocities.

Air temperatures were measured with copper-Copnic thermocouples on a thermocouple potentiometer having 1-deg-F scale divisions. The thermocouples and potentiometer were calibrated against laboratory standards and all temperature measurements were corrected for calibration errors. Radiation shields were used on all thermocouples to minimize errors.

The water circulated through the test coil was taken from an overhead tank equipped with an overflow to insure a constant gravity head. Partial recirculation with make-up water from the city mains was used to maintain constant water temperature to the test section.

Water flow was measured by a sharp-edged orifice, calibrated in place by means of a weigh tank. Colored carbon tetrachloride was used for the manometer fluid in order to magnify the deflection.

Water temperatures were measured by precision-type thermometers inserted directly into the flowing water through packed openings. The thermometer wells were located as close to the test coil as possible and the pipe insulated for a distance of 6 in. on either side of the well. The thermometers were marked in 0.1-deg F scale divisions and were calibrated to 0.01 deg F, against laboratory standards.

The test section consisted of a steel framework to support interchangeable fiberboard tube sheets. Fiberboard side sheets were fastened permanently to the frame. The tubes were standard admiralty-metal condenser tubes wound with copper fins.

The first tests were made for pressure drop over the tube bundle only, and for these tests a length of $^1/_4$ in. was left bare of fins at either end of the tube for insertion into the tube sheets. When the program was extended to include heat-transfer studies the test section was modified so the tubes projected through the tube sheets about 1 in., Fig. 1. Special water headers were made up and connected to the tubes by rubber tubing. Connections between successive rows of tubes in the direction of air flow were also made by rubber tubing. Most of the tests were made with one row of tubes per pass for water flow. The inside of the tubes was carefully cleaned before each test.

RESULTS OF TESTS

Since the tests covered by this paper were made primarily to obtain data for use in the design of cooling equipment for industrial machines, all data were corrected to an average air temperature of 120 F and a pressure of 14.7 psia.

Pressure-Drop Tests. The test results showed the pressure drop over a tube bank of two or more rows depth to be directly proportional to the number of rows of tubes depth. The Fanning equation for flow over a tube bank has therefore been set up as

$$\Delta P = 2fG^2N/\rho g \quad [1]$$

In general, the friction factor is a function of Reynolds number

$$f = C_1\mathbf{R}^{n-2} \quad [2]$$

The pressure drop over a tube bank at a specific pressure and temperature may be expressed as

$$\Delta p = 10^{-7}CG^n \text{ in. water} \quad [3]$$

For flow through a pipe, the value of n is about 1.8. The value of n for pressure drop over a tube bundle was found to vary from about 1.7 to 1.9 in these tests, the highest values being obtained with a very wide tube spacing across air flow and closely

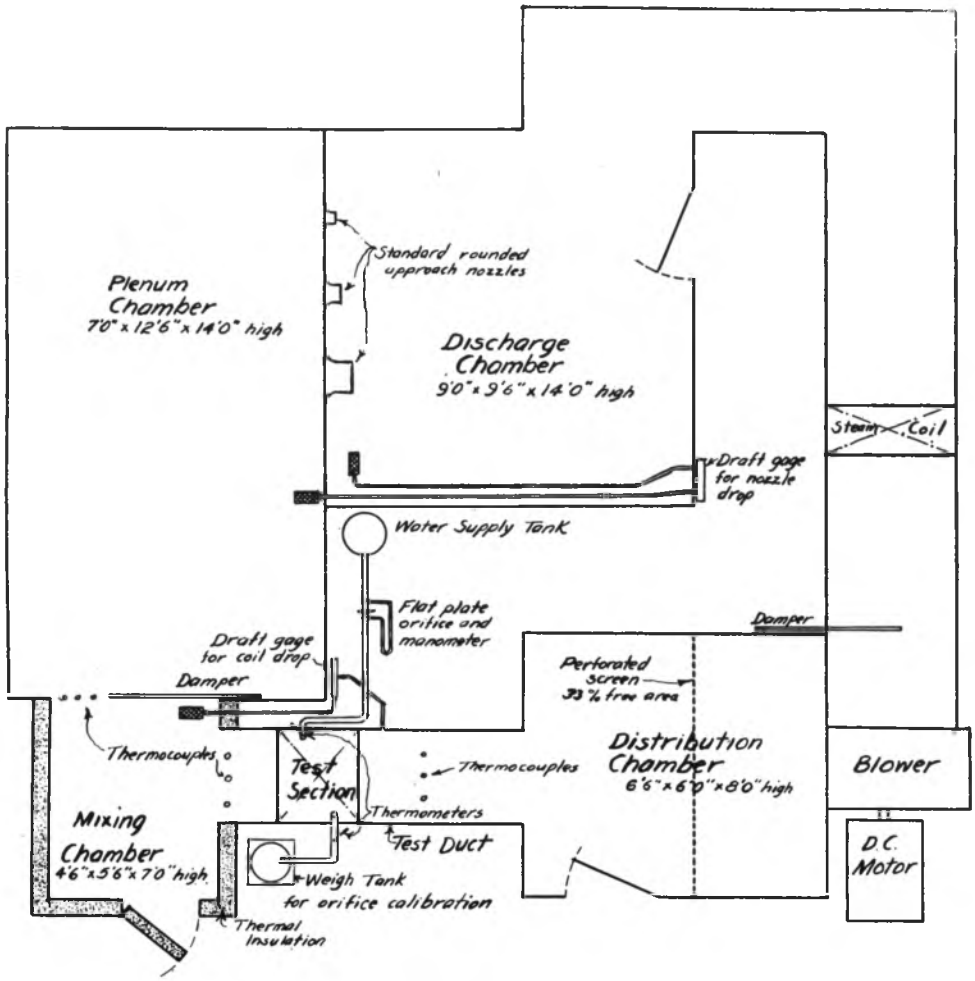

FIG. 3 SKETCH OF TEST DUCT

spaced rows in the direction of air flow. A study of the values of n showed the following:

(*a*) An increase in value as tube spacing across the face of the cooler increased.

(*b*) A minimum value for the spacing between rows at which the free area through the diagonal openings between two successive rows of tubes equaled that in a single row of tubes.

(*c*) A decrease in value as the number of rows of tubes increased.

A possible explanation of these variations is that the pressure drop over a tube bundle is a combination of velocity-head losses, due to the nozzle effect in passing through the minimum spaces between tubes, and frictional losses. The indication from the tests is that the frictional losses would vary as some power of G less than 1.7. The velocity-head loss due to the nozzle effect would vary as the square of G. In the case of close tube spacing, the loss is mostly frictional and the value of n is therefore low. As the tube spacing increases, the frictional component of pressure drop decreases relative to the velocity-head component, and n therefore increases. When the minimum free area through the diagonal openings between two successive rows of tubes equals that in a single row of tubes, the flow path is almost nearly uniform, the velocity head component is a minimum, and the value of n is therefore a minimum.

From the standpoint of obtaining design information and for a general study of the effects of tube spacing it was found convenient to use an average value of n for the various tube arrangements. Equation [3] then becomes

$$\Delta p = 10^{-7} C G^{1.75} \quad [4]$$

The values of C for this approximation and the values of n in Equation [3] are given for the various tube arrangements tested in Table 2.

Using the values of C in Equation [4], the curves in Fig. 4 showing the variation of pressure drop with tube spacing were plotted. The variation in pressure drop with tube spacing across the face is nearly enough independent of the spacing between rows to enable using a single curve for each tube diameter for the correction for tube spacing across the cooler face. The same condition holds for the correction for variation of the spacing between rows in the direction of air flow.

The curves for correction factors for tube spacing given in Fig. 5 are based directly on the curves in Fig. 4. The one exception is the curve for variation in spacing between rows for $^3/_4$-in. tubes. This curve has been drawn more conservatively than would be indicated by Fig. 4, in order better to line up with the curves for $^5/_8$-in. and 1-in. tubes. This may not be completely justified, but from the design standpoint it was felt that any error should be on the conservative side.

The correction factors given in Fig. 5 are adjusted for tube spacing so a single curve of pressure drop versus mass-air velocity may be used for all sizes of finned tubes.

Baffles placed in the spaces at the ends of the short tube rows

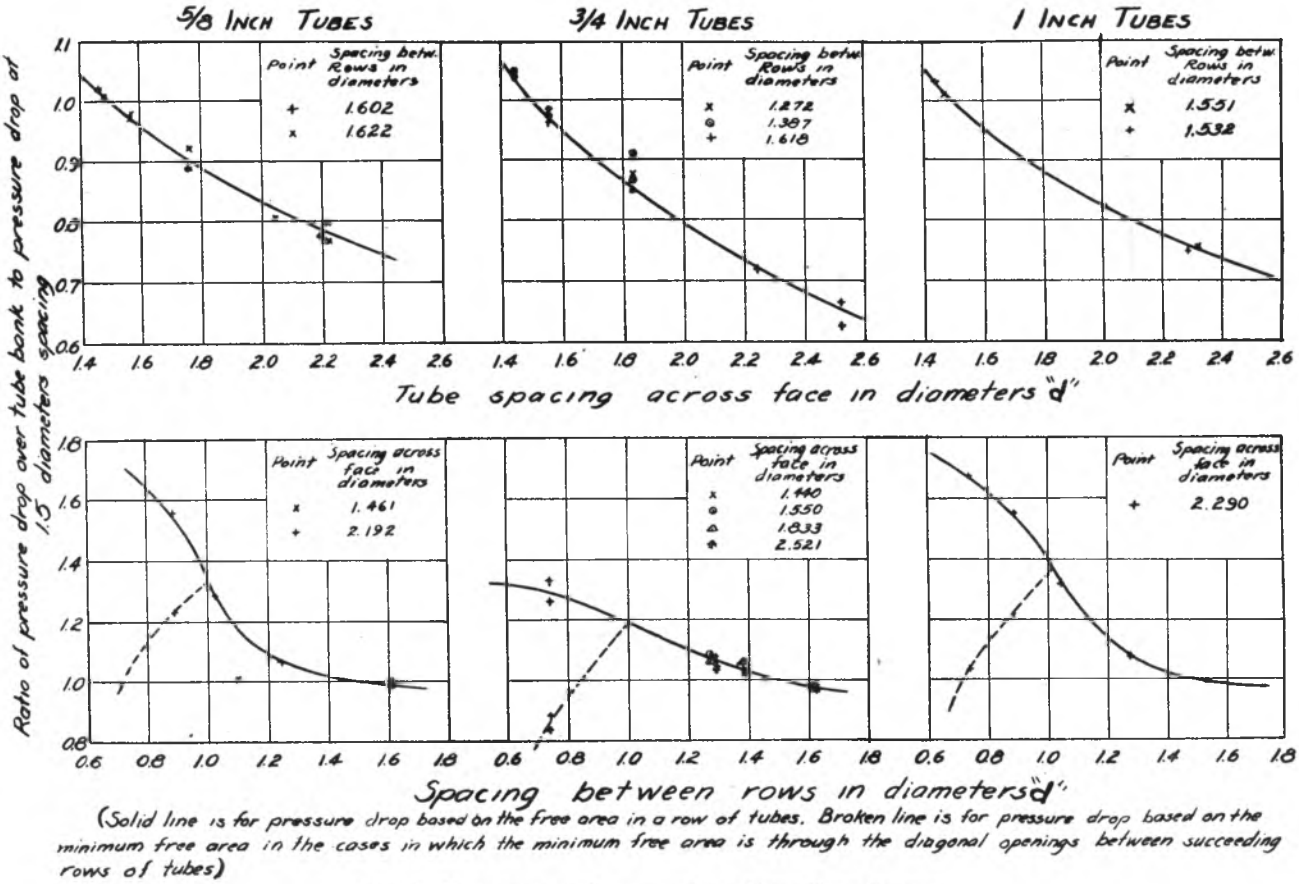

Fig. 4 Variation of Pressure Drop With Tube Spacing

(see Fig. 2, and Table 1) were found to be of considerable value in reducing edge effects, particularly in the case of heat transfer. Check tests showed a baffle made up of an angle with the open side laid against the side of the cooler had the same effect as a half-tube. Since an angle-type baffle is convenient from the standpoint of production, most of the tests were made with angle baffles. The effect of the baffles on pressure drop was found to be about as the 1.75 power of the ratio of the free area in a short tube row to the free area in a long tube row.

The correlation between field tests of coolers installed in machines with the pressure drop calculated by the use of the factors given in Fig. 5 has been very good. The deviation has been less than 5 per cent, even with coolers very narrow across air flow and with closely spaced rows in the direction of air flow.

A relation of the form of the Fanning equation which would correlate the data for all the tube sizes and arrangements tested would be of considerable value in predicting the performance of new finned-tube designs and also in improving present designs. Considerable time was spent trying to obtain such a relation, but without complete success.

The following empirical relation for the "equivalent diameter" of a tube bank correlates the data fairly well for tube banks in which the free area in an individual row of tubes is less than that in the diagonal openings between two successive rows of tubes.

$$D = \frac{d}{\left[\left(\frac{H}{2\sigma}\right)^{0.4}\left(\frac{1}{2\sqrt{s-1}} + \frac{1}{2\sqrt{r-1}}\right)\right]^4} \quad \ldots\ldots [5]$$

Equation [2], using this expression becomes

$$f = 1.532\,\mathbf{R}^{-0.25} \quad \ldots\ldots [6]$$

Equation [4] becomes

$$\Delta p = 9.56 \times 10^{-9} D^{-0.25} N G^{1.75} \text{ in. water} \quad \ldots\ldots [7]$$

(This relation applies only for air at 120 F average temperature and 14.7 psia pressure.)

Although these relations are empirical, they cover the usual range of design and give an indication of the effect of some of the variables on pressure drop. The relations should not be used for Reynolds numbers less than 500 or more than 10,000.

Term f is plotted against $\mathbf{R}$ in Fig. 6 for the highest and lowest test air flows for all tube arrangements tested in which the minimum free area was that in a single row of tubes.

If the test values of f shown in Fig. 6 are approximated by the broken line, this line reflects the increase in the value of n in Equation [3] with tube spacing. An increase in tube spacing increases the "equivalent diameter" of the tube bank, and therefore the Reynolds number.

Fig. 7 shows a comparison between the friction factor for the tube-spacing tests and the friction factors obtained in tests of larger commercial units. Curves d and e cover tests made at pressures up to 15 psig. The comparative data given are for coolers having the free area through the diagonal openings between two successive rows of tubes greater than that in an individual tube row. Test data on a commercial cooler in which the minimum free area was through the diagonal openings between successive tube rows checked that for model tests on a similar spacing closely, but do not line up with the friction-factor curve. Such coolers are definitely outside the range of application of Equations [5], [6], and [7]. The pressure drop over such coolers may be calculated from Fig. 5, however.

Heat-Transfer Tests. There was no apparent variation in the air-side heat-transfer coefficient with tube spacing in any of the tests made with baffles in the spaces at the ends of the short tube rows. The mass-air velocity used for heat-transfer data was based on the free area in a single row of tubes, regardless of the relative magnitude of the free area in the diagonal openings between successive rows of tubes.

Without the baffles in the spaces at the ends of the short tube rows, the apparent air-side heat-transfer coefficient was lower, especially in the case of tubes spaced close together across air flow. In this case the omission of a tube in the short tube row has a slightly greater percentage effect on the free area.

With the baffles omitted the air at the sides of the cooler is only partially cooled. This has been checked several times by thermocouple traverses across the face of a cooler. This partially cooled air has the effect of lowering the apparent heat-transfer coefficient much more than does the decrease in average mass-air velocity due to the increased free area in the short tube rows. The baffles almost completely eliminated these "edge effects."

The improvement in heat transfer gained by the use of baffles in the short tube rows more than compensates for the increase in air pressure drop. In addition, the use of baffles makes the heat-transfer coefficient independent of cooler width and of tube spac-

The standard air pressure drop curve is based on.

1. Air at 14.7 lb/sq in abs. pressure and 120°F average temperature.
2. Staggered tube banks.
3. Baffles in the spaces at the ends of the short rows of tubes.
4. 9 helically wound fins per lineal inch of tube.

Multiply the pressure drop from the standard curve by the factors given below to determine the pressure drop for an individual design.

1. TUBE SPACING

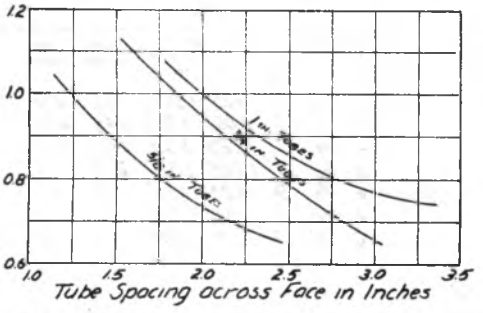

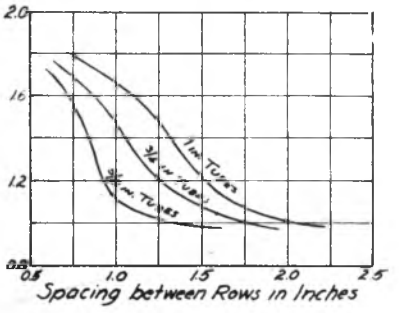

2. AVERAGE AIR TEMPERATURE

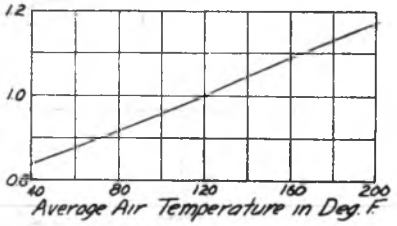

3. AIR PRESSURE

Multiply by 14.7/pressure in lb/sq in. abs.

4. FINS PER LINEAL INCH OF TUBE

Multiply by (Number fins per lineal inch/9)$^{0.4}$

(This is about 4% per fin)

5. OMISSION OF BAFFLES IN SHORT TUBE ROWS.

Multiply by (Free area in long tube row/Free area in short tube row)$^{1.75}$

(This is roughly 0.9 for a 2'6" wide cooler)

NOTES.

1. Correction factors are based on a constant mass air velocity.
2. Use free area in a row of tubes in all cases, even though the free area thru the diagonal openings between successive rows of tubes may be less.

FIG. 5 PRESSURE-DROP CORRECTION FACTORS FOR DESIGN USE
(Air pressure drop over finned-tube banks.)

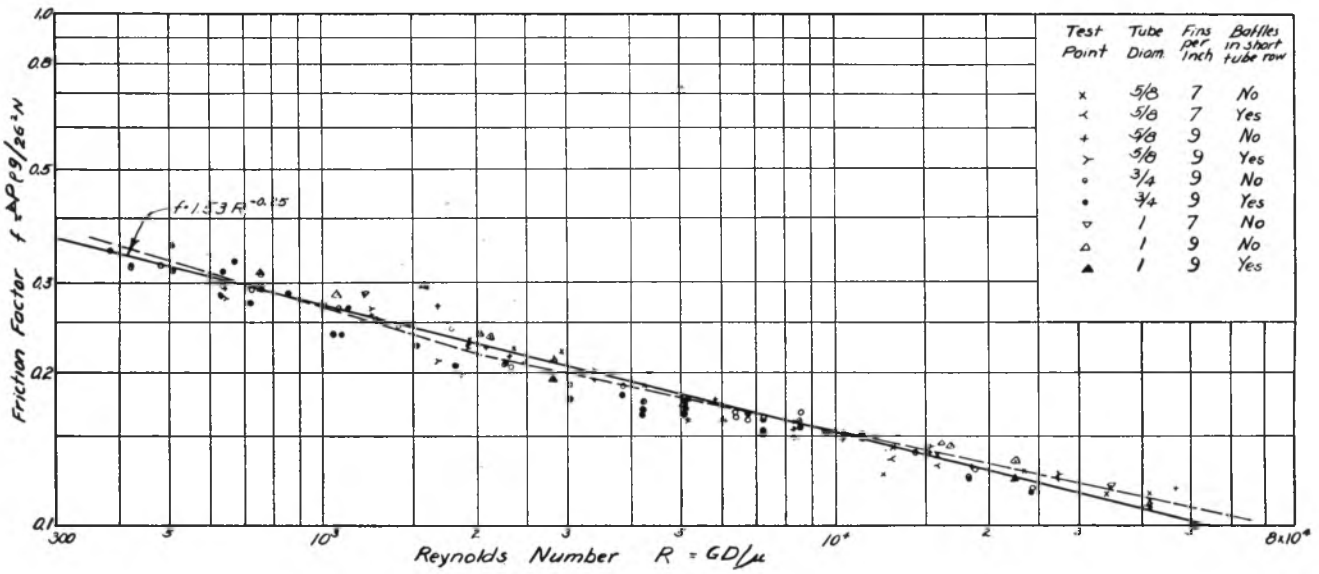

FIG. 6 FRICTION FACTORS FOR TUBE BANKS TESTED
(Points plotted are highest and lowest air-flow test points for each tube arrangement.)

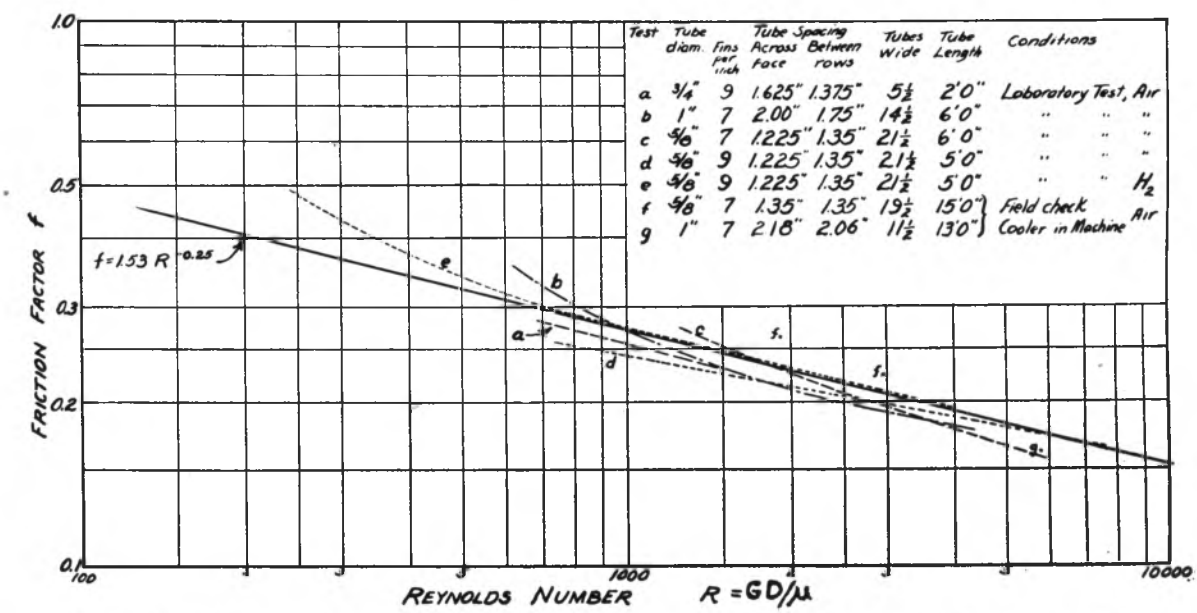

FIG. 7 COMPARISON OF FRICTION FACTOR FROM TUBE-SPACING TESTS WITH TESTS OF COMMERCIAL UNITS

ing. For these reasons baffles are specified for all coolers less than 2 ft in face width and for many wider coolers.

Fig. 8 shows the air-side heat-transfer coefficients obtained for the various tube bundles tested as a function of mass-air velocity.

The dimensionless heat-transfer factor j was plotted against Reynolds number to correlate the tests on various sizes of tubes. The best correlation was obtained using Reynolds number based on the equivalent diameter of an individual tube rather than by using the diameter defined by Equation [5]. The curve of j versus **R** for all tests made with baffles in the short tube rows is given in Fig. 9.

In all cases the average air-side heat-transfer coefficient decreased as the cooler depth decreased. A study of the results indicated that for a cooler of N rows of tubes depth, N-1 rows will have a relative performance of 1.0, and one row will have a relative performance of 0.7. Since most coolers for industrial equipment are more than four rows of tubes deep, the effect of cooler depth on over-all performance may be neglected in design.

A curve showing the heat-transfer factors obtained in tests of a commercial turbine-generator cooler is also given in Fig. 9. The discrepancy between this curve and the results of the tube-spacing tests is in line with previous model tests. For some unexplained reason tests of sample-size coolers usually give a higher air-side heat-transfer coefficient than is obtained in tests of commercial coolers. On the other hand, pressure-drop data usually check closely.

RELATED DATA AND SUGGESTIONS FOR FUTURE TESTS

There are few data available from other sources on the effects of varying tube spacing in finned-tube banks.

Pierson, Huge, and Grimison have reported on a series of tests on the effect of spacing of bare tubes on heat transfer and pressure

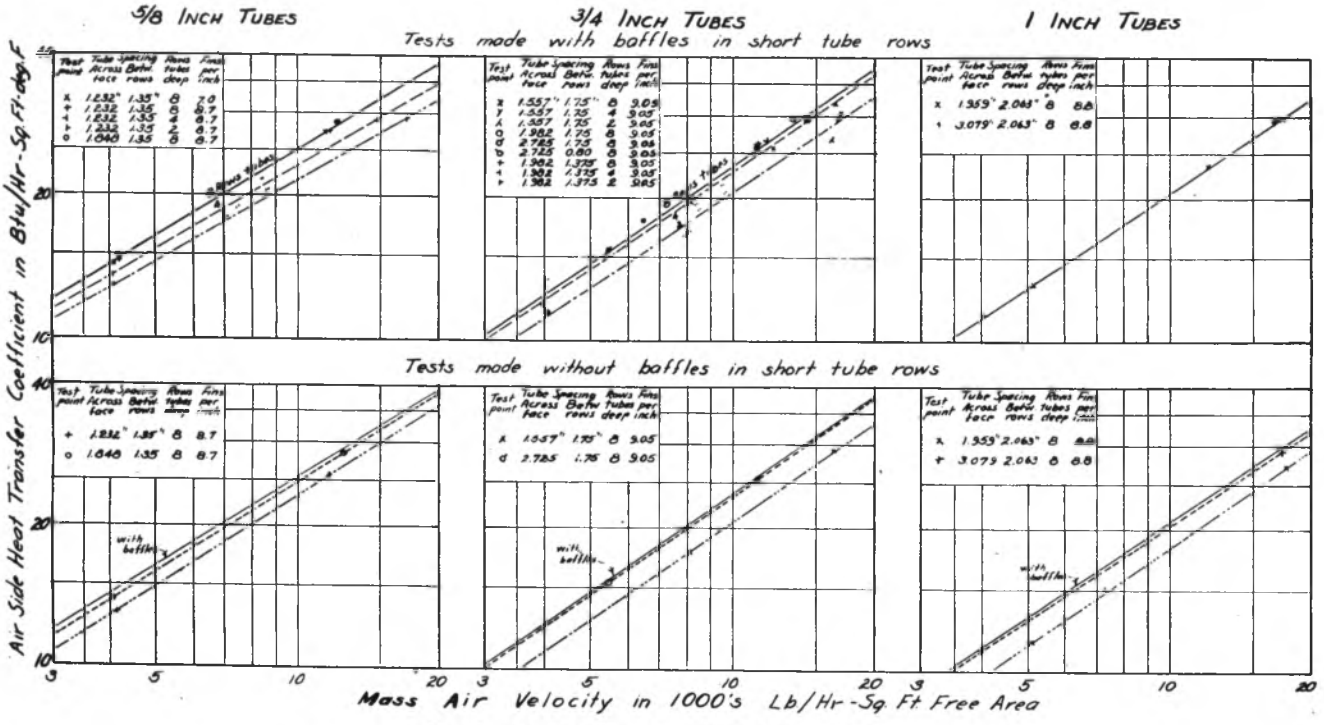

FIG. 8 AIR-SIDE HEAT-TRANSFER COEFFICIENT

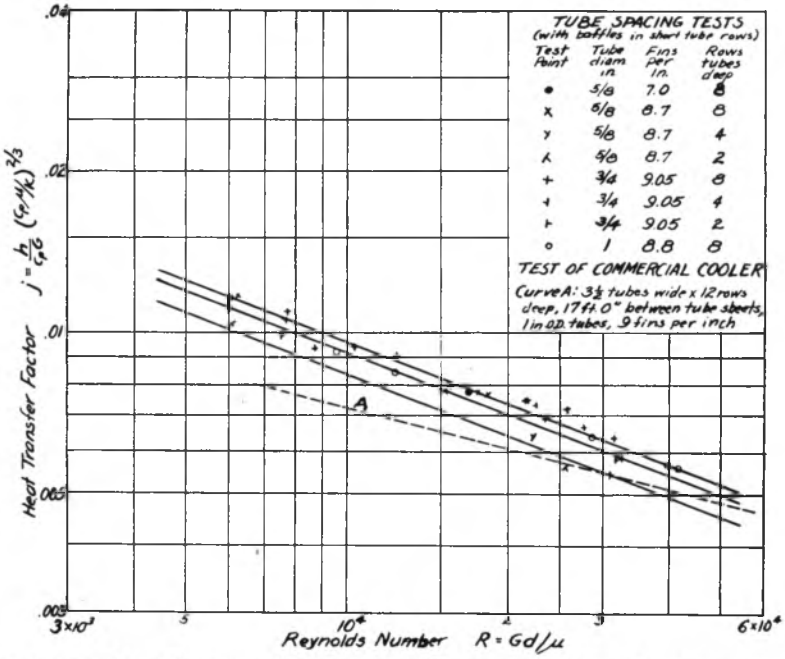

FIG. 9 CORRELATION OF HEAT-TRANSFER TEST DATA FOR TESTS MADE WITH BAFFLES IN SHORT TUBE ROWS

TABLE 2 VALUES OF n IN EQUATION [3], $\Delta p = 10^{-7} CG^n$, AND VALUES OF C IN EQUATION [4], $\Delta p = 10^{-7} CG^{1.75}$

(a) for 5/8 inch O.D. Tube Tests.

Spec. betw. rows, in.	Rows tubes deep	Values of n, $\Delta p = 10^{-7}CG^n$ — Tube spacing across cooler face in inches					Values of C, $\Delta p = 10^{-7}CG^{1.75}$ — Tube spacing across cooler face in inches				
		1.232	1.304	1.478	1.705	1.848	1.232	1.304	1.478	1.705	1.848
7.0 fins per inch											
Without baffles in short tube rows											
1.35	8	1.744	1.749	1.749	1.760	1.779	1.647	1.600	1.522	1.350	1.293
1.35	4					1.835					.653
1.35	2					1.877					.304
With baffles in short tube rows											
1.35	8	1.757	1.758			1.779	1.720	1.674			1.364
8.7 fins per inch											
Without baffles in short tube rows											
0.75	8					1.727*					1.779
0.865	8					1.719					1.864
1.05	8					1.759					1.543
1.063	8	1.719					1.931				
1.35	8	1.726		1.756		1.785	1.809		1.600		1.422
1.35	4	1.740					.905				
1.35	2	1.775					.463				
2.00	8					1.809					1.353
With baffles in short tube rows											
1.063	8	1.739					2.099				
1.35	8	1.736		1.769		1.781	2.094		1.814		1.586
1.35	4	1.790					.917				
1.35	2	1.832					.466				
	1	1.806					.247				

*Minimum free area in diagonal openings between successive tube rows. On frontal plane free area:

0.75	8					1.727					2.254

drop in crossflow over tube banks in a group of three papers.[2] An expression similar to that for the "equivalent diameter" of the tube bank used to correlate the finned-tube-spacing tests was of no value in correlating their data for bare tubes. The finned-tube tests do agree with the data for bare tubes in that the variation of heat transfer with tube spacing was small, but that there was considerable variation in air pressure drop. In both cases the pressure drop at a given mass-air velocity decreased with increase in tube spacing.

On the basis of the results of the tests covered by this paper it is suggested that any future tests on the effects of tube spacing be made with half-tubes or baffles in the spaces at the ends of the short tube rows. This gives much more consistent and more generally applicable data.

A wider range of tube diameters and of the number and height of fins would enable a better determination of the effect of tube-design variables and thereby aid in predicting the performance of new designs.

Discussion

A. Y. Gunter[3] and W. A. Shaw.[4] The author has done an admirable job in the presentation of some usable design data for finned-tube gas coolers.

[2] "Experimental Investigation of Influence of Tube Arrangement on Convection Heat Transfer and Flow Resistance in Crossflow of Gases Over Tube Banks," by O. L. Pierson, Trans. A.S.M.E., vol. 59, 1937, pp. 563–572.

"Experimental Investigation of Effects of Equipment Size on Convection Heat Transfer and Flow Resistance in Crossflow of Gases Over Tube Banks," by E. C. Huge, Trans. A.S.M.E., vol. 59, 1937, pp. 573–581.

"Correlation and Utilization of New Data on Flow Resistance and Heat Transfer for Crossflow of Gases Over Tube Banks," by E. D. Grimison, Trans. A.S.M.E., vol. 59, 1937, pp. 583–594.

[3] Director of Development, Alco Products Division, American Locomotive Company, New York, N. Y. Mem. A.S.M.E.

[4] Heat Transfer Engineer, Research and Development Department, Alco Products Division, American Locomotive Company, New York, N. Y. Jun. A.S.M.E.

TABLE 2 (*Continued*)

(b) for 3/4 inch O.D. Tube Tests.

Spac. betw. rows in.	Rows Tubes deep	Values of n, $\Delta p = 10^{-7} CG^n$					Values of C, $\Delta p = 10^{-7} CG^{1.75}$				
		Tube spacing across cooler face in inches									
		1.557	1.676	1.982	2.422	2.725	1.557	1.676	1.982	2.422	2.725
9.05 fins per inch											
Without baffles in short tube rows											
0.80	8					1.722*					1.155*
0.80	4					1.753*					.632*
0.80	2					1.780*					.304*
1.162	8					1.731					1.668
1.375	8		1.730	1.753				2.013	1.876		
1.400	8					1.754					1.447
1.500	8	1.737	1.754	1.769			2.127	1.988	1.876		
1.750	8	1.676	1.721	1.750	1.775	1.775	2.056	1.896	1.702	1.458	1.356
1.750	4	1.715					1.000				
1.750	2	1.742					0.497				
With baffles in short tube rows											
0.80	8					1.758*					1.323*
1.375	8		1.733	1.771				2.282	2.038		
1.375	4		1.737	1.778				1.098	.969		
1.375	2		1.737	1.775				.533	.481		
1.400	8					1.749					1.600
1.500	8	1.721	1.736	1.745			2.383	2.230	2.013		
1.750	8	1.691	1.710	1.748		1.793	2.396	2.251	1.938		1.434
1.750	4	1.698					1.109				
1.750	2	1.702					.533				
--	1					1.863					.215

*Minimum free area in diagonal openings between successive tube rows.

On frontal plane free area:

0.80	8	Without baffles	1.722	1.742
0.80	4	Without baffles	1.753	.952
0.80	2	Without baffles	1.780	.458
0.80	8	With baffles	1.758	1.997

In a few instances, clarification of certain points seems desirable for a more ready comprehension of the paper:

Under "Nomenclature" in the definitions of r and s, it is suggested that "diameters d" be more specifically stated as being "equivalent diameters, previously defined."

In the tables and in Fig. 2, the "spacing between rows" (shown as b in the figure) should be tied together, with a listing under the nomenclature, to prevent any misinterpretation with rd, the "diagonal spacing."

TABLE 2 (*Continued*)

(c) for 1 inch O.D. Tube Tests.

Spac. betw. rows, in.	Rows tubes deep	Values of n, $\Delta p = 10^{-7} CG^n$				Values of C, $\Delta p = 10^{-7} CG^{1.75}$			
		Tube spacing across cooler face in inches							
		1.959	2.155	2.694	3.079	1.959	2.155	2.694	3.079
7.0 fins per inch									
Without baffles in short tube rows									
2.06	8	1.697			1.750	1.720			1.355
8.8 fins per inch									
Without baffles in short tube rows									
1.00	8				1.725*				1.538*
1.00	4				1.730*				.769*
1.20	8				1.727*				1.805*
1.41	8				1.725				1.948
1.70	8				1.777				1.604
2.06	8	1.717	1.730	1.767	1.781	1.939	1.805	1.601	1.477
With baffles in short tube rows									
2.06	8	1.721			1.781	2.122			1.529
*Minimum free area in diagonal openings between successive tube rows. On frontal plane free area:									
1.00	8				1.725				2.485
1.00	4				1.730				1.243
1.20	8				1.727				2.300

A General Correlation of Friction Factors for Various Types of Surfaces in Crossflow

By A. Y. GUNTER[1] AND W. A. SHAW,[2] NEW YORK, N. Y.

This paper is the elaboration of an unpublished one by the late E. S. Davis and A. Y. Gunter, which was released only to the National Advisory Committee for Aeronautics. The present work, using the friction-factor correlation proposed for bare tubes by Davis and Gunter, demonstrates its merit as a general method for correlating on a single line, pure crossflow friction over both bare and extended surfaces. This result is made possible through the use of an equivalent volumetric hydraulic diameter D_v, in both the Reynolds number and the ordinate, plus configuration ratios of the form $(D_v/S_T)^n$ and $(S_L/S_T)^n$ in the ordinate. Friction factors for bare tubes of diameters from 0.02 in. to 2 in. are included, with transverse and longitudinal pitches ranging from 1.25 to 5 diam. Extended-surface crossflow friction reported on herein covers external round and square cross fins, both meshed and unmeshed, finned cylinders, radiator core-type surface, and one sample of internal wire-mesh fins. It is shown that flat plates and core-type surface with turbulence promoters do not correlate well on the proposed curve.

Nomenclature

The following nomenclature is used in this paper:

D_p, D_t = pipe or tube diameter, ft (except as noted in tables)
D_v = volumetric hydraulic diameter = $\frac{4 \times \text{Net free volume}}{\text{Friction surface}}$, ft
$f'/2$ = half friction factor corrected by viscosity ratio $(\mu/\mu_w)^{0.14}$, dimensionless
$f''/2$ = half friction factor corrected by viscosity ratio $(\mu/\mu_w)^{0.14}$ and $(D_t/S_T)^{0.4}$, dimensionless
$f/2$ = half friction factor corrected by viscosity ratio $(\mu/\mu_w)^{0.14}$, $(D_v/S_T)^{0.4}$, and $(S_L/S_T)^{0.6}$, dimensionless
g = acceleration of gravity = 4.18×10^8 ft/hr per hr
G = fluid mass velocity (based on minimum net free area), psf per hr
L = fluid flow length, ft
n = denotes exponent
ΔP = pressure drop due to "friction," psf
S_L = longitudinal pitch = center-to-center distance from tube in one row to nearest tube in next transverse row
S_T = transverse pitch = center-to-center distance from tube to tube in one transverse row
I = in-line tube arrangement (used in tables)
S = staggered tube arrangement (used in tables)
ϕ = denotes function
μ = absolute viscosity at average main stream temperature, lb per ft per hr
μ_w = absolute viscosity at surface wall temperature, lb per ft per hr
ρ = fluid density, pcf
$(D_v/S_T)^n$, $(S_L/S_T)^n$ = configuration correction factors, dimensionless
$(\mu/\mu_w)^{0.14}$ = viscosity-ratio correction factor (Sieder and Tate), dimensionless

Introduction

Up to the present time, correlations of friction factors for pure crossflow over bare tubes have been based on the use of a hydraulic diameter (D_p or D_t), representing the pipe or tube outside diameter in the conventional Reynolds number, i.e., Colburn (1),[3] Short (2), Bowman (3), Huge (4), Grimison (5), and others; or some form of equivalent diameter based on perimeter for other types of surfaces, e.g., Norris and Spofford (6).

Sieder and Scott (7) suggested an equivalent hydraulic diameter (D_v), but did not make a usable general correlation. Davis and Gunter (8), in an unpublished paper presented to the N.A.C.A., gave correlations for both heat transfer and pressure drop in crossflow over bare-tube banks. These correlations used D_v in the Reynolds number and in the conventional ordinate, plus correction factors for tube arrangement of the form $(D_v/S_T)^n$ and $(S_L/S_T)^n$.

As far as is known, no one has satisfactorily obtained correlation of bare tubes and conventional extended surface in pure crossflow on one line. Many investigators have taken a limited range and obtained curves describing the results therefrom. It was felt that one curve covering a wide range would be of benefit to all.

The present paper, following the lead of Davis and Gunter (8), proposes a general correlation covering both bare and extended surfaces using the correction factors mentioned. This presumes that fins are relatively smooth, and rows of tubes are three or more in depth in conventional arrangements. In addition, crossflow friction on one arrangement of internal fins is shown to correlate in good agreement on the proposed curve.

It should be pointed out that the following discussions do not take into account baffle effects, and for practical use, these factors should be allowed for, where applicable.

General Discussion

In the Davis and Gunter paper (8), it was pointed out that most investigators have found that the classic form of the general Fanning equation for flow inside tubes could be adapted to crossflow outside of bare tubes, using tube outside diameter as hydraulic diameter (D_t). Others used perimeter-type hydraulic

[1] Director of Development, Alco Products Division, American Locomotive Company. Mem. A.S.M.E.

[2] Heat Transfer Engineer, Research and Development, Alco Products Division, American Locomotive Company. Jun. A.S.M.E.

Contributed by the Heat Transfer Division and presented at the Annual Meeting, New York, N. Y., Nov. 27–Dec. 1, 1944, of THE AMERICAN SOCIETY OF MECHANICAL ENGINEERS.

[3] Numbers in parentheses refer to the Bibliography at the end of the paper.

diameter for special surfaces. However, these efforts resulted in having a number of friction-factor curves to cover the various tube sizes and arrangements, Fig. 1. The reference paper further demonstrated that a single curve correlation could be made if certain configuration correction factors for the tube bank be included.

It was found necessary to employ three characteristic dimensions in order to determine completely a particular configuration. This meant therefore the introduction of two dimensionless ratios into any correlation involving the form of the general Fanning equation, in order to produce a complete correlation.

It was debated whether a bank might be completely determined by three dimensions in a conventional shell-and-tube exchanger because of the presence of the shell. This, however, was deemed not true because essentially the shell only ends the bank and should be considered only a quantity determining the mass velocity at any point across the bank.

The problem then was to select three characteristic dimensions which would give a consistent correlation of all data. The tube diameter and the pitch both transversely and longitudinally were one possibility for the three configuration dimensions. However, the original work showed that a much more satisfactory correlation could be obtained if the volumetric hydraulic diameter and the longitudinal and transverse pitches be used. The next step was to decide which of these three characteristic dimensions should be employed in the Reynolds number, and which other two should appear solely in the configuration ratios.

Inasmuch as most authors have found it satisfactory to use diameter in the Reynolds number for any particular tube arrangement, it seemed desirable to use volumetric hydraulic diameter in the Reynolds number and to allow the transverse pitch and longitudinal pitch to appear only in the correction ratios. This was later found to be justified by the excellent correlations which were obtained on this basis.

It has been customary for most authors to measure longitudinal pitch as the perpendicular distance from one row of tubes to the next row in the direction of longitudinal flow. However, in order to obtain a correlation which would present data for both staggered and unstaggered tube arrangements on the same line, it was necessary to define the longitudinal pitch as the center-to-center distance from a tube in one row to the nearest tube in the next row transverse to flow.

For equilateral arrangements both in-line and staggered, there is no difference in the configuration definitions and the $(S_L/S_T)^n$ correction factor becomes unity, disappearing from the equation. However, for nonequilateral arrangements, there is a varying degree of difference, depending on whether the layout is rectangular or isosceles. This is illustrated in Fig. 6.

Much uncertainty has existed in the past concerning whether the $f/2$ values vary as a fixed or variable power of the Reynolds number. The present correlation proposed in this paper does not exhibit this variation to any marked degree and the authors have used straight lines as tangents to a short curve in the transition region. The reason for this is the new Reynolds number against which the data were correlated, and the configuration ratios that were introduced.

Various mean temperatures have been employed by authors in evaluating the properties of the fluid flowing over the banks. The possibilities include the use of a film temperature, an average of the wall and main-stream temperature, the average main-stream temperature, or some intermediate combination of these. There are many arguments in favor of the various possibilities. However, the best proof of validity is the experimental data agreement in the final correlation. For this purpose, in this paper the average main-stream temperature has been used, and a correction for the tube-wall temperature is obtained by using the well-known Sieder and Tate (9) viscosity correction, μ/μ_w. This method appears to give the best correlation and has been well substantiated by checking data on heavy fuel oils and various other petroleum products both for heating and cooling.

The ranges of variables covered in this paper are as follows:

Tube diameter, in.	0.02 to 2
Reynolds number $(D_v G/u)$	0.01 to 300,000
μ/μ_w	0.015 to 8
Transverse pitch, diam	1.25 to 5
Longitudinal pitch, diam	1.25 to 5

Correlation

The proposed equation for pressure drop in crossflow over both bare and extended-surface tubes is

$$\frac{f}{2} = \frac{\Delta P g D_v \rho}{G^2 L}\left(\frac{\mu}{\mu_w}\right)^{0.14}\left(\frac{D_v}{S_T}\right)^{-0.4}\left(\frac{S_L}{S_T}\right)^{-0.6} = \phi(\mathbf{R})$$

For the viscous range, the function of the Reynolds number is $f/2 = 90\,(\mathbf{R})^{-1}$ and in the turbulent region, $f/2 = 0.96\,(\mathbf{R})^{-0.145}$.

The transition point from laminar to turbulent flow occurs at a Reynolds number of about 200, although there is a slight curvature with the main straight lines being tangent thereto.

From inspection of the five major curves, Figs. 1 to 5, inclusive, the relative significance of the new correlation will be immediately evident. Fig. 1 shows an attempted correlation using D_t instead of D_v without the correction factors that are proposed in this paper. This figure shows definitely that such a single-line correlation is impossible.

Fig. 2 shows an attempted correlation using D_v in the Reynolds number and ordinate without the two configuration-ratio correction factors. It will be noted again that this correlation is not satisfactory, although better than Fig. 1. However, it shows the merit of using D_v.

Fig. 3 uses D_v in the Reynolds number and in the ordinate, plus one correction factor, namely, $(D_v/S_T)^n$. This is again better than the first two, but still does not take care of wide pitches, especially in the isosceles or rectangular arrangements.

Fig. 4 uses D_v in the Reynolds number and both of the correction ratios in the ordinate. It will be noted that all of the various tube arrangements now fall on a satisfactory single plot.

Fig. 5 shows extended-surface data correlated on the proposed curve which show surprising agreement.

Friction-factor data are shown in Tables 1 and 2.

Bare Tubes

The extensive data of Sieder and Scott (7) available for pressure drop have been used to establish the viscous and part of the turbulent regions. The power of the μ/μ_w ratio is 0.14 in both the viscous and turbulent regions, unlike flow inside tubes. This correction is included in all plots, Figs. 1 to 5, inclusive.

Norris' (6) data on small wires correlate well on the proposed line. This is encouraging, as it establishes the validity of the equation down to a very low value of tube diameter. Huge's (4) data for pressure drop also correlate satisfactorily.

Inasmuch as within the possible range of variation in this case, the average temperature is not of too great importance in pressure-drop calculations, especially on air, it was possible to use the data of Pierson (10) on 38 different arrangements covering transverse- and longitudinal-pitch arrangements from 1.25 to 3 diam, transverse and longitudinal, both staggered and unstaggered. These 38 arrangements provide an excellent basis for the foregoing correlation.

R. P. Wallis (11) has published extensive friction data on two arrangements. The data have apparently been obtained with a very high degree of accuracy. They substantiate the proposed equation quite exactly.

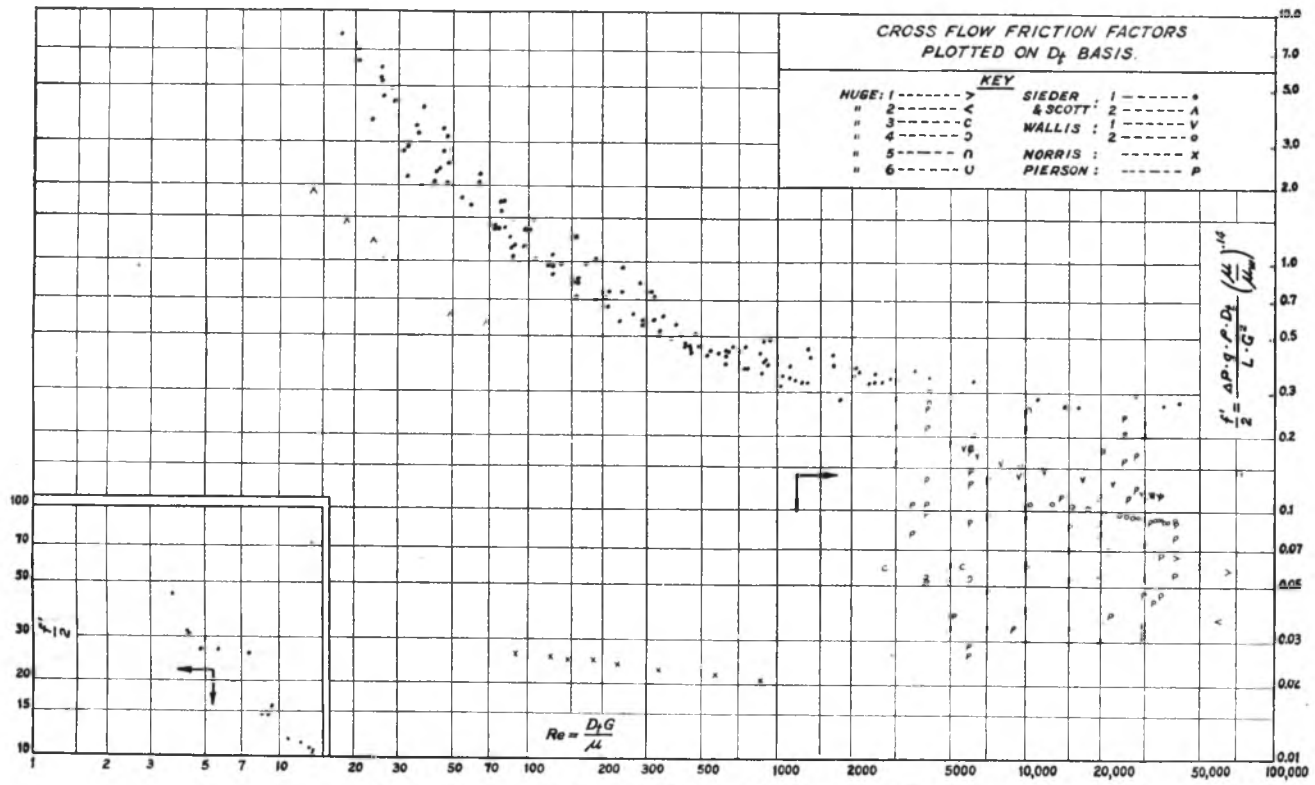

FIG. 1 CROSSFLOW FRICTION FACTORS PLOTTED ON D_t BASIS

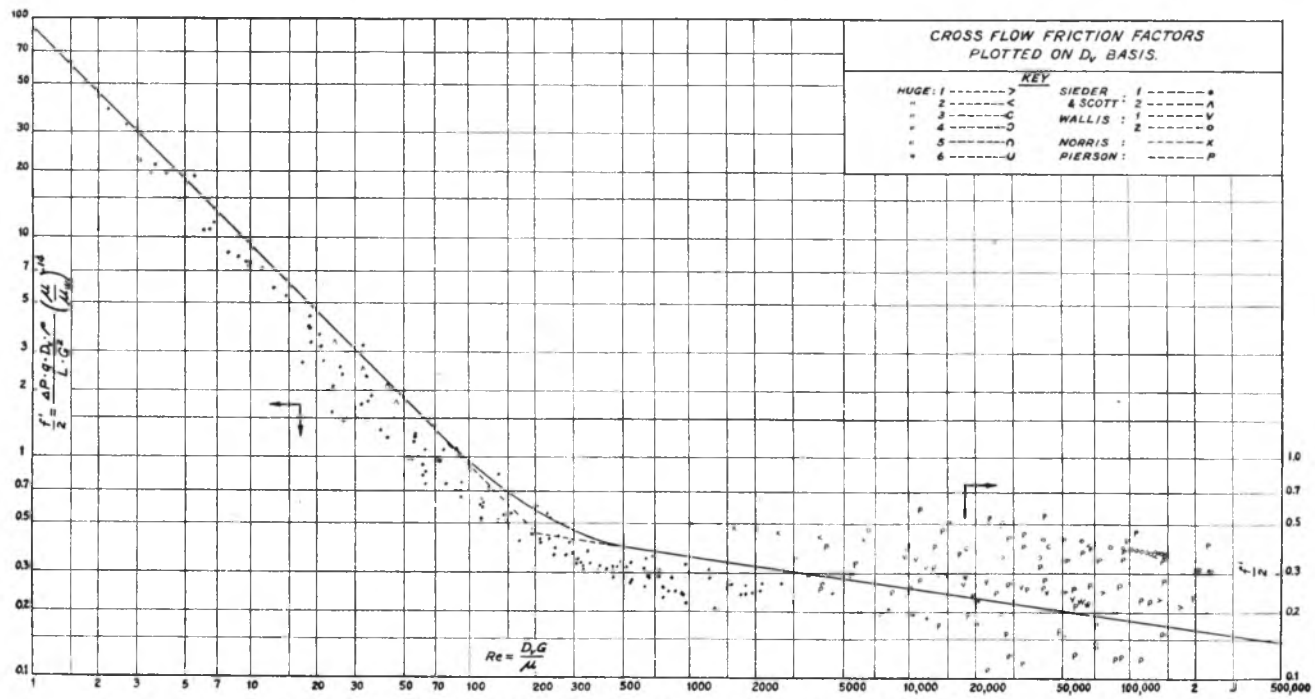

FIG. 2 CROSSFLOW FRICTION FACTORS PLOTTED ON D_r BASIS

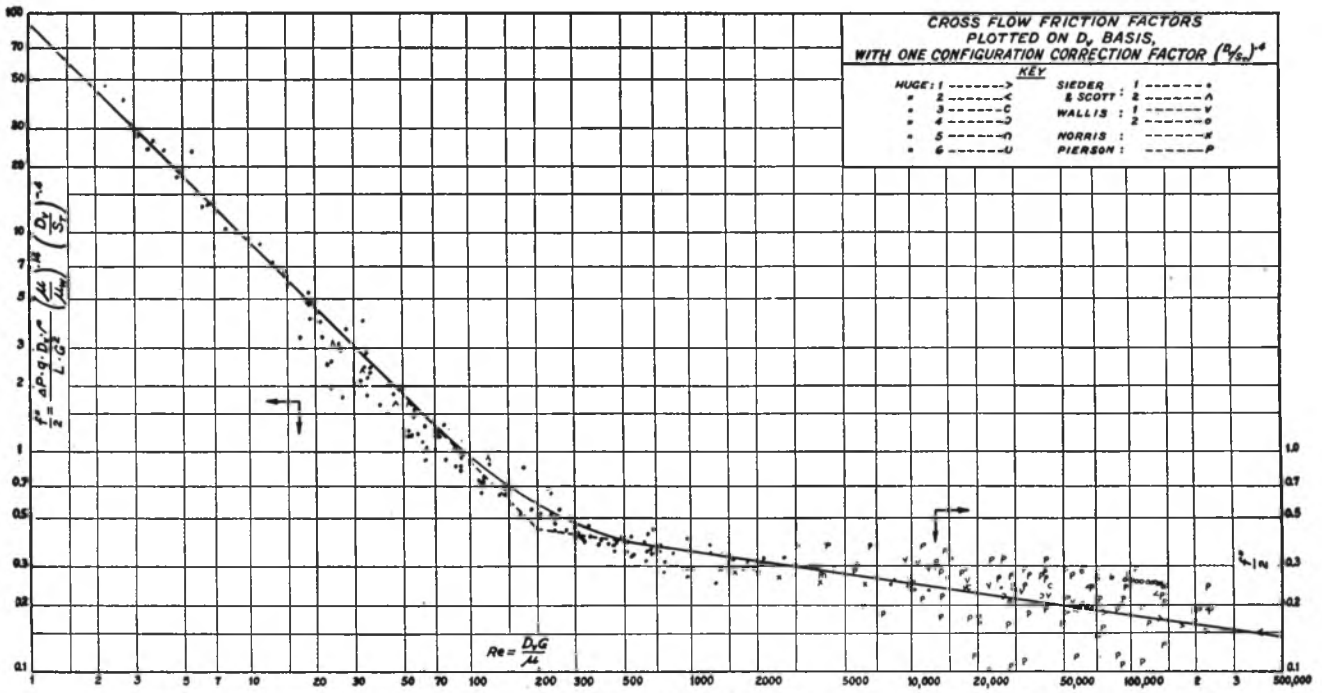

FIG. 3 CROSSFLOW FRICTION FACTORS PLOTTED ON D_v BASIS WITH ONE CONFIGURATION CORRECTION FACTOR, $(D_v/S_T)^{0.4}$

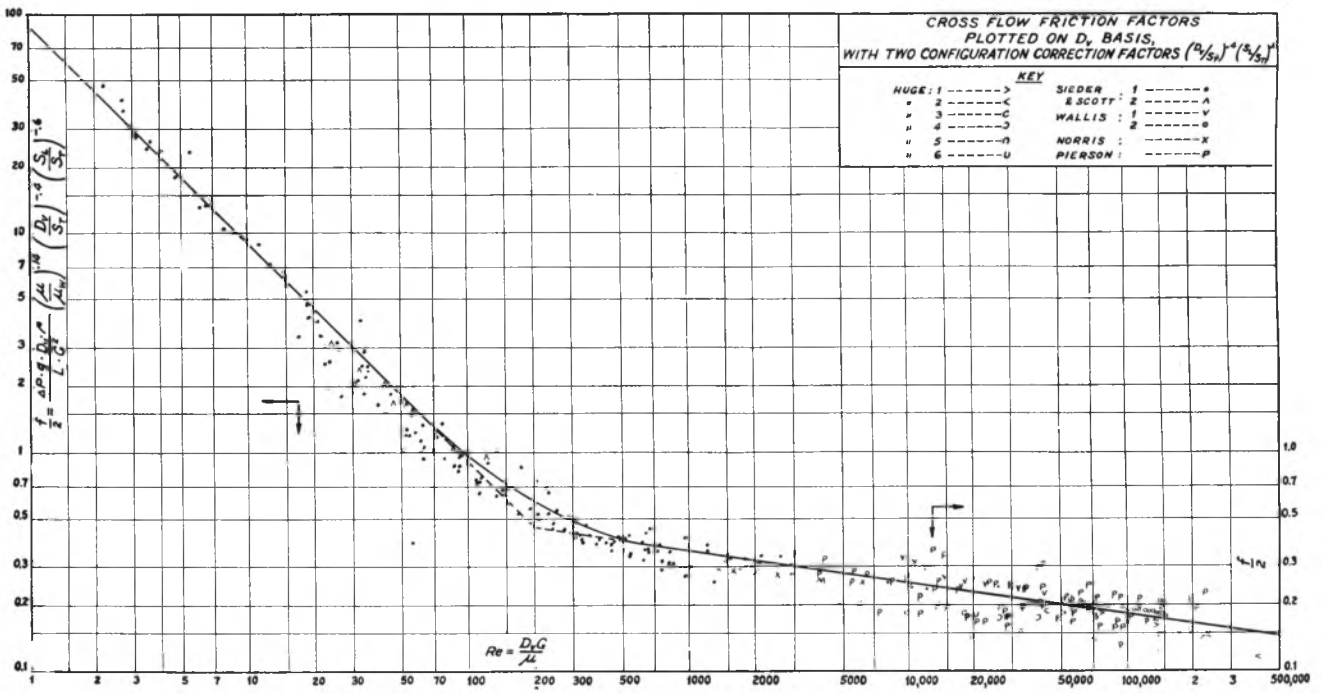

FIG. 4 CROSSFLOW FRICTION FACTORS PLOTTED ON D_v BASIS WITH TWO CONFIGURATION FACTORS, $(D_v/S_T)^{0.4}$, $(S_L/S_T)^{0.6}$

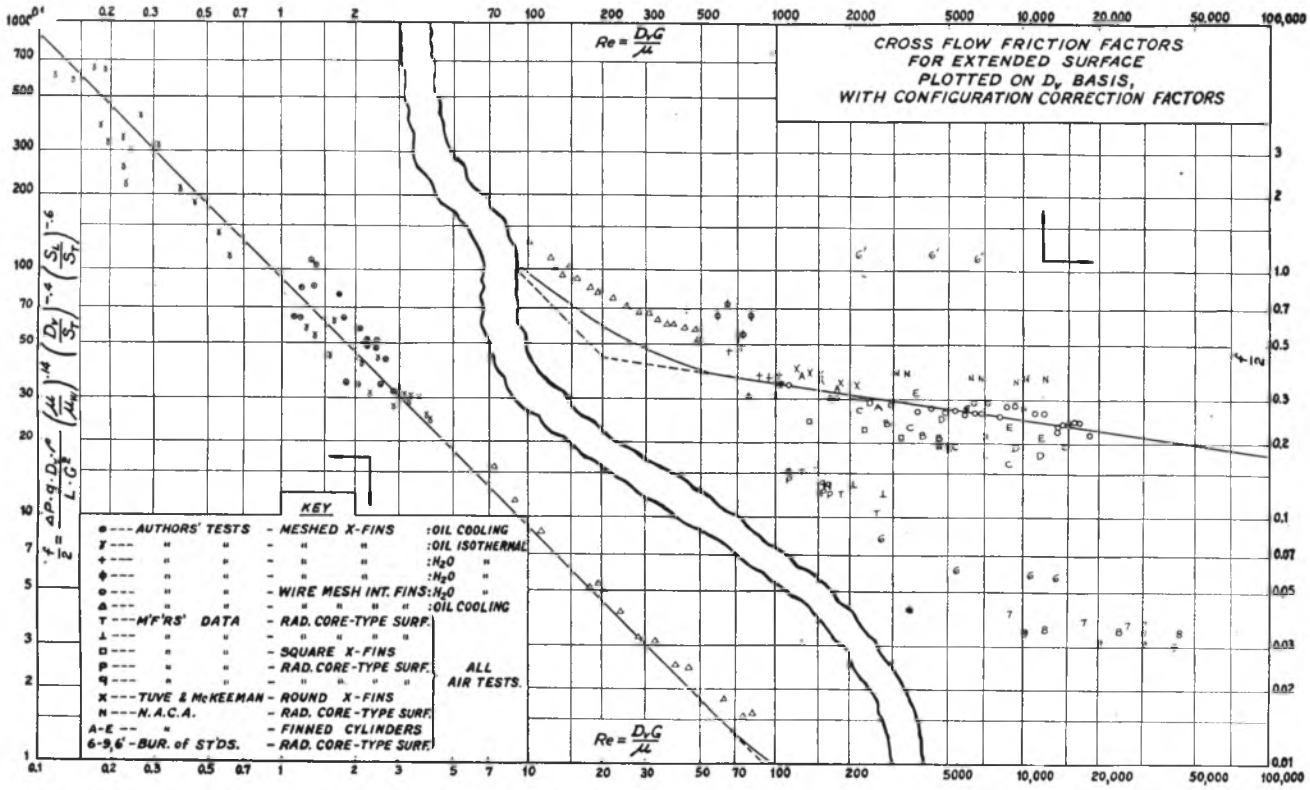

FIG. 5 CROSSFLOW FRICTION FACTORS FOR EXTENDED SURFACE PLOTTED ON D_v BASIS WITH CONFIGURATION CORRECTION FACTORS

TABLE 1 CROSSFLOW FRICTION-FACTOR DATA; BARE TUBES

No.	Arrangement	Source and Material	D_t in.	Basis D_t: Re	Basis D_t: f'/2	D_v ft.	S_L in.	S_T in.	$(D_v/S_T).4$	$(S_L/S_T).6$	Basis D_v: Re	Basis D_v: f'/2	Basis D_v: f"/2	f/2
1	I	Norris	.02	90.3	.0258	.0193	.0625	.0625	1.68	1.0	1,040.	.499	.297	Same
2			or	124.	.0252	or	or	or	-	-	1,385.	.488	.29	as
3		AIR	.04	144.	.0246	.0384	.125	.125	-	-	1,600.	.477	.284	f"/2
4			or	184.	.0244	or	or	or	-	-	2,040.	.472	.281	
5			.125	230.	.0235	.115	.375	.375	-	-	2,550.	.455	.271	
6				339.	.0224				-	-	3,930.	.434	.258	
7				567.	.0217				-	-	6,280.	.42	.25	
8				870.	.0206				-	-	10,000.	.398	.237	
9	I	Wallis	.5	37,200.	.0915	.167	1.3	.755	1.48	1.38	149,000.	.366	.247	.179
10				35,900.	.092	-	-	-	-	-	148,000.	.368	.248	.18
11		AIR		35,350.	.0925	-	-	-	-	-	141,000.	.37	.25	.181
12				34,330.	.0927	-	-	-	-	-	137,000.	.371	.251	.182
13				32,950.	.0935	-	-	-	-	-	132,000.	.374	.253	.183
14				31,600.	.093	-	-	-	-	-	127,000.	.372	.252	.183
15				30,100.	.0945	-	-	-	-	-	121,000.	.378	.256	.186
16				28,500.	.095	-	-	-	-	-	114,000.	.38	.257	.186
17				27,050.	.0955	-	-	-	-	-	108,000.	.382	.258	.187
18				25,530.	.0962	-	-	-	-	-	102,000.	.385	.26	.188
19				23,830.	.0972	-	-	-	-	-	95,500.	.389	.263	.191
20				20,650.	.0994	-	-	-	-	-	82,500.	.398	.269	.195
21				17,740.	.103	-	-	-	-	-	71,000.	.412	.278	.202
22				15,250.	.106	-	-	-	-	-	61,000.	.423	.286	.207
23				12,750.	.1075	-	-	-	-	-	51,000.	.43	.29	.21
24				10,140.	.1065	-	-	-	-	-	40,600.	.427	.288	.209
25	S	Wallis	.5	34,600.	.114	.079	.755	.755	1.095	1.0	65,600.	.217	.198	Same
26				34,200.	.115	-	-	-	-	-	64,800.	.218	.199	as
27		AIR		32,700.	.1165	-	-	-	-	-	62,000.	.221	.202	f"/2
28				31,700.	.1165	-	-	-	-	-	60,200.	.221	.202	
29				29,100.	.119	-	-	-	-	-	55,200.	.226	.206	
30				22,470.	.129	-	-	-	-	-	42,600.	.244	.223	
31				17,000.	.134	-	-	-	-	-	32,300.	.254	.232	
32				11,890.	.143	-	-	-	-	-	22,600.	.271	.248	
33				9,520.	.149	-	-	-	-	-	18,100.	.282	.258	
34				9,395.	.138	-	-	-	-	-	17,800.	.262	.24	
35				7,920.	.154	-	-	-	-	-	14,800.	.292	.267	
36				6,365.	.168	-	-	-	-	-	12,100.	.318	.291	
37				5,630.	.179	-	-	-	-	-	10,700.	.34	.31	
38				4,990.	.186	-	-	-	-	-	9,460.	.352	.322	

TABLE 1 (*Continued*) CROSSFLOW FRICTION-FACTOR DATA; BARE TUBES

No.	Arrangement	Source & Material	D_t	Basis D_t: Re	Basis D_t: $\frac{f'}{2}$	D_v	S_L	S_T	$(\frac{D_v}{S_T})^{.4}$	$(\frac{S_L}{S_T})^{.6}$	Basis D_v: Re	Basis D_v: $\frac{f'}{2}$	Basis D_v: $\frac{f''}{2}$	Basis D_v: $\frac{f}{2}$
39	S	Sieder	.75"	98.2	1.32	.046'	.938"	.938"	.81	1.0	71.4	.965	1.195	Same
40		and		76.8	1.59	-	-	-	-	-	56.	1.16	1.44	as
41		Scott		72.6	1.32	-	-	-	-	-	53.	.965	1.195	$\frac{f''}{2}$
42				45.6	2.72	-	-	-	-	-	33.3	1.98	2.45	
43		FUEL OIL		28.	4.85	-	-	-	-	-	20.6	3.54	4.38	
44		16.7° API		15.5	9.81	-	-	-	-	-	11.3	7.15	8.85	
45		Isothermal		159.	.845	-	-	-	-	-	116.	.616	.765	
46				124.	1.04	-	-	-	-	-	90.6	.758	.94	
47				98.4	1.32	-	-	-	-	-	71.7	.96	1.19	
48				77.8	1.71	-	-	-	-	-	56.7	1.24	1.54	
49				48.4	2.79	-	-	-	-	-	35.3	1.95	2.42	
50				25.6	5.95	-	-	-	-	-	18.7	4.31	5.35	
51				25.4	5.37	-	-	-	-	-	18.5	3.89	4.83	
52				20.7	7.0	-	-	-	-	-	15.1	5.06	6.28	
53				17.4	8.08	-	-	-	-	-	12.7	5.85	7.25	
54				13.6	10.1	-	-	-	-	-	9.9	7.4	9.2	
55				8.48	14.7	-	-	-	-	-	6.18	10.65	13.2	
56				47.7	2.43	-	-	-	-	-	34.8	1.76	2.18	
57				86.2	1.45	-	-	-	-	-	62.8	1.06	1.31	
58				155.	.712	-	-	-	-	-	113.	.52	.642	
59				203.	.71	-	-	-	-	-	148.	.518	.64	
60				425.	.45	-	-	-	-	-	310	.328	.405	
61				333.	.494	-	-	-	-	-	243.	.36	.445	
62				233.	.571	-	-	-	-	-	170.	.417	.515	
63				452.	.439	-	-	-	-	-	330.	.32	.395	
64				289.	.55	-	-	-	-	-	211.	.402	.496	
65				338.	.521	-	-	-	-	-	246.	.381	.47	
66				377.	.488	-	-	-	-	-	275.	.356	.44	
67				428.	.466	-	-	-	-	-	312.	.34	.42	
68				484.	.455	-	-	-	-	-	353.	.332	.41	
69				864.	.354	-	-	-	-	-	630.	.258	.319	
70				706.	.39	-	-	-	-	-	515.	.284	.351	
71				624.	.416	-	-	-	-	-	455.	.304	.376	
72				540.	.439	-	-	-	-	-	394.	.32	.395	
73				455.	.425	-	-	-	-	-	332.	.31	.383	
74	S	Sieder	.75"	1,010.	.389	.046'	.938"	.938"	.81	1.0	735.	.284	.35	Same
75		and Scott		1,270.	.329	-	-	-	-	-	928.	.24	.296	as
76				1,145.	.384	-	-	-	-	-	635.	.28	.346	
77		KEROSENE		1,015.	.416	-	-	-	-	-	740.	.304	.376	$\frac{f''}{2}$
78		31.05°API		852.	.426	-	-	-	-	-	622.	.311	.384	
79		Isothermal		669.	.455	-	-	-	-	-	488.	.332	.41	
80				2,490.	.356	-	-	-	-	-	1,815.	.26	.321	
81				2,080.	.376	-	-	-	-	-	1,515.	.274	.338	
82				1,370.	.411	-	-	-	-	-	1,000.	.301	.374	
83				1,695.	.384	-	-	-	-	-	1,237.	.28	.346	
84				2,040.	.35	-	-	-	-	-	1,490	.256	.316	
85				2,490.	.33	-	-	-	-	-	1,815.	.241	.298	
86				2,880.	.34	-	-	-	-	-	2,100.	.248	.306	
87				4,090.	.304	-	-	-	-	-	2,980.	.222	.274	
88				3,600	.368	-	-	-	-	-	2,630.	.268	.331	
89				2,660.	.33	-	-	-	-	-	1,940.	.241	.298	
90				2,150.	.362	-	-	-	-	-	1,570.	.264	.326	
91	S	Sieder	.75"	41,400.	.276	.046'	.938"	.938"	.81	1.0	30,200.	.193	.238	Same
92		and Scott		16,400.	.261	-	-	-	-	-	12,100.	.189	.234	as
93				35,900.	.268	-	-	-	-	-	26,200	.194	.24	
94		WATER		14,400.	.265	-	-	-	-	-	10,500.	.192	.237	$\frac{f''}{2}$
95		Isothermal		27,800.	.292	-	-	-	-	-	20,300.	.212	.262	
96				11,100.	.282	-	-	-	-	-	8,100.	.204	.25	
97				6,190.	.332	-	-	-	-	-	4,510.	.240	.297	
98	S	Sieder	.75"	188.	.7	.046'	.938"	.938"	.81	1.0	137.	.511	.631	Same
99		and Scott		75.5	1.32	-	-	-	-	-	55.	.963	1.19	as
100				43.9	2.33	-	-	-	-	-	32.	1.7	2.1	
101		FUEL OIL		170.	.98	-	-	-	-	-	124.	.715	.883	$\frac{f''}{2}$
102		10.5° API		96.	1.13	-	-	-	-	-	70.	.827	1.02	
103		Cooling		135.	.98	-	-	-	-	-	98.8	.715	.883	
104				80.	1.34	-	-	-	-	-	58.3	.98	1.21	
105				29.6	3.73	-	-	-	-	-	21.6	2.72	3.36	
106				78.2	1.72	-	-	-	-	-	57.	1.255	1.55	
107				49.	2.56	-	-	-	-	-	35.7	1.865	2.3	
108				35.1	3.47	-	-	-	-	-	25.6	2.53	3.12	
109				6.52	19.9	-	-	-	-	-	4.76	14.55	18.	
110				62.9	2.04	-	-	-	-	-	45.9	1.485	1.83	
111				12.15	11.05	-	-	-	-	-	8.86	8.07	9.97	

TABLE 1 (*Continued*) CROSSFLOW FRICTION-FACTOR DATA; BARE TUBES

No.	Arrangement	Source & Material	D_t	Basis D_t		D_v	S_L	S_T	$(D_v/S_T)^{.4}$	$(S_L/S_T)^{.6}$	Basis D_v			
				Re	$f'/2$						Re	$f'/2$	$f''/2$	$f/2$
112	S	Sieder	.75"	35.9	3.24	.046'	.938"	.938"	.81	1.0	26.2	2.36	2.92	Same
113		and		28.8	4.35	-	-	-	-	-	21.	3.17	3.92	as
114		Scott		13.7	10.3	-	-	-	-	-	10.	7.52	9.29	$f''/2$
115				45.	4.39	-	-	-	-	-	32.8	3.2	3.95	
116		FUEL OIL		25.6	5.24	-	-	-	-	-	18.7	3.82	4.71	
117		10.5° API		20.	7.39	-	-	-	-	-	14.6	5.39	6.65	
118		Cooling		9.35	15.8	-	-	-	-	-	6.82	11.55	14.2	
119				5.64	26.4	-	-	-	-	-	4.12	19.3	23.8	
120				4.25	31.3	-	-	-	-	-	3.1	22.8	28.2	
121				46.6	3.15	-	-	-	-	-	34.	2.3	2.84	
122				26.	4.52	-	-	-	-	-	19.	3.3	4.08	
123				10.9	11.6	-	-	-	-	-	7.95	8.45	10.4	
124				4.8	26.7	-	-	-	-	-	3.5	19.5	24.1	
125				4.99	29.	-	-	-	-	-	3.64	21.2	26.2	
126				37.6	4.09	-	-	-	-	-	27.5	2.98	3.64	
127				20.7	6.33	-	-	-	-	-	15.1	4.62	5.7	
128				9.	14.7	-	-	-	-	-	6.57	10.75	13.3	
129				4.27	30.7	-	-	-	-	-	3.12	22.4	27.7	
130				13.1	10.55	-	-	-	-	-	9.55	7.7	9.52	
131				7.55	25.9	-	-	-	-	-	5.5	18.9	23.4	
132				3.7	44.5	-	-	-	-	-	2.7	32.5	40.1	
133				3.06	52.4	-	-	-	-	-	2.23	38.2	47.1	
134	S	Sieder	.75"	2,360.	.325	.046'	.938"	.938"	.81	1.0	1,730.	.237	.292	Same
135		and		1,690.	.42	-	-	-	-	-	1,230.	.306	.378	as
136		Scott		1,340.	.445	-	-	-	-	-	977.	.325	.4	$f''/2$
137				2,960.	.369	-	-	-	-	-	2,160.	.269	.332	
138		KEROSENE		4,090.	.342	-	-	-	-	-	2,980.	.25	.308	
139		31.05° API		886.	.475	-	-	-	-	-	646.	.346	.426	
140		Heating		902.	.4	-	-	-	-	-	664.	.292	.36	
141				640.	.433	-	-	-	-	-	468.	.316	.389	
142				713.	.436	-	-	-	-	-	520.	.318	.392	
143				1,045.	.315	-	-	-	-	-	762	23	284	
144	S	Sieder	.75"	26.	.99	.111'	1.18"	1.18"	1.05	1.0	46.2	1.77	1.685	Same
145		and		18.3	1.41	-	-	-	-	-	32.6	2.51	2.39	as
146		Scott		29.6	.995	-	-	-	-	-	52.7	1.77	1.685	$f''/2$
147				68.	.56	-	-	-	-	-	121.	.995	.948	
148		FUEL OIL		48.9	.606	-	-	-	-	-	86.8	1.08	1.03	
149		12.8° API		23.7	1.19	-	-	-	-	-	42.2	2.12	2.02	
150		Heating		13.6	1.87	-	-	-	-	-	24.2	3.32	3.16	
151	S	Sieder	.75"	105.	1.47	.046'	.938"	.938"	.81	1.0	76.7	1.075	1.325	Same
152		and		157.5	.809	-	-	-	-	-	115.	.59	.729	as
153		Scott		120.	.96	-	-	-	-	-	87.7	.7	.865	$f''/2$
154				86.4	1.02	-	-	-	-	-	63.	.745	.92	
155		FUEL OIL		36.8	1.99	-	-	-	-	-	26.9	1.455	1.79	
156		16.7°API		32.4	2.16	-	-	-	-	-	23.7	1.58	1.95	
157		Heating		198.5	.746	-	-	-	-	-	145.	.545	.674	
158				263.	.611	-	-	-	-	-	192.	.446	.551	
159				392.	.555	-	-	-	-	-	286.	.405	.5	
160				318.	.576	-	-	-	-	-	232.	.421	.52	
161				156.	.82	-	-	-	-	-	114.	.598	.737	
162				208.	.658	-	-	-	-	-	151.5	.48	.581	
163				581.	.425	-	-	-	-	-	424.	.31	.382	
164				744.	.371	-	-	-	-	-	543.	.271	.334	
165	S	Sieder	.75"	1,800.	.28	.046'	.938"	.938"	.81	1.0	1,315.	.205	.253	Same
166		and		1,320.	.327	-	-	-	-	-	965.	.239	.296	as
167		Scott		747.	.372	-	-	-	-	-	545.	.272	.338	$f''/2$
168				321.	.723	-	-	-	-	-	234.	.527	.65	
169		FUEL OIL		311.	.756	-	-	-	-	-	227.	.553	.683	
170		25.4°API		1,335.	.3	-	-	-	-	-	974.	.219	.27	
171		Cooling		1,190.	.336	-	-	-	-	-	870.	.245	.305	
172				1,050.	.349	-	-	-	-	-	765.	.255	.314	
173				620.	.389	-	-	-	-	-	453.	.284	.352	
174				281.	.818	-	-	-	-	-	205.	.597	.73	
175				1,125.	.341	-	-	-	-	-	822.	.249	.308	
176				915.	.386	-	-	-	-	-	667.	.282	.347	
177				524.	.419	-	-	-	-	-	382.	.306	.378	
178				240.	.945	-	-	-	-	-	175.	.69	.849	
179				880.	.393	-	-	-	-	-	642.	.287	.354	
180				748.	.455	-	-	-	-	-	545.	.333	.41	
181				410.	.501	-	-	-	-	-	299.	.366	.452	
182				187.	1.114	-	-	-	-	-	136.5	.833	1.02	
183				626.	.438	-	-	-	-	-	457.	.32	.394	
184				441.	.454	-	-	-	-	-	322.	.331	.408	
185				288.	.576	-	-	-	-	-	210.	.421	.52	
186				125.5	.959	-	-	-	-	-	91.6	.7	.86	
187				472.	.51	-	-	-	-	-	345.	.373	.46	
188				348.	.6	-	-	-	-	-	254.	.439	.54	
189				212.	.756	-	-	-	-	-	155.	.552	.68	
190				940.	.486	-	-	-	-	-	685.	.355	.442	

TABLE 1 (*Continued*) CROSSFLOW FRICTION-FACTOR DATA; BARE TUBES

No.	Arrangement	Source & Material	D_t in.	Basis D_t Re	Basis D_t f'/2	D_v ft.	S_L in.	S_T in.	$(\frac{D_v}{S_T})^{.4}$	$(\frac{S_L}{S_T})^{.6}$	Basis D_v Re	Basis D_v f'/2	Basis D_v f"/2	f/2
191	S	Sieder &	.75"	238.	.75	.046	.938	.938	.81	1.0	174.	.547	.672	Same
192		Scott		155.	1.25	–	–	–	–	–	113.	.914	1.12	as
193		(Same)		63.9	2.21	–	–	–	–	–	46.6	1.615	2.0	f"/2
194	S	Sieder &	.75	107.	1.02	.046	.938	.938	.81	1.0	78.	.746	.926	Same
195		Scott		87.4	1.15	–	–	–	–	–	63.7	.84	1.04	as
196				69.5	1.12	–	–	–	–	–	50.7	.82	1.01	f"/2
197		FUEL OIL		41.4	2.07	–	–	–	–	–	30.2	1.51	1.86	
198		11.7° API		84.	1.24	–	–	–	–	–	61.3	.902	1.11	
199		Heating		73.	1.38	–	–	–	–	–	53.3	1.01	1.24	
200				58.2	1.67	–	–	–	–	–	42.5	1.22	1.5	
201				46.9	2.02	–	–	–	–	–	34.2	1.47	1.81	
202				31.1	2.74	–	–	–	–	–	22.7	2.0	2.5	
203				53.9	1.795	–	–	–	–	–	39.3	1.31	1.63	
204				42.4	2.26	–	–	–	–	–	30.9	1.65	2.06	
205				32.6	2.85	–	–	–	–	–	23.8	2.08	2.58	
206				23.4	3.66	–	–	–	–	–	17.1	2.67	3.33	
207				152.	.818	–	–	–	–	–	111.	.597	.74	
208				125.	.886	–	–	–	–	–	91.5	.647	.816	
209				84.8	1.12	–	–	–	–	–	61.8	.817	1.0	
210	I	Huge	2.0	15,000.	.07	.575	4.0	3.5	1.31	1.08	51,800.	.244	.185	.171
211				22,000.	.07	–	–	–	–	–	76,000.	.244	.185	.171
212		AIR		40,000.	.066	–	–	–	–	–	138,000.	.229	.174	.161
213		Heating		50,000.	.061	–	–	–	–	–	172,500.	.212	.16	.148
214				65,000.	.058	–	–	–	–	–	224,000.	.202	.153	.142
215	S	"	2.0	60,000.	.0367	1.1	6.33	4.0	1.61	1.32	400,000.	.245	.152	.115
216				35,000.	.0467	–	–	–	–	–	232,000.	.312	.193	.146
217				20,000.	.0547	–	–	–	–	–	133,000.	.365	.226	.171
218				10,000.	.06	–	–	–	–	–	66,500.	.40	.248	.188
219	S	"	.5	1,500.	.0587	.276	1.58	1.0	1.61	1.316	9,950.	.37	.242	.183
220				2,750.	.0587	–	–	–	–	–	18,300.	.39	.242	.183
221				5,600.	.06	–	–	–	–	–	43,800.	.398	.247	.187
222	I	"	.5	4,000.	.0534	.276	1.5	1.0	1.61	1.28	26,600.	.354	.22	.172
223				6,000.	.0534	–	–	–	–	–	39,800.	.354	.22	.172
224	S	"	2.0	71,500.	.147	.163	2.78	2.5	.996	1.068	70,800.	.146	.1466	.137
225				10,200.	.256	–	–	–	–	–	10,100.	.254	.255	.239
226				4,080.	.272	–	–	–	–	–	4,040.	.269	.27	.252
227	I	"	.5	6,120.	.20	.041	.625	.625	.996	1.0	6,000.	.198	.199	.199
228				20,400.	.176	–	–	–	–	–	20,200.	.174	.175	.175

No.	Arrangement	Source & Material	D_t	Basis D_t Re	Basis D_t f'/2	D_v ft.	S_L in.	S_T in.	$(\frac{D_v}{S_T})^{.4}$	$(\frac{S_L}{S_T})^{.6}$	Basis D_v Re	Basis D_v f'/2	Basis D_v f"/2	f/2
229	I	Pierson	.31"	5,000.	.0334	.268	.93	.93	1.645	1.0	52,000.	.348	.212	.212
230				7,000.	.0334	–	–	–	–	–	72,800.	.348	.212	.212
231		AIR		9,000.	.0334	–	–	–	–	–	93,600.	.348	.212	.212
232		Heating		20,000.	.03	–	–	–	–	–	208,000.	.312	.19	.19
233	"	"	"	5,200.	.038	.171	.62	.93	1.38	0.79	34,400.	.252	.183	.231
234				10,000.	.04	–	–	–	–	–	66,000.	.264	.191	.242
235				30,000.	.035	–	–	–	–	–	198,000.	.232	.168	.212
236	"	"	"	6,000.	.0266	.121	.465	.93	1.19	0.66	28,200.	.125	.105	.159
237				30,000.	.0332	–	–	–	–	–	141,000.	.157	.132	.2
238				15,000.	.0292	–	–	–	–	–	70,500.	.138	.111	.175
239	"	"	"	6,000.	.0288	.096	.388	.93	1.09	0.592	22,600.	.108	.1	.167
240				15,000.	.0336	–	–	–	–	–	56,500.	.127	.1165	.197
241				30,000.	.032	–	–	–	–	–	113,000.	.121	.111	.1875
242	"	"	"	5,000.	.06	.171	.93	.62	1.61	1.27	33,000.	.396	.246	.194
243				10,000.	.06	–	–	–	–	–	66,000.	.396	.246	.194
244				30,000.	.0467	–	–	–	–	–	198,000.	.308	.191	.1505
245	"	"	"	5,000.	.053	.106	.62	.62	1.33	1.0	20,500.	.218	.164	.164
246				10,000.	.062	–	–	–	–	–	41,000.	.255	.192	.192
247				30,000.	.054	–	–	–	–	–	123,000.	.222	.167	.167
248	"	"	"	7,000.	.0479	.072	.465	.62	1.14	0.84	19,600.	.134	.1175	.14
249				33,000.	.0439	–	–	–	–	–	92,500.	.123	.108	.129
250	"	"	"	15,000.	.0528	.056	.388	.62	1.03	0.752	32,700.	.115	.112	.149
251				40,000.	.056	–	–	–	–	–	87,500.	.122	.1185	.1575
252	"	"	"	7,000.	.0967	.121	.93	.465	1.57	1.51	33,000.	.456	.291	.193
253				15,000.	.0868	–	–	–	–	–	70,500.	.409	.26	.172
254				30,000.	.0734	–	–	–	–	–	141,000.	.346	.22	.146
255	"	"	"	4,000.	.098	.073	.62	.465	1.28	1.19	11,200.	.274	.214	.18
256				10,000.	.094	–	–	–	–	–	28,000.	.263	.206	.173
257				20,000.	.09	–	–	–	–	–	56,000.	.252	.197	.166
258	"	"	"	40,000.	.093	.039	.465	.465	1.09	1.0	74,500.	.173	.159	.159
259				10,000.	.103	–	–	–	–	–	18,600.	.192	.176	.176
260				4,000.	.106	–	–	–	–	–	7,450.	.197	.181	.181
261	"	"	"	10,000.	.125	.036	.388	.465	.97	.9	13,800.	.172	.177	.197
262				20,000.	.115	–	–	–	–	–	27,600.	.159	.164	.182
263	"	"	"	4,000.	.133	.099	.93	.388	1.55	1.69	15,100.	.502	.324	.191
264				28,000.	.123	–	–	–	–	–	106,000.	.464	.299	.177
265	"	"	"	6,000.	.18	.057	.62	.388	1.25	1.33	13,100.	.392	.314	.236
266				28,000.	.17	–	–	–	–	–	61,000.	.371	.296	.223

TABLE 1 (*Continued*) CROSSFLOW FRICTION-FACTOR DATA; BARE TUBES

No.	Arrangement	Source & Material	D_t in.	Basis D_t Re	Basis D_t f'/2	D_v ft.	S_L in.	S_T in.	$(\frac{D_v}{S_T})^{.4}$	$(\frac{S_L}{S_T})^{.6}$	Basis D_v Re	Basis D_v f'/2	Basis D_v f"/2	Basis D_v f/2
267	I	Pierson	.31	4,000.	.214	.036	.465	.388	1.04	1.12	5,520.	.296	.285	.254
268		AIR		10,000.	.214	–	–	–	–	–	13,800.	.296	.285	.254
269		Heating		30,000.	.201	–	–	–	–	–	41,400.	.276	.266	.298
270	I	"	"	4,000.	.258	.026	.388	.388	.91	1.0	3,940.	.252	.278	.278
271				10,000.	.25	–	–	–	–	–	9,850.	.244	.268	.268
272				30,000.	.226	–	–	–	–	–	29,600.	.221	.243	.243
273	S	"	"	3,000.	.154	.097	.952	.388	1.55	1.71	11,300.	.58	.374	.218
274				7,000.	.134	–	–	–	–	–	26,400.	.505	.326	.19
275				26,000.	.113	–	–	–	–	–	98,000.	.425	.274	.16
276	"	"	"	25,000.	.16	.056	.65	.388	1.25	1.36	52,300.	.347	.278	.204
277				3,000.	.215	–	–	–	–	–	6,500.	.467	.374	.275
278	"	"	"	3,000.	.28	.036	.505	.388	1.04	1.17	4,180.	.39	.375	.32
279				25,000.	.206	–	–	–	–	–	34,900.	.288	.277	.236
280	"	"	"	3,000.	.336	.026	.434	.388	.91	1.07	3,030.	.34	.374	.349
281				25,000.	.24	–	–	–	–	–	25,200.	.242	.266	.248
282	"	"	"	6,000.	.09	.122	.96	.465	1.58	1.54	28,600.	.43	.272	.177
283				20,000.	.08	–	–	–	–	–	95,500.	.382	.242	.157
284	"	"	"	6,000.	.13	.073	.661	.465	1.28	1.235	17,000.	.368	.288	.234
285				32,000.	.092	–	–	–	–	–	90,500.	.26	.203	.164
286	"	"	"	3,000.	.173	.049	.522	.465	1.09	1.07	5,700.	.329	.302	.282
287				30,000.	.112	–	–	–	–	–	57,000.	.213	.195	.182
288	"	"	"	35,000.	.117	.036	.451	.465	.97	.982	48,800.	.163	.168	.171
289				6,000.	.176	–	–	–	–	–	8,360.	.246	.254	.258
290	"	"	"	3,500.	.08	.171	.98	.62	1.61	1.315	23,200.	.53	.329	.25
291				35,000.	.0468	–	–	–	–	–	232,000.	.31	.193	.147
292	"	"	"	3,500.	.105	.106	.693	.62	1.33	1.07	14,300.	.472	.355	.332
293				35,000.	.067	–	–	–	–	–	143,000.	.274	.206	.193
294	"	"	"	40,000.	.0798	.073	.557	.62	1.15	.94	113,000.	.226	.197	.21
295				14,000.	.113	–	–	–	–	–	39,600.	.32	.278	.296
296	"	"	"	6,000.	.144	.056	.496	.62	1.03	.874	13,000.	.314	.305	.35
297				40,000.	.091	–	–	–	–	–	86,800.	.198	.192	.22
298	"	"	"	4,000.	.052	.268	1.04	.93	1.65	1.07	41,400.	.541	.328	.306
299				22,000.	.0387	–	–	–	–	–	229,000.	.402	.244	.228

TABLE 2 CROSSFLOW FRICTION DATA; EXTENDED SURFACE

No.	Arrangement	Source and Material	D_t	Basis D_t Re	Basis D_t $\frac{f'}{2}$	D_v	S_L	S_T	$(\frac{D_v}{S_T})^{.4}$	$(\frac{S_L}{S_T})^{.6}$	Basis D_v Re	Basis D_v $\frac{f'}{2}$	Basis D_v $\frac{f''}{2}$	Basis D_v $\frac{f}{2}$
300	S	Authors'	–	–	–	.0265'	.1094'	.1094'	.566	1.0	2.62	24.2	42.7	Same
301		Tests				–	–	–	–	–	2.46	29.1	51.4	as
302	Meshed		NOTE:			–	–	–	–	–	2.22	27.2	48.0	$\frac{f''}{2}$
303	Round	OIL				–	–	–	–	–	1.79	35.5	62.8	
304	X-fins	Cooling	These Tests			–	–	–	–	–	1.32	61.1	108.0	
305			Not Evaluated			–	–	–	–	–	2.84	17.9	31.6	
306			on			–	–	–	–	–	2.54	19.2	33.9	
307			D_t Basis			–	–	–	–	–	2.24	28.8	50.9	
308						–	–	–	–	–	2.20	28.0	49.5	
309						–	–	–	–	–	2.44	26.9	47.5	
310						–	–	–	–	–	1.35	47.9	84.5	
311						–	–	–	–	–	2.07	32.5	57.4	
312						–	–	–	–	–	1.71	44.5	78.5	
313						–	–	–	–	–	1.38	59.0	104.0	
314						–	–	–	–	–	2.06	19.0	33.6	
315						–	–	–	–	–	1.83	19.6	34.6	
316						–	–	–	–	–	1.20	35.6	62.8	
317						–	–	–	–	–	1.145	35.9	63.4	
318						–	–	–	–	–	1.205	47.5	83.8	
319	S	Authors'	"	"		.0265'	.1094'	.1094'	.566	1.0	.548	79.3	140.0	Same
320		Tests				–	–	–	–	–	.495	90.0	159.0	as
321	Meshed					–	–	–	–	–	.613	63.5	112.0	$\frac{f''}{2}$
322	Round	OIL				–	–	–	–	–	.440	104.5	184.5	
323	X-fins	Isothermal				–	–	–	–	–	.386	120.0	212.0	
324						–	–	–	–	–	.262	235.0	416.0	
325						–	–	–	–	–	.312	178.5	315.	
326						–	–	–	–	–	.187	366.	645.	
327						–	–	–	–	–	.169	375.	660.	
328						–	–	–	–	–	3.33	17.	30.	
329						–	–	–	–	–	2.46	24.7	43.6	
330						–	–	–	–	–	1.62	34.6	61.2	
331						–	–	–	–	–	.24	172.	304.	
332						–	–	–	–	–	.23	125.	221.	
333						–	–	–	–	–	.193	185.	327.	
334						–	–	–	–	–	.222	144.	254.	
335						–	–	–	–	–	.221	193.	341.	
336						–	–	–	–	–	.180	214.	378.	

TABLE 2 (*Continued*) CROSS FLOWFRICTION DATA; EXTENDED SURFACE

No.	Arrangement	Source and Material	D_t	Basis D_t: Re	Basis D_t: $\frac{f'}{2}$	D_y	S_L	S_T	$(\frac{D_y}{S_T})^{.4}$	$(\frac{S_L}{S_T})^{.6}$	Basis D_y: Re	Basis D_y: $\frac{f'}{2}$	Basis D_y: $\frac{f''}{2}$	$\frac{f}{2}$
337	S	Authors'	-	-	-	.0265'	.1094'	.1094'	.566	1.0	.139	330.	583.	Same
338		Tests				-	-	-	-	-	.116	349.	616.	as
339	Meshed		NOTE:			-	-	-	-	-	2.26	17.5	30.9	$\frac{f''}{2}$
340	Round	OIL				-	-	-	-	-	2.81	15.75	27.8	
341	X-fins	Isothermal	These Tests			-	-	-	-	-	2.91	17.85	31.5	
342			Not Evaluated on			-	-	-	-	-	3.14	17.5	30.9	
343			D_t Basis.			-	-	-	-	-	3.28	16.25	28.7	
344						-	-	-	-	-	3.21	16.85	29.8	
345						-	-	-	-	-	3.6	16.9	29.9	
346						-	-	-	-	-	3.88	14.15	25.	
347						-	-	-	-	-	3.94	13.7	24.2	
348						-	-	-	-	-	1.01	45.5	80.2	
349						-	-	-	-	-	1.25	32.4	57.3	
350						-	-	-	-	-	1.35	30.3	53.5	
351						-	-	-	-	-	1.56	25.3	44.7	
352						-	-	-	-	-	2.11	23.6	41.7	
353						-	-	-	-	-	3.0	18.35	32.4	
354	S	Authors'	"			.0265'	.1094'	.1094'	.566	1.0	1,025.	.212	.375	Same
355		Tests				-	-	-	-	-	923.	.208	.367	as
356	Meshed					-	-	-	-	-	636.	.264	.465	$\frac{f''}{2}$
357	Round	WATER				-	-	-	-	-	848.	.211	.372	
358	X-fins	Isothermal				-	-	-	-	-	1,065.	.197	.348	
359						-	-	-	-	-	1,010.	.178	.315	
360						-	-	-	-	-	704.	.296	.521	
361						-	-	-	-	-	439.	.385	.68	
362						-	-	-	-	-	1,060.	.195	.345	
363						-	-	-	-	-	729.	.276	.486	
364						-	-	-	-	-	575.	.361	.637	
365						-	-	-	-	-	648.	.4	.707	
366						-	-	-	-	-	765.	.172	.304	
367						-	-	-	-	-	733.	.304	.537	
368						-	-	-	-	-	800.	.321	.65	
369	Wire	Authors'	"	"		.0220'	.0104'	.0104'	1.35	1.0	14,000.	.3175	.235	Same
370	Mesh	Tests				-	-	-	-	Assumed	15,150.	.32	.237	as
371	In-					-	-	-	-	-	16,150.	.331	.245	$\frac{f''}{2}$
372	ternal	WATER				-	-	-	-	-	16,900.	.326	.2415	
373	Fins	Isothermal				-	-	-	-	-	18,700.	.296	.219	
374						-	-	-	-	-	13,950.	.301	.223	

No.	Arrangement	Source and Material	D_t	Basis D_t: Re	Basis D_t: $\frac{f'}{2}$	D_y	S_L	S_T	$(\frac{D_y}{S_T})^{.4}$	$(\frac{S_L}{S_T})^{.6}$	Basis D_y: Re	Basis D_y: $\frac{f'}{2}$	Basis D_y: $\frac{f''}{2}$	$\frac{f}{2}$
375	Wire	Authors'	NOTE:			.0220'	.0104'	.0104'	1.35	1.0	14,650.	.322	.238	Same
376	Mesh	Tests				-	-	-	-	Assumed	10,100.	.374	.277	as
377	Internal		These Tests			-	-	-	-	-	11,300.	.36	.266	$\frac{f''}{2}$
378	Fins	WATER	Not Evaluated			-	-	-	-	-	12,320.	.356	.264	
379		Isothermal	On D_t Basis			-	-	-	-	-	1,135.	.456	.338	
380						-	-	-	-	-	1,750.	.413	.306	
381						-	-	-	-	-	2,900.	.389	.288	
382						-	-	-	-	-	3,740.	.364	.270	
383						-	-	-	-	-	4,260.	.375	.278	
384						-	-	-	-	-	4,800.	.362	.268	
385						-	-	-	-	-	5,300.	.373	.276	
386						-	-	-	-	-	5,810.	.361	.2675	
387						-	-	-	-	-	6,400.	.358	.267	
388						-	-	-	-	-	6,780.	.363	.269	
389						-	-	-	-	-	6,310.	.394	.292	
390						-	-	-	-	-	7,230.	.396	.294	
391						-	-	-	-	-	8,150.	.344	.255	
392						-	-	-	-	-	8,780.	.379	.281	
393						-	-	-	-	-	9,350.	.390	.289	
394	Wire	Authors'	"	"		.0220'	.0104'	.0104'	1.35	1.0	488.	.715	.53	Same
395	Mesh	Tests				-	-	-	-	Assumed	471.	.775	.575	as
396	Internal					-	-	-	-	-	427.	.798	.591	$\frac{f''}{2}$
397	Fins	OIL				-	-	-	-	-	388.	.812	.602	
398		Cooling				-	-	-	-	-	366.	.82	.608	
399						-	-	-	-	-	332.	.852	.631	
400						-	-	-	-	-	309.	.91	.675	
401						-	-	-	-	-	280.	.912	.676	
402						-	-	-	-	-	250.	.967	.716	
403						-	-	-	-	-	221.	1.03	.762	
404						-	-	-	-	-	190.	1.09	.808	
405						-	-	-	-	-	177.	1.155	.856	
406						-	-	-	-	-	168.5	1.26	.934	
407						-	-	-	-	-	137.5	1.285	.952	
408						-	-	-	-	-	129.	1.353	1.002	
409						-	-	-	-	-	149.	1.403	1.04	
410						-	-	-	-	-	123.	1.53	1.135	
411						-	-	-	-	-	101.	1.755	1.3	

TABLE 2 *(Continued)* CROSSFLOW FRICTION DATA; EXTENDED SURFACE

No.	Arrangement	Source and Material	D_t	Basis D_t: Re	Basis D_t: $\frac{f'}{2}$	D_v	S_L	S_T	$(\frac{D_v}{S_T})^{.4}$	$(\frac{S_L}{S_T})^{.6}$	Basis D_v: Re	Basis D_v: $\frac{f'}{2}$	Basis D_v: $\frac{f''}{2}$	$\frac{f}{2}$
412	Radiator	Manufac-	NOTE:			.0137'	-	.052'	.586	1.0	1,280.	.0895	.1525	Same
413	Core-(A)	turers'				-	-	-	-	Assumed	1,830.	.074	.126	as
414	Type ___	Data	These tests not			-	-	-	-	since	2,570.	.0619	.1055	$\frac{f''}{2}$
415	Surface	AIR	evaluated on			.0156'	-	-	.618	indeter-	1,460.	.10	.162	
416	(B)		D_t Basis.			-	-	-	-	minate	2,080.	.0822	.133	
417						-	-	-	-		2,730.	.0767	.124	
418	Square	Manufac-	"	"		.024'	.198'	.198'	.43	1.0	1,360.	.1055	.245	Same
419	X-fins	turers'				-	-	-	-	-	2,260.	.0972	.226	as
420		Data				-	-	-	-	-	3,180.	.0912	.212	$\frac{f''}{2}$
421		AIR				-	-	-	-	-	4,530.	.0856	.199	
422	Radiator	Manufac-				.0152'	-	.0364'	.705	1.0	1,120.	.10	.142	Same
423	Core-(I)	turers'				-	-	-	-	Assumed	1,570.	.0895	.127	as
424	Type ___	Data				-	-	-	-	since	1,620.	.0882	.125	$\frac{f''}{2}$
425	Surface	AIR				.0152'	-	.0364'	.705	indeter-	1,120.	.1065	.151	
426	(II)					-	-	-	-	minate	1,570.	.0955	.1355	
427						-	-	-	-		1,620.	.0952	.135	
428	Round	Tuve	"	"		.0297'	-	.1354'	.545	1.0	1,227.	.2165	.397	Same
429	X-fins					-	One	-	-	Assumed	1,380.	.208	.382	as
430		AIR				-	Row	-	-	because	1,533.	.204	.374	$\frac{f''}{2}$
431						-	Deep	-	-	only one	1,840.	.189	.347	
432						-		-	-	row deep	2,150.	.186	.3415	
433	Radiator	N.A.C.A.	"			.0207'	.0417'	.0834'	.574	.66	3,390.	.144	.261	.38
434	Core-					-	-	-	-	-	6,770.	.141	.246	.372
435	Type	AIR				-	-	-	-	-	10,200.	.140	.244	.369
436	Surface					-	-	-	-	-	3,080.	.1463	.255	.386
437						-	-	-	-	-	6,160.	.140	.244	.369
438						-	-	-	-	-	9,270.	.1342	.234	.355
439						-	-	-	-	-	12,300.	.139	.242	.366
440	Finned	N.A.C.A.	"	"		.00364'	-	.591'	.130	1.0	1,280.	.0489	.376	Same
441	Cylinders					-	Single	-	-	Assumed	1,540.	.0468	.36	as
442		AIR				-	Cylinder	-	-	because	1,795.	.0432	.333	$\frac{f''}{2}$
443	(A)					-	in	-	-	of	2,050.	.0398	.306	
444						-	Shroud	-	-	Shroud	2,560.	.0365	.281	
445						.00784'		.591'	.176	Effect	1,660.	.0542	.308	
446	(B)					-		-	-		2,760.	.0423	.240	
447						-		-	-		3,870.	.0384	.218	
448						-		-	-		4,430.	.0364	.201	
449						-		-	-		4,980.	.0342	.194	

No.	Arrangement	Source and Material	D_t	Basis D_t: Re	Basis D_t: $\frac{f'}{2}$	D_v	S_L	S_T	$(\frac{D_v}{S_T})^{.4}$	$(\frac{S_L}{S_T})^{.6}$	Basis D_v: Re	Basis D_v: $\frac{f'}{2}$	Basis D_v: $\frac{f''}{2}$	$\frac{f}{2}$
450	Finned		NOTE:			.0124'	Single	.591'	.213	1.0	2,190.	.0578	.271	Same
451	Cylinders	N.A.C.A.				-	Cylinder	-	-	Assumed	3,500.	.049	.230	as
452			These tests not			-	in	-	-	because	5,250.	.0418	.196	$\frac{f''}{2}$
453	(C)	AIR	evaluated on			-	Shroud	-	-	of	7,000.	.0384	.180	
454			D_t Basis.			-		-	-	Shroud	8,760.	.0352	.165	
455	(D)					.0163'	"	.591'	.237	Effect	2,880.	.0697	.294	"
456						-		-	-		4,600.	.0593	.250	
457						-		-	-		6,910.	.0503	.212	
458						-		-	-		9,220.	.0462	.195	
459						-		-	-		11,500.	.0425	.1795	
460	(E)					.0207'	"	.591'	.260		3,660.	.0836	.321	"
461						-		-	-		5,850.	.0707	.272	
462						-		-	-		8,770.	.0603	.232	
463						-		-	-		11,700.	.0551	.212	
464						-		-	-		14,600.	.051	.196	
465	Radiator	Bureau of	"	"		.033'	Flat	.0208'	1.22	1.0	2,700.	.0988	.081	"
466	Core-Type	Standards				-	Plate	-	-	Assumed	5,400.	.0739	.0605	
467	Surface					-	Tubes	-	-	since	10,800.	.0718	.0588	
468	(E-6)	AIR				-		-	-	inde-	13,500.	.0697	.0571	
469	(E-7)					.0543'	Flat	.0312'	1.248	terminate	8,900.	.0514	.0412	"
470						-	Plate	-	-		17,800.	.0477	.0382	
471						-	Tubes	-	-		26,600.	.0467	.0374	
472						-		-	-		31,100.	.0464	.0372	
473	(E-8)					.076'	Flat	.0417'	1.27		12,450.	.0455	.0358	
474						-	Plate	-	-		24,900.	.0446	.0351	
475						-	Tubes	-	-		31,000.	.0446	.0351	
476						-		-	-		43,500.	.0446	.0351	
477	(E-9)					.127'	Flat	.0625'	1.33		10,400.	.0457	.0344	"
478						-	Plate	-	-		20,800.	.0418	.0314	
479						-	Tubes	-	-		31,200.	.0417	.0313	
480						-		-	-		41,500.	.0402	.0302	
481	(F-6)					.0266'	.0417'	.0834'	.634	.66	2,170.	.498	.785	1.19
482						-	-	-	-	-	4,340.	.498	.785	1.19
483						-	-	-	-	-	6,510.	.437	.69	1.145

Friction data of Carrier, Allen, Soule, Dehn, Reiher, and Reitschel for a great variety of tube arrangements have also been used to establish the equation, but are not shown.

There are certain discrepancies and deviations from the proposed main line in the data of Pierson. However, the magnitude of these deviations is in general not more than 10 or 15 per cent. Another point of importance is that no other authors have found friction factors which increase with Reynolds number, which is reported over limited ranges by both Pierson and Huge. Lindmark, in his discussion of this paper, pointed this out and stated that he found no such increase in experiments he conducted. A certain amount of these deviations may be accounted for by the fact that entrance and exit losses are contained in the over-all pressure drop reported by these authors.

Jakob (12) proposed two equations of rather complex form for the correlation of Pierson's data. It appears that the present equation is simpler to use, and probably more accurate as it is substantiated by data from many other sources.

Extended Surface

Fig. 5 illustrates how extended surface, both external and internal, will plot on this same proposed correlation.

It will be noted that some forms of extended surface, namely, flat plates and fins with turbulence promoters, do not correlate well on the suggested curve as would be expected.

McAdams (13), Colburn (14), Norris and Streid (15), and many others have pointed out that flat plates and turbulence promoters will produce different flow characteristics. Flat plates show low $f/2$ values, and turbulence promoters give high values. The published and authors' data included in the paper bear out these conclusions.

The authors' data on meshed round-cross-fin tubes (eight $^1/_4$-in. fins per in.) with no turbulence promoters, Figs. 6(h) and 7(a), show good agreement with the proposed correlation. They cover both heavy lubricating-oil and water tests.

The N.A.C.A. tests on finned airplane-engine cylinders (16), Fig. 6n, in an air stream show ±20 per cent, which is well in line. These results are encouraging, since fin heights are 1.22 in. and spacing varies from 0.057 to 0.166 in.

Authors' results on one sample of internal-fin tubes, Fig. 7b, show good correlation. This is especially interesting, since the tests represent a combination of cross- and internal-tube flow.

Tuve and McKeeman's tests on unmeshed cross-fin tubes (17), Fig. 6g, (for only one row), show agreement within 15 per cent, on the proposed curve.

For comparative purposes, data from the Bureau of Standards reports (18, 19), on various types of aircraft nose radiators, are included. These data show flat plates some 80 per cent low, and round tubes and flat plates with turbulence promoters approximately 300 per cent high for friction factors on the suggested basis.

In addition, manufacturers' data on flat-tube core-type radiators are included to show that where not too much turbulence-promoter effect is present, these too correlate on the curve within —60 per cent.

Reference to Table 2 will show that for the factor $(S_L/S_T)^n$, as applied to some of the extended-surface samples, assumptions of unity were made in certain instances.

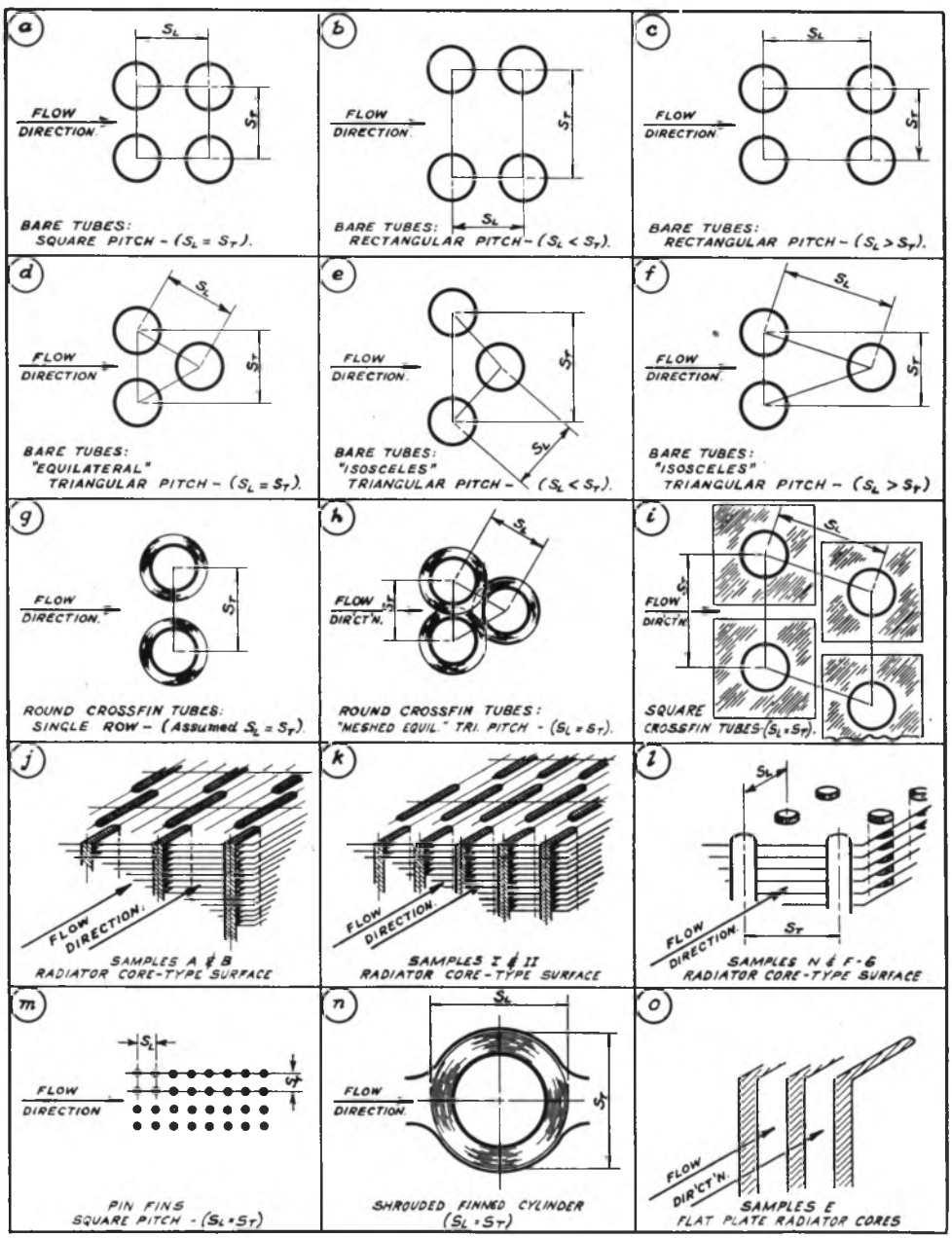

Fig. 6 Various Types of Crossflow Surfaces

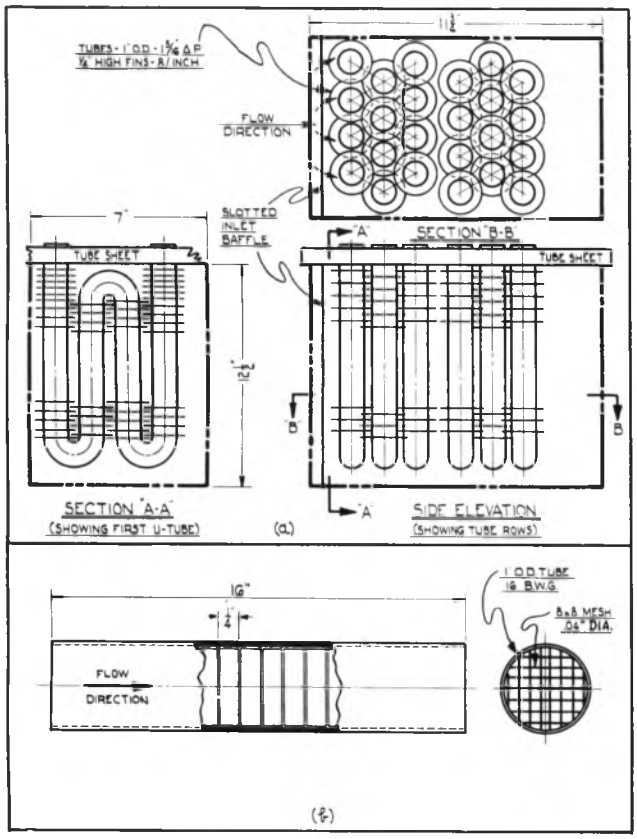

FIG. 7 AUTHORS' TEST SAMPLES
(*a*, External meshed round cross fins.
b, Internal wire-mesh fins.)

In the case of the wire-mesh internal fins, Fig. 7*b* (Tests No. 369–411), an 8 × 8 screen wire mesh was used for the inserts. It was reasoned that the symmetrical spacing of the cross-wires at 0.125 in. centers was the equivalent of equilateral pitch in a conventional tube bank; hence the use of $(S_L/S_T)^{0.6} = 1$.

For the various samples of radiator core-type surface, using flat tubes with relatively smooth plate-type fins, the evaluation of the configuration ratio was deemed indeterminate. Since these samples were included solely for comparative purposes, the factor was taken as unity.

Tuve and McKeeman's tests on round cross-fin tubes, unmeshed, were for only one row deep in the direction of flow. While no finite value of S_L is determinable for this arrangement, t was assumed that sufficient exit turbulence was present to give at least some of the effect of additional rows. Therefore, $(S_L/S_T)^{0.6}$ was assumed as 1 for the plot.

With the shrouded-finned cylinders reported on by the N.A.C.A., a variation of the foregoing is found. In this case, the single "tube" is surrounded by a close-fitting baffle just clearing the outer periphery of the fins, Fig. 6*n*. It was felt that this produced the effect of an equilateral tube arrangement, and therefore, the configuration factor would become unity.

CONCLUSIONS

1 The use of D_v and the configuration factors proposed herein is recommended for a general correlation of pure crossflow friction on a single curve.

2 This same type of correlation can be applied to heat transfer, although demonstration of this is beyond the scope of the present paper.

3 It has been shown that certain types of extended surface, approximating conventional tube arrangements, correlate well on the general plot. This statement is qualified by the assumption that fins are relatively smooth and tubes are disposed in three or more rows deep, transverse to flow. It is admitted that where flat-plate or turbulence-promoter effects become significant, the suggested correlation does not apply.

4 It should be pointed out that additional data for the viscous range, on a greater variety of tube sizes and surface arrangements, are needed to establish more definitely this portion of the plot. This will be evident from an inspection of Figs. 1 to 5.

ACKNOWLEDGMENT

The authors wish to take this opportunity of crediting their late colleague, Mr. E. S. Davis, with his full due for the original mathematical analysis which formed the basis for the correlation revealed herein.

As in the unpublished reference work, appreciation is expressed to Messrs. E. N. Sieder and N. A. Scott, Jr., of Foster-Wheeler Corporation for making available extensive original crossflow data, and to Mr. R. H. Norris for his courtesy in supplying exact values of his published data.

In addition, the authors must acknowledge their debt to the National Advisory Committee for Aeronautics, the Bureau of Standards, and to all the other investigators whose published data were made free use of in this paper.

Finally, thanks are due to Mr. C. P. Byrne, who carried out most of the authors' test work; and to Miss B. L. Samson and Mrs. D. G. Davis for their efforts in working up the test calculations, tabulations, and plots.

Appendix

As mentioned previously, the present paper incorporates data from many diverse sources. The basic bare-tube plots are taken directly from the published data of various investigators, as set forth in the Bibliography. Some of the extended-surface plots are from published data; the rest from private manufacturers' data made available for this work, and from actual authors' tests. The last specifically are the external meshed cross-fin plots and those for the internal wire-mesh fins.

Meshed Cross Fins. The meshed-cross-fin-surface sample tested is detailed in Fig. 7*a*. Conventional spiral cross-fin tubes (1 in. OD with $1^1/_2$-in-OD fins, 0.012 in. in thickness, 8 per in.), were arranged on $1^5/_{16}$-in. triangular pitch with fins intermeshed, as shown, in two nests of three rows each. The open tube ends were rolled into a tube sheet in the conventional manner, with the return bends disposed as shown. This assembly was enclosed in a rectangular box-type shell with suitable inlet and outlet nozzles at the narrow ends for installation in the test setup piping. A slotted baffle plate was placed at the inlet end of the test section to insure proper distribution of the entering fluid over the full face of the tube bundle.

Cooling and isothermal test runs, Table 2 (No. 300–368), for both lube oil and water were made to fill in as complete a range of the curve as possible. It will be noted that the oil tests fall along the viscous portion of the line, with those for water in the turbulent region.

Internal Wire-Mesh Fins. The internal wire-mesh fin-tube sample tested is shown in Fig. 7*b*. This was a 1-in. OD, No. 16 Bwg copper tube with tinned wire-mesh inserts (8 × 8 mesh, 0.04-in-diam wire), disposed inside throughout its length. The test sample was then installed with suitable entrance and exit straightening tubes in the piping setup, and the water and oil tests run as listed in Table 2 (No. 369–411).

ADDENDA

It is recognized that the admirable work of Chilton and Genereaux (20) was seemingly overlooked in the presentation of the present correlation. It must be explained that, while the data of all the investigators covered by these authors were utilized to establish the new recommended curve, preprint deadline limitations prohibited a direct comparison with this earlier work.

BIBLIOGRAPHY

1 "A Method of Correlating Forced-Convection Heat-Transfer Data and a Comparison With Fluid Friction," by A. P. Colburn, Trans. American Institute of Chemical Engineers, vol. 29, 1933, pp. 174–210.

2 "A Review of Heat-Transfer Coefficients and Friction Factors for Tubular Heat Exchangers," by B. E. Short, Trans. A.S.M.E., vol. 64, 1942, pp. 779–785.

3 "Investigation of Heat Transfer Rates on the External Surface of Baffled Tube Banks," by R. A. Bowman, in "Heat Transfer," A.S.M.E. unpublished papers, no. 28, 1936, pp. 75–81.

4 "Experimental Investigation of Effects of Equipment Size on Convection Heat Transfer and Flow Resistance in Crossflow of Gases Over Tube Banks," by E. C. Huge, Trans. A.S.M.E., vol. 59, 1937, pp. 573–581.

5 "Correlation and Utilization of New Data on Flow Resistance and Heat Transfer for Crossflow of Gases Over Tube Banks," by E. D. Grimison, Trans. A.S.M.E., vol. 59, 1937, pp. 583–594.

6 "High-Performance Fins for Heat Transfer," by R. H. Norris and W. A. Spofford, Trans. A.S.M.E., vol. 64, 1942, pp. 489–496.

7 "Fluid Friction at Parallel and Right Angles to Tubes and Tube Bundles," by E. N. Sieder and N. A. Scott, Jr., A.S.M.E. unpublished papers, No. 83, 1932.

8 "Heat Transfer and Pressure Drop in Crossflow Over Bare Tube Banks," by E. S. Davis and A. Y. Gunter, unpublished paper released only to N.A.C.A., 1943.

9 "Heat Transfer and Pressure Drop of Liquids in Tubes," by E. N. Sieder and G. E. Tate, *Industrial and Engineering Chemistry*, vol. 28, 1936, pp. 1429–1435.

10 "Experimental Investigation of the Influence of Tube Arrangement on Convection Heat Transfer and Flow Resistance in Crossflow of Gases Over Tube Banks," by O. L. Pierson, Trans. A.S.M.E., vol. 59, 1937, pp. 563–572.

11 "Resistance to Flow Through Nests of Tubes," by R. Pendennis Wallis and C. M. White, *Engineering*, vol. 146, 1938, pp. 605–607, 665–666, and 723–725.

12 "Discussion of Pierson, Huge, and Grimison Papers," by Max Jakob, Trans. A.S.M.E., vol. 60, 1938, pp. 384–386.

13 "Heat Transmission," by W. H. McAdams, McGraw-Hill Book Company, Inc., New York, N. Y., 1942, pp. 123–124, 197–198.

14 "Heat Transfer by Natural and Forced Convection," by A. P. Colburn, Purdue University, Engineering Experiment Station, Research Series No. 84, Jan., 1942, pp. 38–40, 51.

15 "Laminar-Flow Heat-Transfer Coefficients for Ducts," by R. H. Norris and D. D. Streid, Trans. A.S.M.E., vol. 62, 1940, pp. 525–533.

16 "Blower Cooling of Finned Cylinders," by O. W. Schey and H. H. Ellerbrock, Jr., U. S. N.A.C.A., Report No. 587, 1937, p. 269.

17 "Heat Transfer From Direct and Extended Surfaces With Forced Air Circulation," by G. L. Tuve and C. A. McKeeman, Trans. American Society of Heating and Ventilating Engineers, vol. 40, No. 997, 1934, pp. 427–442.

18 "Radiators for Aircraft Engines," by S. R. Parsons and D. R. Harper 3rd, U.S. Bureau of Standards, Technical Paper No. 211, 1922, pp. 369–371, 391–392.

19 "Heat Dissipation and Other Properties of Radiators," by H. C. Dickinson, W. S. James, and R. V. Kleinschmidt, N.A.C.A. Report No. 63, 1919.

20 "Pressure Drop Across Tube Banks," by T. H. Chilton and R. P. Genereaux, Trans. American Institute of Chemical Engineers, vol. 29, 1933, pp. 161–173.

Discussion

D. F. Boucher[4] and C. E. Lapple.[4] The authors have undertaken the formulation of a generalized method for estimating pressure drop across tube banks, a field in which a large amount of conflicting data are available and in which correlation is sorely needed. The advantages claimed for the proposed method are that it attempts to combine the data for tubes of both plain and extended surfaces in a single empirical correlation, and that the same method of representation is applied to the streamline- and turbulent-flow regimes, as well as to staggered and in-line tube arrangements.

An empirical generalization of this type is a useful design tool and has much to recommend it. However, as is usually the case in such instances, a certain sacrifice in accuracy is entailed. For banks of plain tubes, the accuracy is fairly good in the range of spacings commonly used in practice but becomes progressively worse as more extreme spacings are approached. Unfortunately, this is not made clear by the authors since their plots ascribe almost one half of all the points plotted to an arrangement tested by Sieder and Scott, while each of the two Wallis-White arrangements is given considerably more weight than each of the numerous arrangements tested by Huge and Pierson. Figs. 8 and 9 of this discussion show all the available data on pressure drop for turbulent flow across plain tube banks on the authors' method of presentation, giving equal weight to each arrangement reported. It is apparent that the deviation of the data from the line proposed by the authors is as much as three- to fourfold as compared with less than twofold indicated by their Fig. 4. This greater deviation is due to the additional data of Allen, Andreas, Brandt and Dingler, Carlson and Hurt, Dehn, Jauernick, Reiher, Rietschel, Soule, and ter Linden, as well as some of Pierson's and Huge's data that had not been included in the original presentation by the authors.

Their line for streamline flow appears to be based on isothermal data for only a single arrangement. All other points are based on heating and cooling runs. In view of the uncertainty as to the proper interpretation of data for banks in which heat transfer occurs, it would hardly appear justifiable to use them for the fundamental correlation, particularly when isothermal data are available. The isothermal correlation should then be used to determine the proper way to handle data for the case of heat transfer.

Fig. 10 of this discussion has been prepared to compare the available isothermal data on the basis of the authors' method of presentation. The points shown represent all the isothermal streamline data originally reported by Sieder and Scott as well as some additional data obtained by Sieder and reported by the authors. All of the data represent staggered equilateral tube-bank arrangements. By reference to the original Sieder-Scott method of presentation, subsequently adopted by Chilton and Genereaux for the streamline region, it becomes apparent that the authors' method does not give as good a representation of the data.

It is to be expected that the effect of tube spacing will be different for turbulent and for streamline flow. In one case, kinetic energy or inertia forces are predominant, while in the other shear or frictional forces are controlling. It is only by pure coincidence that tube spacing can affect each to the same degree. The fact that the authors obtained a fairly good correlation for both streamline and turbulent flow would appear to indicate that an equal effect is closely approximated. However, it should be pointed out that the available data for streamline flow, while copious, cover a very limited range of spacings (two staggered equilateral and no in-line arrangements). Consequently, acceptance of the possibility of a single correlation for both regions must be made with considerable reservation until more data become available.

In the case of the Wallis-White staggered arrangement, the authors apparently used a value of D_e of 0.079 ft, whereas it

[4] Engineering Department, Experimental Station, E. I. du Pont de Nemours & Co., Wilmington, Del.

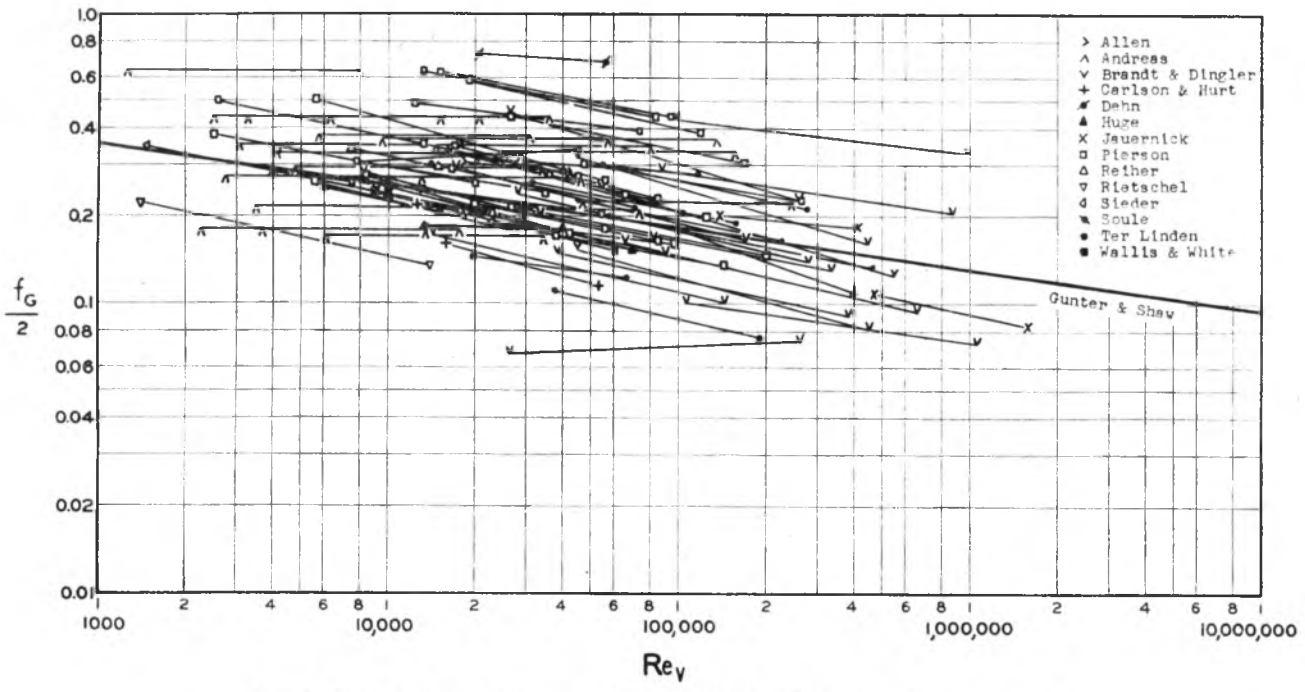

FIG. 8 COMPARISON OF TURBULENT-FLOW DATA FOR STAGGERED ARRANGEMENTS
(Gunter-Shaw method of representation.)

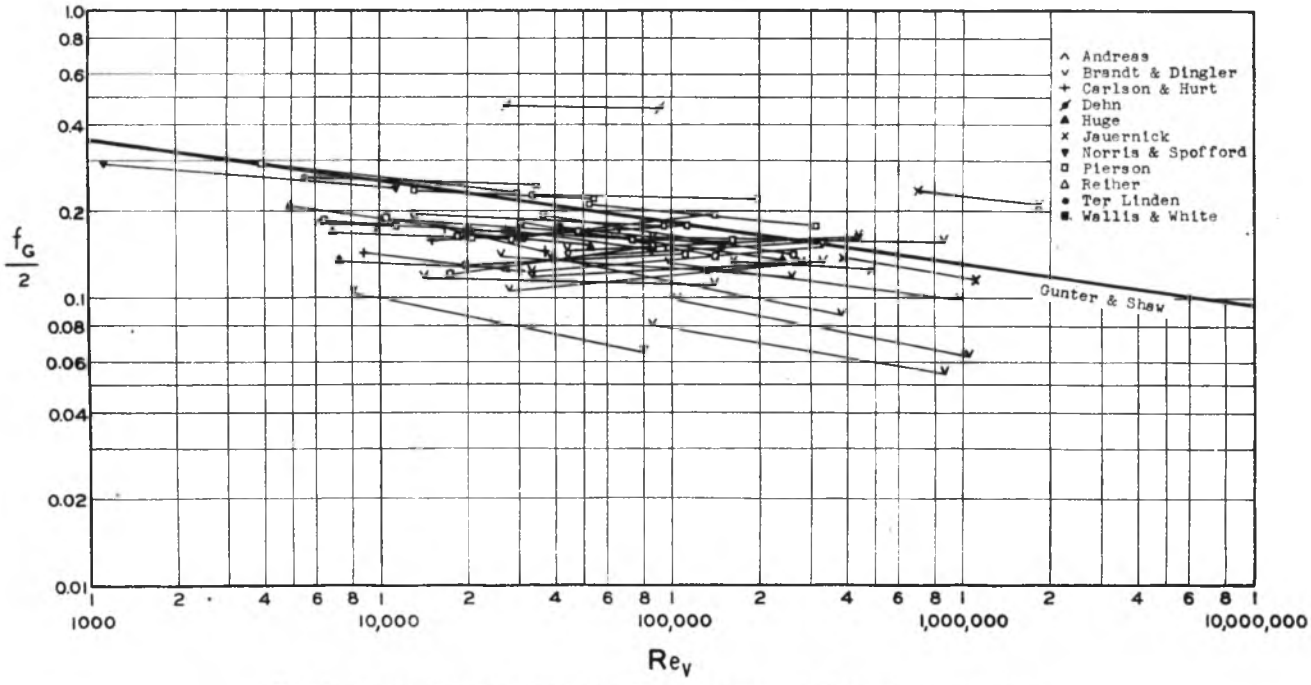

FIG. 9 COMPARISON OF TURBULENT-FLOW DATA FOR IN-LINE ARRANGEMENTS
(Gunter-Shaw method of representation.)

should have been 0.0625 ft, which results in their friction factors being high by 25 per cent. The original calculations of the Sieder-Scott data reported by the authors also contained some errors, which, when rectified, resulted in most of the values originally reported for Reynolds numbers, $D_e G/\mu$, less than 20 being shifted to a Reynolds number tenfold higher. The corrected values are given in Fig. 10 of this discussion. (See page 658).

Summarizing, it would appear that the effect of tube spacing is considerably more complex than the authors' method would imply. The foregoing discussion largely represents excerpts from a forthcoming review paper on the same subject. This paper will compare the various methods that have been proposed for the representation of data on pressure drop across plain tube banks, using all available data. It will be shown that other methods are considerably more accurate and simpler to employ for design calculations in the case of plain tube banks than that

proposed by the authors. Extended surfaces have not been considered, since data are considered still too meager to permit any critical comparison.

S. L. Jameson.[5] The equation for pressure drop in crossflow proposed by the authors is very interesting, both from the degree of correlation they have obtained, and from the ease with which it may be used in design. However, a study of data on the effect of tube spacing in staggered banks of helically finned tubes[6] indicates that the equation requires further study and refinement before it can be generally used.

In Figs. 11 and 12 of this discussion, friction factors are plotted against Reynolds number, as defined by the authors, for the highest and lowest test air flows for the arrangements reported.[6] In all cases the friction factor is calculated on the basis of the free area in a single row of tubes, regardless of the relative free area through the diagonal openings between successive tube rows.

Fig. 11 shows the friction factors for various $^3/_4$-in. tube arrangements as calculated from the authors' equation. The points diverge widely from their curve, and show definite trends of divergence with variation of either the tube spacing across the face of the tube bank, or of variation of the spacing between tube rows.

The authors' equation revised by interchanging S_L and S_T gave a much better correlation of the friction factors for crossflow over finned-tube banks. The revised equation is

$$\frac{f}{2} = \frac{\Delta P\, g\, D_{vp}}{G^2 L}\left(\frac{\mu}{\mu_w}\right)^{0.14}\left(\frac{D_v}{S_L}\right)^{-0.4}\left(\frac{S_T}{S_L}\right)^{-0.6} = \phi\,(\mathbf{R})$$

All symbols are as defined by the authors. The friction factors for all tube arrangements tested[6] are plotted against Reynolds number in Fig. 12. The equation of the curve approximating the data is $f/2 = 1.69\,(\mathbf{R})^{-0.25}$.

A factor to correct air pressure drop for tube spacing in a finned-tube bank is very useful in design (see Fig. 5 of the writer's paper[6]). Factors based on constant air-mass velocity, pressure, and temperature are plotted in Fig. 13 of this discussion. The factors calculated from the revised equation given previously check the test results satisfactorily. The factors calculated using the original relation of the authors show about double the test correction for tube spacing across the face of the tube bundle, and a decrease in pressure drop with a decrease in spacing between rows, rather than an increase as found in the tests.

The revised equation indicates about double the effect of change in number of fins on pressure drop as was obtained in tests of finned-tube banks.

The revised equation correlates the data for cross-

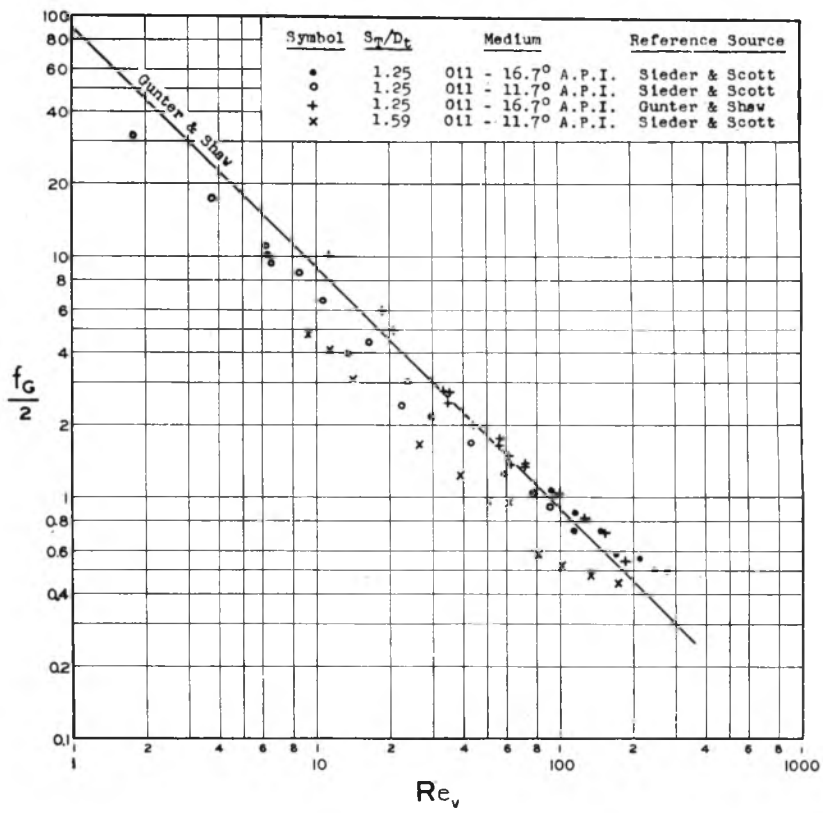

Fig. 10 Comparison of Streamline-Flow Data on Gunter-Shaw Method of Representation

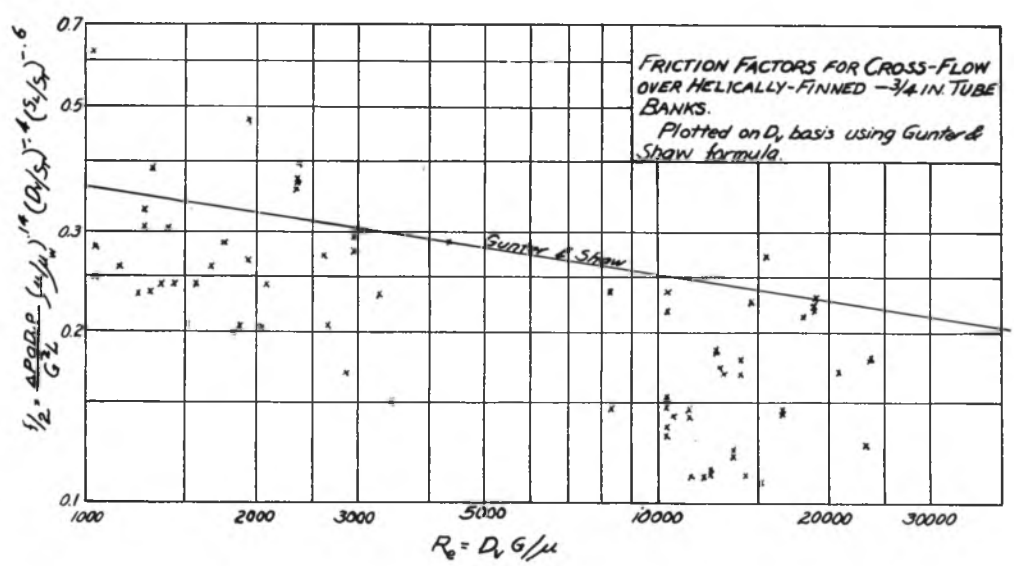

Fig. 11 Friction Factors for Crossflow Over Helically Finned $^3/_4$-In. Tube Banks (Plotted on D_v basis using Gunter and Shaw formula.)

[5] Construction Engineering Division, General Electric Company, Schenectady, N. Y. Mem. A.S.M.E.

[6] "Tube Spacing in Finned Tube Banks," by S. L. Jameson, Trans. A.S.M.E., vol. 67, 1945, pp. 633–642.

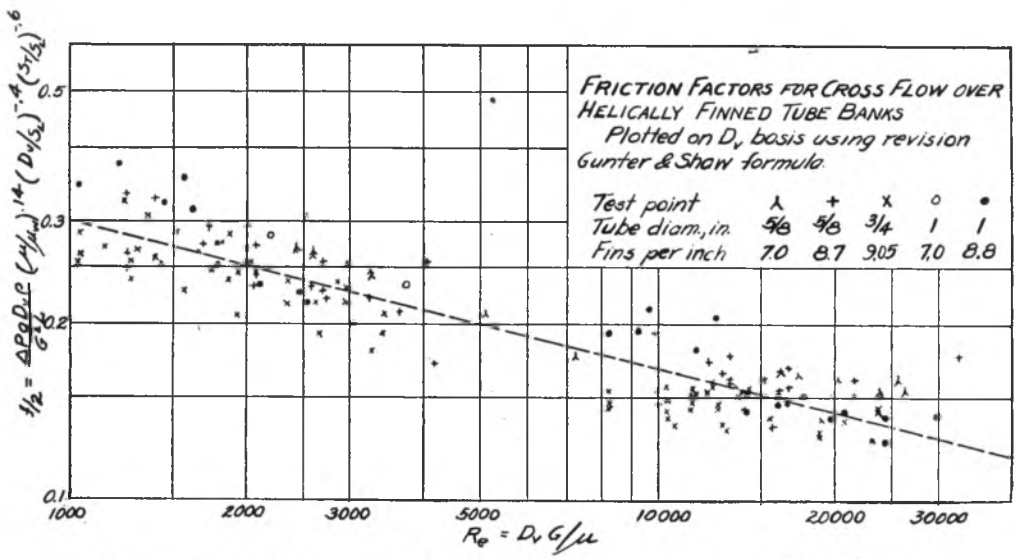

FIG. 12 FRICTION FACTORS FOR CROSSFLOW OVER HELICALLY FINNED TUBE BANKS
(Plotted on D_v basis using revision Gunter and Shaw formula.)

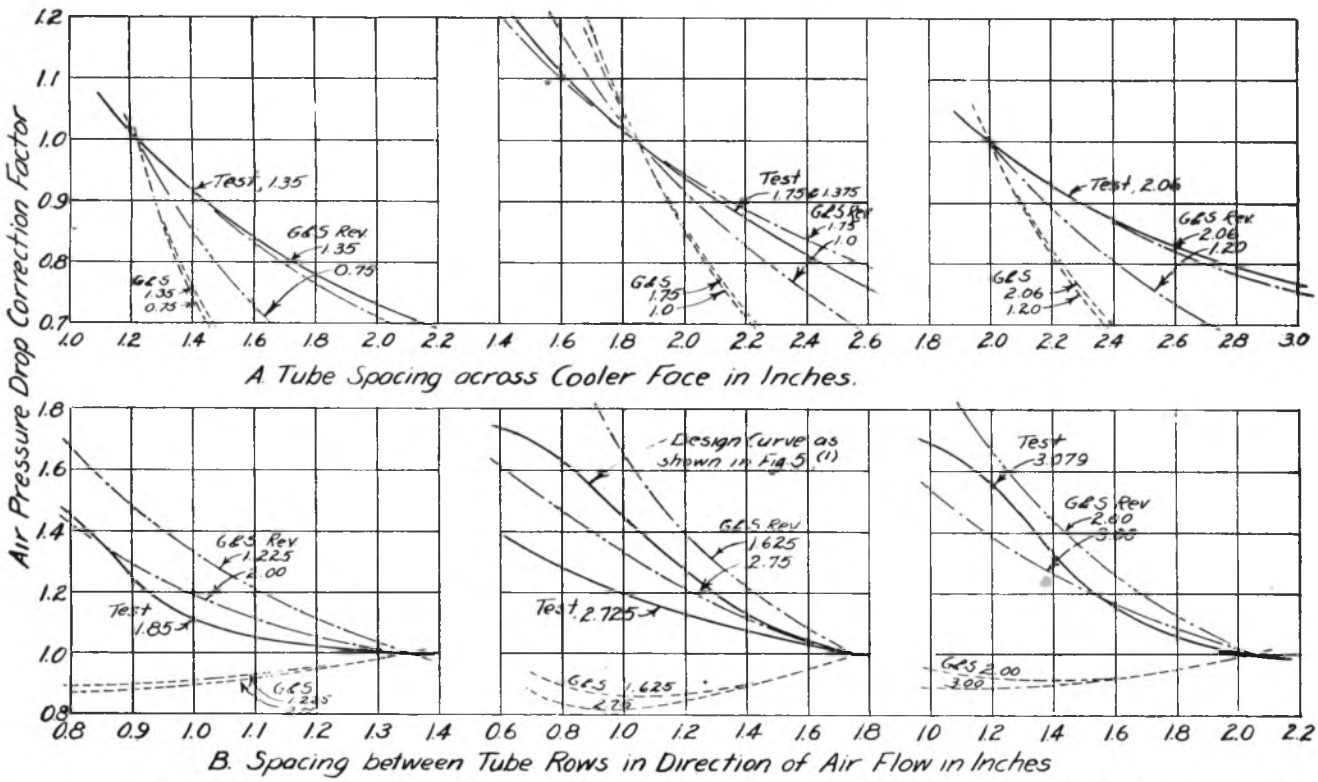

FIG. 13 FACTORS TO CORRECT AIR PRESSURE DROP FOR TUBE SPACING IN BANKS OF HELICALLY FINNED TUBES
(Correction factors are based on constant air-mass velocity and on $f/2$ varying as $R_e^{-0.25}$. Curves are designated as follows: G&S factors based on Gunter & Shaw equation. G&S Rev.: Factors based on a revision of Gunter & Shaw equation. Test: Factors based on actual test data. Figures: In curves A, spacing between rows; in curves B, tube spacing across cooler face.)

flow across banks of helically finned tubes much better than does the original equation of the authors, but both require much study and revision before they may be applied to all types of surface in crossflow.

AUTHORS' CLOSURE

The authors appreciate the contribution, by Messrs. Boucher and Lapple and Mr. Jameson, of some thought-provoking discussion material on the subject paper. Although their comments seemingly refute certain parts of the over-all correlation these are welcome, since it is only by constructive criticism that progress can be made in a field in which, admittedly, such advances are desirable.

With regard to the Boucher and Lapple comments, it is agreed that some over-all accuracy is lost in attempting a crossflow friction correlation which presumes to take care of both staggered and in-line, bare and extended-surface tubes; at the same time it is observed that a single curve covering both streamline and

turbulent flow is most advantageous for practical engineering application. It might be well to point out that a majority of the additional data cited by Messrs. Boucher and Lapple fall outside the "conventional arrangement" limitations imposed by the paper, and that "single cylinder" effects predominate.

Further, as originally mentioned under "Bare Tubes" in the paper, "friction data of Carrier, Allen, Soule, Dehn, Reiher and Reitschel..... (were) used to establish the correlation but are not shown." Recheck of this material against discussers' Figs. 8 and 9 reveals inconsistencies of their plots here. The reference to Pierson's and Huge's data "not included" is refuted by the statement that a majority of the minimum and maximum cases of these investigators were reported on in the paper while random tests of the remainder were made to check the validity of the correlation, but were not published.

With regard to the streamline region of the curve, it is unfortunate that only two tube arrangements were available. However, a number of extended-surface arrangements were applied which confirm this portion of the plot, in good agreement with the bare-tube data. Moreover, from a practical standpoint, the authors have used a large number of heating and cooling streamline flow tests which fall on the suggested line, using the well-known Sieder and Tate μ/μ_w viscosity correction ratio. Conclusion 4 of the paper admitted this scarcity of variety in the data available for this range of the correlation, and thereby justified the foregoing procedures. In any case, the authors' curve is found to be more conservative than that of Chilton and Genereaux (20).

In this connection, critical study was made of the evaluation of the final ΔP values as produced by the two methods. As a result it may be stated that the Chilton and Genereaux correlation gives calculated results for the Seider and Scott isothermal data, for example, with average deviation of approximately -20 per cent, as against approximately $+10$ per cent for the new correlation recommended by the authors. Since practical applications always countenance a certain amount of safety factor, and since, in the final analysis, it is the ultimate values of ΔP which should carry the most weight in establishing the validity of a correlation against actual results, it is felt that the proposed curve is more acceptable in this regard.

In Mr. Sieder's published discussion of the Chilton and Genereaux paper (20) he indicated that the use of two individual plots, covering streamline and turbulent flow, might be confusing and that there definitely is a gradual transition from one type of flow to the other, which is lost in the separate curve presentation. From a practical standpoint as brought out previously, a single curve is also very desirable for commercial use. For these reasons the development of the present correlation was undertaken.

The authors must admit to an error in the published value of D_v for the Wallis-White staggered arrangement, (Line No. 25–38, Table 1). The corresponding in-line data, however, are correctly shown. Further reference to the original plots of authors' Fig. 4 and corrected replots of these data in discussers' Fig. 8 will show that the 20 per cent discrepancy reported by the latter is of minor significance. Whereas the incorrect plotting first fell some 10 per cent above the recommended line, the true replotting positions these points an approximately equivalent amount below. The net result of this shift does not warrant any change in the published curve.

With regard to the tenfold correction reported by the discussers in certain of the Sieder and Scott data for Reynolds numbers originally less than 20, the authors cannot identify the tests referred to, only one run having been located which contained such a change. In addition, four points appear to have been omitted from Boucher and Lapple's Fig. 10 which fall on the published line at Reynolds numbers between 6 through 20.

With reference to Mr. Jameson's discussion, there are several items which warrant comment. In the first place, his reproduction of the authors' basic line as given in Fig. 11 is not strictly correct, being slightly high for the turbulent region shown (compare with Figs. 4 and 5). Moreover, it is to be noted that Fig. 11 is restricted to but one tube size, $^3/_4$ in. A more complete plotting by the authors, including the $^5/_8$-inch and 1-in. tube data shown in Fig. 12 transposed to original basis, falls both above and below the published curve, which represents a good average of these plots (see Fig. 14).

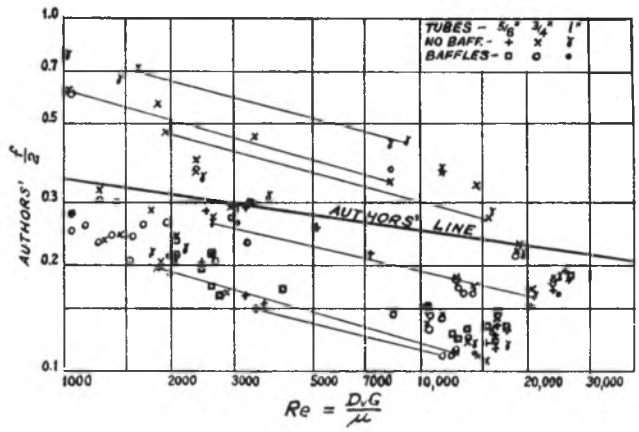

FIG. 14 COMPARISON OF JAMESON FINNED-TUBE DATA WITH TURBULENT REGION OF AUTHORS' RECOMMENDED LINE

It must be pointed out that a minimum of three rows was stipulated as the lower limit of accuracy for the recommended correlation. Since some of Mr. Jameson's work was on one or two rows, it might be expected that these points would plot low, which they do.

As to the suggested revision of the basic equation by interchanging S_L and S_T, the authors cannot subscribe to this as a definitely established, recommended revision of the proposed general correlation. Application of this reversal to bare-tube data destroys the alignment there; hence for general correlation of both bare and extended surfaces, the original published version of the equation and correlation is preferred, at least for the present. The interchanged factor idea, is, however, most interesting, and as a demonstration of possible future work toward refinement of the basic correlation for more over-all accuracy, has much to recommend it.

It is believed that when heat transfer and pressure drop can each be correlated on a single line for both turbulent and streamline flow, using dimensionless correction factor ratios, this is a major advance in crossflow analysis.

Further development of the basic equation must consider the following groups of surfaces—round bare tubes and single cylinders, round tubes plus flat plates (crossfin tubes), and flat tubes plus flat plates (core-type surface).

Air-Cooled Steam Condensers

By R. A. BOWMAN,[1] PHILADELPHIA, PA.

In connection with the rehabilitation of the war-torn areas of the world, there is a great need for power plants which can be moved from one location to another without difficulty, and which can be put into operation in a short period of time. In some of the locations where these power plants must operate, cooling water will be unavailable, or obtainable only at a great premium. To take care of such cases, a number of power trains have been built to use air as a cooling medium rather than water. The trains in general have been widely described. The present paper is devoted to a more complete description of the condensers and to a report on their operation.

POWER trains are expected to operate at temperatures varying from 40 F below zero to + 95 F. The primary purpose of the condenser is to recover condensate and not to reduce the heat rate of the plant by the production of vacuum. Back-pressure operation was chosen for design conditions because the condenser size and power requirements of the blowers would be excessive if a vacuum of any magnitude is to be maintained. At lower air temperatures or at partial loads, vacuum will, of course, be practical, and a single-stage ejector is supplied to take advantage of these conditions.

Details of Condenser and Operating Considerations

The condenser for a 5000-kw power train is placed on two cars, each car containing eight separate condenser sections, air for which is supplied by four propeller-type blowers. Fig. 1 is a general view of the condenser cars. Steam is supplied to the cars through a manifold from the turbine, connecting to a pair of longitudinal steam ducts running the length of the car. The condenser sections are set on these ducts so that steam enters them from the bottom, is condensed, and the condensate drains back into the ducts from which it is removed by a condensate pump. This counterflow relationship between steam and condensate was chosen because it not only serves to heat and deaerate the condensate but also prevents its freezing.

The condensing sections themselves consist of ten rows of finned tubes, mounted vertically. Each section contains 370 tubes, giving 5625 sq ft of finned surface, or a total of 90,000 sq ft for the train. The face area of each section is 42.5 sq ft. The dimensions of the tubes are given in Fig. 2. They are arranged on a 2-in. staggered pitch. The tubes are constructed of steel, with steel fins, and the tube assembly is galvanized inside and out. Steel was chosen for the material because it is adequate for the service and was more available at the time the design was prepared than were the copper-base alloys.

In all condensing apparatus where the latent heat of steam is transferred to a cooling fluid as sensible heat, there will be variations in the condensing capacity of different sections of the condenser. In order to supply each part of the condenser with the steam it requires, it is necessary either to provide a varying pressure drop to the different parts, or to arrange the flow paths so that they will have the proper resistance to limit the steam to that required by the condensing surface. In the ordinary surface condenser this can be accomplished in a natural manner by arrangement of tubes and tube plates. In those cases where the steam is inside of the tubes, nothing can be done to vary the resistance of the individual flow paths, but resistances can be added in the form of orifices to bring about a balance in the steam-flow paths.

A section through the individual condensing unit is shown in Fig. 3, illustrating the method used in this air-cooled condenser to provide balanced steam flows. The tube bank is divided into five separate groups, each group comprising two rows of tubes. The first four of these groups exhaust into the fifth group through orifices. The fifth group of tubes serves as a final condensing section, or what is frequently called an "air-cooler section." The orifices limit the amount of steam which any group can supply to the air cooler, and in order to pass the total steam required by the air-cooler section it is necessary that steam be supplied through all the other four groups of tubes, giving an adequate balance of steam flows.

The requirement that the condenser operate satisfactorily at a temperature of —40 F makes it imperative that every possible precaution be taken to prevent freezing inside the condenser. The greatest danger of freezing arises in those areas which, because of poor distribution or light loading, are not fully supplied with steam. Fortunately, the design which leads to efficient use of the condenser surface by supplying steam to all the tubes in accordance with their capacity to condense it, also serves to keep all areas warm and free from ice.

Avoiding Difficulties at Low Temperatures

Under conditions of light load and cold air the vacuum determined from heat-transfer considerations will exceed that produced by the ejector, and the condenser will begin to fill with air until the point is reached at which the remaining surface supplied with steam is just sufficient to satisfy the heat-transfer equation. As soon as a tube fills with air its temperature will drop approximately to that of the air outside the tube. If this temperature is below the freezing point the condensate which is formed within the tube or flows into it from other sections will freeze. The first tubes in which this will occur are those in the air-cooler section; but since this section is located on the air-discharge side, the air will have been warmed up to a temperature above 32 F in almost all cases. Any reduction in load occurring after the air-cooler section has been blanked off will introduce air at the top of the tubes in the first row where danger of freezing is great.

Each section of the condenser is supplied with a distant-reading thermometer, the bulb of which is located in the top of the center tube of the first row. Since this thermometer bulb is located at a point where freezing is most likely to occur, the operator is given a reliable guide on the danger of ice formation. The operating instructions of the train state that when the temperature as measured by this thermometer falls below 150 F, the amount of air circulated should be reduced by closing down one or more blowers.

In the case of extremely low temperatures and very light loads, it is possible that even with only one car in service and one

[1] Manager, Condenser Engineering, Westinghouse Electric Corporation. Mem. A.S.M.E.

Contributed by the Heat Transfer Division and presented at the Annual Meeting, New York, N. Y., Nov. 27–Dec. 1, 1944, of The American Society of Mechanical Engineers.

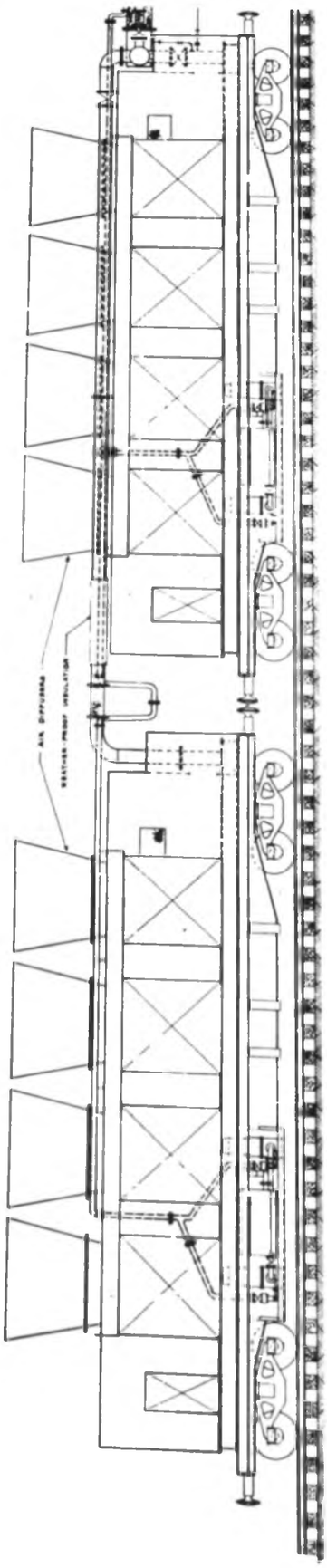

FIG. 1 GENERAL ARRANGEMENT OF CONDENSER CARS

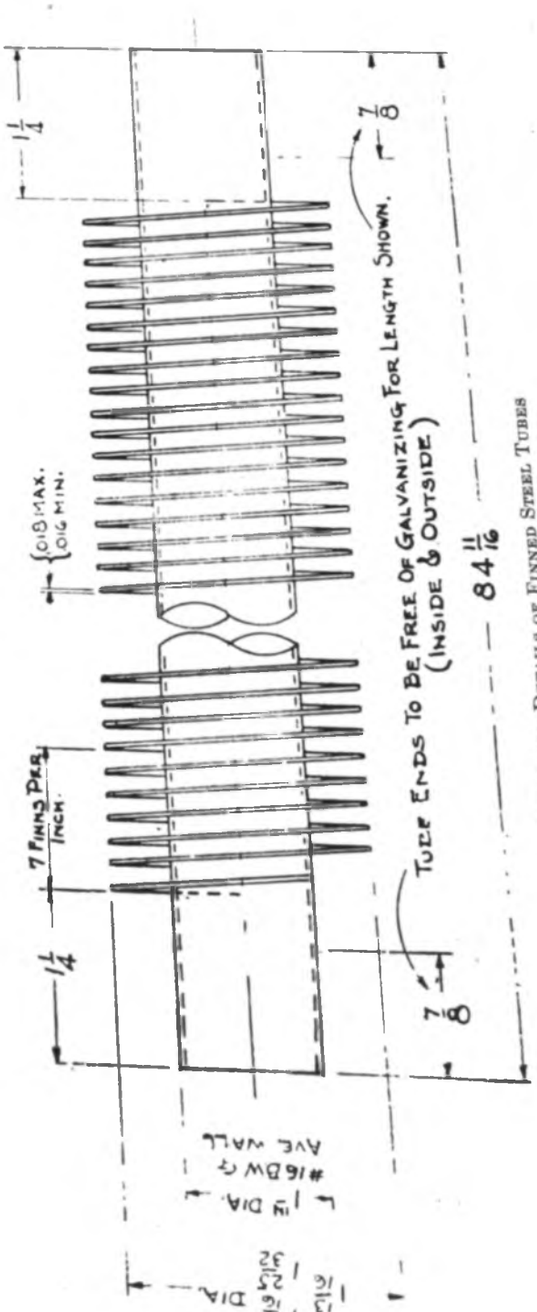

FIG. 2 DIMENSION DETAILS OF FINNED STEEL TUBES

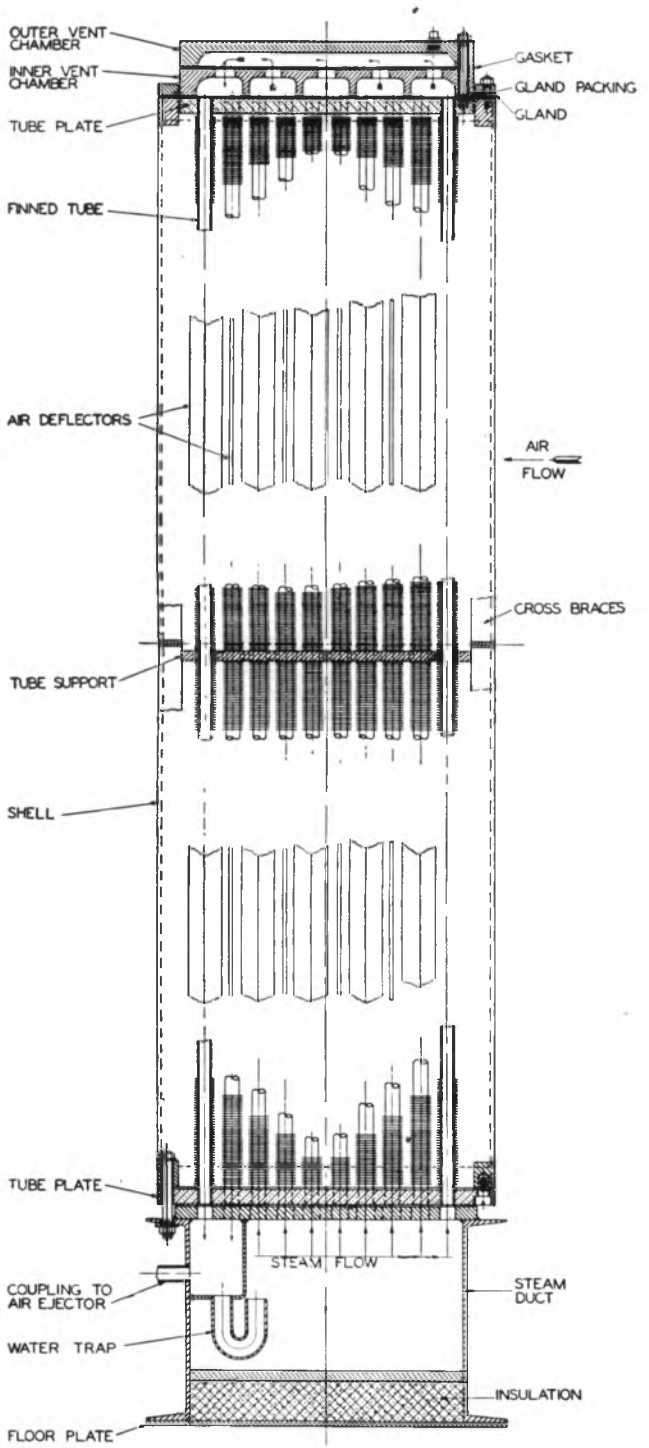

FIG. 3 SECTION THROUGH CONDENSING UNIT

blower operating on that car, the temperature as read on the thermometer will still tend to fall to a dangerous degree. To provide for such an eventuality condensers are equipped with cover plates which can be used to cover a part of the surface of each section to reduce the cooling area and amount of air flowing.

The air-removal system from the sections consists of a manifold running along the car, connected to the air off-take from each section. This manifold delivers the air to the suction of a single-stage ejector which in turn is served by an air-cooled after condenser.

CONDENSER TESTS CONDUCTED

At the time the entire train was tested, readings were made on the condenser. The purpose of these tests was to determine the amount of heat which could be transferred by the condenser under design conditions and were limited to this objective. Time was not available to run tests under carefully controlled conditions or to develop careful instrumentation. Test data were obtained on the following items:

1 Ambient temperature.
2 Barometer.
3 Air temperature leaving condenser.
4 Steam temperature.
5 Steam flow to the condenser.
6 Air-pressure drop through condenser.

The temperatures were measured with glass thermometers, except for the temperature of the air leaving the condenser which was measured by means of thermocouples. The steam pressure in the duct was measured with a mercury column, the pressure drop through the condenser with a water column, and the amount of steam flowing with a calibrated commercial flowmeter at the boiler. The test results are given in Table 1.

TABLE 1 TEST RESULTS ON CONDENSER

Test no.	1	2	3
Ambient temperature, deg F	94.25	86.8	70.3
Barometer, in. Hg	28.95	28.93	28.86
Air temperature from condenser, deg F	202.2	184.2	171.3
Steam temperature, deg F	225.4	217.2	202.4
Steam condensed, lb per hr	79860	78640	78140
Air-pressure drop, in. H_2O	2.4	2.53	2.64
Heat load, Btu per hr	75,330,000	74,360,000	75,830,000
Heat-transfer rate	13.4	11.7	12.0
Face velocity, psf per hr	4300	4700	4640

Tests on the air-cooled condenser for the power train indicate that such a condenser is entirely practical where conditions justify its use. It has the advantage that no water is required for cooling and can be put into operation without connection to an outside source of cooling medium. Because of the poor heat-transfer properties and the low specific heat of air, such a condenser in general requires higher auxiliary power, greater investment, and higher back pressure on the turbine than would the usual water-cooled condenser. For this reason it is not likely to find many profitable applications in the power-generation field, and its use will be confined to those extreme conditions where water is not available, and the increased cost and reduced operating efficiencies can be justified.

Discussion

S. KOPP.[2] The air-cooled steam condenser described by the author is an interesting application of extended heat-transfer surface to meet a wartime need in the power-generation field. As mentioned by the author, only in rare cases will such condensers be used in peacetime for this purpose. The power requirements for the blowers is high, although this could be reduced by increasing the amount of heat-transfer surface.

At the present time several companies are manufacturing standardized air-cooled heat exchangers which are being used in those sections where water is scarce or may only be obtained at a premium. Several of these installations are quite large and justify their installation from an economical standpoint. The writer knows of one case where the cost of installing a water line plus the cost of a cooling tower alone far exceeded the total cost of an air-cooled heat exchanger.

[2] American Locomotive Company, Alco Products Division, New York, N. Y. Mem. A.S.M.E.

Heat Transfer Through Tubes With Integral Spiral Fins

By D. L. KATZ,[1] K. O. BEATTY, JR.,[1] AND A. S. FOUST[1]

Heat-transfer data are presented for a group of tubes having integral spiral fins. The group includes tubes with a range of from 4 to 24 fins per in. and from 0.05 to 0.38 in. fin height. Seven series of measurements were made, using steam, air, water, and oil as fluids. The data are compared, when possible, with theoretical equations which apply to the particular heat transfer. The performance of tubes with the extended surface is compared in all cases with that of plain tubes tested under similar conditions.

Nomenclature

The following nomenclature is used in the paper:

A_0 = outside area of tube, sq ft per ft
A_1 = inside area of tube, sq ft per ft
c_p = heat capacity of fluid, Btu per lb per deg F
D_0 = diameter of tube over fins, in.
D_1 = inside diameter of tube, in.
D_E = equivalent diameter or diameter of a plain tube which has the same longitudinal cross section as the finned tube (including fins)
D' = inside diameter of outside wall of annulus minus D_E of inner tube
G = mass velocity, lb per sq ft per sec
h = film coefficient, Btu per hr per deg F per sq ft
k = thermal conductivity, Btu (ft per hr per deg F per sq ft)
L = length of tube, ft
q = rate of heat transfer, Btu per hr
Δt = logarithmic-mean temperature difference
U_0 = over-all heat-transfer coefficient, Btu per hr per deg F per sq ft outside surface
U_L = over-all heat-transfer coefficient, Btu per hr per deg F per ft length of tube
V = velocity, fpm, V_{max} = velocity at minimum cross section
μ = viscosity, lb per ft sec

Introduction

Heat-transfer measurements have been made on eighteen tubes with integral spiral fins and two plain tubes. The tubes were made of copper and were either of $^1/_2$ or $^5/_8$ in. nominal diameter with actual dimensions as given in Table 1. Fig. 1 shows the nature of the integral spiral fins which are formed from a plain thick-walled tube. With the exception of tubes Nos. 13, 14, and 24, the fins have a small uniform taper; the tip of the fin is from 60 to 80 per cent as thick as the base. Fig. 1(*a*) shows the nature and magnitude of corrugations inside the tubes.

Seven groups of heat-transfer measurements were made with steam, air, water, and a mineral oil as fluids, as follows:

Series A: Heat transfer from steam inside single horizontal tubes to air in forced convection outside.

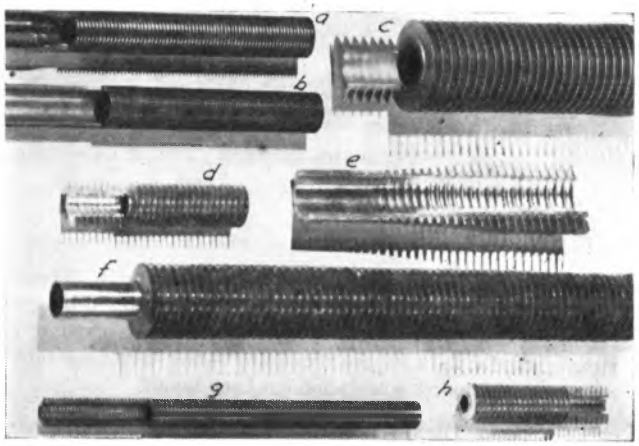

Fig. 1 Integral Spiral-Finned Tubing

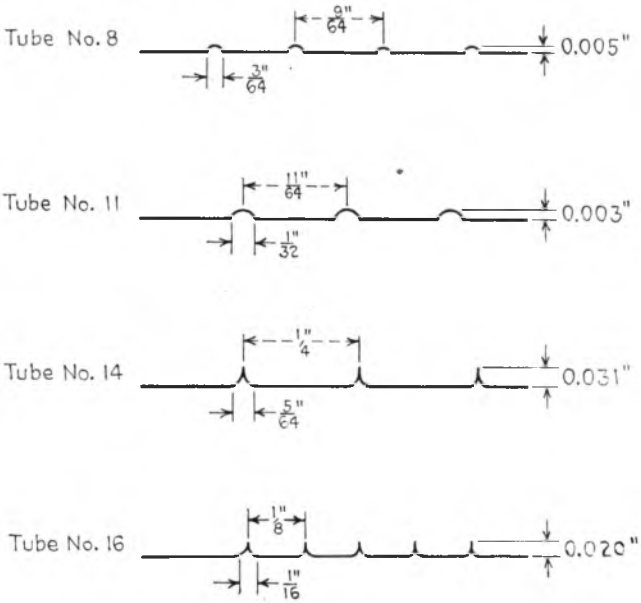

Fig. 1(*a*) Dimensions of Corrugations on Inside of Typical Tubes

Series B: Heat transfer from steam inside banks of vertical tubes to air in forced convection outside.

Series C: Heat transfer between cold water inside single horizontal tubes and humid air in forced convection outside.

Series D: Heat transfer between water inside single horizontal tubes and steam outside.

Series E: Heat transfer between steam inside single horizontal tubes and water in annular space outside.

Series F: Heat transfer between water inside single horizontal tubes and hot oil in annular space outside.

Series G: Heat transfer between steam inside single horizontal tubes and oil in annular space outside.

[1] Department of Engineering Research, University of Michigan, Ann Arbor, Mich.

Contributed by the Heat Transfer Division and presented at the Annual Meeting, New York, N. Y., Nov. 27–Dec. 1, 1944, of The American Society of Mechanical Engineers.

TABLE 1 DIMENSIONS OF TUBES TESTED

Tube no.	Fins per in.	Fin height, in.	A_0 ft² per ft	A_1 ft² per ft	Root diam, in.	Inside diam, in.	Outside fin diam, in.	Fin thickness, in.	D_E, in.[a]	Face depth of duct during Series A, in.
1	16.1	0.050	0.46	0.144	0.640	0.550	0.740	0.016	0.666	1.25
4	24	0.044	0.556	0.143	0.628	0.548	0.717	0.012	0.654	1.00
7	None	0	0.163	0.143	0.625	0.547	...	...	0.625	1.00
8	7.5	0.228	0.964	0.147	0.662	0.562	1.115	0.020	0.730	1.50
9	None	0	0.131	0.110	0.500	0.422	...	...	0.500	1.00
10	7.7	0.335	1.46	0.141	0.620	0.540	1.291	0.024	0.744	1.291
11	5.8	0.300	1.01	0.142	0.622	0.542	1.223	0.024	0.706	1.223
12	8.1	0.320	1.47	0.148	0.640	0.564	1.280	0.024	0.764	1.280
13	4.0	0.123	0.281	0.106	0.481	0.404	0.725	0.035[b]	0.515	1.50
14	4.0	0.235	0.505	0.111	0.500	0.424	0.970	0.032	0.560	1.50
15	3.9	0.380	0.81	0.111	0.500	0.424	1.260	0.027	0.580	1.50
16	8.0	0.285	1.28	0.149	0.645	0.569	1.215	0.024	0.754	1.215
22	8.33	0.166	0.617	0.114	0.503	0.436	0.835	0.024	0.569	1.215
23	9.00	0.119	0.471	0.113	0.492	0.432	0.730	0.022	0.539	1.215
24	3.8	0.157	0.336	0.102	0.500	0.390	0.815	0.037	0.544	1.215
25	3.8	0.286	0.594	0.104	0.518	0.398	1.090	0.032	0.588	1.09
26	3.8	0.316	0.66	0.104	0.518	0.398	1.150	0.032	0.595	1.15
27	5.8	0.250	0.74	0.111	0.510	0.424	1.010	0.027	0.588	1.01
28	6.0	0.141	0.43	0.115	0.521	0.441	0.840	0.027	0.567	1.01
29	6.0	0.347	1.09	0.116	0.525	0.445	1.220	0.024	0.625	1.22

[a] D_E is the diameter of a plain tube which has the same longitudinal cross section as the finned tube (including fins).
[b] Estimated.
NOTE: A_0 = outside area. A_1 = inside area.

Over-all coefficients of heat transfer were measured in all cases. The results for Series A, B, and C have been correlated by generally accepted methods and are presented as correlation curves. The experimental data for the remaining series have been tabulated, since no complete correlation has been found.

SERIES A HEAT TRANSFER FROM STEAM INSIDE SINGLE HORIZONTAL TUBES TO AIR IN FORCED CONVECTION OUTSIDE

Single tubes 3 ft long were placed in a horizontal position as shown in Fig. 2. Air blown normal to the axis of the tube was controlled by vanes which had a spacing at the position of the tube as listed in Table 1. Calming was accomplished by six vertical vanes 16 in. long, as indicated in Fig. 2. Inlet- and outlet-air temperatures were measured by mercury-in-glass thermometers.

Steam was admitted to the inside of the tubes at 10 psig, and the condensate was collected in a calibrated tank. Care was exercised that noncondensable gases did not accumulate in the condensate receiver.

The observed rate of steam condensation, corrected for radiation losses, was used to calculate the rate of heat transfer. The air rate on a weight basis was calculated from the measured rise in air temperature and the heat-transfer rate.

Over-all coefficients of heat transfer are expressed either as U_L or U_0, as calculated from the following equations

$$U_L = \frac{q}{L\Delta t} = \frac{\text{Btu}}{\text{(hr) (deg F) (ft)}} \quad \ldots\ldots [1]$$

$$U_0 = \frac{q}{LA_0\Delta t} = \frac{\text{Btu}}{\text{(hr) (deg F) (sq ft)}} \quad \ldots\ldots [2]$$

where q = heat-transfer rate, Btu per hr
L = length of tube, ft
A_0 = sq ft of outside tube surface per ft of length
Δt = logarithmic-mean temperature difference between steam and air

The relation between the two coefficients is

$$U_L = U_0 A_0 \quad \ldots\ldots [3]$$

From the data obtained, correlations have been developed between the heat-transfer coefficient U_0, and the air velocity at the minimum free cross section, V_{max}. Air velocity is expressed in feet per minute of standard air defined at 70 F, 29.92 in. mercury barometer, and 50 per cent relative humidity. At these conditions, the specific volume of air is 13.5 cu ft per lb. In calculating the minimum free cross section, allowance is made for the longitudinal cross-sectional area of the tube, including the fins.

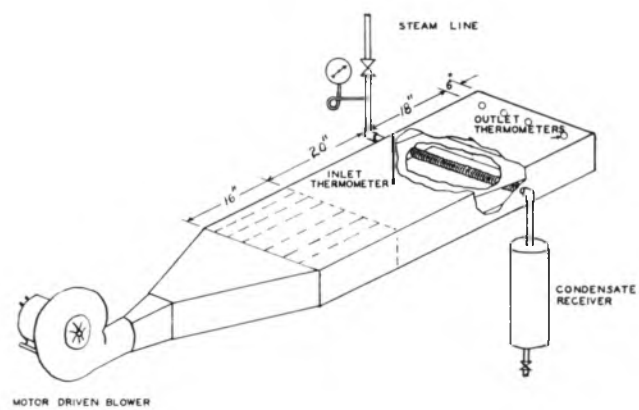

FIG. 2 APPARATUS USED FOR HEAT-TRANSFER MEASUREMENTS ON SINGLE TUBES
(Section through duct and top vane to show tube.)

The correlations for the data on the tubes of Table 1 are presented in Figs. 3, 4, and 5, as plots on logarithmic co-ordinates. Fig. 3 includes the data for tubes having outside-surface areas in excess of 0.65 sq ft per ft. Fig. 4 shows the data for tubes having outside-surface areas less than 0.65 sq ft per ft. In each figure, the tubes included range from those having 4 to those having 9 fins per in. The straight line in Fig. 3 has the equation

$$U_0 = 0.229\, V_{max}^{0.53} \quad \ldots\ldots [4]$$

In Fig. 4 the straight line drawn corresponds to

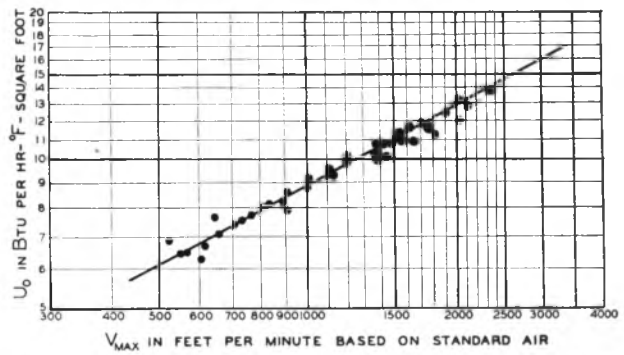

FIG. 3 OVER-ALL COEFFICIENTS OF HEAT TRANSFER FOR SINGLE TUBES AGAINST AIR VELOCITY AT MINIMUM FREE CROSS SECTION
(Data for tubes Nos. 10, 12, 15, 16, 26, 27, and 29.)

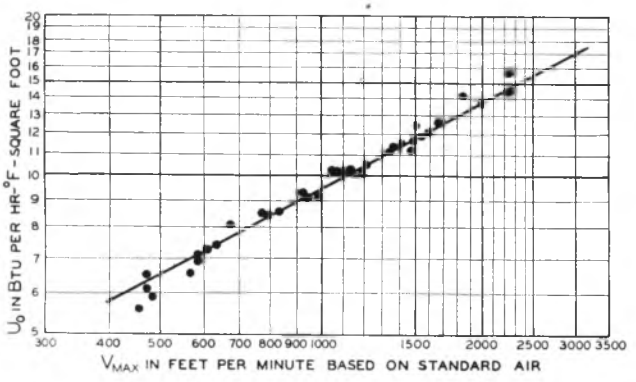

FIG. 4 OVER-ALL COEFFICIENTS OF HEAT TRANSFER FOR SINGLE TUBES AGAINST AIR VELOCITY AT MINIMUM FREE CROSS SECTION
(Data for tubes Nos. 11, 22, 23, 24, 25, and 28.)

$$U_0 = 0.244\, V_{max}^{0.53} \quad [5]$$

Both groups of data agree within approximately ±7 per cent with a single line drawn in between the two lines shown. This line has the equation

$$U_0 = 0.236\, V_{max}^{0.53} \quad [6]$$

Fig. 5 contains the data on the two low-finned tubes Nos. 1 and 4 and the plain tubes, Nos. 7 and 9. Equation [6] is plotted as a dashed line for comparison. The extended surface of the fins for the tubes in Figs. 3 and 4 is slightly more effective per square foot than the surface of the plain tube. The tubes 1 and 4 are low-fin tubes having 16 and 24 fins per in. The curves show

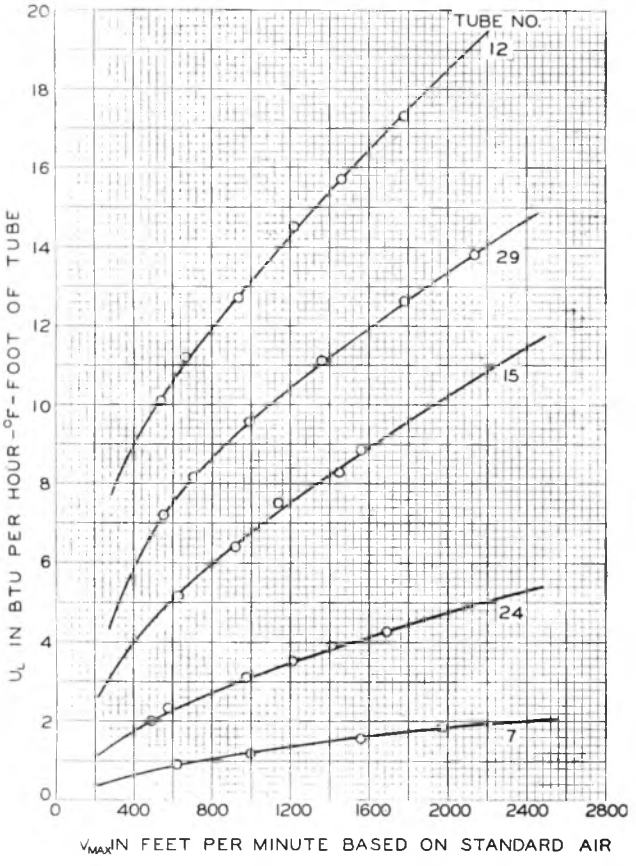

FIG. 6 HEAT-TRANSFER COEFFICIENTS PER FOOT FOR TYPICAL TUBES FROM THOSE TESTED

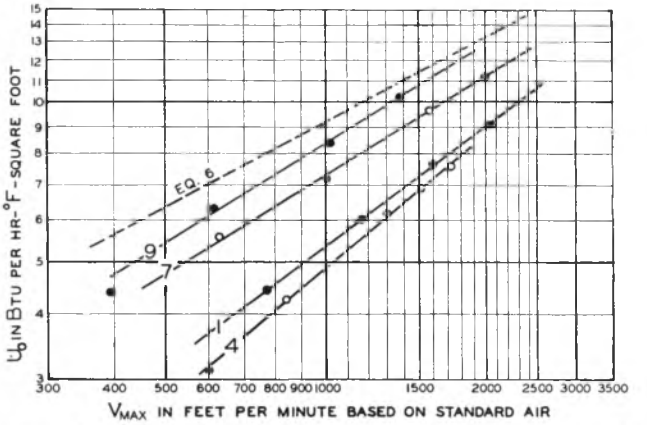

FIG. 5 OVER-ALL COEFFICIENTS OF HEAT TRANSFER FOR SINGLE TUBES AGAINST AIR VELOCITY AT MINIMUM FREE CROSS SECTION
(Data for tube numbers as labeled on curves.)

that the increase in surface produced by the fins does not cause a proportionate increase in the heat-transfer coefficient per foot of length. This is probably because the fins are too close together to permit free passage of air between them.

In Fig. 6 certain of the data have been plotted as U_L, the heat-transfer coefficient per foot of length, against the air velocity at minimum free cross section. This figure illustrates the wide differences in fin heights and fin pitches of the tubes tested. The consequent variations in outside tube surface per foot of length make great differences in the heat-transfer coefficients, based on the length of the tube.

SERIES B HEAT TRANSFER FROM STEAM INSIDE BANKS OF VERTICAL TUBES TO AIR IN FORCED CONVECTION OUTSIDE

One single row of 12 tubes and one double-row unit were used for heat-transfer measurements on banks of tubes. The dimensions of the units and of the finned tubes used in them are given in Table 2. Fig. 7 is a sketch of the apparatus used in testing the two finned-tube units. The units were set with tubes vertical in a duct of cross section equal to the face dimensions of the unit. Measurements of steam condensed and air-temperature rise were made at a variety of constant air velocities for each of several different steam pressures. Steam pressures used were 5, 25, 50, 75, 100, and 125 psig. Face air velocities were varied from 200 to 750 fpm, based on standard air.

Calculations of the data were made in the same manner as with single tubes. The calculated values of U_0 are plotted against V_{max}, on logarithmic co-ordinates in Fig. 8. No distinction has been made between points obtained at various steam pressures,

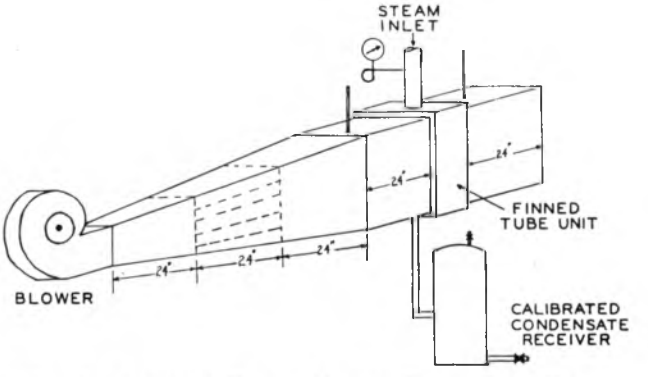

FIG. 7 APPARATUS USED IN TESTING FINNED-TUBE UNITS

TABLE 2 DIMENSIONS OF UNITS TESTED

SINGLE-ROW UNIT

Dimensions:

Face, in. high × in. wide	24.5 × 17.6
Face area, sq ft	3.0
Minimum free area, sq ft	1.55
Number of tubes	12
Number of rows	1
Total length of tubes, ft	24.5
Total heat-transfer area, sq ft	25.95
Center-to-center tube spacing, in.	1.41

Data on tube in single-row unit:

N = 5.80 fins per in.
H = 0.314 in. = fin height
A_0 = 1.056 sq ft per ft = outside tube surface
D = 0.622 in. = root diam of tube
D_0 = 1.250 in. = outside fin diam
D_E = 0.709 in.

DOUBLE-ROW UNIT

Dimensions:

Face, in. high × in. wide	24.5 × 17.6
Face area, sq ft	3.0
Minimum free area, sq ft	1.461
Number of tubes	24
Number of rows	2
Total length of tubes, ft	49
Total heat-transfer area, sq ft	75
Tube arrangement	Staggered 2 rows, 1.5 in.
Center line to center line	12 tubes, 1.41 in., center to center in each row

Data on tube in double-row unit:

N = 7.80 fins per in.
H = 0.347 in. = fin height
A_0 = 1.056 sq ft per ft = outside tube surface
D = 0.621 in. = root diam of tube
D_0 = 1.315 in. = outside fin diam
D_E = 0.751 in.

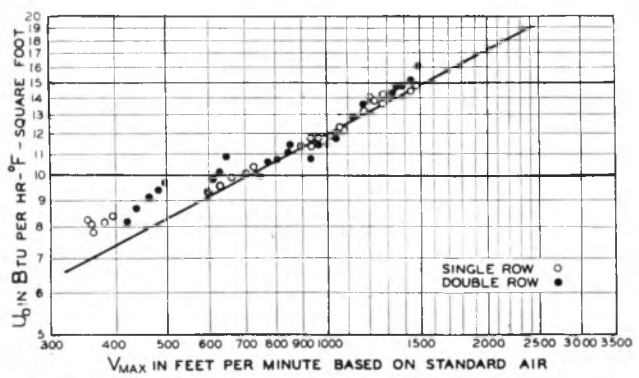

FIG. 8 OVER-ALL COEFFICIENTS OF HEAT TRANSFER FOR TUBE BANKS AGAINST AIR VELOCITY AT MINIMUM FREE CROSS SECTION

since no trend was observed. The straight line in the figure has the equation

$$U_0 = 0.308\ V_{max}^{0.53} \quad [7]$$

A comparison of this equation with Equation [6] for similar single tubes shows that the heat-transfer coefficients at a given air velocity are approximately 30 per cent higher when the tubes are arranged in banks than when they are used singly. This increase is probably caused by a greater turbulence of the air around the tubes in banks, or could be attributed partially to the layer of condensate accumulating inside the horizontal tube. The effect of turbulence has been observed by other investigators[2,3] between a single row and a bank of several rows with plain tubes. It appears that a single row of finned tubes causes turbulence equivalent to several rows of plain tubes and that only minor increases in turbulence occur with added rows of finned tubes. When tubes are to be used vertically in banks, the coefficient should be estimated from the solid line in Fig. 8 and not from Fig. 3 or 4.

SERIES C HEAT TRANSFER BETWEEN COLD WATER INSIDE SINGLE HORIZONTAL TUBES AND HUMID AIR IN FORCED CONVECTION OUTSIDE

Measurements of heat transfer between humid air and cold water were made, using the apparatus in Fig. 2, with modifications. Air entering the blower was conditioned to 80 F, with 50 per cent relative humidity, and held constant. Water cooled to 40 F was circulated through the tube at a velocity of about 200 fpm in the tube. Actual water rates were determined by a calibrated orifice, and the rise in water temperature was measured by Beckmann thermometers in the inlet and outlet streams.

Wet- and dry-bulb temperatures of the inlet air and dry-bulb temperature of the outlet air were measured by mercury-in-glass

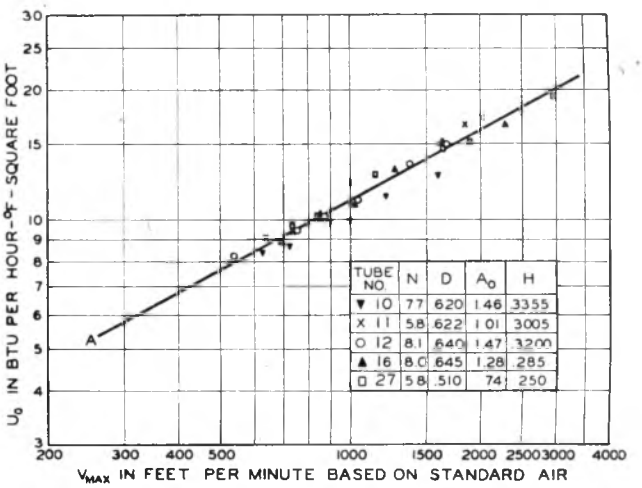

FIG. 9 OVER-ALL HEAT-TRANSFER COEFFICIENTS, HUMID AIR TO COLD WATER FOR TUBES WITH EIGHT HIGH FINS PER INCH

thermometers. The rate of heat transfer was computed from the measurements on the water side. The air rate was computed by a heat balance, assuming the air to have been cooled and dehumidified according to the "contact-mixture theory."[4] This method was considered more reliable than wet-bulb measurements on the outlet air because of the possibility of condensate from the tube being entrained in the air stream.

The over-all coefficients of heat transfer were computed using Equation [2]. The results for five high-finned tubes which follow the same curve A are given in Fig. 9. A similar curve was drawn for tubes Nos. 15, 25, 26, and 28. It is shown in Fig. 10, as curve B, which figure also includes curve A of Fig. 9 and the data for seven individual tubes. Fig. 11 is a comparison of the plain tubes, the low-finned tubes and the curves A and B. The equations for curves A and B are as follows

$$\text{Curve } A \quad U_0 = 0.286\ V_{max}^{0.53} \quad [8]$$

$$\text{Curve } B \quad U_0 = 0.353\ V_{max}^{0.53} \quad [9]$$

In calculating the minimum free cross section of the duct to obtain V_{max} in feet per minute of standard air, allowance was made for a condensate film approximately 0.01 in. thick covering the entire outer tube surface in addition to the longitudinal cross section of the dry tube.

[2] "Correlation and Utilization of New Data on Flow Resistance and Heat Transfer for Crossflow of Gases Over Tube Banks," by E. D. Grimison, Trans. A.S.M.E., vol. 59, 1937, pp. 583–594.

[3] "Heat Transmission," by W. H. McAdams, second edition, McGraw-Hill Book Company, Inc., New York, N. Y., 1942, p. 228.

[4] "Contact Mixture Analogy Applied to Heat Transfer With Mixtures of Air and Water Vapor," by W. H. Carrier, Trans. A.S.M.E., vol. 59, 1937, p. 49.

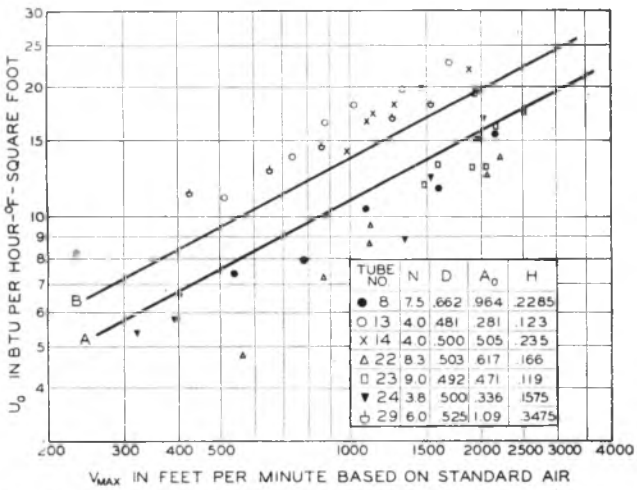

FIG. 10 OVER-ALL HEAT-TRANSFER COEFFICIENTS, HUMID AIR TO COLD WATER FOR TUBES SHOWING HIGH OR LOW COEFFICIENTS

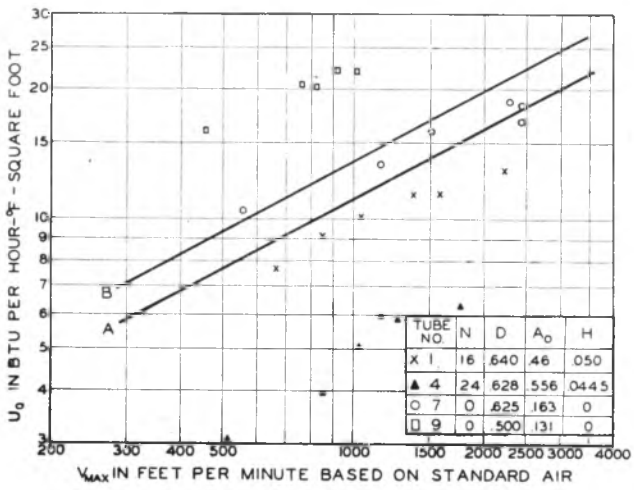

FIG. 11 OVER-ALL HEAT-TRANSFER COEFFICIENTS, HUMID AIR TO COLD WATER FOR PLAIN AND LOW-FIN TUBES

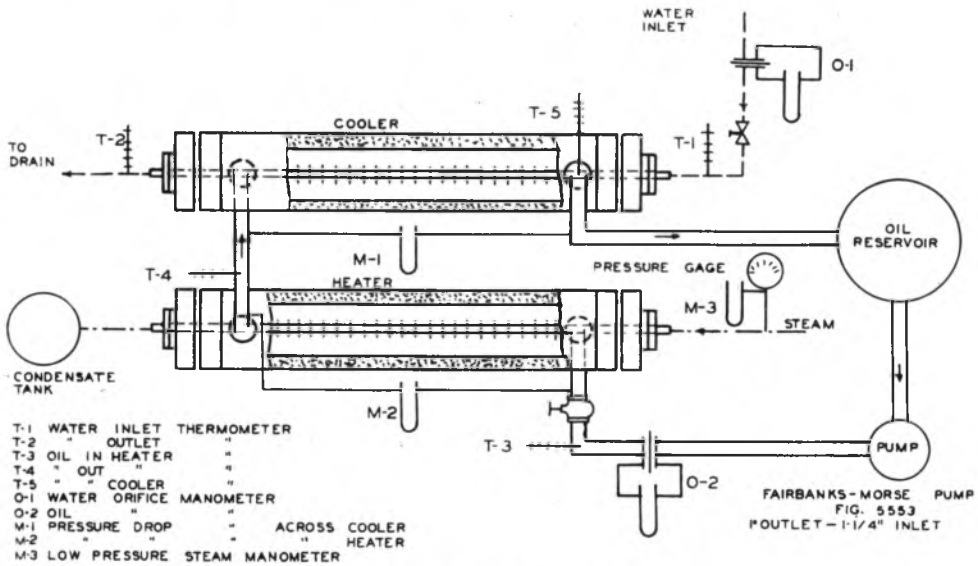

FIG. 12 FLOW DIAGRAM

The fin shape, height, and pitch appear to have considerably more effect on the heat-transfer coefficients of the tubes when they are wet than when dry. In general, the large number of fins per inch give lower coefficients with the extreme effect shown by tube No. 4 with 24 fins (0.044 in. high) per inch, Fig. 11. No explanation can be given for the high coefficients for plain tube No. 9. It should be appreciated that the temperature rise measured for the water was lowest for the plain tubes and rose with increased surface for the finned tubes.

SERIES D HEAT TRANSFER BETWEEN WATER INSIDE SINGLE HORIZONTAL TUBES AND STEAM OUTSIDE

The last four series of tests were made using variations of the apparatus shown in Fig. 12. For Series D, the cooler section only was used with water flow as indicated in Fig. 12, and steam at 25 psig in the annular space outside the tube with condensate going to a calibrated receiver.

The experimental data and calculated coefficients are given in Table 3. The over-all coefficient is composed of the steam-film coefficient on the outside which should remain substantially constant, the copper resistance, and the water-film coefficient on the inside, which should vary as the 0.8 power of the Reynolds number. It was possible to select steam-film coefficients for the outside by the Wilson method,[5,6] which give straight lines of slope equal to 0.8 for the water-film coefficient as plotted in Fig. 13. For many of the tubes no constant value for the resistance of the steam film plus the metal resistance could be found which would give straight lines in Fig. 13. A possible explanation could be that dropwise condensation occurred during the early runs at low water velocity and filmwise condensation gradually set in. In several cases the over-all coefficient was reduced for an increased water velocity, although further increase in water velocity always gave a net increase in the coefficient.

For all finned tubes the water-film coefficient was greater than that predicted by the Dittus-Boelter type equation recommended by McAdams[7]

[5] "Basis for Rational Design of Heat-Transfer Apparatus," by E. E. Wilson, Trans. A.S.M.E., vol. 37, 1915, p. 47.

[6] Reference 3, p. 272.

[7] Ibid., 3, p. 168.

TABLE 3 DATA ON FINNED TUBES; WATER INSIDE, STEAM OUTSIDE

Tube No	Water Temperature Inlet °F	Water Temperature Outlet °F	Water Temperature ΔT °F	Ln Mean ΔT °F	Water Velocity Ft/Sec	Steam Condensed Lbs/Hr	Heat Transferred Steam Btu/Hr	Heat Transferred Water Btu/Hr	Coefficient Btu per Hr per °F per Sq Ft*	Coefficient Btu per Hr per °F per Ft
1	66.2	136.6	70.4	162.0	1.85	56.6	49000	47700	696	99.7
	66.6	129.2	62.6	166.8	3.44	81.6	81900	80100	1130	162.0
	65.1	123.7	58.6	170.0	4.76	114.4	106400	102600	1428	205.0
	64.5	117.3	52.8	172.2	6.43	135.2	126400	124000	1695	242.0
4	66.9	136.9	70.0	164.8	1.70	46.2	43200	45200	610	87.5
	65.9	128.3	62.4	169.7	3.50	83.0	83200	79800	1120	160.0
	65.5	121.1	55.6	173.5	4.85	106.6	99600	98400	1330	190.0
	65.3	117.9	52.6	172.0	6.34	126.5	120000	122000	1655	239.0
7	66.5	129.1	62.6	165.5	1.55	36.9	36400	35400	505	72.5
	65.4	113.0	47.6	178.0	3.57	62.4	58300	48700	765	109.5
	64.8	105.7	40.9	183.0	4.80	78.9	75700	71600	925	132.2
	64.4	100.0	35.6	184.5	6.42	89.6	83800	83500	1050	151.0
8	67.5	142.4	74.9	156.0	1.98	63.5	59000	57700	848	124.5
	66.85	138.6	71.7	163.0	3.45	105.3	98000	90300	1310	192.7
	66.3	133.9	67.6	165.2	4.78	130.0	126100	117500	1670	246.0
	66.2	130.0	63.8	166.3	6.52	161.0	150000	147500	2065	304.0
9	67.1	134.4	67.3	162.8	2.61	46.3	42300	41300	777	85.0
	67.2	125.8	58.6	167.0	5.19	77.5	72300	71500	1310	144.0
	66.9	121.2	54.3	171.2	7.36	103.5	96600	93800	1680	185.0
	66.7	118.0	51.3	173.0	10.10	131.1	122300	121500	2125	234.0
10	66.5	144.5	78.0	157.0	1.82	54.6	50900	49600	766	106.5
	65.6	134.0	68.4	161.5	3.86	99.9	93200	87500	1335	186.2
	65.6	129.4	63.8	166.2	5.15	132.0	123000	115000	1770	230.2
	65.3	126.2	60.9	167.5	6.55	151.0	141000	140000	2000	279.0
11	67.1	144.3	77.2	158.0	1.85	57.9	54100	53300	794	113.0
	66.8	135.2	68.4	163.0	3.35	96.0	89500	84100	1248	178.0
	65.8	128.7	62.9	177.0	5.06	130.0	121200	119800	1550	221.0
	65.4	126.4	61.0	168.0	6.40	158.7	148000	145000	2020	288.0
12	66.0	170.5	104.5	142.4	2.12	97.5	90900	87900	1401	209.0
	65.7	159.2	93.5	149.0	3.19	135.6	126500	118000	1840	274.0
	65.5	149.8	84.3	154.5	4.55	175.7	163800	151800	2280	341.0
	65.5	144.3	78.8	157.5	6.00	206.0	192000	186500	2685	400.0
13	67.7	202.4	134.7	119.0	2.86	96.0	89600	90600	2380	252.0
	67.3	180.8	113.5	135.0	5.42	162.1	151800	144800	3450	366.0
	67.0	171.8	104.8	140.5	7.41	206.0	192500	183000	4200	445.0
	66.8	165.3	98.5	148.7	9.33	239.0	223500	215500	4650	492.0
14	68.2	183.8	115.6	132.0	3.85	112.2	106000	104000	2300	244.0
	68.2	173.1	104.9	139.5	5.65	153.1	143100	138500	2940	332.0
	68.0	163.7	95.7	146.4	7.45	187.2	175000	167000	3420	392.0
	67.8	157.5	89.7	149.5	9.50	220.5	206000	199000	3940	452.0
15	67.3	185.9	118.6	131.0	3.08	90.1	84200	83100	1865	214.0
	66.4	169.7	103.3	142.0	5.98	144.5	135000	132000	2730	314.0
	66.6	157.4	90.8	150.0	7.21	175.7	164000	164000	3180	364.0
	65.8	154.2	88.4	152.0	9.12	217.0	203000	201000	3870	443.0
16	66.6	169.0	102.4	142.5	1.62	70.6	66000	65800	1037	154.0
	65.8	157.7	91.9	150.0	3.52	133.0	124200	120800	1850	272.0
	65.2	151.5	86.3	155.0	4.54	174.7	163200	155200	2310	343.0
	65.2	146.0	80.8	157.5	5.95	206.0	192000	191000	2120	495.0
22	60.7	184.6	123.9	134.6	3.41	112.0	104600	98500	2205	252.0
	60.5	173.8	113.3	141.8	4.05	114.0	106400	107200	2195	251.0
	60.1	153.6	93.5	155.2	5.09	121.0	113700	111300	2120	241.5
	60.0	147.6	87.6	158.7	5.97	128.8	120100	122300	2255	254.7
	59.0	134.8	75.8	164.7	8.08	155.9	145600	145400	2538	289.0
	58.6	130.8	72.2	163.2	9.62	169.8	158300	162600	2775	316.0
23	60.5	180.8	120.3	137.3	3.31	100.5	93800	90900	1980	224.0
	60.4	162.4	102.0	149.5	4.35	113.0	105600	101000	2040	231.0
	60.0	148.0	88.0	158.2	5.38	117.8	110000	108200	2036	230.0
	59.9	139.8	79.9	165.5	6.10	131.8	123000	122100	2210	250.0
	59.5	130.4	70.9	169.0	8.24	143.0	133100	134000	2380	269.0
	59.3	129.0	69.7	170.0	9.35	157.0	146500	148800	2558	289.0
24	60.0	199.0	139.0	124.0	4.06	120.0	112000	105000	2860	292.0
	60.0	180.0	120.0	137.0	5.03	128.5	120000	114000	2815	287.0
	60.0	166.0	106.0	141.0	6.75	146.7	137000	134000	3005	307.0
	60.0	160.0	100.0	151.0	8.05	164.9	154000	150000	3295	336.0
	60.0	151.0	97.0	153.0	8.95	178.7	167000	162000	3520	359.0
	60.0	154.0	94.0	154.0	9.46	186.5	174000	172000	3645	372.0
25	60.0	203.0	143.0	124.0	4.35	130.5	122000	116,000	3160	321.0
	60.0	181.0	121.0	131.0	5.58	136.0	127000	123000	2985	306.0
	60.0	171.0	111.0	143.8	6.44	153.0	143000	134000	3180	324.0
	60.0	162.0	102.0	149.0	8.37	165.0	154000	159000	3450	350.0
	60.0	159.0	99.8	151.0	8.70	182.0	170000	160000	3580	365.0
	60.0	155.0	95.0	156.0	9.66	188.3	176000	172000	3696	372.0
26	59.0	209.8	154.8	115.0	3.09	109.0	102000	90400	2780	289.0
	59.0	175.8	136.8	139.0	4.26	128.6	120000	113000	2690	280.0
	59.0	168.6	109.6	145.0	6.15	145.0	135500	130900	2940	306.0
	59.8	164.0	104.8	148.0	7.16	163.0	152000	146000	3240	337.0
	59.0	154.0	95.4	154.0	8.25	171.3	160000	165000	3260	339.0
	59.0	146.4	87.4	160.0	10.20	192.5	180000	173000	3540	368.0
27	59.6	208.6	149.0	116.0	3.08	116.6	108000	101000	2770	300.0
	59.8	189.4	130.6	132.0	4.23	141.3	132000	121000	2955	320.6
	58.6	175.0	114.4	145.0	5.08	144.6	135000	128000	2825	306.0
	58.6	158.4	99.8	152.0	6.52	160.5	150000	143400	2975	322.0
	58.6	155.2	96.6	153.0	7.25	171.1	160000	154000	3160	342.0
	58.4	152.2	93.8	165.0	8.33	195.0	182000	172000	3520	380.0
28	60.0	200.0	140.0	123.0	3.15	121.0	113000	105000	2565	296.0
	60.0	165.0	105.0	148.0	5.04	142.4	133000	126000	2550	294.0
	60.0	150.0	90.0	164.0	6.45	156.2	146000	138000	2635	300.0
	60.0	145.0	85.0	160.0	7.56	166.0	155000	153000	2790	321.0
	60.0	141.0	81.0	162.0	8.43	181.0	163000	163000	2960	342.0
	60.0	137.0	77.0	164.0	9.33	192.5	180000	171000	3095	357.0
29	60.0	209.0	149.0	116.0	3.84	158.3	148000	141000	3500	408.0
	60.0	192.0	132.0	129.0	5.31	193.9	181000	171000	3900	455.0
	60.0	176.0	116.0	140.0	6.67	211.0	197000	188000	3340	459.0
	60.0	167.0	107.0	146.0	7.55	221.4	207000	197000	3945	460.0
	60.0	168.0	108.0	146.0	8.55	238.0	222000	224000	4360	509.0
	60.0	162.0	102.0	149.0	9.40	260.0	243000	233000	4560	432.0

*Based on Inside Area

$$\frac{hD}{k} = 0.023 \left(\frac{DG}{\mu}\right)^{0.8} \left(\frac{c_p\mu}{k}\right)^{0.4} \qquad [10]$$

This increase is caused by corrugations on the inside diameter which were made during the processing of the tube. Finned tubes having lower corrugations would be expected to have water-film coefficients similar to plain tubes and would follow Equation [10].

Series E Heat Transfer Between Steam Inside Single Horizontal Tubes and Water in Annular Space Outside

Series E was run in a manner similar to Series D but with steam inside the tubes and water outside. The data are presented in Table 4. Over-all coefficients per foot of tube are plotted for some of the tubes in Fig. 14, using water rate as the variable.

In the absence of methods for predicting the film coefficients for the steam inside and the water outside, no correlation was made. For finned tubes the outside area may be several times the inside area. Therefore, even a high film coefficient on the inside such as for steam may become a major portion of the resistance. For example, tube No. 12 at 162 lb of water per min had an over-all coefficient of 453 Btu per hr per deg F per ft of length, or 308 Btu per hr per deg F per sq ft outside area, or 3060 Btu per hr per deg F per sq ft of inside area. The steam-film

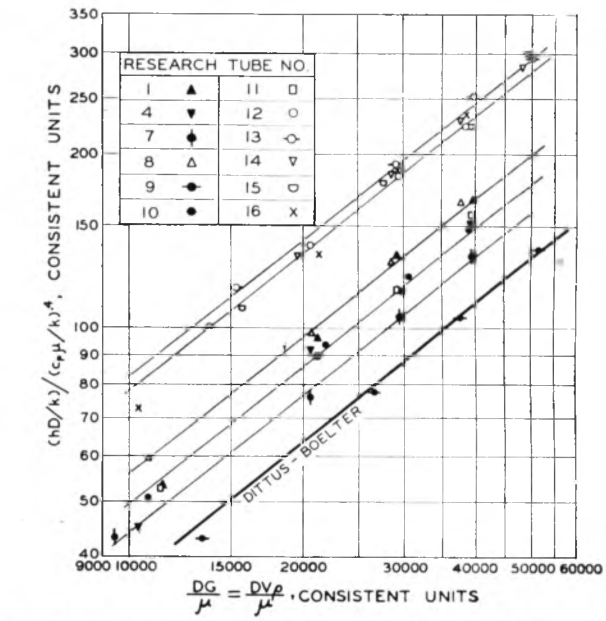

Fig. 13 Data for Film Coefficients of Fluids Inside Unifin Tubes Based on Measurements With Water Inside Tubes Being Heated by Steam Condensing on Outside

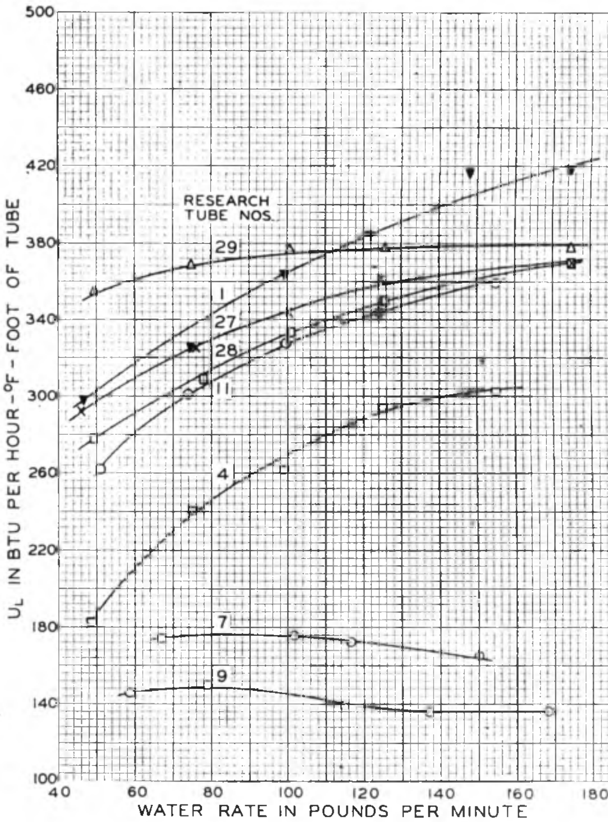

Fig. 14 Over-All Heat-Transfer Coefficients Steam Inside to Water Outside for Tubes With Six Fins per Inch and Plain Tubes

TABLE 4 DATA ON FINNED TUBES; WATER OUTSIDE, STEAM INSIDE

Tube No.	Water Temperature Inlet °F	Outlet °F	ΔT °F	LN Mean ΔT °F	Water Velocity Lbs/Min	Steam Condensed Lbs/Hr	Heat Transferred Water Btu/Hr	Heat Transferred Steam Btu/Hr	Coefficient Btu/Hr/°F Per Sq Ft	Per Ft
1	69.4	123.6	54.2	179.8	46.7	168.3	153,300	157,200	607	298
	65.1	104.9	39.8	181.5	75.0	188	179,200	175,900	668	326
	67.1	101.3	34.2	182.3	99.5	208	204,000	194,000	757	364
	66.1	94.9	28.8	186.0	122.0	231	212,000	216,000	810	384
	66.3	92.9	26.6	186.9	148.0	247	236,000	232,000	880	417
	66.0	88.4	22.4	189.3	175.0	255	238,000	238,000	886	418
4	67.8	101.6	33.8	181.8	48.5	108.2	98,200	101,000	322	183
	67.6	97.0	29.4	184.2	75	144.1	132,000	134,800	426	241
	67.1	91.6	24.5	187.2	97	162.6	142,800	152,000	465	262
	66.9	89.4	22.5	188.4	125	177.0	167,600	165,600	571	294
	66.2	84.4	18.2	191.2	155	191.0	169,000	178,600	534	302
7	67.5	91.4	23.9	187.0	67	113.1	96,500	98,300	1060	173.6
	66.7	83.3	16.6	191.6	102	118.8	101,000	101,000	1074	176.0
	66.7	80.7	14.0	192.8	117	112.9	98,400	101,000	1053	172.5
	67.1	77.4	10.3	194.2	150	108.1	92,600	100,000	1010	165.0
8	67.9	117.9	50.0	174.1	53	33.0	156,000	164,000	348	297
	67.1	107.0	39.9	178.9	76	37.3	183,000	172,600	348	336
	66.7	99.5	32.8	183.4	99	38.9	194,600	192,000	364	352
	66.7	95.0	28.3	185.6	121	40.2	205,000	199,400	376	367
	66.6	89.3	22.7	188.6	153	40.9	208,000	210,000	382	370
	66.3	87.6	21.3	189.5	172	42.6	220,000	217,000	398	385
9	67.8	90.9	23.1	187.7	58.5	89.5	81,300	83,600	1145	146.5
	67.4	85.4	18.0	189.5	79	91.6	85,100	85,600	1175	150
	67.8	79.2	11.4	193.0	115	86.9	78,800	83,500	1092	139
	68.0	77.0	9.0	194.0	137	89.5	74,600	83,600	1063	136
	68.0	75.5	7.5	194.8	168	89.5	75,500	83,600	1063	136
10	48.0	96.7	48.7	194.1	49.5	159.0	144,800	148,200	174	252
	48.0	87.5	39.5	198.7	76.0	192.0	188,200	179,200	208	301
	48.0	80	32.0	202.5	103.0	220.5	198,400	206,000	229	332
	48.0	76.3	28.3	204.3	127.0	235.5	216,000	218,000	244	354
	48.0	71.1	23.1	207.0	164.0	250.5	227,000	234,000	256	371
11	66.5	112.3	46.8	177.3	51.0	149.0	148,000	138,000	259	262
	66.0	103.7	33.7	181.7	74.0	173.8	167,000	162,000	298	301
	66.0	103.8	33.8	185.2	89.5	195.0	181,000	182,000	325	328
	66.1	92.2	26.1	187.3	124	206.6	194,500	192,000	341	334
	66.5	86.3	19.8	189.2	155	216.3	203,800	202,000	356	339
12	48.0	110.1	62.1	187.4	51	204.5	190,400	191,000	231	339
	48.0	97.3	49.3	193.8	69	218.5	200,000	204,000	236	347
	48.0	88.0	40.0	198.5	98	247.5	235,000	231,000	266	391
	48.0	82.2	34.2	201.4	125	278.5	256,000	269,000	291	427
	48.0	76.8	28.8	204.1	162	317.5	280,000	282,000	308	453
13	64.6	108.6	42.0	180.2	47	126.8	124,000	118,200	790	222
	64.4	95.0	30.6	187.0	72.5	142.0	133,000	132,800	845	237
	64.8	84.6	19.8	192.0	120	150.0	142,400	140,000	872	245
	64.6	81.0	16.4	194.0	155	159.0	152,000	148,200	919	258
14	65.4	107.6	42.2	180.2	63	144.0	134,500	134,500	492	248
	65.0	99.7	34.7	184.3	77.5	173.5	161,000	162,000	578	292
	64.8	92.6	27.8	188.1	102	182.0	170,000	170,000	597	301
	64.4	88.4	24.0	190.3	124	189.0	178,500	176,600	615	310
	64.2	83.2	19.0	192.1	166	198.7	189,100	185,500	640	323
15	65.0	113.4	48.4	177.2	51.3	160.5	149,000	150,000	347	281
	64.6	100.9	36.3	183.7	75	165.6	163,000	154,800	356	288
	64.4	92.0	27.6	188.2	99	174.7	164,000	163,000	358	290
	64.7	87.5	22.8	190.2	124	184.0	176,600	172,000	377	305
	64.1	83.8	19.7	192.3	161	198.0	190,500	184,800	401	325
16	47.5	101.5	54.0	192.0	52.0	187.2	168,500	174,900	233	298
	47.5	90.4	42.9	197.5	77	217.5	198,000	203,000	264	338
	47.5	83.7	36.2	200.9	98	241.0	213,000	225,000	284	364
	47.5	79.0	31.5	203.2	125	262.5	240,000	245,000	311	398
	47.5	74.1	26.6	205.7	163	282.5	260,000	264,000	332	425
22	42.8	81.8	39.0	201.7	52	135.6	122,000	126,000	381	205.5
	42.8	78.6	35.8	206.9	76	169.8	162,000	158,300	422	260
	42.6	71.1	28.5	209.6	102	172.5	175,100	165,800	438	270
	42.6	67.9	24.3	211.2	125	187.4	189,600	175,000	465	287
	42.0	64.2	21.6	213.1	166	217.5	215,500	203,000	530	327
23	41.9	78.2	36.3	206.5	56	128.5	121,800	120,000	413	135
	41.9	75.0	33.1	208.1	76	152.0	157,000	142,000	477	235
	41.9	71.3	29.4	209.9	100	180.0	176,800	168,200	581	274
	41.9	66.0	24.1	212.6	126	189.0	182,900	176,500	598	282
	41.9	60.4	18.6	215.3	175	202.6	194,900	188,300	630	297
24	42.2	81.1	38.9	204.8	44.5	121.9	104,800	113,800	528	178
	42.4	76.2	32.8	207.8	74	160.0	146,200	149,200	701	236
	42.0	69.2	27.2	210.8	98.5	175.4	161,900	163,900	766	258
	42.0	64.9	22.9	213.6	125	188.1	172,000	175,800	808	272
	42.0	60.2	18.2	215.5	174	199.6	188,900	186,500	862	290
25	43.4	82.5	39.0	203.5	42.6	118.0	111,000	110,000	305	181
	43.3	74.6	31.3	207.5	74	142.5	139,000	133,000	368	218
	43.3	68.1	24.8	210.8	102	158.0	157,300	147,600	398	236
	43.3	68.1	24.8	210.8	126	191.8	187,000	179,000	487	289
	42.9	62.6	19.7	215.7	177	214.0	208,000	200,000	536	318
26	42.9	83.5	40.6	203.5	48	119.0	116,000	111,000	284	187
	42.8	74.5	31.7	208.0	76	150.0	144,000	140,000	346	228
	42.8	71.9	29.1	209.0	94	168.8	164,100	157,500	388	256
	42.9	67.5	24.6	211.0	128	195.0	189,000	182,000	444	293
	43.1	63.6	20.5	212.0	179	227.0	222,000	212,000	515	340
27	43.6	104.2	60.6	192.0	46	176.2	171,800	164,800	393	292
	43.5	87.4	43.9	201.0	76	191.0	201,000	191,000	439	325
	43.5	79.6	36.1	205.0	100	221.5	217,000	206,000	465	344
	43.5	74.0	30.5	208.0	126	236.5	230,000	221,000	487	361
	43.6	66.4	22.9	211.5	175	244.0	241,000	228,000	500	370
28	43.6	99.7	63.1	195.0	49.5	163.8	166,500	158,300	647	278
	43.3	84.3	41.0	202.5	78	197.0	191,400	184,000	719	309
	43.1	78.2	35.1	206.0	101	214	212,000	200,000	775	333
	43.1	72.8	29.7	208.0	126	239	224,000	214,000	815	350
	43.3	66.4	23.1	211.0	175	247	242,000	227,000	860	370
29	43.5	112.2	68.9	188.8	49.5	203.5	204,000	190,000	326	333
	43.1	92.8	49.7	196.5	75	226	224,000	211,500	339	369
	42.9	82.0	39.1	204.0	101	240	236,000	224,000	345	376
	42.7	75.4	32.7	207.5	126	238.5	246,000	223,000	346	377
	42.9	66.6	23.7	211.7	175	247.5	249,000	231,000	347	378

coefficient must have been in excess of the 3060 Btu per hr per deg F per sq ft.

Series F Heat Transfer Between Water Inside Single Horizontal Tubes and Hot Oil in Annular Space Outside

The apparatus in Fig. 12 was used with measurements for Series F on the cooler. The 37-deg A.P.I. mineral-seal oil had viscosities of 3.20 centipoise at 100 F, and 1.03 centipoise at 210 F. The boiling range was from 525 F at 10 per cent to 644 F at 90 per cent with a 50 per cent temperature of 568 F. Two sets of heat-transfer data were taken, one for an annulus with a diameter 2.073 in. for the inside diameter of the outer pipe, and the other for an annulus of 1.583 in. The data are given in Tables 5 and 6.

The measurements on plain tubes Nos. 7 and 9 are the usual over-all coefficients for the inside wall of an annulus. In the case of finned tubes, the spiral fins affect the path of the oil through the annulus.

Water-film coefficients inside the tube under conditions similar to these were computed in Series E. These water-film coefficients and the assumption that the resistance of the copper may be neglected were used along with the over-all coefficients to compute film coefficients for the oil in the annulus.

A comparison between the experimental coefficients and those calculated by Nusselt-type equation, Equation [10], requires equivalent diameters for the annuli. A procedure for plain tubes is to use the difference between the inside and outside diameters of the annulus. For the finned tubes, the inside diameter of the annulus has been taken as equal to D_E. For the twelve tubes which gave essentially straight lines for the water-film coefficients in Fig. 13, a plot was made of the product of hD' versus Reynolds number, Figs. 15 and 16. If the Prandtl number $\left(\frac{c_p\mu}{k}\right)$ and the thermal conductivity k are assumed to be constant over the small temperature range used, Equation [10] may be simplified as shown by Equation [11]

$$hD' = 0.023\left(\frac{c_p\mu}{k}\right)^{0.4} k\left(\frac{DG}{\mu}\right)^{0.8} = b\left(\frac{DG}{\mu}\right)^{0.8} \quad \ldots [11]$$

By using average values for c_p, μ, and k (Prandtl number =

TABLE 5 DATA ON FINNED TUBES; OIL OUTSIDE, WATER INSIDE

Tube No.	Water Temperature Inlet C	Outlet C	ΔT C	Oil Temperature Inlet C	Outlet C	ΔT C	LN Mean ΔT F	Velocity Lbs/Min Water	Oil	Heat Transferred Btu/Hr Water	Oil	Coefficient Btu per Hr per °F per Sq Ft	Per Ft
1	19.39	26.92	7.53	88.05	85.48	2.57	114.5	14.3	92.0	11600	13300	71.9*	33.8
	19.27	25.11	5.84	88.41	85.69	2.72	116.8	14.3	64.0	9000	9870	57.3	26.9
	19.27	23.48	4.21	87.94	87.11	2.83	117.2	14.4	44.0	6700	7000	41.1	19.3
	19.33	22.18	2.85	87.50	84.02	3.48	117.0	14.5	22.9	4460	4480	27.1	12.7
4	19.70	27.37	8.67	88.21	86.25	2.96	113.8	14.60	84.25	12700	14000	70.3	39.2
	17.40	25.65	8.25	88.30	85.40	2.90	117.6	14.7	79.5	13100	12800	65.9	36.7
	17.40	24.70	7.30	88.30	85.45	2.85	118.3	14.7	73.0	11600	11700	58.9	82.8
	19.12	24.85	5.73	88.34	85.46	2.70	116.7	14.5	64.0	8390	9710	48.0	26.7
	19.08	23.47	4.39	88.21	85.32	2.89	117.8	14.4	45.0	6830	7310	35.6	19.9
	17.45	20.90	3.45	89.60	85.65	3.85	123.0	14.5	24.5	5400	5164	25.1	14.3
	19.06	22.00	2.94	87.47	83.82	3.65	117.1	14.0	22.9	4450	4690	22.4	13.0
7	19.16	22.77	3.61	87.60	86.32	1.28	118.9	13.9	84.25	5410	5910	37.0	15.8
	19.08	22.23	3.15	87.97	86.54	1.43	120.0	14.32	64.5	4880	5780	85.5	14.0
	19.13	21.73	2.60	88.11	86.36	1.75	120.1	14.2	44.2	3990	4330	70.6	11.5
	19.20	21.27	2.07	87.82	85.33	2.49	119.2	13.95	24.5	3120	3425	56.0	9.2
8	19.71	34.97	15.26	88.17	83.49	4.68	104.3	13.45	84.0	22200	22100	73.4	70.7
	19.75	32.10	12.35	88.01	82.79	5.22	108.2	13.5	64.0	18000	18000	58.9	56.8
	19.75	30.61	10.86	88.18	81.95	6.23	108.4	13.5	45.0	15800	15000	50.5	48.6
	19.76	28.06	8.30	87.81	79.32	8.49	107.3	13.2	24.5	11800	11700	38.0	36.6
9	18.81	22.43	3.62	82.49	81.44	1.05	110.0	10.5	86.4	4680	5030	108.0*	14.1*
	18.84	22.87	4.03	81.90	80.69	1.21	108.8	10.3	64.0	4480	4360	104.8*	13.7*
	18.90	21.36	2.46	81.12	79.97	1.42	108.3	10.4	41.6	2766	3470	64.7*	8.5*
	19.02	20.92	1.90	78.80	77.00	1.80	104.1	10.25	24.5	2105	2480	51.4*	6.7*
10	19.62	33.97	14.35	87.82	82.74	5.08	106.1	14.5	82.6	22500	23600	56.0	72.4
	19.49	32.75	13.26	87.78	81.89	5.89	104.5	14.5	64.8	20800	21500	48.7	62.5
	19.56	31.67	12.11	87.97	80.77	7.20	106.7	13.2	44.6	17300	18000	38.6	55.7
	19.17	29.35	10.18	87.97	77.80	10.17	101.1	12.8	23.75	13800	13600	31.5	45.5
11	19.15	32.26	13.11	88.28	83.72	4.56	102.5	14.3	84.0	20300	21500	64.1	64.8
	19.08	31.07	11.99	87.60	82.36	5.24	102.6	14.3	65.0	18500	19100	58.4	58.2
	18.95	29.60	10.65	87.77	81.34	6.43	108.5	14.35	45.0	16500	16300	51.3	51.1
	18.95	26.62	7.67	87.42	78.01	9.41	107.9	16.4	23.75	13600	13100	41.4	41.2
12	20.07	36.97	16.90	88.14	83.54	5.60	100.8	13.8	84.0	26200	26400	58.0	85.2
	20.00	35.40	15.40	87.79	81.47	6.32	102.5	13.8	64.0	23000	22700	50.8	74.6
	19.68	34.04	14.32	88.26	80.56	7.70	103.6	12.75	44.0	19700	18500	42.3	62.1
	19.58	31.01	11.43	87.50	76.90	10.60	101.2	12.6	23.75	15600	14100	33.2	48.9
13	19.67	27.35	7.68	87.69	84.34	2.61	111.7	14.5	84.0	12000	12300	128.1	36.3
	19.70	26.27	6.57	87.95	85.49	2.86	114.5	13.8	65.0	9700	10400	107.1	30.1
	19.62	24.84	5.37	82.28	84.05	3.23	114.3	13.6	45.0	7900	8150	83.4	23.4
	18.47	23.58	4.11	87.60	83.21	4.39	115.0	13.65	24.5	6050	6050	62.3	17.6
14	20.30	32.06	11.67	88.04	83.97	4.07	107.7	14.10	84.0	17300	18100	113.5	67.3
	20.30	30.41	10.11	88.12	83.49	4.71	108.5	14.1	63.5	15400	16800	98.0	48.4
	19.85	28.41	8.56	88.03	82.95	5.14	112.5	14.3	43.0	13200	14100	81.6	41.2
	20.20	26.46	6.26	87.97	81.35	6.62	110.2	13.8	25.0	9380	9500	56.3	28.4
15	20.75	29.67	8.92	87.57	81.95	5.62	107.0	25.9	82.0	25200	25800	98.1	79.4
	20.71	30.01	9.30	88.16	82.06	6.10	107.5	23.0	69.0	23100	23600	89.4	72.3
	20.68	31.07	10.36	87.95	81.41	6.54	104.8	16.6	46.5	18600	18400	72.8	58.8
	21.20	32.38	11.15	87.75	78.15	9.6	100.8	10.0	21.2	12100	11400	47.9	38.8
16	19.41	37.08	17.57	88.18	82.28	5.90	102.1	14.4	85.0	27300	28200	70.5	90.4
	19.36	34.85	15.49	87.81	81.26	6.55	103.1	14.45	64.5	24200	23800	60.4	77.4
	19.33	32.67	13.34	87.91	80.21	7.70	104.6	14.2	44.5	20400	19300	49.4	63.3
	19.34	29.88	10.54	87.93	76.81	11.12	104.0	14.2	23.75	16200	14800	38.8	49.6
22	20.59	31.73	11.14	87.04	83.88	3.36	107.1	14.5	86.0	17440	19100	92.1	56.9
	20.40	30.47	10.07	87.78	83.32	4.46	107.7	14.4	62.1	15600	15600	78.4	48.1
	20.40	29.10	8.70	87.99	82.74	5.25	103.8	14.0	45.0	13200	13400	65.0	40.1
	20.35	26.82	6.47	87.68	80.76	6.92	105.0	14.2	24.6	9910	9650	48.2	29.8
23	20.78	31.52	10.74	88.30	84.88	3.42	107.5	13.7	84.3	14800	16200	108.7	47.4
	20.67	29.20	8.53	88.21	84.40	3.81	118.3	13.8	64.1	12700	13800	85.0	40.1
	20.62	27.88	7.26	87.98	83.70	4.28	109.9	14.3	45.0	11200	10800	71.0	33.5
	20.65	26.07	6.52	87.59	82.04	5.55	116.7	13.8	24.6	8200	7700	52.9	25.0
24	19.86	28.70	8.84	88.14	84.98	3.16	112.8	14.0	84.0	13500	14900	124.4	41.9
	19.10	26.52	7.42	87.77	83.65	4.12	113.9	14.5	65.0	11900	12900	108.0	36.4
	18.44	26.36	5.92	87.70	83.70	4.00	114.0	15.0	44.5	9600	10000	85.1	28.7
	19.21	23.88	4.67	87.82	82.52	5.30	114.5	14.5	23.8	7310	7070	62.1	21.0
25	20.40	33.15	12.75	87.63	83.31	4.32	105.3	14.3	86.6	19700	21000	108.7	64.4
	20.42	31.59	11.17	87.89	82.86	5.03	106.9	14.4	64.1	17400	18200	93.5	55.4
	20.30	29.83	9.53	87.70	81.70	6.00	107.2	14.3	45.0	14700	16200	78.4	46.5
	20.05	27.40	7.35	87.70	79.70	8.00	108.0	14.25	24.6	11300	11000	58.1	34.5
26	20.79	33.67	12.88	88.08	83.64	4.43	106.6	14.4	86.3	19900	21200	98.2	64.8
	20.71	32.16	11.45	87.81	82.71	5.10	109.4	14.3	64.1	17700	18300	83.2	54.9
	20.78	31.17	10.39	87.95	82.20	5.75	106.6	14.0	48.2	15700	15600	74.3	49.0
	20.68	28.43	7.75	87.62	79.89	7.73	106.5	14.35	26.3	12000	11400	44.8	36.6
27	20.75	34.48	13.73	88.33	83.63	4.70	104.9	15.6	89.0	22300	25500	98.3	72.7
	20.75	33.11	12.36	88.07	82.67	5.40	105.0	14.2	65.0	18900	19700	85.1	63.4
	20.75	31.16	10.41	87.66	81.21	6.45	105.1	14.3	47.0	16100	17100	71.0	52.5
	20.65	28.86	8.21	87.73	79.17	8.56	105.5	14.3	24.6	12700	11800	52.2	38.7
28	20.94	30.84	9.90	87.65	84.10	3.55	108.0	14.2	85.8	16300	16900	115.2	49.6
	20.95	29.56	8.61	87.72	83.75	3.97	108.9	14.3	64.1	13300	14300	98.2	42.2
	20.95	28.20	7.25	87.56	82.99	4.57	109.2	13.8	41.0	10800	11300	78.5	33.8
	20.90	26.24	5.34	87.78	81.63	6.15	110.0	14.3	24.6	8240	8500	63.0	25.4
29	21.10	29.24	8.14	87.96	80.83	7.13	106.9	35.1	72.0	31200	30800	88.6	96.5
	20.63	28.72	8.09	88.07	80.45	7.62	107.2	33.6	68.5	29300	29300	83.7	91.2
	20.55	28.36	7.81	87.91	79.10	8.81	106.5	26.0	46.0	21300	22800	64.3	70.0
	20.55	28.47	7.92	88.21	77.60	10.61	104.8	20.5	25.0	15500	14300	44.2	48.2

ANNULUS - 2.0[illegible] IN.

TABLE 6 DATA ON FINNED TUBES; OIL OUTSIDE, WATER INSIDE

TUBE NO.	WATER TEMPERATURE INLET °C	WATER TEMPERATURE OUTLET °C	WATER TEMPERATURE ΔT °C	OIL TEMPERATURE INLET °C	OIL TEMPERATURE OUTLET °C	OIL TEMPERATURE ΔT	LN MEAN ΔT °F	VELOCITY LBS/MIN WATER	VELOCITY LBS/MIN OIL	HEAT TRANSFERRED BTU/HR. WATER	HEAT TRANSFERRED BTU/HR. OIL	COEFFICIENT BTU PER HR PER SQ FT	COEFFICIENT PER °F PER FT
1	16.42	26.61	10.19	87.78	84.79	2.99	116.5	13.9	91.0	15300	15400	93.3	43.8
	16.36	25.36	9.00	88.23	84.63	3.60	118.0	13.8	66.0	13100	13300	79.6	37.4
	16.33	23.75	7.42	87.85	83.68	4.17	118.2	13.7	46.0	10800	11000	66.2	30.7
	16.64	20.64	4.00	88.16	83.76	4.40	123.2	13.2	21.8	5700	5890	33.1	15.6
4	16.38	29.23	12.85	87.64	83.85	3.79	115.0	14.75	92.0	20500	19600	106.2	53.2
	16.11	27.28	11.17	88.21	83.94	4.27	115.5	14.75	69.5	17800	16700	89.4	49.8
	16.16	23.75	7.42	87.68	83.06	4.71	118.8	13.8	41.0	11100	10800	56.1	30.7
	16.18	19.93	3.75	88.06	83.59	4.47	122.0	14.75	21.6	5970	5770	28.8	16.0
7	16.30	21.26	4.96	87.75	86.20	1.55	122.8	14.6	94.0	7600	8190	131.2	21.4
	16.25	20.62	4.37	87.70	86.02	1.68	123.3	13.7	74.0	6470	6990	111.2	18.2
	16.30	19.71	3.41	87.58	85.67	1.91	123.6	13.9	53.0	5130	5690	88.6	14.4
	16.32	18.88	2.56	87.61	85.28	2.33	124.0	13.9	32.8	3780	4300	66.5	10.9
8	17.35	36.26	17.90	88.09	82.84	6.25	106.0	13.75	85.0	26600	25100	84.4	81.2
	16.99	34.47	17.48	88.08	81.99	6.09	106.3	12.6	66.0	23600	22300	74.2	71.5
	17.22	31.86	14.64	88.12	80.39	7.73	107.5	13.4	44.5	21200	19400	65.3	62.5
	17.10	28.30	11.20	88.22	76.18	12.04	107.0	13.0	22.45	15700	15900	61.1	49.2
9	15.49	19.23	3.47	88.44	87.08	1.36	126.8	13.8	86.0	5560	6660	122.5	16.1
	15.30	18.37	3.07	87.67	86.19	1.48	126.1	13.6	63.8	4500	5300	98.7	12.0
	15.30	17.68	2.38	87.35	85.67	1.68	126.0	14.0	42.0	3600	3965	76.3	10.0
	15.21	17.08	1.87	87.88	85.52	2.36	126.5	14.15	28.5	2860	3000	55.0	7.7
10	16.23	34.24	18.01	88.00	82.04	5.96	107.0	14.3	78.8	27800	26400	58.4	84.4
	17.08	35.17	18.09	87.77	80.72	7.05	104.5	12.25	57.0	23900	22600	57.8	74.7
	17.10	34.84	17.74	87.49	78.66	8.83	102.3	11.0	39.4	21100	19600	45.8	66.2
	17.14	33.19	16.05	87.88	76.17	11.71	102.3	9.4	21.0	16300	15100	35.5	57.2
11	16.09	32.08	15.99	88.37	82.73	5.64	111.0	14.8	78.0	25600	25000	75.1	75.8
	15.96	37.92	15.96	88.19	81.54	6.65	109.4	12.8	57.0	22100	21300	65.4	66.0
	16.38	31.07	14.96	87.92	80.09	7.83	108.4	13.0	45.5	21000	20000	62.4	63.0
	16.88	29.19	12.31	87.78	76.40	11.38	106.5	12.3	23.7	16400	15200	48.0	49.5
12	17.30	38.30	21.00	88.20	81.48	6.72	102.0	14.1	81.0	32000	31400	70.7	103.5
	17.22	37.16	19.94	87.64	79.74	7.90	101.3	13.8	65.5	29800	29100	65.9	96.9
	17.05	35.05	18.00	87.99	77.55	10.44	101.9	13.8	43.5	26900	25600	57.3	84.2
	16.81	31.82	15.01	87.77	73.02	14.75	101.0	13.2	23.6	21400	19800	45.9	67.5
13	15.95	28.02	12.57	85.47	81.73	3.74	109.9	12.3	85.5	16700	18000	167.2	57.6
	15.83	26.56	10.73	83.45	79.38	4.07	108.4	12.2	65.9	14100	15100	160.0	47.9
	15.70	24.13	8.43	81.43	76.85	4.58	106.7	12.6	43.0	11500	11100	125.2	35.2
	15.70	22.21	6.51	80.94	75.39	5.55	106.7	11.8	24.5	8290	7640	88.6	24.9
14	14.67	29.13	14.46	87.85	82.58	5.27	113.7	15.4	86.5	24100	26400	143.2	72.4
	14.44	27.82	13.38	87.94	82.01	5.93	114.4	14.8	66.7	21400	21900	124.7	63.0
	14.52	26.37	10.85	87.61	80.61	7.00	115.6	16.25	43.7	18000	17200	100.4	50.8
	14.35	23.27	8.92	87.77	78.67	9.10	116.9	14.30	24.9	13800	12800	75.4	38.1
15	14.18	34.90	20.72	87.39	81.43	6.56	107.5	14.1	85.0	31500	31400	120.2	97.5
	14.85	33.34	18.50	87.62	79.97	7.65	106.7	14.25	64.8	28500	27800	108.2	87.9
	15.19	31.55	16.36	87.61	77.97	9.64	107.0	14.3	43.6	25300	23600	94.0	76.1
	15.40	29.54	14.14	88.12	75.14	12.98	106.5	13.9	29.4	21200	21400	82.4	66.7
16	16.97	38.93	21.94	88.22	81.46	6.19	102.3	12.5	84.3	29400	29300	74.8	95.6
	16.84	37.72	20.88	88.30	81.04	7.26	102.6	12.4	65.8	28900	26900	71.0	90.7
	17.33	35.83	18.50	88.07	78.67	9.40	102.0	12.3	44.0	24600	23200	59.9	76.6
	17.30	31.82	14.62	88.09	74.37	13.72	101.9	12.1	29.0	19000	17800	47.1	62.3
22	15.55	30.11	14.56	87.94	83.04	4.89	112.2	14.3	85.0	23900	23400	113.9	70.3
	15.70	28.58	12.88	87.88	82.42	5.46	112.9	14.3	65.0	19800	19300	96.2	58.7
	15.70	26.60	10.90	87.77	81.14	6.63	113.9	14.2	43.0	16700	16000	77.6	47.8
	15.70	24.39	8.69	87.82	79.51	8.31	114.5	14.35	23.0	12500	13600	64.0	39.4
23	15.16	28.44	12.78	87.72	83.55	4.17	113.9	13.75	85.0	18900	19800	120.1	56.6
	15.70	27.14	11.44	87.93	83.09	4.84	115.3	14.0	65.5	17800	17800	107.8	57.8
	15.70	25.28	9.58	87.68	82.07	5.61	115.9	14.2	43.5	14700	13700	86.6	40.9
	15.60	23.11	7.51	88.11	80.98	7.14	117.3	14.1	25.0	11400	10200	65.2	30.8
24	15.45	28.72	13.32	87.70	83.32	4.38	113.7	13.8	84.5	19800	20800	176.9	59.5
	15.56	27.65	12.04	88.06	83.10	4.96	114.8	14.0	65.5	18200	18300	167.0	53.0
	15.55	25.57	10.02	87.14	82.28	5.86	116.4	13.9	43.6	15000	16000	131.8	44.4
	15.50	23.35	7.85	88.27	81.05	7.22	117.8	14.0	28.5	11900	11500	98.3	33.1
25	15.67	32.70	17.03	87.91	82.08	5.83	109.6	14.7	85.0	27100	27900	141.6	84.0
	15.69	31.29	15.60	87.84	81.14	6.70	109.4	14.6	65.0	24600	24600	126.1	74.8
	15.70	28.91	13.21	87.87	78.57	8.30	110.5	14.8	43.0	20900	20100	104.1	61.7
	15.70	26.59	10.89	88.18	77.53	10.65	111.1	14.8	31.0	17400	18500	90.7	45.9
26	15.87	33.27	17.40	88.23	82.58	5.65	108.8	14.5	86.0	27300	27400	127.2	83.6
	15.56	31.25	15.69	87.78	81.30	6.48	109.8	14.5	65.0	24600	23600	111.3	73.2
	15.47	28.90	13.43	87.66	79.44	8.22	110.4	14.5	43.5	21000	20,100	94.0	62.6
	15.47	26.57	11.10	87.90	77.27	10.63	110.8	14.25	30.0	17100	17900	78.4	62.7
27	15.56	33.16	17.60	87.68	81.85	5.83	108.2	14.3	86.0	27500	28200	116.8	85.7
	15.41	31.76	16.35	87.73	80.73	7.00	108.6	14.5	65.0	25600	25600	106.0	78.5
	15.38	29.54	14.16	87.81	79.23	8.58	108.9	14.3	43.5	21900	21500	88.8	66.7
	15.40	26.87	11.47	87.35	77.18	10.77	110.6	14.25	29.0	17600	17500	71.6	52.9
28	15.50	31.26	15.76	88.10	83.06	5.04	111.1	13.5	85.0	23000	24100	165.4	71.2
	15.11	29.62	14.51	88.13	82.40	5.73	113.0	13.3	65.0	20900	20900	143.3	61.7
	15.34	27.11	[illegible]	87.93	81.22	6.71	113.9	13.3	43.5	16700	16400	112.2	48.4
	15.43	24.73	9.30	87.52	79.43	7.99	114.1	12.5	28.0	12600	13000	86.6	37.3
29	15.90	39.36	23.46	87.72	80.34	7.38	100.5	13.8	86.2	35000	35300	107.0	116.6
	15.79	37.72	21.93	87.93	79.13	8.80	101.6	13.7	64.3	32400	31600	96.6	105.3
	15.80	35.44	19.64	87.43	76.65	10.78	101.1	13.5	43.0	28400	26000	82.4	89.8
	15.78	32.13	16.35	82.77	73.45	14.32	102.0	13.27	29.4	23400	23700	70.5	76.3

ANNULUS = 1.583 IN.

21), b was computed to be **0.072**. For the No. 7 plain tube and the 1.583-in. annulus, the film coefficient was computed by Equation [11] and plotted in Figs. 15 and 16 for reference. It may be seen that the oil-film coefficients are all above those for plain tubes, probably due to the turbulence caused by the fins.

The increase in turbulence may be offset by the increased resistance of the metal, especially for those tubes having high fins and thin fin sections. It is significant to observe that the higher coefficients were for tubes which had 4 fins per in. In nearly all cases the measurements on the larger annulus gave higher coefficients for a given Reynolds number.

Series G Heat Transfer Between Steam Inside Single Horizontal Tubes and Oil in Annular Space Outside

Series G comprises the measurements in the heater, while Series F was being made in the cooler in Fig. 12. Only a portion of the tubes was used in Series G, but both sizes of annuli, 2.073 and 1.583 in., were included. The data and calculated coefficients are given in Tables 7 and 8. The complexity of the factors in the over-all coefficients forbids analysis on the basis of individual films. However, the data may be used as a guide for similar conditions of heat transfer.

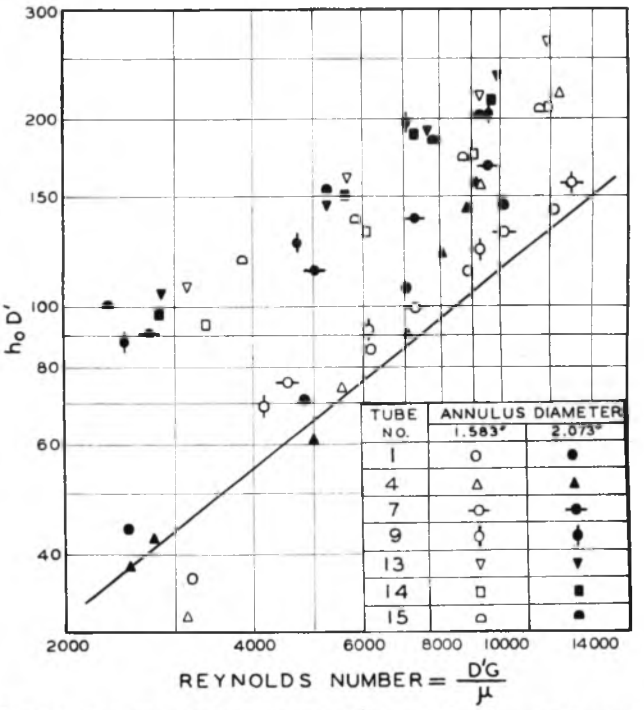

FIG. 15 CALCULATED FILM COEFFICIENTS FOR OIL OUTSIDE FINNED TUBES

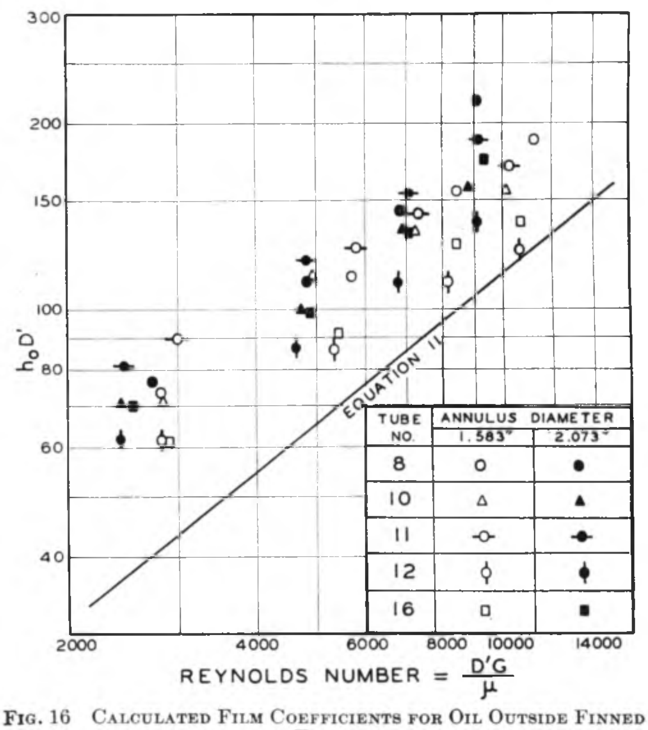

FIG. 16 CALCULATED FILM COEFFICIENTS FOR OIL OUTSIDE FINNED TUBES

ACKNOWLEDGMENT

The data presented in this paper were obtained as part of a project at the University of Michigan for the Wolverine Tube Division of the Calumet and Hecla Consolidated Copper Company. The authors wish to thank the Wolverine Tube Division for permission to publish these results.

TABLE 7 DATA ON FINNED TUBES; OIL OUTSIDE, STEAM INSIDE

Tube No.	Oil Temperature Inlet °C	Oil Temperature Outlet °C	Oil Temperature ΔT °C	Steam Data Pressure PSIA	Steam Data Temp °F	Steam Data Condensed Lbs./Hr.	LN Mean ΔT °F	Oil Velocity Lbs./Min.	Heat Transferred BTU/Hr Oil	Heat Transferred BTU/Hr Steam	Coefficient BTU per Hr per °F per Sq Ft	Coefficient BTU per Hr per °F per Ft
10	82.16	87.83	5.67	34.4	258.26	31.95	72.9	85.5	27300	27400	85.9	134.0
	81.33	87.98	6.65	34.68	255.23	27.75	70.4	65.7	23600	23300	76.5	110.7
	79.94	87.61	7.67	30.16	250.43	23.55	67.5	43.7	18800	18500	63.5	91.83
	77.79	87.77	10.05	26.90	244.53	18.6	58.69	24.9	14100	14700	62.9	91.0
	82.00	88.23	6.23	36.40	261.76	35.6	76.3	86.0	30200	30400	91.5	132.2
	80.70	87.78	7.08	34.30	258.97	30.15	74.97	65.0	26800	25800	84.8	122.6
	78.74	87.66	8.92	31.66	256.95	25.85	73.70	43.5	21800	21400	66.6	96.27
	76.25	87.90	11.65	32.34	247.1	23.15	74.64	34.0	19600	17900	58.0	83.79
	81.40	87.60	6.20	37.3	261.36	35.65	71.76	86.0	30400	30600	97.9	141.5
	80.23	87.73	7.50	32.64	258.30	30.88	71.70	65.0	27400	26000	86.0	124.1
	78.47	87.81	9.16	32.94	255.80	27.55	73.10	43.5	24400	23800	73.0	105.63
	76.17	87.38	11.38	31.20	243.54	24.15	72.87	29.0	19200	17900	58.7	84.90
11	82.80	87.70	4.90	36.65	262.8	24.75	76.23	89.5	23500	21100	100.8	147.8
	82.52	88.06	5.54	36.79	262.6	23.65	76.10	65.5	20400	19500	86.4	87.28
	81.58	88.14	6.56	38.45	258.7	22.65	75.13	47.6	17900	17700	80.4	81.66
	79.60	85.23	8.63	41.19	260.9	16.22	84.62	28.5	13900	13100	54.8	[illegible]
	82.44	87.94	5.50	41.73	264.9	29.35	83.5	85.0	26700	24400	104.0	145.0
	81.87	87.88	6.01	39.2	266.0	26.36	81.23	65.0	21900	21600	88.5	89.75
	80.31	87.77	7.46	36.59	261.8	22.76	78.12	45.0	17500	18300	75.5	76.3
	78.58	87.82	9.24	34.43	248.4	17.3	74.8	29.0	15700	17200	64.8	46.5
	83.20	87.74	4.52	32.43	259.4	27.15	68.65	85.0	21600	22400	105.5	146.6
	83.05	87.93	4.88	32.19	254.4	22.25	68.85	65.5	19400	17900	82.9	93.7
	81.24	87.48	6.15	31.43	253.1	21.0	67.60	47.5	15000	16800	73.1	73.9
	80.12	88.11	7.90	29.27	244.9	17.78	65.16	25.0	11200	11300	58.5	59.8
	82.34	88.1	5.56	36.4	261.6	30.71	76.43	86.0	26600	25800	113.8	146.9
	81.83	88.11	6.28	34.8	259.0	25.9	74.0	65.0	24900	24700	109.3	110.6
	80.45	87.91	7.46	32.34	257.7	21.75	71.76	43.5	18200	18500	84.2	85.0
	78.34	87.52	9.16	30.09	251.4	16.55	69.4	29.0	14900	14504	70.5	71.1
14	85.60	87.75	2.15	25.25	240.6	15.66	52.5	94.0	11400	14600	194.2	67.4
	85.36	87.70	2.34	24.71	239.7	11.8	51.6	74.0	9740	8230	134.8	63.9
	84.75	87.53	2.79	23.23	240.6	11.48	52.4	53.0	8510	7630	102.8	51.9
	83.92	87.61	3.65	22.75	247.6	8.64	57.1	32.8	6800	7453	78.6	39.65
22	84.25	87.76	3.55	48.21	211.9	25.50	85.03	91.0	18100	18900	117.5	72.4
	83.99	88.25	4.26	45.11	212.9	20.75	85.91	66.0	15700	16500	99.5	61.4
	82.36	87.85	5.10	41.54	269.2	15.38	82.20	46.0	13200	11500	86.7	53.5 *
	82.26	88.16	5.90	34.59	257.1	11.08	68.60	23.0	7880	7400	64.1	37.2
	84.20	87.52	3.32	33.51	259.8	19.06	72.60	86.0	16000	14900	116.1	71.0
	84.24	88.06	3.82	37.11	262.7	17.78	76.50	65.0	13900	13800	98.1	60.6
	82.83	87.74	4.91	34.95	262.7	15.31	77.08	45.8	12100	11400	82.4	50.8
	82.15	88.10	5.95	34.05	257.6	11.25	72.12	24.6	8270	8580	62.5	38.6
	83.43	87.78	4.35	45.58	215.8	24.45	89.90	85.0	20800	19600	118.8	73.2
	83.12	88.10	4.98	47.98	218.4	22.65	92.30	64.0	17900	17900	104.7	64.5
	81.78	88.00	6.22	47.98	218.4	19.42	92.70	42.4	14800	15000	93.5	58.0
	81.00	87.83	6.83	41.26	268.7	14.69	84.10	25.0	9600	10300	61.2	38.8
26	82.22	88.09	5.87	63.00	298.5	33.10	110.40	85.0	28100	27800	121.8	84.3
	81.42	88.08	6.66	65.36	296.5	31.30	108.50	65.0	24440	25600	116.2	76.8
	79.61	88.12	8.49	64.45	298.4	29.55	123.10	46.5	22800	21500	93.5	61.8
	74.64	88.22	13.68	64.77	301.2	23.45	121.18	22.4	17900	18300	75.5	49.7
	81.61	88.00	6.39	[illegible]	296.5	34.45	111.30	78.5	26100	28000	124.8	82.5
	[illegible]	87.27	7.60	[illegible]	298.5	31.50	115.30	47.0	25000	26600	116.8	73.1
	[illegible]	87.49	9.69	[illegible]	301.1	27.45	118.80	37.4	21500	22200	92.8	61.2
	[illegible]	87.88	13.06	[illegible]	296.5	22.85	120.40	25.0	16800	17800	72.6	47.9
	82.07	88.37	6.30	[illegible]	298.0	33.10	111.60	79.0	28000	27200	124.9	82.5
	80.80	88.15	7.34	[illegible]	297.4	27.35	110.10	67.0	25300	22400	105.0	69.5
	79.99	87.52	8.55	[illegible]	297.6	27.46	114.60	46.5	21800	22200	96.9	64.0
	[illegible]	87.78	12.11	[illegible]	301.2	22.15	125.00	25.7	16900	17100	69.9	46.1
28	[illegible]	87.66	4.30	46.18	271.0	26.45	90.10	92.0	22500	21400	168.2	81.0
	83.28	88.27	4.93	46.84	272.0	23.35	90.63	69.0	19300	19100	165.2	70.5
	82.01	87.65	5.64	41.62	269.4	17.19	83.46	41.0	13000	13000	120.7	51.8
	82.34	88.06	6.82	36.14	259.3	11.09	85.00	25.0	7770	7400	69.5	23.6
	[illegible]	88.11	3.49	38.80	265.6	25.15	78.48	92.0	20100	20500	198.1	85.5
	83.07	87.85	4.78	41.08	269.7	21.06	82.90	64.6	17200	16700	161.0	68.2
	[illegible]	87.99	5.98	44.18	275.4	18.60	88.47	45.8	14300	14500	127.2	54.8
	[illegible]	88.38	7.22	44.58	276.4	15.25	89.70	23.9	9650	11200	85.7	34.0
	[illegible]	[illegible]	4.06	[illegible]	[illegible]	24.50	80.90	91.5	20900	19900	194.8	85.8
	[illegible]	87.46	4.68	41.00	268.7	21.40	84.00	66.0	17100	17000	157.5	64.7
	[illegible]	87.54	5.90	[illegible]	[illegible]	18.94	90.12	45.0	14300	14400	124.2	53.5
	[illegible]	87.85	6.75	[illegible]	[illegible]	14.02	81.80	23.8	8980	10100	85.1	36.6 *
29	[illegible]	[illegible]	7.25	48.40	279.0	39.55	93.20	83.0	35800	35400	110.7	120.7
	[illegible]	87.14	8.80	49.55	280.2	37.65	97.40	65.5	31400	31500	98.8	107.6
	[illegible]	[illegible]	11.12	50.31	281.5	32.85	[illegible]	43.5	27200	27350	85.0	[illegible]
	[illegible]	[illegible]	13.95	[illegible]	[illegible]	21.10	[illegible]	23.6	21200	21100	65.6	[illegible]
	[illegible]	[illegible]	6.76	[illegible]	276.3	37.36	[illegible]	84.5	32000	31600	106.0	115.6
	[illegible]	[illegible]	7.66	45.29	274.1	34.95	90.00	68.8	29100	29400	99.4	108.5
	[illegible]	[illegible]	10.24	45.11	274.3	32.35	92.30	44.0	25200	27000	85.2	96.1 *
	[illegible]	88.09	14.85	43.51	232.8	25.65	95.00	25.0	19200	20800	64.1	70.0
	[illegible]	88.51	7.20	46.36	276.4	40.80	91.75	85.0	34400	34800	115.1	125.8
	79.92	87.78	8.36	46.70	277.9	36.25	95.30	64.0	30800	30600	98.5	101.5
	76.46	87.68	11.22	49.90	280.0	32.45	100.20	42.5	26600	27000	82.0	85.5
	72.11	88.18	16.07	49.6	280.5	28.30	103.80	24.8	21100	23200	64.1	72.1
				ANNULUS 2.073								

TABLE 8 DATA ON FINNED TUBES; OIL OUTSIDE, STEAM INSIDE

Tube No.	Oil Temperature Inlet °C	Oil Temperature Outlet °C	Oil Temperature ΔT °C	Steam Data Pressure PSIA	Steam Data Temp °F	Steam Data Condensed Lbs./Hr.	LN Mean ΔT °F	Oil Velocity Lbs./Min.	Heat Transferred BTU/Hr Steam	Heat Transferred BTU/Hr Oil	Coefficient BTU per Hr per °F per Sq Ft	Coefficient BTU per Hr per °F per Ft
7	80.68	82.49	1.81	48.27	279.1	11.35	100.2	85.4	8460	7710	[illegible]	[illegible]
	79.98	81.90	1.92	54.37	286.5	10.90	108.9	64.0	6510	7000	[illegible]	[illegible]
	78.83	81.12	2.29	60.61	293.2	9.68	117.1	43.6	5600	3850	[illegible]	[illegible]
	75.72	78.80	3.08	63.39	296.7	9.04	125.8	24.5	4140	5290	[illegible]	[illegible]
8	83.15	88.06	4.95	27.15	246.0	27.20	59.1	85.3	23100	22800	[illegible]	151.1
	82.23	87.81	5.58	23.65	236.8	22.20	52.2	64.1	20100	21200	137.0	[illegible]
	81.83	87.95	6.12	22.85	235.0	21.60	50.0	48.2	16500	17800	118.8	[illegible]
	78.84	87.62	8.78	19.60	231.6	16.78	49.4	26.5	13000	13100	91.1	37.9
	83.25	88.33	5.08	25.60	236.8	27.35	50.8	89.0	25400	25000	166.0	159.0
	82.16	88.07	5.91	21.65	231.6	24.30	46.2	65.0	21600	20500	156.4	151.0
	80.62	87.66	7.04	20.85	230.0	21.45	46.3	47.0	18600	17600	134.9	130.0
	78.25	87.73	9.48	20.95	230.1	17.45	48.5	24.6	13000	13100	93.6	92.2
12	81.88	87.57	5.69	20.60	229.3	32.25	45.0	82.0	28700	28000	142.3	209.5
	81.52	88.16	6.64	20.60	229.1	28.10	44.1	63.0	25800	24500	126.8	186.5
	80.69	87.95	7.26	19.30	225.5	25.80	41.8	46.5	20400	19900	108.8	160.0
	76.29	87.75	11.46	18.71	224.0	18.25	43.3	21.2	15600	14600	69.6	101.1
	80.17	87.96	7.79	25.40	240.7	40.25	56.7	77.0	33200	35300	137.6	201.5
	79.99	88.07	8.08	24.75	239.5	36.65	55.9	68.5	31100	31900	127.8	187.8
	78.50	87.91	9.41	22.85	235.0	30.40	52.9	46.0	24300	26110	108.1	159.0
	76.67	88.21	11.54	21.60	232.0	23.60	50.7	25.0	16200	19600	66.6	98.0
13	85.17	87.60	1.85	21.96	233.0	11.16	41.2	84.2	8660	7690	249.5	70.1
	85.81	87.97	2.10	24.47	239.1	10.87	50.6	64.5	7610	7340	175.5	49.5
	85.54	88.11	2.57	24.15	239.5	9.92	50.9	44.2	6510	6450	151.0	42.4
	83.90	87.82	3.92	26.67	245.3	9.91	54.6	24.5	5400	6400	118.2	31.8
15	82.89	88.17	5.28	29.55	248.5	29.7	62.3	84.0	24900	25100	162.9	132.0
	82.11	88.01	5.92	27.29	245.0	25.4	59.7	64.0	21300	21100	146.2	118.5
	81.05	88.18	7.15	26.41	245.3	22.25	59.2	45.0	18100	18100	125.2	101.6
	88.19	87.81	9.62	24.99	240.0	17.64	58.2	24.5	13500	13600	95.5	77.4
	82.18	87.82	5.64	29.55	248.9	29.40	65.9	82.6	26200	24800	175.0	140.1
	81.27	87.78	6.51	29.57	248.9	27.15	64.0	64.8	23100	23300	155.8	124.6
	80.06	87.97	7.91	29.05	248.4	25.35		44.5	19800	21000	150.2	105.5
	76.70	87.91	11.21	27.17	245.9	21.05	66.0	23.8	15000	17000	95.0	77.0
	83.19	88.28	5.09	26.45	245.5	28.55	66.4	84.0	24000	24100	175.3	142.1
	81.76	87.60	5.84	25.61	240.2	26.50	55.8	66.0	21300	22200	160.1	129.9
	80.57	87.77	7.20	25.83	245.0	25.53	59.1	46.0	18200	19400	150.9	106.0
	76.86	87.42	10.56	25.81	243.0	20.10	62.5	23.8	14700	16200	96.4	78.2
	81.97	88.14	6.17	34.55	258.3	33.45	73.2	84.0	29100	29400	164.8	133.3
	80.78	87.79	7.01	33.21	256.2	30.15	72.5	64.0	25400	25400	144.0	116.8
	79.88	88.26	8.38	31.25	252.6	27.05	68.9	44.0	20700	22500	129.0	104.5
	75.73	87.50	11.77	30.09	250.6	20.60	71.0	25.8	15700	16500	93.2	75.5
16	84.14	87.05	2.91	14.78	212.3	17.58	26.20	81.0	13200	14200	135.6	173.5
	84.50	87.90	3.40	15.52	214.5	16.40	27.40	66.0	12600	12780	120.6	154.2
	83.96	87.84	3.88	14.58	211.5	13.19	24.60	45.0	9800	9800	104.0	133.0
	82.49	87.76	5.27	14.48	211.5	11.43	25.95	23.0	6800	8100	71.8	92.0
	83.41	88.04	4.63	19.11	225.5	24.75	38.75	84.0	21400	20800	141.6	181.2
	82.80	88.12	5.32	18.35	225.0	21.85	38.80	63.5	18900	18000	123.8	158.2
	82.16	88.09	5.93	18.22	222.6	19.48	37.35	49.0	16300	15750	111.5	142.6
	80.11	87.97	7.86	18.18	222.5	15.65	39.03	25.0	11200	12100	77.6	99.5
	83.43	87.84	4.41	17.28	220.0	24.15	33.75	86.0	21300	20300	160.1	206.5
	82.79	87.78	4.99	17.10	219.2	21.50	33.50	62.1	17400	17600	136.8	175.1
	82.09	87.99	5.90	17.10	219.2	18.40	33.96	46.0	14900	14180	114.0	146.0
	79.84	87.68	7.84	17.20	219.6	14.70	36.40	23.5	10800	11200	78.0	100.0
	82.79	87.63	4.84	17.80	221.5	26.00	35.40	86.5	23600	22000	168.0	215.0
	82.25	87.89	5.64	18.30	222.8	24.15	37.55	64.1	20400	19800	138.5	177.5
	81.08	87.70	6.62	18.10	222.5	20.85	38.25	46.0	16700	17000	115.0	147.2
	78.67	87.70	9.03	18.10	222.5	17.54	40.10	24.6	12500	13900	81.1	105.8 *
29	81.85	88.18	6.33	29.68	249.2	34.55	64.40	85.0	30200	29700	141.9	[illegible]
	80.76	87.81	7.07	27.22	244.8	30.00	60.40	64.5	25600	25500	129.0	148.9
	79.54	87.91	8.37	26.08	242.5	29.10	59.00	44.5	21000	24700	108.4	113.2
	75.81	87.95	12.12	24.62	239.0	21.40	59.00	25.8	16800	10440	91.0	79.5
	83.20	87.84	4.64	21.84	232.8	24.50	47.00	84.2	22000	20300	151.2	149.7
	82.29	87.64	5.65	21.28	231.2	24.00	46.30	64.5	19400	20000	130.5	142.0
	81.47	88.16	6.69	21.96	235.0	21.15	48.50	44.0	16500	17500	107.0	116.6
	77.88	87.71	9.83	22.09	233.8	16.66	51.50	24.5	15500	14800	84.1	91.6
	81.45	87.70	6.25	26.81	243.8	32.84	58.60	84.5	29300	28100	150.2	163.8
	80.60	87.81	7.21	26.65	245.4	30.35	59.2	66.0	26500	25800	142.4	155.1
	79.39	88.19	8.80	26.49	243.0	27.40	60.3	44.0	21700	25000	115.1	123.3
	76.51	88.03	11.52	26.19	242.6	20.75	62.0	26.5	17100	16700	85.5	90.7
						ANNULUS - 1.58						

Discussion

C. M. Ashley.[8] This paper is of considerable interest, particularly from the standpoint of presenting a correlation of the results of tests on a number of different sizes of finned tubes. There are two specific points which the writer would like to mention:

1 In Fig. 8 of the paper it is believed that the discrepancy in the results of tests at low air velocities can readily be accounted for by the fact that these are in the streamline-flow region which, according to our experience, begins somewhere near 600 fpm maximum velocity.

2 It is presumed that the apparatus sketches shown as Figs. 2 and 7 are schematic in character.

It has been our experience that great care is necessary to obtain superheated steam, uniformity of inlet temperature and velocity, and outlet temperature, and also adequate accuracy in the measurement of air quantity. The apparatus as shown in these two figures is scarcely calculated to accomplish these desired results. It would be interesting to learn from the author what provisions were made to assure uniformity and accurate measurement.

Another point relative to the test procedure, on which information might be of interest, is the method of shielding the thermometers from the radiant heat.

[8] Director of Development, Carrier Corporation, Syracuse, N. Y.

C. T. Paugh.[9] The writer can now comment from a disinterested standpoint but, at the time of the original development of this integral-finned tubing, he personally devised the tools and method of manufacture which made the high-fin type possible and practical to produce and was granted four of the patents on it.

In the section of the paper, designated as "Series D," the authors state, "the water coefficient was greater than that predicted by . . . . equation recommended . . . ." and, "This increase is caused by corrugations on the inside diameter which were made during the processing of the tube." The writer wishes to point out that the condition stated is by no means accidental and that the feature of wall corrugation was incorporated for two very good reasons, one being to produce turbulent flow inside the tube and thus accomplish increased heat transfer as here reported, and the other being a feature outside the scope of the paper which permits this finned tube to be bent, by simple means, on a comparatively short radius without removing the fins or weakening the tube.

This product is inherently comparatively costly to produce, but it has distinct valuable qualities peculiar to its being of integral metal, and hence warrants consideration on many severe applications where its characteristics are of distinct value.

R. G. Vanderweil.[10] Several film coefficients are mentioned in the paper. Working with heat-transfer problems, the writer has found that the task of finding correct film coefficients in literature is most annoying and in most cases results in highly questionable data. Have the authors had an opportunity to check the

[9] Utilities Consultant, U. S. Industrial Chemicals, Inc., Baltimore, Md. Fellow, A.S.M.E.

[10] Office of Consulting Engineer, Chase Brass & Copper Company, Waterbury, Conn.

relations between temperature of fluids, velocity of fluids, viscosity of fluids, etc., and the film coefficient, in the course of their tests?

Authors' Closure

The authors appreciate the comments by Messrs. Ashley, Paugh, and Vanderweil.

Mr. Ashley states that his experience shows that the high coefficient noted at low air velocities in Fig. 8 may be "accounted for by the fact that these are in streamline flow." At 600 fpm the Reynolds number is approximately 3300, a value normally considered to be in the critical region between viscous and turbulent flow. However, because of the doubt as to the proper value of D to use in calculating the Reynolds number for banks of finned tubes and because other independent data available to the authors showed a straight line for the data down to a velocity of 380 fpm, we were reluctant to interpret the data below 600 fpm as being in the viscous region. It is quite possible that the data are in the transition region between viscous and turbulent flow at velocities of 300 to 500 fpm.

In regard to Mr. Ashley's second point, steam was always taken from a line at 125 psi gage and throttled directly to the unit. Since many of the tests were run at low pressures such as 5, 25, and 50 lb per sq in. gage it was felt that this throttling gave adequate assurance of dry steam entering the unit at least for the lower pressures. Concerning the uniformity of air velocities and the accuracy of the temperature measurements, vanes were present as shown in the sketches of this paper but which were not present on the preprint. Pitot-tube traverses made of the air stream leaving the unit were used to check the general accuracy of the heat balance. The thermometer was placed in several positions before selecting the one used. The outlet thermometer was always shielded to avoid errors due to radiation. The inlet thermometer was not shielded in the tests reported in the paper but a correction was made based on similar tests with and without a shielded inlet thermometer.

Mr. Vanderweil asked about film coefficients. In the case of heating air with steam in series A and B, the steam film resistance is so low that the over-all coefficient is substantially equal to the air film coefficient. In such cases the over-all coefficient is used directly for design purposes without investigating the detail of the film coefficient. In other cases such as series E and F an understanding of the data requires that the over-all coefficient be broken down into the film coefficient for the two sides of the heat-transfer surface. It may be possible to vary these film coefficients independently and so no general correlation is available for over-all coefficients but only for the film coefficients. The viscosity, velocity, and density of the flowing fluids were correlated with the film coefficient for the cases of oil and water in series E and F.

Heat Transfer and Pressure Loss in Small Commercial Shell-and-Finned-Tube Heat Exchangers

By R. M. ARMSTRONG,[1] DOWNINGTOWN, PA.

Preliminary results are submitted covering heat transfer and pressure loss for fluids flowing through the shells of small shell and finned-tube heat exchangers in crossflow. These results are compared to the calculated performance of similar exchangers with bare tubes, and the comparisons noted. It is brought out that this type of exchanger can now be applied to duties where finned tubes heretofore have not been used, namely, where over-all heat-transfer rates for bare-tube service would be from about 25 to 250 Btu/(hr)(sq ft)(deg F). It is also pointed out that this type unit is not suitable for many services. Actual field experiences are related.

Nomenclature

The following nomenclature is used in the paper:

- A_s = cross-sectional area for flow across tubes, sq ft
- c = specific heat of fluid at constant pressure and average temperature
- D_s = inside diameter of shell, ft
- d_t = outside diameter of tube, ft
- F = MTD correction factor for pass, from TEMA Standards (p. 20)
- G_s = mass velocity through shell, lb/(hr)(sq ft)
- h_m = heat-transfer rate through metal wall of tube, Btu/(hr)(sq ft)(deg F)
- h_s = film heat-transfer rate on shell side, Btu/(hr)(sq ft)(deg F)
- h_{sd} = scale heat-transfer rate on shell side, Btu/(hr)(sq ft)(deg F)
- h_t = film heat-transfer rate on tube side, Btu/(hr)(sq ft)(deg F)
- h_{td} = scale heat-transfer rate on tube side, Btu/(hr)(sq ft)(deg F)
- J = dimensionless number $\left(\frac{h_s}{cG_s}\right)\left(\frac{c\mu}{k}\right)^{2/3}$
- K = pass correction factor, from TEMA Standards, p. 20
- k = thermal conductivity of fluid at average temperature, Btu/(hr)(sq ft)(deg F/ft)
- n = number of tubes in shell of heat exchanger
- R = pass correction factor, from TEMA Standards (p. 20)
- S = baffle spacing, ft
- U = over-all heat-transfer rate, Btu/(hr)(sq ft)(deg F)
- W = pounds fluid flowing through shell per hour
- μ = viscosity of fluid at average temperature, lb/(hr)(ft)
- μ_ω = viscosity of fluid at wall temperature, lb/(hr)(ft

Introduction

Several years ago a new type of finned tube, extruded from the base metal itself and with low ratio of outside to inside surface, became available for use in heat exchangers. It was decided to consider the application of this tube to shell-and-tube exchangers for crossflow and liquid-to-liquid service, since the compact nature of the tube made it possible to get about 3 times as much outside surface with the finned tube as with a bare tube, in a given shell diameter. No published data were available for heat transfer to baffled banks of finned tubes and experiments were begun to obtain such data.

Some advantages and disadvantages were rather obvious from the examination of the tube, details of which are shown in Figs. 1 and 2. These are as follows:

Advantages:

(*a*) Low ratio of outside to inside surface, about 3.5 to 1. Most previous finned tubes for similar service had run from 7 or 10 to 1. The low ratio makes possible the use of the tube for higher film heat-transfer rates.

(*b*) Low metal resistance, due to very low fin height, absence of any metal-to-metal bond. The calculated metal-wall resistance for this type tube runs about 0.0004 for admiralty metal, compared to as much as 0.015 for steel, and 0.006 for admiralty in high-ratio tubes with a bond.

(*c*) Mechanically the tube is stable and due to low outside diameter gives a large amount of surface per unit of volume. The tube is so built that it can be withdrawn from a bundle and otherwise handled the same as a bare tube.

Disadvantages:

(*a*) The most obvious and immediate disadvantage is the danger of fouling of the space between the fins, greatly reducing the outside area in contact with the fluid.

(*b*) The fins are thin and subject to attack by corrosion if the fluid and metal used are not entirely suited to each other. Fortunately, several metal choices are available.

(*c*) Many services are not suitable for finned-tube work under any circumstances, particularly high-efficiency operations like steam condensing where the compensating effect of finned surface is not needed and therefore is an unnecessary expense.

One of the questions which immediately arises from a heat-transfer and pressure-loss standpoint is whether or not the finned surface gives results qualitatively the same as a bare tube, if coefficients are based on the outside finned area, as they are in this paper. Experiments on this score are still continuing and this paper reports only a small portion of the work done to date, but the following statements can be made at this time, and some preliminary data are shown to bear out the statements:

1 The shell-side heat-transfer film coefficient, based on the outside finned area, is at the very least equal to the rate which would be obtained at a like Reynolds number with bare tube, at a Reynolds number of 300 or higher, using the nomenclature and units given in this paper. Fig. 5 shows experimental results from a set of tests on 8.5-centipose oil. At Reynolds numbers materially above 300 the experimental results are seen to be materially higher than those predicted by bare-tube data.

---

[1] Downingtown Iron Works, Inc.

Contributed by the Heat Transfer Divison and presented at the Annual Meeting, New York, N. Y., Nov. 27-Dec. 1, 1944, of The American Society of Mechanical Engineers.

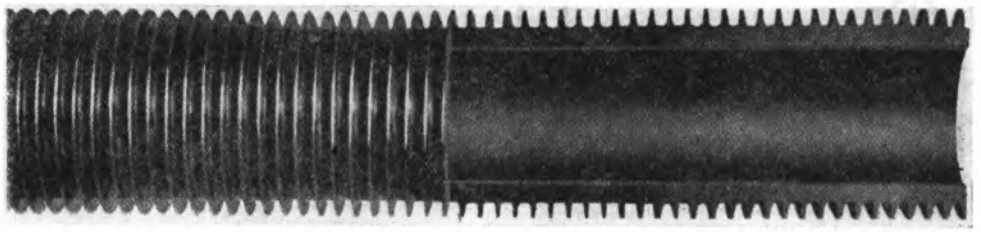

FIG. 1 SECTION OF TUBE USED IN EXPERIMENTS

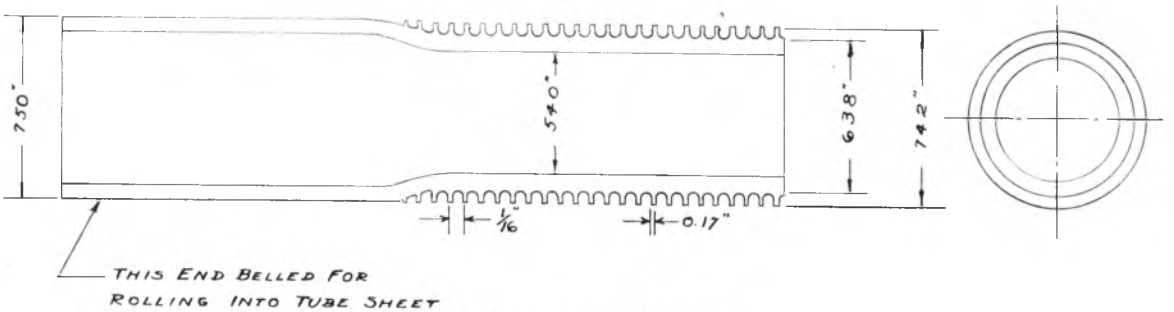

FIG. 2 DIMENSIONS OF TUBE USED

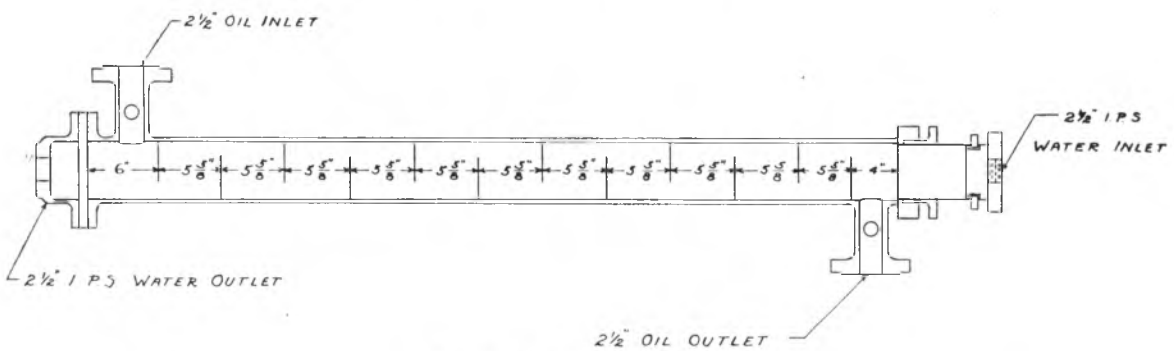

FIG. 3 TEST HEAT EXCHANGER

2 The crossflow friction is undoubtedly greater for the finned tube than for a bare tube. Determination of the friction loss for finned-tube bundles has been run on a research project concurrently with bare-tube bundles. While finned tubes show greater losses, other features of bundle design are vastly more important in determining the over-all pressure loss, so that the effect of the finned surface alone does not represent more than a small percentage of the total.

TEST PROCEDURE

The heat-transfer data shown in Fig. 5 were developed in tests on a 5-in-shell-size unit with 6-ft-long finned tubes. This is a full-size standardized unit developed for finned-tube work. The tests reported here were run with an oil in the shell of about 8.5 centipoises average viscosity at the test conditions. The test unit is shown in Fig. 3. Baffle height was 3.68 in.

The oil was pumped in a closed circuit, Fig. 4, through the exchanger and into a reservoir where it was heated. The water for cooling came in from the supply main and was discharged to the sewer after passing through the tubes.

The quantities of oil and water were measured by calibrated orifices to which were attached 36-in. mercury manometers. The temperatures were measured at the points marked T in Fig. 4 by the use of $^1/_5$ deg F thermometers with 15-in. scales. The pressure loss of oil flowing through the shell was measured using a 36-in. mercury manometer with taps in the shell nozzles, as shown in Fig. 4.

Unfortunately, it was found that the capacity of the system was considerably greater than had been anticipated, and as a result the water velocity going through the tubes was neces-

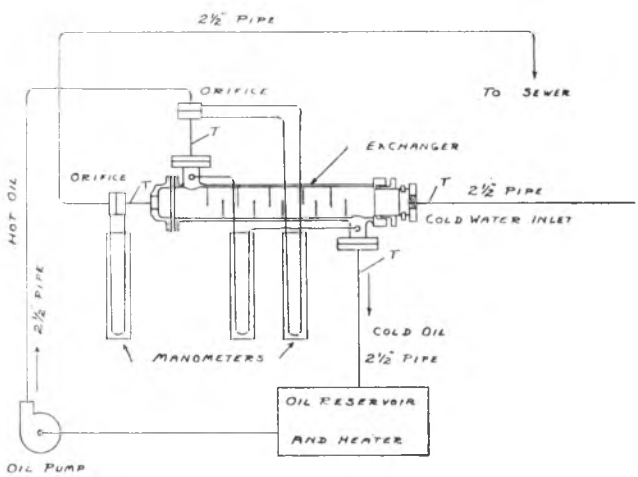

FIG. 4 TEST ARRANGEMENTS AND FLOW PATTERNS

sarily slow as the water temperature was low and there was no available means of heating the water at that time.

The over-all heat-transfer rate was calculated from the test results, based on total outside finned surface. The individual film rates were calculated from the curves given by the TEMA Standards (page 42). Then the metal-wall resistance and the water-film resistance were subtracted from the over-all measured resistance, and the remainder was taken as the oil-side resistance. This method is somewhat conservative in one respect as it makes no allowance whatsoever for fouling, and the tests took up a sufficient period of time so that it is likely some fouling actually did occur. The method of figuring water-film resistance by the TEMA curves, however, we feel to be conservative on the other side, as we found a number of tests, not reported here, where the calculated water-film resistance alone was greater than the over-all resistance as measured. These were mostly at very low water-flow rates.

In several instances we have noted that when cooling a fluid with water in the tubes at low velocity, obviously higher results are obtained than would be predicted by TEMA curves (page 42). Some of this is undoubtedly due to natural convection, as suggested by Dr. A. C. Mueller, and could perhaps be evaluated further by suggested methods.[2] However, from an entirely practical viewpoint there are also other factors, notably possibility of fouling, which would counteract this factor somewhat for the purposes for which these tests were made.

The agreement of the heat balances was quite good throughout and since in all but two or three cases the water heat balance was the lower and in general considered the more reliable, it was used as a basis of figuring.

Discussion of Results of Tests

The results shown in Fig. 5, as plotted with $\frac{d_s G_s}{\mu}$ versus J are based on a diameter of tube taken on a weighted basis referred to

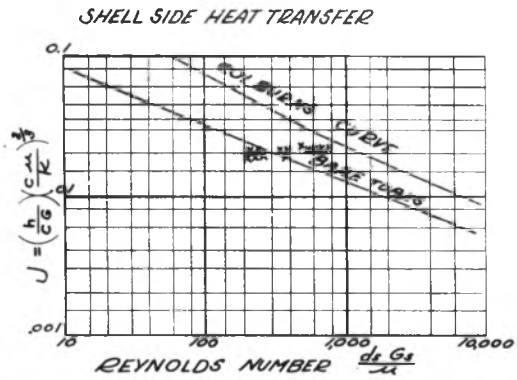

Fig. 5 Heat-Transfer-Rate Curves, Bare Versus Finned Tubes

the outside area of fin across which the flow occurs. The outside diameter of the fin is 0.742 in., and the diameter at the base of the fin 0.638 in. The weighted outside diameter works out to be 0.656 in., or somewhat below the mean of outside diameter and inside diameter.

The area for flow on which G is based is determined by the formula

$$G_s = \frac{W}{S\left(D_s - d_s\sqrt{\frac{4n}{\pi}}\right)}$$

This is a modified form of the equation suggested by Bowman,[3] and the main difference is that the so-called leakage factor is eliminated. These data have been plotted both with and without the leakage factor and just as good agreement is obtained without the factor as with it. Since the area is much simpler to handle without the factor the modified form is used.

It will be seen that the data fall well underneath the "Colburn curve" reported in Bowman's paper, but they fall partly above and partly below a conservative line drawn through the lower area of experimental points on Bowman's plot.

Considerable plotting of experimental points on a plot of this type for both bare- and finned-tube data, using the modified form of G, will show that the line given falls in the lower area of the majority of points and for this reason the author considers it a fair comparison against which to consider the finned-tube data reported herewith.

Evidence is shown that in the small shell unit with finned tubing, the flow is not entirely the same as in a larger unit. The shell-side fluid does not have time to straighten out into pure crossflow before it is again broken into eddy currents and turbulence. As a result, we should expect the performance of the unit tested to be better than the performance of the same tube in a larger shell where the crossflow distance is materially larger. The relatively low performance at low Reynolds numbers indicates that basically the finned tube does not exert a 100 per cent quality of surface efficiency when compared to bare tube in pure crossflow. The lesser slope of the curve we feel indicates that when the flow is reversed at frequent intervals and a good deal of the flow is quite turbulent in nature, the performance is greater than would be predicted by normal bare-tube rating methods.

Field experience with this type of unit has indicated that if the flow conditions are such that the Reynolds number always exceeds 300 on the shell side, calculated as indicated here, the performance of the exchanger can be conservatively calculated by holding to the bare-tube performance as shown on the curve.

As further indication of field performance, in the Appendix are data and calculations resulting from a spot check on the performance of a 16-in-shell-diam by 8-ft-tube-length compressed-air aftercooler which had been in operation about 6 months at the time of test. Unfortunately, this test was run with an extremely low water velocity in the tubes, only 0.287 fps. This was far below the design conditions and resulted in a very low over-all heat-transfer coefficient. However, the actual observed rate of 15 Btu/(hr)(sq ft)(deg F) was slightly below the calculated performance for a bare $^5/_8$-in-OD, 18-gage, copper tube under the identical conditions, namely, 16.4 Btu/(hr)(sq ft)(deg F), and we should point out that in calculating the MTD, which is almost off the scale on the correction curves, the highest possible value was taken. As this was on the flat part of the curve, it could easily be as much as 25 per cent on the conservative side. This amount would be reflected by an increased actual rate on the test unit, and in this case the actual rate would be greater than the calculated rate for the bare tube.

To give an idea of how this works out in practice Example 1 is given in which the film coefficients are the same on the bare tube

[2] "The Effect of Free Convection on Viscous Heat Transfer in Horizontal Tubes," by D. Q. Kern and D. F. Othmer, Trans. of American Institute of Chemical Engineers, vol. 39, 1943, pp. 517–555.

[3] "Investigation of Heat Transfer Rates on the External Surface of Baffled Tube Banks," by R. A. Bowman, A.S.M.E., Miscellaneous Papers, 1934.

EXAMPLE 1 EFFECT OF RATIO OF OUTSIDE TO INSIDE AREAS OF TUBES

Basic Data

Size	Bare tubes 5/8-in. × 18-gage admiralty	Finned tubes 3/4-in. nominal, 16 fins per in., admiralty
Ratio outside to inside surface	1.19	3.5
Shell-side-film rate	50	50
Tube-side-film rate	400	400
Fouling, both sides	1000	1000

Calculation of Heat-Transfer Rate

Resistance, shell film	0.02000	0.02000
Resistance, shell fouling	0.00100	0.00100
Metal-wall resistance	0.00002	0.00040
Resistance, tube fouling	0.00119	0.00350
Resistance, tube film	0.00298	0.00875
Total resistance	0.02519	0.03365
Over-all heat-transfer rate	39.7	29.7

as on the finned tube, showing the effect of the ratio of outside to inside areas.

While the bare-tube coefficient is 1/3 greater than that of the finned tube, the amount of surface on the finned tube is roughly 3 times as great, resulting in a net gain of volume inside the exchanger of about 2 to 1. As an example, in the case cited, if the same size shell is used then the length of the finned-tube unit will be roughly one half the length of the bare-tube unit. If the baffle pitch must be substantially the same on both, then the pressure loss in the finned unit, while somewhat higher per baffle, will likely be less over-all since fewer baffles would be required.

The finned unit works out most advantageously when the inside coefficient is fairly high, and at least 2 or 3 times as great as the outside coefficient.

Comparison of Results in Practice

To gain some impression of how the heat-transfer rates compare in practice, refer to Fig. 6 which shows a plot of test results on

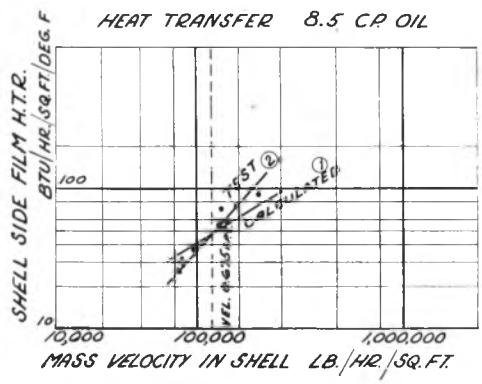

Fig. 6 Comparison of Oil-Film Heat-Transfer Rates, Bare Versus Finned Tubes

(Curve 1: Calculated rate for 5/8-in-OD bare tube in conventional shell-and-tube exchanger.
Curve 2: Test results for 5-in. shell unit 19 finned tubes, 5 1/2-in. baffle spacing; effective tube length 6 ft; baffle height 3.68 in.)

the 5-in. exchanger against calculated bare-tube results for the same conditions. This shows that at relatively low flow rates the finned tube has a lower shell-side heat-transfer rate, while when the flow exceeds what is about 1 fps, the rate catches the bare tube and begins to pull away. From a practical viewpoint it is desirable to have at least a velocity of 1 fps to keep the surface swept clean and also to get a high enough film factor so that the unit as a whole is economical. We feel therefore that the policy of rating the finned-tube unit with an outside film coefficient equal to that used for the bare tube, with velocities of at least 1 fps, is conservative and so it has worked out in practice.

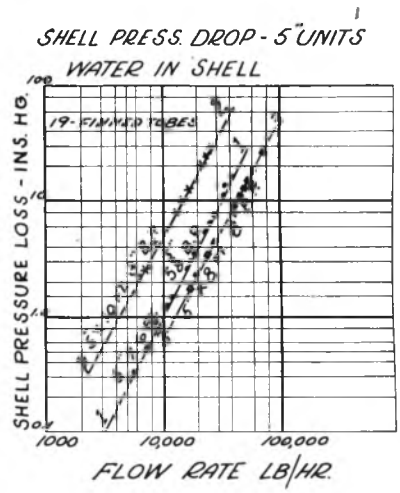

Fig. 7 Shell-Side Pressure Loss in 5-In. Unit With Water in Shell

(Curve 1: 5-in. × 6-ft unit, 5 5/8-in. baffle pitch; baffle height 3.68 in.
Curve 2: 5-in. × 10-ft. unit, 3-in. baffle pitch; baffle height 3.68 in.
Curve 3: 5-in. × 8-ft unit, 8-in. baffle pitch, with reduced segment cut; baffle height 3.25 in.)

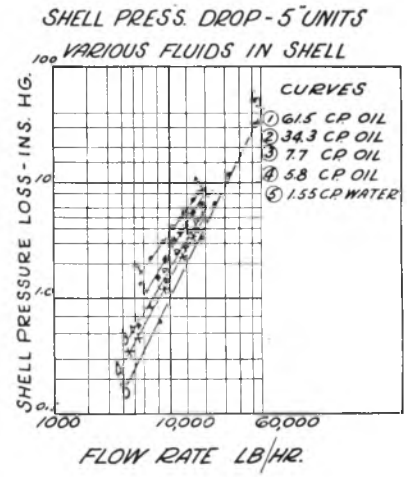

Fig. 8 Shell-Side Pressure Loss in 5-In. Unit With Various Fluids in Shell

(Baffle height, 3.68 in.)

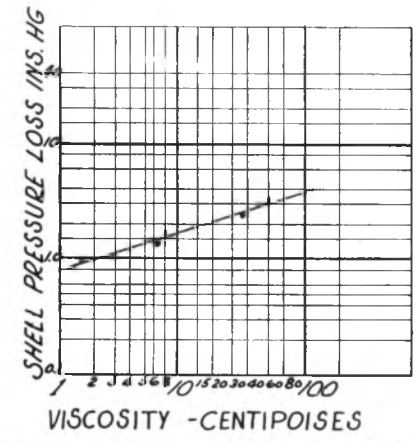

Fig. 9 Effect of Viscosity on Pressure Loss in 5-In. Shell

(Baffle height, 3.68 in.)

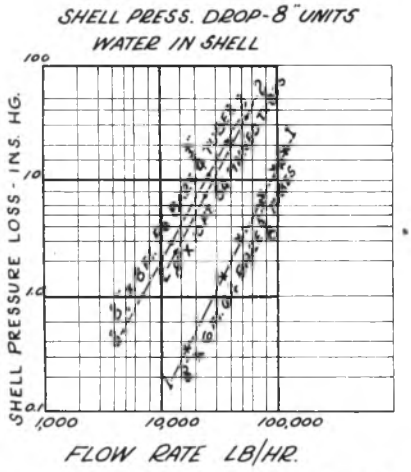

FIG. 10 SHELL-SIDE PRESSURE LOSS IN 8-IN. UNIT WITH WATER IN SHELL

(Curve 1: 8-in. × 6-ft unit, 64 tubes 3/4 in. OD on 13/16-in. triangular pitch, 7-in. baffle pitch, bare tubes; baffle height, 5.44 in.
Curve 2: 8-in. × 10-ft unit, 34 finned tubes 3/4 in. OD on 15/16-in. triangular pitch, 2 1/2-in. baffle pitch; baffle height, 5.66 in.
Curve 3: 8-in. × 8-ft unit, 55 bare tubes 3/4 in. OD on 15/16-in. triangular pitch, 2-in. baffle pitch; baffle height, 5.38 in.)

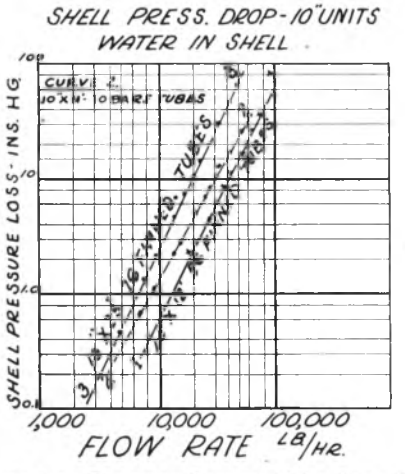

FIG. 11 SHELL-SIDE PRESSURE LOSS IN 10-IN. UNIT WITH WATER IN SHELL

(Curve 1: 10-in. × 12-ft unit, 56 finned tubes 3/4 in. OD on 15/16-in. triangular pitch, 3-in. baffle pitch; baffle height, 6.625 in.
Curve 2: 10-in. × 11-ft unit, 70 bare tubes, 3/4 in. OD on 15/16-in. triangular pitch, 2 1/2-in. baffle pitch; baffle height, 7.18 in.
Curve 3: 10-in. × 25-in. unit, 76 finned tubes, 3/4 in. OD on 15/16-in. triangular pitch, 1-in. baffle pitch; baffle height, 7.25 in.)

PRESSURE LOSS IN SHELL SIDE

To pass on to the subject of pressure loss in the shell side, we report here the results of a series of tests on small heat exchangers with both finned and bare tubes. We can say that the results of these tests on small units agree rather well with a much more extensive set of tests on units of larger size and widely varying description as to tube size, pitch, baffle spacing, etc.

At the outset we can state briefly that it seems rather obvious that one of the main factors in determining the pressure loss of a fluid through a baffled shell is the relation of the actual flow area to the by-pass or clearance area. The clearance area is the summation of cracks between tube and baffle and between the baffle and the shell. On close baffle pitches with normal tolerances, as recommended by the TEMA and the WPB, the amount of crack area may easily almost equal the normal flow area. In such cases our tests have shown that the pressure loss calculated without regard to by-pass area may be as much as 800 per cent high when the equipment is new and the effect of fouling has not come into play. There are several methods now in use to compensate for the effect of this by-pass area. None of these methods, however, can be any more accurate than the shop tolerances and in general we find variations from one exchanger to another are enough to upset seriously any exact method of compensating for by-pass area. Also we can state definitely that the relation of the baffle (segment-cut) flow to crossflow may have a serious effect on the over-all friction loss. This effect is so much greater than the surface effect of the finned tube that while the finned tube does have a greater friction loss, it is only a small part of the over-all drop in most cases. The shell inside diameter of the experimental unit was 5.047 in., baffle outside diameter was exactly 5 in., and baffle holes were 49/64 in.

The tests, Figs, 7, 8, 9, 10, 11, show actual pressure-loss measurements taken with water and with oil flowing through the shells of the heat exchangers tested. The manometer taps were located in the nozzles of the exchangers tested at an average distance of about 3 in. from the shell.

The effect of baffle height is clearly shown in Fig. 7. On curves 1 and 3 the number of baffles in the shell was almost the same, namely, 11 and 12. The tube length was 2 ft greater on 3 than on 1, or 33 per cent. Yet, by merely cutting the baffle height from 3.68 in. to 3.25 in. the friction loss was reduced in the face of the greater length. We cannot account for the slight variation in slope, although we do find from time to time that there will be some such minor differences in test results.

The effect of viscosity on pressure loss is indicated in Figs. 8 and 9, first showing that the lines, while at slightly different slope with higher viscosities, in general follow the same pattern. Fig. 9 shows the effect of viscosity taken at one flow rate. The test

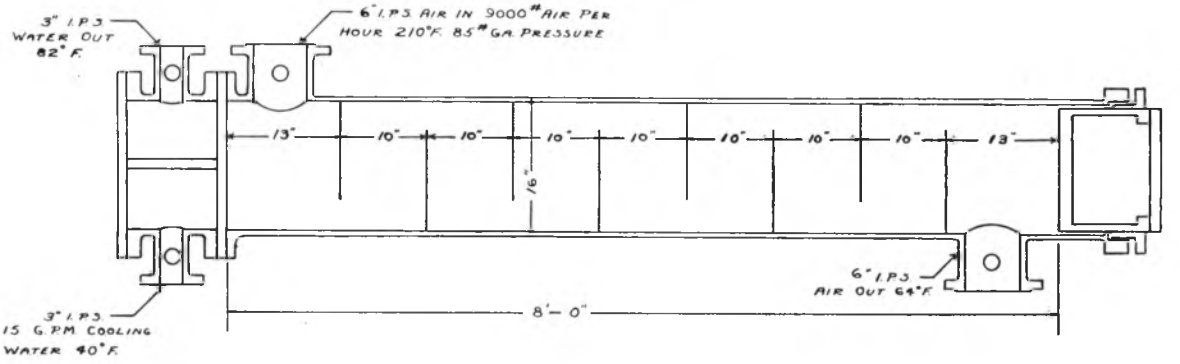

FIG. 12 TEST AIR AFTERCOOLER WITH FINNED-TUBE BUNDLE

points are in remarkably close agreement and we feel that the effect of viscosity on the particular exchanger tested is definitely greater than the effect on a larger unit of bare-tube design. The segment flow of oil passing along the tube perpendicular to the fins, introduces a considerable drag that would not be found in a bare-tube unit and it is possible that this effect increases with the viscosity.

Figs. 10 and 11 are given to show the trend in pressure-loss measurements on 8-in. and 10-in. units and to indicate that in general the same slope applies. The results shown were all taken on new and clean units.

From a practical standpoint we can state that finned-type shell-and-tube heat exchangers of this type have been in commercial use for the following purposes:

Cooling quench oil.
Cooling lubricating oil on Diesel engines.
Cooling circulating oil on hydraulic presses.
Cooling of air and compressed gases.
Cooling and condensation of organic vapors.
Condensation and subcooling of propane.
Vaporization of organic solvents.
Cooling of jacket water on Diesel engines.

To date, the performance of the finned tube in the services listed has been satisfactory when designed in accordance with the recommended procedure mentioned before.

As an example of field conditions, a metal-quench-bath oil cooler which had been in operation about 6 months on a continuous system, with oil temperatures varying from 50 F to 200 F, was taken apart and cleaned. Sludge had formed between the fins on the major portion of the bundle, but the edges of the fins were quite visible. On the baffles and tie rods the sludge had bridged over completely, indicating that the finned surface does not offer a firm footing for the sludge. The oil was about 0.9 specific gravity and 100 SSU at 100 F. The fouled performance was about 33 per cent of clean performance. The bundle was removed, sludge cleaned off by pouring solvent over the bundle, then a water hose stream removed most of the foreign material. The bundle was blown clean with compressed air and reinstalled, all in a period of approximately 2 hr. When reconnected the cooler gave approximately new performance.

Quenching-oil duty is relatively dirty and, in our opinion, about as dirty an application as should be considered for this type of finned surface.

Conclusion

The availability of a new low-ratio (3.5 to 1) finned tube of extruded manufacture opens a new field of application for liquid-to-liquid heat transfer for finned tubing.

Preliminary experimental results indicate that the surface is active at all points and that the heat-transfer rate from the fluid to the outside of the finned tube is in general somewhat better than that to the bare tube. It is felt that a conservative practice is to base designs on film-heat-transfer rates used for bare tubes for like service, using a minimum Reynolds number of 300.

The resistance to pressure loss is somewhat greater than the corresponding loss to a bare-tube bundle of the same dimensions, but other factors of design are very much more important in determining the pressure loss in a given unit.

Commercial heat exchangers incorporating finned tubes of the type described, are in service on several types of duty. Field experience with these has been satisfactory.

It is recommended that in the interest of furthering the application of finned tubes to industrial heat transfer, extreme care be applied in choosing the type to be used. Finned tubes of

TABLE 1 HEAT-TRANSFER TESTS—OIL IN SHELL TO WATER INSIDE TUBES OF 5-IN. × 6-FT FINNED UNIT

Basic Data

Externa lsurface, sq ft	57	Oil viscosity, tested, SSU at 210 F	41
Internal surface, sq ft	16.3	Oil viscosity, tested, SSU at 100 F	115
Crossflow area between baffles, sq ft	0.0669	Number of tubes	19
Baffle pitch, in. center to center	5/8	Single pass both sides	Counterflow
Oil specific heat, at 150 F	0.49	Water-side viscosity correction $\left(\frac{Z}{Z_w}\right)^{0.14}$	1.10
Oil specific gravity, at 150 F	0.855		

Tabulated Data

Oil flow rate, lb per sec	Pressure loss through shell, in. Hg	Temp oil entering, deg F	Temp oil leaving, deg F	Temp drop, deg F	Viscosity (cp) oil at avg temp, deg F	Water flow rate, gpm	Temp water entering, deg F	Temp water leaving, deg F	Temp rise, deg F	Heat balance—oil, Btu per hr	Heat balance—water, Btu per hr	MTD, deg F	Over-all heat-transfer rate, U	Film heat-transfer rate, water inside tubes $h_i\left(\frac{Z}{Z_w}\right)^{0.14}$	Film resistance inside tube plus metal resistance, $\frac{3.5}{h_i\left(\frac{Z}{Z_w}\right)^{0.14}} + \frac{1}{h_m}$	Film heat transfer rate on oil side h_s
2.92	1.6	177	135.3	41.7	7.6	18.8	36.2	61.2	25	215000	235000	106	38.8	280	0.0117	71.95
3.6	2.35	169	132.2	36.8	8.2	18.4	36.4	62	25.6	234000	235500	102	40.5	278	0.0118	77.5
1.68	0.60	175.3	127.8	47.5	8.1	19.3	36.4	51.6	15.2	141000	146500	109	23.6	270	0.0122	33.1
1.55	0.60	172	124.7	47.3	8.45	19.3	36.2	50	13.8	129300	133100	103	22.7	270	0.0122	31.3
1.55	0.57	169.7	122.2	47.5	8.77	19.3	36.2	49.2	13	130000	125300	102	21.6	270	0.0122	29.35
1.46	0.52	174.8	125.4	49.4	8.3	15.8	36.2	51.7	15.5	127000	122500	105	20.4	220	0.0148	29.2
1.44	0.50	172	123.6	48.4	8.55	15.8	36	50.8	14.8	123000	116900	103	19.9	220	0.0148	28.25
1.44	0.50	170	122.5	47.5	8.65	15.8	36	50	14	120800	110600	102	19.0	220	0.0148	26.5
2.6	1.28	170.4	128.7	41.7	8.33	15.8	35.8	57.6	21.8	191200	172200	102	29.7	225	0.0145	52.1
2.7	1.43	169.4	129.4	40	8.4	15.8	35.8	58.4	22.6	191000	178500	102	30.7	225	0.0145	55.3
2.65	1.45	162	125.6	36.4	9.24	15.8	35.8	56.6	20.8	170500	164500	98	29.4	225	0.0145	51.3
4.5	3.45	164	135.6	28.4	8.3	13.8	36.8	67	30.2	226000	208500	97.8	37.4	195	0.0107	100.0
4.6	3.7	160.6	133.4	27.2	8.68	13.8	36.4	65.8	29.4	220500	202600	95.9	37.1	195	0.0167	98.0
4.6	3.75	152	127.8	24.2	9.75	13.8	36.2	62.6	26.4	196500	182000	90	35.5	195	0.0167	87.7

low ratio and close fin spacing should not be used where the fouling is severe, or where the fluid is definitely corrosive to the tube metal available. There are a number of applications where the finned tube is not mathematically desirable, principally where the film rate on the finned side is equal to or greater than the film rate on the plain side.

Appendix

Tables 1, 2, and 3 make up the Appendix.

TABLE 2 CALCULATIONS FOR HEAT-TRANSFER CURVE, $\frac{DG_s}{\mu}$ VERSUS $\left(\frac{h}{cG_s}\right)\left(\frac{c\mu}{k}\right)^{2/3}$

Basic Data

c = specific heat, taken at 0.49 (from TEMA Standards)
D = tube diameter 0.0547 ft
G_s = shell-side mass velocity, lb/(hr)(sq ft). Leakage factor omitted
k = thermal conductivity, taken at 0.074 Btu/(hr)(sq ft)(deg F/ft) (from TEMA Standards)
μ = viscosity at average body temperature, lb/(hr)(ft)

Tabulated Data

G	μ	$\frac{d_s G_s}{\mu}$	$\left(\frac{c\mu}{k}\right)^{2/3}$	h_s	$\frac{h_s}{cG_s}$	J
157200	18.4	468	24.5	71.95	0.000932	0.0228
194000	19.85	535	25.8	77.5	0.000815	0.0210
90500	19.6	253	25.6	33.1	0.000748	0.0192
83500	20.5	223	26.5	31.3	0.000765	0.0203
83500	21.2	216	27.1	29.35	0.000716	0.0194
78600	20.1	214	26.1	29.20	0.000758	0.0198
77500	20.7	205	26.6	28.25	0.000745	0.0198
77500	20.9	203	26.7	26.50	0.000698	0.01865
140000	20.2	379	26.2	52.1	0.000760	0.01990
145500	20.3	393	26.25	55.30	0.000775	0.0204
142800	22.4	348	28	51.3	0.000735	0.0206
242300	20.1	660	26.1	100.0	0.000838	0.0219
248000	21.0	645	26.8	98.0	0.000806	0.0216
248000	24.6	551	29.8	87.7	0.000723	0.0216

J = dimensionless number $\left(\frac{h_s}{cG_s}\right)\left(\frac{c\mu}{k}\right)^{2/3}$

TABLE 3 PERFORMANCE DATA AND CALCULATIONS FOR 16-IN-SHELL × 8-FT-TUBE-LENGTH FINNED-TUBE AIR AFTERCOOLER; AIR IN SHELL, WATER IN TUBES

Basic Data

Number of tubes	154
Length of tubes, ft	8
Outside surface, sq ft	616
Inside surface, sq ft	176
Arrangement	Air-single pass Water-two pass
Baffle pitch, in.	10
Area for crossflow over tubes, sq ft	0.443
Water quantity, gpm	15.0
Water temperature:	
Entering, deg F	40
Leaving, deg F	82
Air quantity, lb per hr	9000
Air temperature:	
Entering, deg F	210
Leaving, deg F	64

Calculations

Greater temperature difference	Lesser temperature difference
210	64
82	40
128	24

Uncorrected MTD ..... 62 deg F
To correct MTD refer to pass-correction plot (TEMA Standards, p. 20)

$$K = \frac{42}{170} = 0.247$$

$$R = \frac{146}{42} = 3.47$$

F is on flat of curve. The most conservative estimate gives F as a maximum value of 0.55
Corrected MTD = 62 × 0.55 = 34.1 deg F
Heat load = 15 × 500 × 42 = 315,000 Btu per hr

$$\text{Heat-transfer rate} = \frac{315{,}000}{34.1 \times 616} = 15.0 \text{ Btu/(hr)(sq ft)(deg F)}$$

Discussion

R. G. Vanderweil.[4] It seems quite encouraging that this paper gives the designing engineer a chance to compare test data with actual data taken on commercial heat-transfer equipment. As to the use of finned and unfinned surfaces, the writer would like to complement the author's statements with the following:

It seems that the only criterion not only in selecting between finned or unfinned tubes, but also in selecting the fin spacing, thickness, and the width of the fin, is the ratio of the two film coefficients f_s/f_o.

In this connection, the writer would like to know if tests have been carried out with one fin arrangement only, or by any chance a second set of tubes with fins of less thickness and pitch but of the same width has been tested? Finally, it would be interesting to know how the over-all heat output of exchangers compares if shells of the same over-all dimensions are used and provided with prime surface in one case and with finned tubes in another.

Author's Closure

It should be emphasized that the tests were made on equipment of commercial scale and may not entirely agree with tests on single tubes or tests made under conditions which might be different from commercial practice.

It is suggested by Mr. London that there may be a break in the curve in Fig. 5 resulting in a change of slope, at the point where there may be a change-over from viscous flow to turbulent flow. The available data are found to be so scattered, however, that there is no clear-cut line, and frankly at this time we feel that the accuracy of the test data reported so far in the literature would not allow that much refinement.

The tests reported cover only one type of finned tube. This type is the only type tested and was chosen for a combination of mechanical and thermal reasons. It is a question of using an available tube which has desirable features mechanically and which for a number of uses is also suitable thermally. To cover a wide range of applications different ratios can be employed, but testing these goes beyond the scope of this paper.

Mr. Donahue suggests that the data be plotted using the Nusselt method rather than Dr. Colburn's method which has been used. This may well give a better agreement and it is regretted that the time to do this has not been available.

The tests were made using comparatively clean city water, which is not thought to have had much tendency toward fouling in the time the tests were run. The orifices were calibrated by separate calibration runs during which the fluid discharged was actually weighed.

The question has been raised whether the type of finned tube used has given difficulty from cutting tube walls at the baffle or tube support due to vibration. So far in normal crossflow service we have seen no evidence of this—certainly no greater tendency on the part of this tube than on a bare tube. Most duties have been with close baffle pitches where the tendency toward extreme vibration is considerably curbed.

Again it must be stressed that this report is preliminary in nature and is only a first indication of what may be expected from shell-and-finned-tube exchangers of this type. A number of these are in commercial service and so far have proved satisfactory.

[4] Office of Consulting Engineer, Chase Brass & Copper Company, Waterbury, Conn.

Heat-Transfer Coefficients and Other Data on Individual Serrated-Finned Surface

By E. A. SCHRYBER,[1] BROOKLYN, N. Y.

The purpose of this paper is to provide data on the serrated (segmented) type of finned surface; also to show the ease of fabrication and the flexibility of sizes, i.e., the ability to alter the ratio of secondary to prime surface without difficulty.

THE individual serrated-finned surface under discussion is made from relatively thin flat metal strip. As the finned surface is wound around the tube, each individual fin takes the shape, roughly, of the letter L. The foot of the L is the shoulder of the fin and is used to secure a bond between the fin and the tube wall. The thickness, width, and length of the fin may vary to suit the need, but the general appearance and method of manufacture remain the same. The shoulder, or base, of the finned surface is continuous and is wound around the tube in a helical manner. The individual fins, being perpendicular to the shoulder, are caused by this winding operation to stand out from the tube in much the same manner as spokes from the hub of a wheel. Each individual fin is given a slight twist so that its flat surfaces do not follow the helical wind but lie in planes parallel to all other fins and perpendicular to the axis of the tube. These details are indicated in Fig. 1.

With the serrated form of tube surface, no material is removed in forming the fins. The total width of all the fins in one row will therefore substantially equal the circumference of the tube. The fin height times the circumference of the tube, doubled to cover the area of both sides of the fin, plus the area of the fin edges, will substantially total the area of one row of fins. Where the same fin length is used, larger- or smaller-diameter tubes will have a surface area directly in proportion to the diameter of the tube. Changing the number of rows of fins per inch of tube or using longer or shorter fins will give a wide range of ratios of secondary to prime surface.

It is not the purpose of this paper to go into a lengthy discussion of the relative value of individual serrated surface compared with other surface designs. Considerable work has been done by others, among them the interesting paper by Norris and Spofford.[2] Evidence has frequently been presented that the design of extended surface greatly influences its over-all heat transfer per square foot of surface and per foot of tube length. Extensive laboratory tests[3] were made to establish the performance data for the surface under discussion. An all-copper tube, solder-bonded, was used, having a $^5/_8$-in. tube, $1^1/_2$ in. diam over the fins, 7 rows of fins per inch. The results, together with a description of the test apparatus and procedure, follow.

Details of Test Setup

The construction details of the test setup should be carefully noted, Figs. 2 and 3. They were selected to give the nearest approach to basic data and take into consideration the fact that units of this sort are sensitive to installation details, such as rounded versus sharp edges, and forced versus induced convection. Air was drawn through the test section, thence through the calibrated bellmouth orifice, by which the quantity of air was measured, then through an exhauster fan which was operated at various speeds. Air temperatures were taken by thermocouples ahead and behind the heater section, all shielded by aluminum foil to minimize radiation errors. The flow of air was measured at the bellmouth orifice by a pitot tube.

Three assembly units were tested. The first was a single row of 15 vertical tubes, each 2 ft long, assembled on $1^1/_2$-in. centers. The gross duct area was practically 4 sq ft (2 ft × 2 ft) where occupied by the coil. The second assembly consisted of two rows, each identical to the single-row section, but placed with the second row slightly offset so that the center line of the rear row of tubes was at the mid-point of the front row (known as staggered arrangement). The third test assembly consisted of three rows of tubes, all identical, and also assembled in a staggered arrangement.

Table 1 gives the important dimensions of the units tested.

TABLE 1 UNIT DIMENSIONS

	Unit 1	Unit 2	Unit 3
Tube inside diameter, in.	0.575	0.575	0.575
Tube outside diameter, in.	0.652	0.652	0.652
Outside diameter extended surface, in.	1.5	1.5	1.5
Thickness extended surface, in.	0.010	0.010	0.010
No. of fins per inch	7	7	7
Numbers of rows	1	2	3
Number of tubes per row	15	15	15
Air-side area, sq ft per ft tube	1.245	1.245	1.245
Air-side area of unit, sq ft	37.4	74.8	112.2
Steam-side area of unit, sq ft	4.51	9.02	13.53
Ratio air-side to steam-side area	8.29	8.29	8.29
Approach-face area, sq ft	3.9	3.9	3.9
Net area between tubes, sq ft	2.03	2.03	2.03
Length of tubes, ft	2	2	2

Three sets of curves represent the results of these tests. Only the over-all coefficient of heat transfer and pressure-drop[4] curves are shown here, Figs. 4 and 5. Equations for the heat-transfer curves are as follows:

Row (1) $U = 0.165\ G^{0.523}$
Rows (2) $U = 0.143\ G^{0.542}$
Rows (3) $U = 0.0838\ G^{0.6}$

U = Btu per hr per sq ft total air-side area per deg F, L.T.D.
G = lb air per hr per sq ft net or free area

Conducting the Tests

As the test runs were being conducted, a check was made from time to time of the heat balance between the air-temperature rise and the steam condensed. As this balance was found to be in accord, within reasonable test limits, the tests were recorded and

[1] Extended Surface, Inc.

[2] "High-Performance Fins for Heat Transfer," by R. H. Norris and W. A. Spofford, Trans. A.S.M.E., vol. 64, July, 1942, pp. 489–495.

[3] These tests were made in the laboratory of The Pennsylvania State College under the personal supervision of H.A. Everett and F. C. Stewart, and the results presented in a private report from which the data herewith are abstracted.

Contributed by the Heat Transfer Division and presented at the Annual Meeting, New York, N. Y., Nov. 27–Dec. 1, 1944, of The American Society of Mechanical Engineers.

[4] The schematic drawing of the test layout, Fig. 3, shows an ordinary slant gage as the device for determining the pressure drop through the test sections. However, to insure utmost accuracy, a manometer calibrated in thousandths of an inch was used to determine the exact pressure drop as shown on the curves.

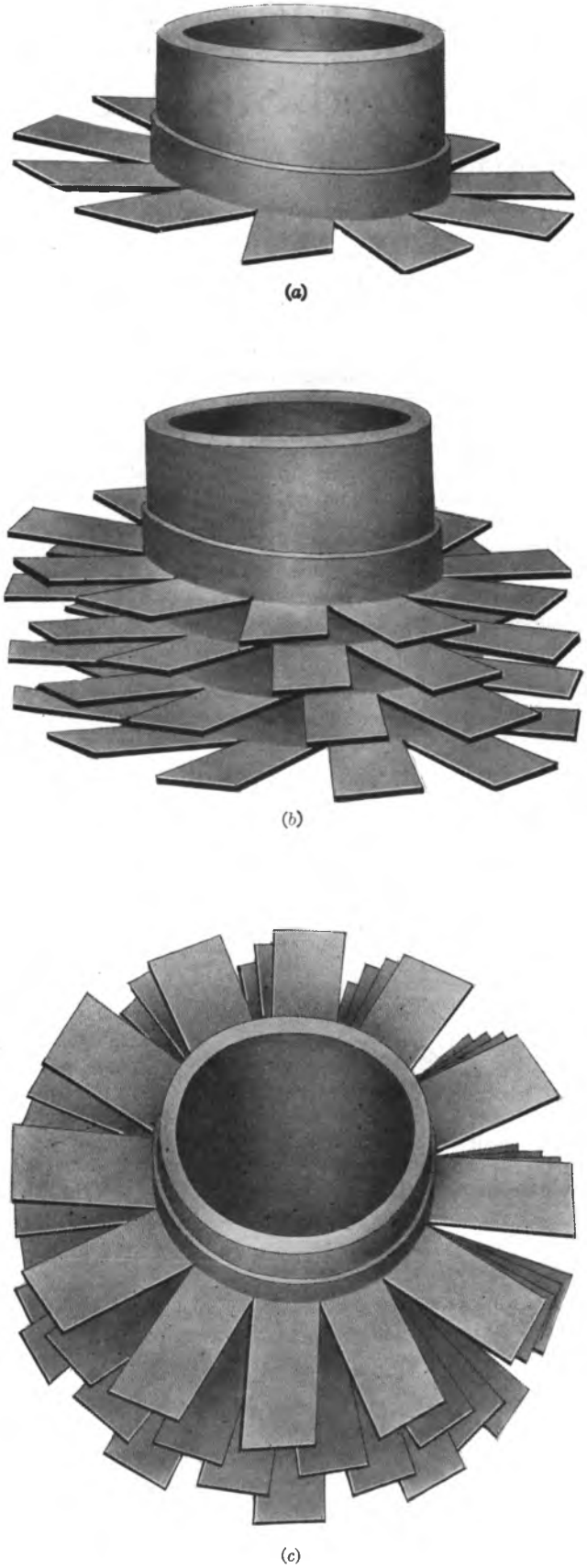

FIG. 1 DETAILS OF SERRATED-FINNED TYPE OF TUBE SURFACE

checked using the air-temperature rise to calculate the total Btu transfer. Special care was taken to limit heat losses so that the heat taken up by the air would equal the heat given up by the steam.

Reference to the schematic drawing of the test apparatus, Fig. 3, will show five thermocouples, connected in series, ahead of the test section to measure the temperature of the incoming air. Behind the test section are nine thermocouples, connected in three series of three each, to measure leaving-air temperature. There is an air-mixing and straightening chamber about 4 ft long immediately behind the test section, at the discharge end of which was placed the nine thermocouples. Checking one series of thermocouples against another, on the discharge side, indicated an even temperature distribution at this point.

Attention is called to the fact that but one-, two-, and three-row assemblies were tested. The primary objective of these tests was to ascertain the heat-transfer characteristics and pressure-drop characteristics of the surface design. The results of these tests therefore are not directly comparable with tests of multiple-row assemblies.

METHOD OF MANUFACTURE

To build the individual serrated-finned-surface tube, a simple but complete machine designed solely for this purpose is used. The bare tube is fed into the side of the machine and reels of fin stock are fed from the rear. The turning and forward progression of the tube, the serrating and bending of the fin stock, the winding of the fin stock on the tube, are all accomplished simultaneously and synchronized. The use of wider or narrower fin stock will result in longer or shorter fins, but the fabricating operation remains the same. Also, by winding the fins at a greater or lesser number of turns per inch the ratio of prime to secondary surface can be altered at will.

Securing the fins to the tube is accomplished in one of two ways. Either the tube, as it passes through the winding operation, now progresses through a fluxing and soldering bath, or the shoulder of the fins is welded to the tube by continuous electric-resistance welding simultaneously with the winding operation. All nonferrous metals can be easily bonded by the soldering method. Capillary attraction causes the solder to flow under the shoulder of the fin creating a metallic bond with an area far greater than the cross-sectional area of the fin itself. Most metals can be readily resistance-welded by known techniques and some of the more difficult metals to weld, including aluminum and copper, are now being welded, and commercially acceptable welding techniques are being developed. The joining of metals by welding, as it applies to extended-surface tubes, opens a new field for this product. Subzero temperatures, as well as very high temperatures, can be handled without thought to bond rupture or disintegration. This development of the resistance-welding method of securing a bond is a substantial improvement over metallic or mechanical bonds.

For the handling of corrosive fluids or gases on either side of the tube, bimetal extended-surface tubes can be fabricated by the welding method to the great advantage of the coil designer. Combinations of bimetal tubes using steel, copper, monel metal, cupronickel, admiralty metal, etc., can be fabricated. In this manner the most durable and satisfactory metal surface, either inside or on the outside of the tube, can be presented to the destructive action of many commonly handled materials, such as hot oil, ammonia, acid or alkaline solutions, many corrosive gases, etc. Fin materials would be the same as the outside surface of the tube thereby presenting a corrosion-resistant surface with a welded bond. The structure of the bond would be such that durability and full flow of heat through this important point could be expected.

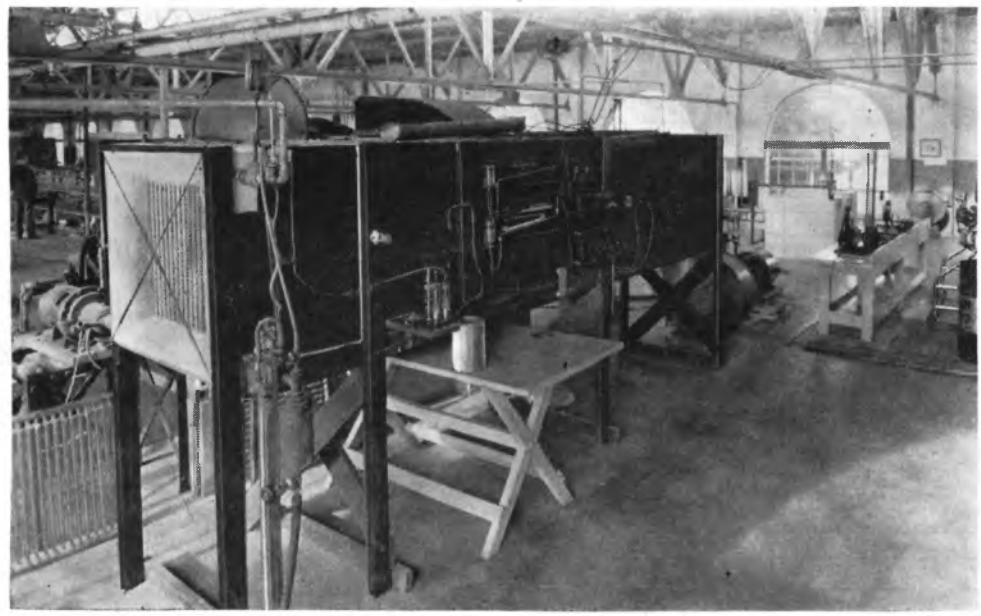

FIG. 2 VIEW OF TEST APPARATUS SET UP IN LABORATORY

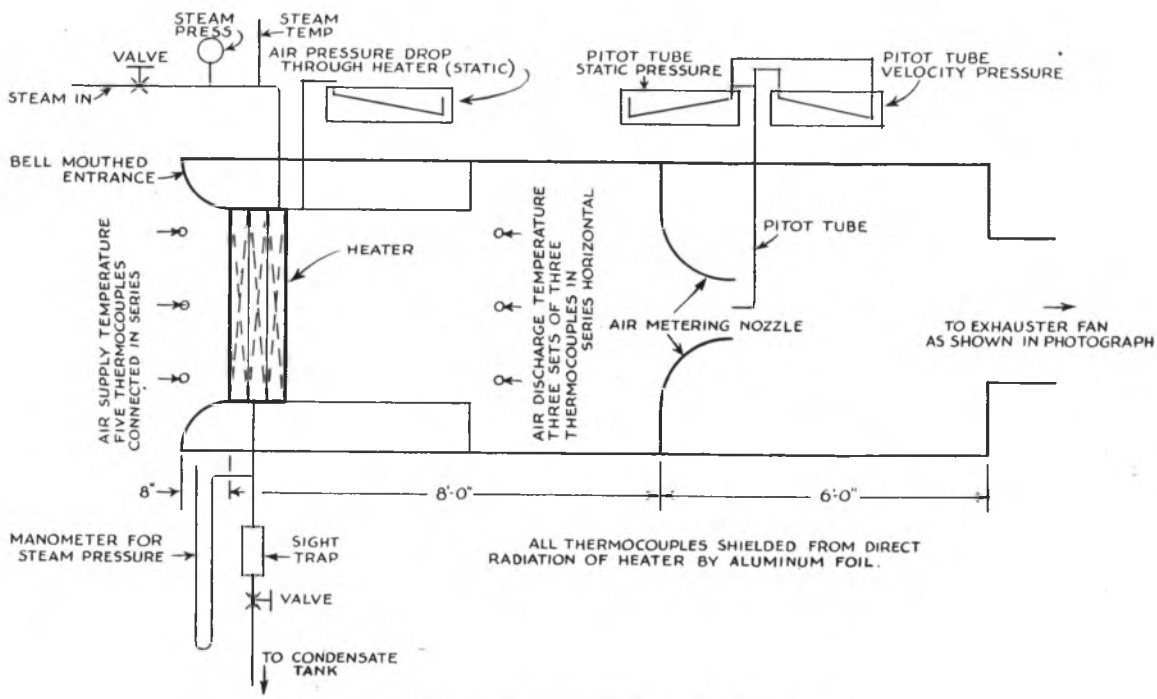

FIG. 3 SCHEMATIC DIAGRAM OF TEST APPARATUS

SPECIAL APPLICATIONS

Distinct and apart from the foregoing tests has been the application of individual serrated-finned surface in tube-within-tube heat exchangers. In this application the V-shaped openings between the individual fins form a definitely controllable and computable free opening in direction of flow. Full test data on the performance of this surface in such applications is not presently available. While the surface arrangements are not directly comparable, the paper by Gunter and Shaw[5] shows the value of many short surfaces, instead of long continuous-surface arrangements, in direction of flow. Of similar character is the application of extended-surface tubes in standard shell-and-tube heat exchangers. Their definite worth is being demonstrated in many installations; however, their comparatively recent widespread use is handicapped by the lack of generally acceptable data except for specific applications.

Individual segmented-finned surface, because of its high heat-transfer coefficient, is economical to use. If higher values of U are obtained per square foot of outside surface, it is axiomatic that economy of surface, and therefore economy of metal used, will result. For full commercial realization of this economy of de-

[5] "Heat Transfer, Pressure Drop, and Fouling Rates of Liquids for Continuous and Noncontinuous Longitudinal Fins," by A. Y. Gunter and W. A. Shaw, Trans. A.S.M.E., vol. 64, 1942, pp. 795–802.

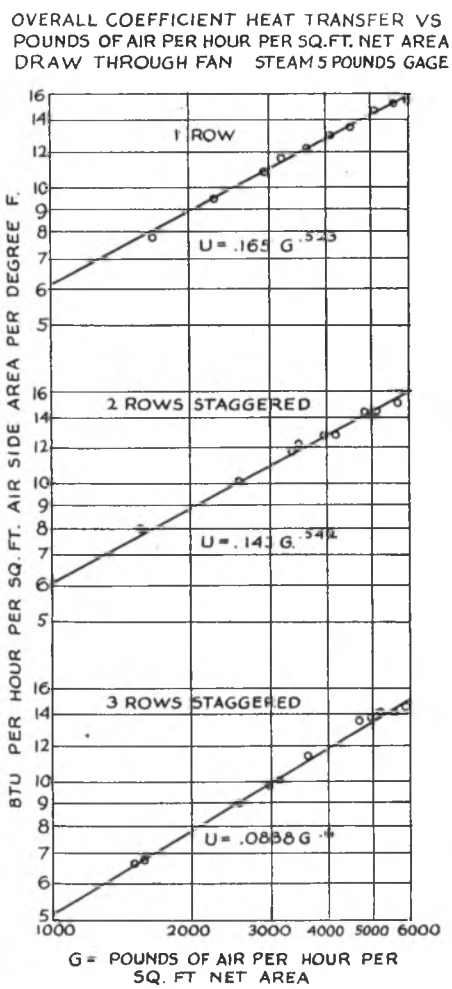

FIG. 4 OVER-ALL COEFFICIENT OF HEAT TRANSFER VERSUS POUNDS OF AIR PER HOUR PER SQUARE FOOT NET AREA DRAW THROUGH FAN
(Steam 5 lb per sq in. gage.)

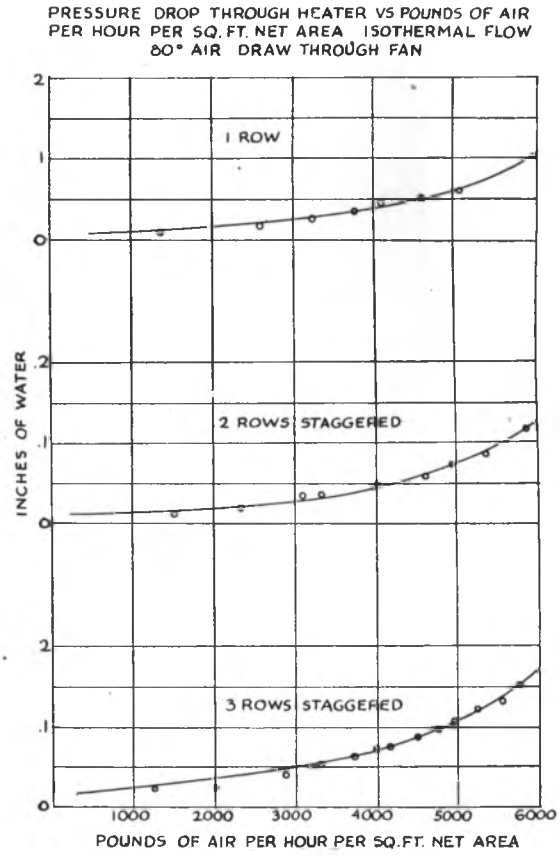

FIG. 5 PRESSURE DROP THROUGH HEATER VERSUS POUNDS OF AIR PER HOUR PER SQUARE FOOT NET AREA
(Isothermal flow, 80 F air draw through fan.)

sign, it is necessary that it be coupled to economy of manufacture. Rapid automatic single-purpose machines, building the tube in one operation, complete the team of engineering and technological progress. Individual segmented-finned surface which can be made with a wide range of fin lengths, with a wide range of fin spacings per inch and wound on any size of tube, is therefore an extended-surface tube, the design of which gives use and manufacturing economy.

Discussion

R. G. VANDERWEIL.[6] Is it possible to apply successfully the soldering and welding equipment mentioned to narrowly spaced fins, say $^1/_{16}$ in. spacing, of a height of 1 to 2 in.? Another question arises in connection with the application of the flux: We have found that the flux applied between fin and tube will accumulate at certain spots in the joint and thus decrease the effectiveness of the bond. This is particularly true for fins of small spacing and where no openings were provided to accommodate the exit of the flux from the joint.

[6] Office of Consulting Engineer, Chase Brass & Copper Company, Waterbury, Conn.

AUTHOR'S CLOSURE

In reply to the questions by Mr. Vanderweil, the fabrication of narrowly spaced fins, both solder-bonded and welded, has been done experimentally. However, there is a practical difficulty; the foot of the fin strip must be strong enough to stand the stress of fabrication and is usually not less than $^7/_{64}$ in. wide. Therefore, the building of tubes of more than 8 rows of fins per inch necessitates a partial overlapping of the fin shoulder. This overlapping brings up new problems and the fabrication of very narrowly spaced fins has not been done in normal production. The height of the fin is of no consequence.

It has been the practice to use an aqueous mixture of ammomium chloride and zinc chloride, together with a wetting agent, in mild solution as a flux. This is jetted on the tube after the winding operation, and thoroughly wets all exterior surfaces. The surface between the tube wall and the fin shoulder is wetted by capillary attraction. The molten solder, applied immediately after and in like manner, apparently flushes off all acid residue. No evidence of acid inclusion has yet been found.

Disk Extended Surfaces for High Heat-Absorption Rates

By G. E. TATE[1] and JOHN CARTINHOUR,[2] NEW YORK, N. Y.

Four types of disk-on-tube extended-surface heat exchangers are discussed in this paper, i.e., interlocking cast-iron sections of nine disks each; die-cast aluminum-alloy disks each with shroud and hub; two surfaces die-pressed from wrought-iron sheet, each with a flue; and one a sixteen-pronged star. Data for both the cast-iron and aluminum surfaces were obtained from tests of full-sized economizers in conjunction with boiler tests, while data on the wrought-iron disks were obtained from laboratory studies. Details are given of the testing procedure, and the results in terms of effectiveness of the various surfaces are analyzed and correlated.

THE advantages of using extended surfaces in commercial-sized heat exchangers have long been generally recognized. Convenient proportions, greater compactness, fewer pressure joints, ease of arranging counterflow of the heat-exchanging fluids, and ease of achieving equal flows in the parallel circuits being traversed are the principal advantages realized. A requisite of commercial heat exchangers, unless their use is to be restricted to clean fluids, is provision for cleaning the heat-exchanging surfaces with ease and speed. A type of extended surface having these features is the disk-on-tube, four varieties of which are illustrated in Figs. 1 to 3, inclusive.

Types of Heat-Absorbing Surfaces

The first variety, Fig. 1, consists of interlocking cast-iron sections of nine disks each, shrunk onto steel tubes. Sand molds are used in the casting process. The internal surface, which is to be in contact with the tube, is broached to a diameter slightly less than that of the tube; the joint faces are finished on semiautomatic machines. The external surface requires neither machining nor finishing. The contact between tube and cast-iron section, after the latter is shrunk on, has a thermal resistance of the order of 0.002 deg F hr/Btu per ft length of finned tube. This value includes the resistance of the hub metal.

This form of extended surface has been most frequently applied to superheaters and economizers for stationary and marine boilers, waste-heat boilers, and oil heaters. Another interesting application is to gas coolers for chemical processes where the resistance of cast iron to highly corrosive gases is utilized. For example, cast-iron surface is advantageously used in the sulphur-dioxide coolers required after the initial sulphur-burning step of the contact process of making sulphuric acid. Here the primary function of the heat exchanger is to cool the reactant mixture of gases to the temperature required for the next step; the conservation of useful heat is a valuable secondary function.

The second type, Fig. 2, consists of individually die-cast aluminum-alloy disks, each having a shroud and hub. The

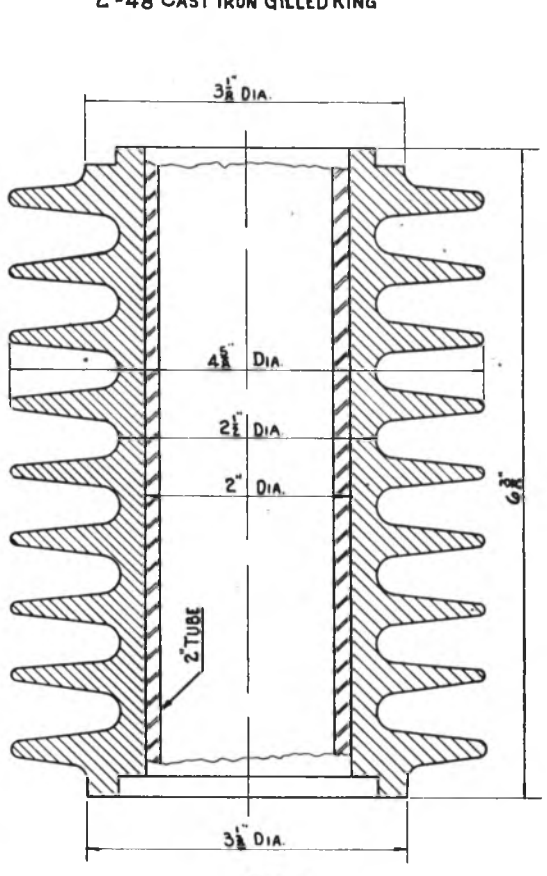

Fig. 1

accuracy of the casting and the condition of its surface are such as to require no machining. In assembly a hydraulic ram is used to force each disk, the internal diameter of which is less than the outer diameter of the tube, onto the tube and against the preceding disk. As may be seen from the assembly figure, the tip of the shroud of the preceding disk is encased in a groove in the leading end (gill) of the disk being put in place. At the same time, the steel hoop ring is forced onto the hub underneath the shroud. Tubes of particularly close tolerance are used in order to insure good contact between hub and tube.

Under service conditions the hoop ring and tube expand less than the aluminum hub, on account of the lower coefficient of thermal expansion of steel. The function of the hoop ring is to hold the aluminum hub in good thermal contact with the tube. The thermal resistance of this contact, including the metal of the hub, is approximately 0.002 deg F hr/Btu per ft length of finned tube. This value represents a mean of extensive tests wherein test elements 1 ft long and comprising 22 disks are heated in a 9-kw electric furnace. The element is in effect the heating surface of a natural-circulation boiler, and the heat absorbed is obtained from the measured electric power as well as from the steam pro-

[1] Research Physicist, Foster Wheeler Corporation.
[2] Engineer, Foster Wheeler Corporation.
Contributed by the Heat Transfer Division and presented at the Annual Meeting, New York, N. Y., Nov. 27–Dec. 1, 1944, of The American Society of Mechanical Engineers.

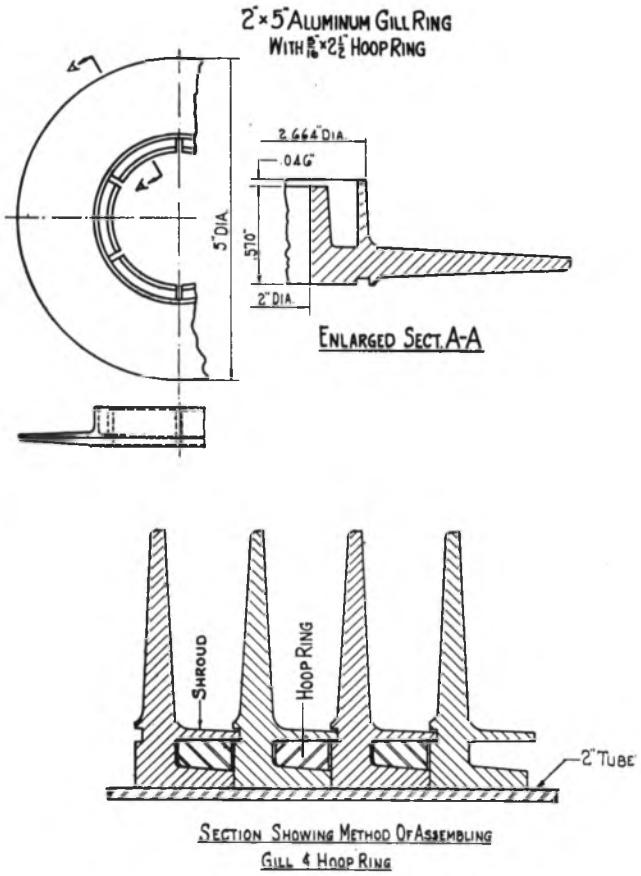

Fig. 2

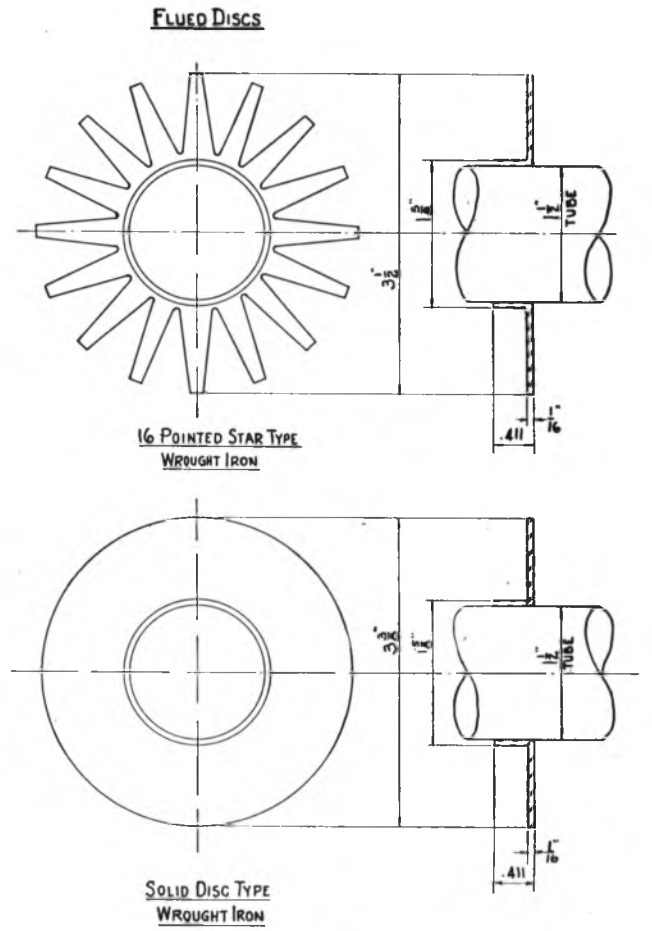

Fig. 3

duced. The temperature of the disks, hubs, and tube are measured with thermocouples.

The aluminum disk was developed for application to economizers of marine boilers where space and weight are of primary importance. Its use obviously is not limited to this application. A limit to the maximum, feasible, heat-absorption rate does exist, however, as the tips of the disks must be kept below the softening temperature (approximately 1000 F). By means of the theoretical formulas of Schmidt (1),[3] which relate the temperature drop, fin tip to base, to the heat-absorption rate, the theoretically safe maximum rate of heat absorption can be expressed as a function of tube temperature. In actual service a heat-absorption rate of 43,000 Btu/hr per ft length of 2-in. tube has been reached with a tube temperature of 480 F, without impairment of the tips of the disks.

The third and fourth surfaces are formed from wrought-iron sheet by a series of die-press operations. The resulting shape is a disk with a flue. In one case portions of the disk are cut out by stamping, leaving a sixteen-pronged "star." Wrought iron is used because of its thermal conductivity and ductility. These disks are then attached to the tube by seam-welding the flues to the tubes by means of automatic welding machines. Fusion between the metal of the flue and that of the tube takes place over approximately 50 per cent of the flue width. The thermal resistance of the flue, including the weld, is found to be less than 0.002 deg F hr/Btu per ft length of finned tube. These disks are used in economizers where weight and space are at a premium.

[3] Numbers in parentheses refer to the Bibliography at the end of the paper.

Taking Test Data

The data for both the cast-iron and aluminum surfaces were obtained from tests of full-sized economizers in conjunction with tests of the boilers proper. The flue-gas temperature ranged between 1150 F maximum at the inlet and 200 F minimum at the outlet; the inlet feedwater temperature ranged between 150 F minimum and 410 F maximum. In the aluminum-ring-economizer tests the fuel was oil, while for the cast iron several types of coal are included, as well as oil.

It is recognized that the accuracy of some of the data is not of a high order. True average gas temperatures are difficult to measure on large-scale equipment, particularly at the inlets of economizers placed close to the boiler outlet, where little mixing of the gas has taken place. Radiation losses from thermocouples also add to the difficulty. Hence a selection from the data obtained over a period of several years was made, using the heat balance as a criterion in judging the accuracy of the temperature measured with thermocouples. Only tests in which the feedwater flow, the fuel-consumption rate, the fuel analysis, and the flue-gas analysis were accurately determined are included.

The data presented on the wrought-iron disks were obtained by laboratory tests of air heaters, wherein room air passing over the fins was heated by steam condensing inside the tubes. Finned elements 1 ft long were arranged in staggered rows, four elements in each of the five rows, on $4^1/_8$-in. equilateral centers. Dummy half-elements were used at each end of alternate rows in order to effect the same flow pattern around the end elements as obtained about the middle ones. The tubes were vertical in order to

insure free drainage of the condensate. The temperature of the air was measured by means of thermometers in regions where the air was well mixed. Standard orifices were used to meter the air. The heat absorbed by the air was in good agreement with the heat given up by the steam, as calculated from the measured quantity of condensate, steam pressure and temperature, and condensate temperature.

The results of the laboratory tests have been compared with tests on economizers used to cool the flue gas from boilers with the feedwater, and substantial agreement was found. The data from the laboratory tests are presented in preference to those from full-sized economizers for two reasons:

1 Absence of soot.

2 Small variation of thermal properties of the air over the small temperature range obtaining.

As a matter of interest results of a test of unflued disks $4^3/_4$ in. diam and $^1/_{16}$ in. thick, silver-soldered to 2-in. tubes, have been included. Five staggered rows, each of three tubes 1 ft long, comprised the air heater. The tubes were on $5^1/_4$-in. centers.

From the over-all coefficients of heat transfer from the gas to the water U', the corresponding coefficient of heat transfer from gas to fin surface h, was computed by means of the relation

$$1/h = 1/U' - (S_1 + S_2)\Sigma R$$

Here ΣR is the sum of the following thermal resistances: Fluid inside tube to inner tube wall; the rust layer on this surface; the tube wall itself; contact between tube and flue, or hub; flue or hub; disk. No allowance for soot deposits on the fin and flue surface was made in the case of the full-sized economizers, because of the arbitrary assumptions that would be involved.

In calculating the resistance of the inner fluid, also that of the tube wall, the ample data of various investigators (2) were utilized. The resistance of the rust deposit was calculated from its measured thickness on the assumption that the deposit was porous and therefore the thermal conductivity was equal to that of the water filling the pores.

The method of measuring the thermal resistance of the contact between tubes and aluminum hub, together with that of the hub, in the electric furnace has been described previously. This method was applied to the shrunk-on cast-iron elements and to the wrought-iron disks having their flues welded to the tubes. In the latter case a more rapid test by electrical means was also employed, wherein a current of 200 amp was passed into the periphery of one disk, and the voltage drops along the flue and across to tube were explored by means of a probe and a precision millivoltmeter. The electrical resistivity of the flue material was

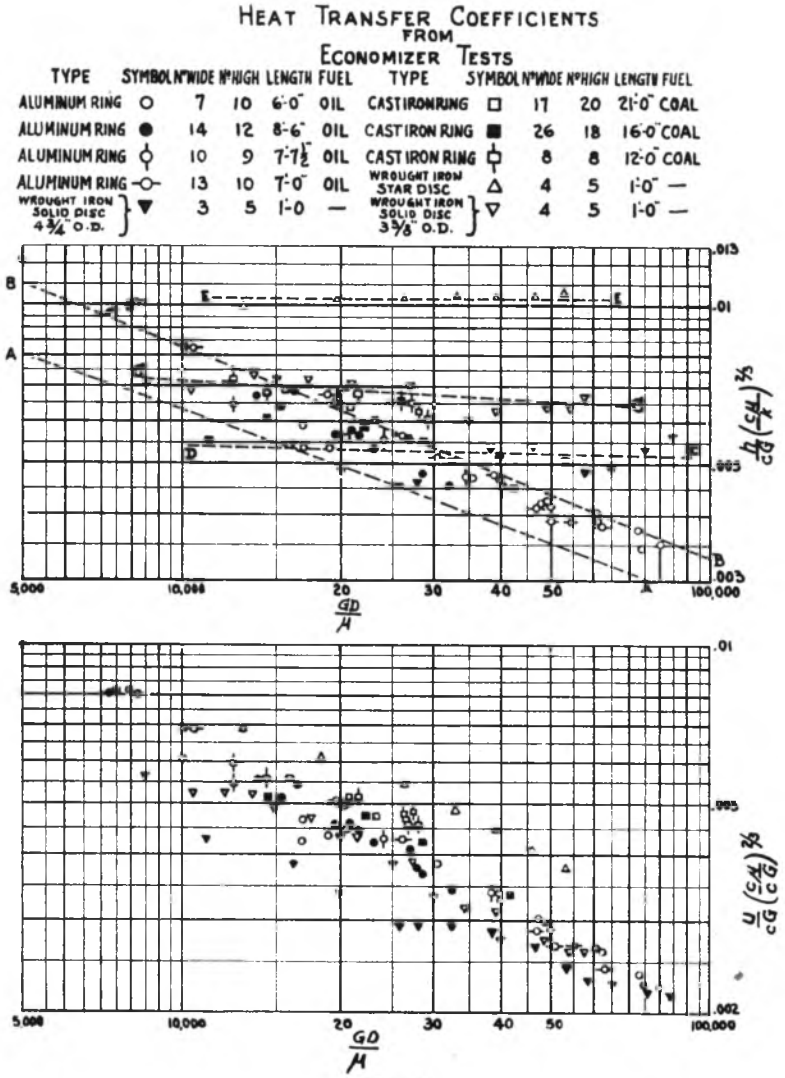

FIG. 4

measured, using specimens machined to accurate dimensions, and the thermal conductivity was deduced approximately by means of data available in the literature (3).

The average value of the ratio, length of path to cross-sectional area of path, was calculated from the electrical resistance and resistivity. The shape factor so obtained, when divided by the thermal conductivity, gave the thermal resistance. However, before comparing with the results of the first method (measured temperatures and heat-absorption rate), an allowance had to be made for the heat absorbed by the flue direct from the gas. When this was done the results of the two methods were found to be comparable.

Probably a more satisfactory electrical method, except from the standpoint of routine tests of full-sized elements, would be to surround a disk and flue with mercury, thus providing an anode analogous to the gas from which heat is transferred in the thermal case. In this manner the resistance from anode to the tube, or including it, could be obtained from the measured current, voltage drop, and resistivity of the fin material. If the flue were cut away the resistance of the disk alone could be obtained; thus the adequacy of the theoretical treatment of variously shaped disks could be checked.

Values of the thermal resistance of the disks were calculated by means of theoretical formulas derived by Harper and Brown (4). A graphical representation of disk resistance and effectiveness, based on the foregoing theoretical analysis, is shown in Fig. 5. Here h is the heat-transfer coefficient from gas to fin surface, U that from gas to base of disk, and M is

$$2k_F t_F \sqrt{D_1}/\sqrt{D_2}\,(D_2 - D_1)^2$$

M/h and M/U are dimensionless. The derivation is discussed in the Appendix.

In the case of a disk and shroud, e.g., Fig. 2, we have in effect two fins of unequal dimensions in parallel. If we assume that the values of the coefficients of heat transfer from gas to fin surface are the same for both disk and shroud, the respective heat flows are

$$Q_1 = ehS_1 \times \text{temperature drop from gas to hub}$$
$$Q_2 = EhS_2 \times \text{temperature drop from gas to hub}$$

Defining U and U' by the relation

$$Q_1 + Q_2 = U(S_1 + S_2) \times \text{temperature drop gas to hub}$$
$$= U'(S_1 + S_2) \times \text{temperature drop gas to water}$$

we obtain $$\frac{1}{U'} - (R_s + R_r + R_w + R_c)(S_1 + S_2) = \frac{1}{U}$$

$$= \frac{1}{h}\,\frac{S_1 + S_2}{eS_1 + ES_2}$$

Treating the shroud as a strip, receiving heat on one side only, its effectiveness e, was calculated from the well-known hyperbolic-tangent formula, and the disk effectiveness E was read from Fig. 5; so a plot of

$$\frac{1}{U'} \text{ versus } \frac{1}{h}\,\frac{S_1 + S_2}{eS_1 + ES_2}$$

was prepared. From this subsidiary graph values of h, corresponding to test values of U', were easily computed.

Correlation of Test Data

The values of h calculated in the manner described were incorporated into the dimensionless group $(h/cG)(c\mu/k)^{2/3}$, and plotted against Reynolds number DG/μ, as shown in Fig. 4. Here the mass flow of the gas G is that through the minimum area available. The equivalent diameter D, used in Re is that of a

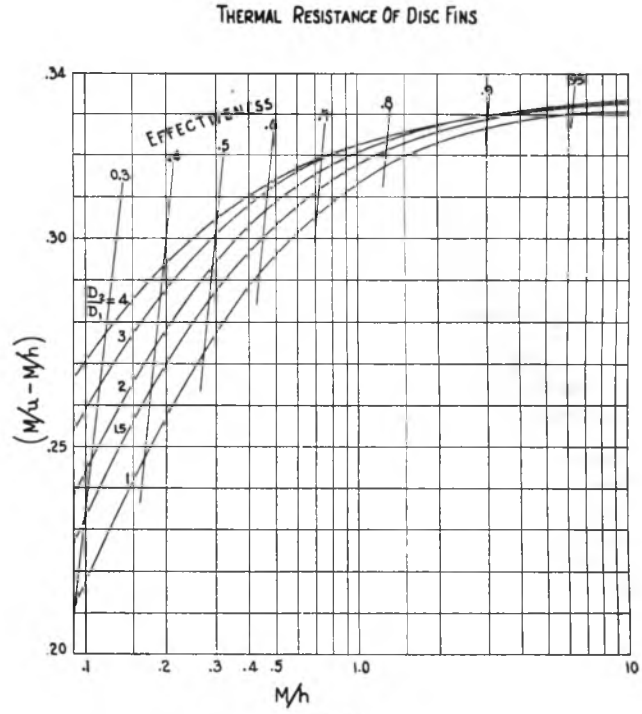

Fig. 5

cylinder having the same projected area as the finned tube. It was chosen somewhat arbitrarily. The particular grouping of the heat-transfer factors used here is preferred because the diameter, the choice of which is to be substantiated, appears only in the abscissa.

Values of U were plotted in the same manner, as shown in the lower plot of Fig. 4. In Table 1 the various resistances, the

TABLE 1 RESISTANCES, DIMENSIONS, AND THERMAL CONDUCTIVITIES OF VARIOUS SURFACES

Surface	Cast iron	Aluminum	3⅜-In. wrought iron	4¾-In. wrought iron	Star
D_1	0.208	0.225	0.134	0.167	0.134
D_2	0.387	0.417	0.282	0.396	0.292
D	0.275	0.282	0.158	0.201	0.158
S	3.10	4.50	3.29	6.50	2.16
d_1	0.139	0.139	0.100	0.146	0.100
d_2	0.167	0.167	0.125	0.167	0.150
R_r	0.0023	0.0035	0	0	0
R_T	0.0030	0.0045	0.0039	0.0046	0.0026
R_c	0.0060	0.0090	0.0061	0.0070	0.0040
k_F	29	87	36	36	36
k_T	29	29	29	29	29
t_F	0.0207	0.0117	0.0052	0.0052	0.0052

sum of which was subtracted from the over-all resistance in obtaining U, are listed together with pertinent dimensions and thermal conductivities. U was chosen in preference to the over-all heat-transfer coefficient U', in order to show the characteristic performance of the various disks unencumbered by the particular resistances which are imposed by the inner fluid and its conduit and which have no general relation to the convective process occurring at the external surface.

The temperature at which the thermal properties of the gas were evaluated was the arithmetic average of the gas and fin temperatures at inlet and outlet. The viscosity and thermal conductivity of the flue gas were assumed to be the same as those of air. The specific heat was calculated from the known composition of the gas, using current values of specific heats derived from spectroscopic data (5).

It will be noted in Fig. 4 that the surface heat-transfer coefficients h of the cast-iron and aluminum disks are fairly con-

sistent, and that they are approximately represented by curve *B-B*. This curve, which is drawn for purpose of comparison, represents a rough average of the results obtained by Pierson (6) for banks of staggered bare tubes. Curve *A-A*, also shown for comparison, represents average values for single bare tubes (7). The scattering of the points is attributable to experimental inaccuracy, due chiefly to nonuniform temperature distribution in the gas stream to and from large-scale apparatus, and to the deposition of soot on the fin surface. The rate and character of the soot deposits are believed to depend on the nature of the ash in the fuel, the concentration of solid carbonaceous matter in the gas, the gas temperature, and its velocity. The tendency of the points to converge to a single curve at the higher flows is considered to have a basis in reality; for it is a common observation that much less soot is blown free by the soot blowers at the end of tests at high gas flows than at the end of tests of the same duration at low rates of flow.

A notable feature of the surface heat-transfer group in the case of the solid wrought-iron disks, lines *C-C* and *D-D* in Fig. 4, is its independence of Reynolds number over the range covered in the tests. Any alternate choice of mean of disk and tube diameter would merely displace the points to right or left, parallel to the axis of the abscissa, while leaving their ordinates unchanged. Obviously, the ordinates of the points represented by *C-C* and *D-D* require a factor in order to merge with one or the other extremity of *B-B*, after suitable modification of the abscissa as well.

In the case of the star disks, disposition of the disk surface in the form of prongs apparently increases the turbulence in the bank of finned tubes to such a degree that the heat-transfer group, line *E-E*, is increased by 50 per cent. The heat absorbed per unit length of finned tube is nearly the same for the star disks with segments cut out as for the solid disk of the same diameter.

The effect is similar to that found by Norris and Spofford (8) for strip fins. If their method of correlation is applied to the prongs of the star disks, using 0.56 in. as the average perimeter of a prong, the test points form a nearly horizontal line. The middle of this line is approximately the point of intersection with the sloping line representing their results. An alternate procedure is to divide the perimeter of the prongs by π, and seek a way of averaging this and the tube diameter. In view of the complex nature of the flow, however, probably no such simple parameter would suffice.

Two undoubtedly important factors are tube spacing and fin spacing. The data presented here are too meager to warrant any conclusions. However, the persistence of eddies from one row to the next and their penetration of the passageway between adjacent fins are undoubtedly involved. A possible basis for extending the correlation to cover further data may be:

1 Incorporation of the square root of the ratio, fin-passageway width to height, into the heat-transfer group.

2 Use of some implicit function of tube diameter and pitch, together with fin spacing and height, such as hydraulic diameter, in the expression for Reynolds number.

3 Use of the ratio of tube pitch to diameter as a separate explicit parameter.

The first two are suggested by the results of Ellerbrock and Biermann (9) on single-finned cylinders.

No account has been taken of the variation of h locally over the surface of a disk. In the case of single-finned cylinders, considerable variation was found by Biermann and Pinkel (10). If the thermal resistance of a disk is appreciably affected by this variation, as well as the average value of h, allowance for this might change the slope of lines *C-C* and *D-D*.

Appendix

Nomenclature

The following nomenclature is used in this paper.

R_F = resistance of fin, (deg F)(hr)/Btu
R_s = resistance, fluid inside tube to inner tube wall, (deg F)(hr)/Btu
R_R = resistance of rust on inner tube wall, (deg F)(hr)/Btu
R_T = resistance of tube wall, (deg F)(hr)/Btu
R_c = resistance of contact and hub of disk, (deg F)(hr)/Btu
h_i = heat-transfer coefficient, fluid inside tube to inner tube wall, Btu/(hr)(sq ft)(deg F)
h = coefficient of heat transfer, gas to fin surface, Btu/(hr)(sq ft)(deg F)
U = heat-transfer coefficient, gas to base of disk, Btu/(hr)(sq ft)(deg F)
U' = over-all heat-transfer coefficient, gas to fluid inside tube, Btu/(hr)(sq ft)(deg F)
S_1 = surface of flue per foot length of tube, sq ft per ft
S_2 = surface of disk per foot length of tube, sq ft per ft
$S = S_1 + S_2$
E = effectiveness of fin
e = effectiveness of flue
k_F = thermal conductivity of disk metal, Btu/(hr)(ft)(deg F)
k_T = thermal conductivity of tube metal, Btu/(hr)(ft)(deg F)
k_G = thermal conductivity of gas, Btu/(hr)(ft)(deg F)
μ = viscosity of gas, lb/(hr)(ft)
c = specific heat of gas at constant pressure
G = mass flow of gas, lb/(hr)(sq ft)
W = weight flow of fluid per tube, lb/hr
D = equivalent diameter of surface, ft
D_1 = inner diameter of disk, ft
D_2 = outer diameter of disk, ft
d_1 = inner diameter of tube, ft
d_2 = outer diameter of tube, ft
t_1 = thickness of fin at D_1, ft
t_2 = thickness of fin at D_2, ft
t_F = mean fin thickness, ft

Thermal Resistance of Disk Fins

The heat balance for a differential element of volume of a disk, neglecting temperature gradients in all directions except the radial, is for steady flow

$$d\left(2\pi k\, rz\, \frac{d\theta}{dr}\right) = 4\pi h\theta r \sqrt{1 + {}^1/_4\left(\frac{dz}{dr}\right)^2}\, dr \qquad [1]$$

Here θ is the temperature difference between gas and the surface of the disk at radius r, z is the thickness at radius r, k is the thermal conductivity of the disk material, and h the surface coefficient of convective heat transfer.

If the disk is tapered, and its thickness varies with radius according to

$$z = z_1 \frac{r_1^{2m}}{r} \qquad [2]$$

Equation [1] assumes the form

$$\frac{d^2\theta}{dx^2} + \frac{1 - 2m}{x}\frac{d\theta}{dx} - \lambda^2 x^{2m}\theta = 0 \qquad [3]$$

where

$$x \equiv \frac{r}{r_1} \text{ and } \lambda^2 \equiv \frac{2hr_1^2}{kz_1}\left[1 + \frac{m^2 z_1^2}{r_1^2 x^{4m+2}}\right]^{1/2}_{\text{Mean}} \qquad [4]$$

Use of the mean value of the radical in Equation [1] is justifiable where $\frac{z_1}{r_1}$ is small compared to x.

The solution of Equation [3] is

$$\theta = x^m \left[AI_{\frac{m}{m+1}} \left(\frac{\lambda}{m+1} x^{m+1} \right) + BK_{\frac{m}{m+1}} \left(\frac{\lambda}{m+1} x^{m+1} \right) \right] \quad \ldots\ldots [5]$$

where A and B are integration constants to be determined from the boundary conditions

$$\left.\begin{aligned} &\theta = \theta_1 \text{ when } x = x_1 = 1 \\ &\frac{d\theta}{dx} = 0 \text{ when } x = x_2 \\ &-2\pi z_1 r_1 k \frac{d\theta}{dz} = 2\pi U \theta_1 \int_{r_1}^{r_2} r \sqrt{1 + {}^1/_4 \left(\frac{dz}{dr}\right)^2}\, dr \\ &\qquad\qquad \text{when } x = x_1 \end{aligned}\right\} \ldots [6]$$

Here $I_{\frac{m}{m+1}}$ and $K_{\frac{m}{m+1}}$ are modified Bessel functions of first and second kind, respectively, and order $\frac{m}{m+1}$.

The case $m = 0$ has been treated by Harper and Brown (4), and Schmidt (1), who used Hankel's notation for the Bessel functions. The case $m = {}^1/_2$ was treated by Carrier and Anderson (11) without identification of the series obtained as solutions.

In the case $m = 0$, i.e., a disk of constant thickness, the disk effectiveness E, is found to be (in the notation employed here)

$$E = \frac{U}{h} = \frac{2}{(x_2^2 - 1)\lambda} \frac{I_1(\lambda x_2)K_1(\lambda) - I_1(\lambda)K_1(\lambda x_2)}{I_0(\lambda x_2)K_0(\lambda) + I_0(\lambda)K_1(\lambda x_2)} \quad \ldots [7]$$

Ten-place tables of the I and K functions of integral order are given by Gray and Mathews (12). By means of these the numerator in Equation [7] can be calculated with precision more than ample for our purpose.

A graphical representation of Equation [7] in a form frequently convenient is shown in Fig. 5. Use of the parameter

$$M = \frac{kz_1}{2(r_2 - r_1)^2} \sqrt{\frac{r_1}{r_2}} = \frac{2kz_1}{(D_2 - D_1)^2} \sqrt{\frac{D_1}{D_2}}$$

effects a merger of the individual curves at large values of the abscissa M/h, to a degree of accuracy exceeding that required for most purposes. This parameter M involves the dimensions of the disk and the thermal conductivity of its material. Values of the ordinate were obtained from Equation [7] and the relation

$$\frac{M}{U} - \frac{M}{h} = \frac{1 - E}{E} \frac{M}{h} \quad \ldots\ldots [8]$$

Lines of constant disk effectiveness E were drawn by plotting $\frac{1 - E}{E} \frac{M}{h}$ as ordinate, assigning decimal values successively to E.

As r_1 becomes very large, while $(r_2 - r_1)$ remains small in comparison, the influence of curvature diminishes, and as a limit we approach the strip fin of height $(r_2 - r_1)$. The equation of the curve denoted by $D_2/D_1 = 1$ in Fig. 5 is easily derived from the usual hyperbolic-tangent formula for effectiveness, together with Equation [8], yielding

$$\frac{M}{U} - \frac{M}{h} = \sqrt{M/h} \coth \sqrt{\frac{h}{M}} - \frac{M}{h} \quad \ldots\ldots [9]$$

The chart may be used directly in calculating the unit resistance $\left(\frac{1}{U} - \frac{1}{h}\right)$, of a disk when h, k, and the dimensions are specified. When U instead of h is specified, a subsidiary plot with M/U as abscissa is more convenient, and is easily constructed. Correction for the heat flow into the edge of the disk may be made approximately by adding one half the disk thickness to $(r_2 - r_1)$, following the procedure of Harper and Brown.

In the case of a disk having a parabolic profile, $m = 1$ in Equation [4], the Bessel functions of Equation [5] are of order ${}^1/_2$ and reduce to hyperbolic functions, yielding

$$\theta = A \cosh (\lambda x^2/2) + B \sinh (\lambda x^2/2) \quad \ldots\ldots [10]$$

and

$$E = \frac{U}{h} = \frac{2 \tanh \{\lambda(x_2^2 - 1)/2\}}{\lambda(x_2^2 - 1)} \quad \ldots\ldots [11]$$

after determination of A and B by means of the boundary conditions Equations [6]. By assigning to M the value

$$M = \frac{2kz_1z_2}{(r_2 - r_1)^2(\sqrt{z_1} + \sqrt{z_2})^2} \left(1 - \frac{z_1^2 + z_2^2}{4r_1^2 z_1}\right)$$

the curve labeled $D_2/D_1 = 1$ may be used for the parabolic disk.

Correction for the temperature gradients other than radial was treated by Harper and Brown and shown to be small in ordinary cases. In the case examined in detail by them M/h had the value 0.2967, and the correction to effectiveness 0.6 per cent. The corresponding correction to be added to $\left(\frac{M}{U} - \frac{M}{h}\right)$ amounts to 1 per cent.

No account was taken of the local variation of h over the disk surface. An influence as great as that due to curvature and shape would be anticipated.

BIBLIOGRAPHY

1 "Wärmeübertragung Durch Rippen," by E. Schmidt, *Zeitschrift des Vereines deutscher Ingenieure*, vol. 70, 1926, p. 947.

2 "Heat Transmission," by W. H. McAdams, McGraw-Hill Book Company, Inc., New York, N. Y., second edition, 1942, p. 180.

3 "Further Measurements of the Thermal and Electrical Conductivity of Iron at High Temperatures," by R. W. Powell, Proceedings of the Philosophical Society, vol. 51, 1939, pp. 407–418.

4 "Mathematical Equations for Heat Conduction in the Fins of Air-Cooled Engines," by D. R. Harper and W. B. Brown, N.A.C.A. Report No. 158, 1923, pp. 679–703.

5 "Spezifische Wärme, Enthalpie, Entropy und Dissoziation Technischer Gase," by E. Justi, J. Springer, Berlin, 1938, pp. 143–147.

6 "Experimental Investigation of the Influence of Tube Arrangement on Convection Heat Transfer and Flow Resistance in Cross-flow of Gases Over Tube Banks," by O. L. Pierson, Trans. A.S.M.E., vol. 59, 1937, pp. 563–572.

7 "Heat Transmission," by W. H. McAdams, McGraw-Hill Book Company, Inc., New York, N. Y., 1942, p. 221.

8 "High-Performance Fins for Heat Transfer," by R. H. Norris and W. A. Spofford, Trans. A.S.M.E., vol. 64, 1942, pp. 489–495.

9 "Surface Heat Transfer Coefficients of Finned Cylinders," by H. H. Ellerbrock and A. Biermann, N.A.C.A. Report No. 676, 1939, pp. 1–14.

10 "Heat Transfer From Finned Metal Cylinders in an Air Stream," by A. E. Biermann and B. Pinkel, N.A.C.A. Report No. 488, 1934, pp. 1–22.

11 "The Resistance to Heat Flow Through Finned Tubing," by W. H. Carrier and S. W. Anderson, *A.S.H.V.E. Journal* section of *Heating Piping and Air Conditioning*, May, 1944, pp. 304–318.

12 "A Treatise on Bessel Functions," by A. Gray and G. B. Mathews, The Macmillan Co., New York, N. Y., 1931.

Heat-Flux Pattern in Fin Tubes Under Radiation

By A. R. MUMFORD[1] and E. M. POWELL,[2] NEW YORK, N. Y.

In this paper data are presented showing heat-flux patterns as indicated by temperature-drop curves from field measurements and from an electrical analogy in the laboratory. Data of this kind may become of some importance if the use of tube-surface temperatures in furnace-testing technique is successfully developed.

SEVERAL examples of the use of surface temperatures to indicate the heat-flux variation around the circumference of a tube have appeared in technical publications. Although this method is fascinating and gives promise of producing data which will aid in a more complete understanding of what is going on in the furnace and at the walls, it is apparent that the variations caused by slag deposits in coal-fired furnaces are of such magnitude that many more data than are at present available will be required before we can say with assurance that this condition or that condition represents the normal at a given location and rating.

Fig. 1 shows a plan section through a furnace having a slagging bottom and fired tangentially with pulverized coal. The furnace walls are made up of finned tubes, one of which, as indicated, was selected for the measurement of surface temperatures. A section of the finned tubes used in the construction of the walls of this furnace is shown in Fig. 1. Thermocouples were installed at several points around the circumference of the tube at an elevation of approximately 13 ft from the floor of the furnace. The method of installing the thermocouples for measuring the surface temperatures of tubes has been described by C. G. R. Humphreys.[3] When couples were installed on the back of the tubes in a position not exposed to furnace gases or ash, the temperatures indicated were within a degree or two of the saturation temperature corresponding to the boiler pressure. It is therefore probable that this method of surface-temperature measurement provides a means which can be expected to be accurate within 0.5 per cent of the indicated temperature.

Fig. 2 gives a number of curves showing the difference between the tube-surface temperature and the saturation temperature around the exposed semicircumference of that tube at intervals after the unit was lit-off. Curve *a* represents the condition shortly after lighting-off when the load was less than 1/2 normal. Only a small amount of coal had been burned up to that time, and it is probable that the tube surface was clean and exposed. The temperature elevation varies about 50 F with the peak to the right of the normal to the wall. Fourteen hours later the boiler was operating at about 90 per cent of normal and no lancing had been done. Some ash had accumulated on the surface because the surface temperature of the metal had dropped as shown on curve *b*, in spite of the fact that the rate of heat release in the furnace had doubled. It may be significant that the greater drop in surface temperature occurred in the right quadrant of the tube. At least, from an examination of the geometry of the furnace, noting the direction of the fuel stream and the point of highest heat intensity, this quadrant is the point at which we would expect ash to deposit.

Curve *c* represents the conditions about 6 days after the boiler was lit. The load was normal but apparently a fairly uniform coating of ash had accumulated which reduced the rate of heat transfer to such a point that the surface temperature of the tube was only 60–70 F above saturation.

Curve *d* represents conditions a week after the unit was lit-off,

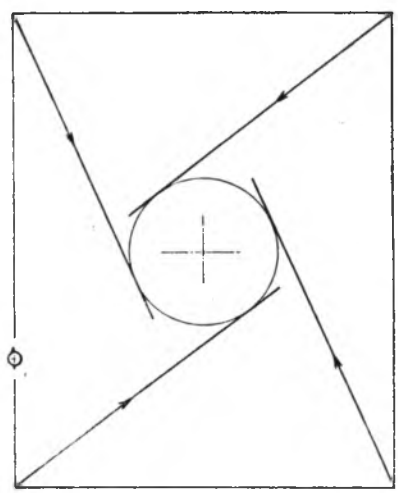

FIG. 1 PLAN SECTION THROUGH PULVERIZED-COAL-FIRED FURNACE

with only routine lancing and with a load of about 90 per cent of normal. This curve is of particular interest because of the small variation around the circumference. The evidence of these observations would indicate that the normal temperatures would be higher in the right quadrant.

Six days later, or 13 days after lighting-off, the conditions are represented by curve *e*. These surface temperatures are the lowest observations at full load and indicate the existence of a heavy coating of slag with more heat being transmitted through the right quadrant. This curve represents the condition immediately preceding a thorough lancing of the walls.

Curve *f* represents conditions immediately after the wall had been lanced. The largest temperature drop, and probably the largest rate of heat transfer, exists in the right-hand quadrant. The comparatively low drop which is shown at 30 deg from the face of the wall in the left-hand quadrant is probably due to the continued adherence of some insulating slag in this region.

Period Preceding and Following Lancing of Furnace Wall

A more detailed examination of the period immediately pre-

[1] Research and Development Department, Combustion Engineering Company, Inc. Fellow A.S.M.E.

[2] Engineering Department, Combustion Engineering Company, Inc.

[3] "Thermocouples for Furnace-Tube-Surface Temperature Measurements," by C. G. R. Humphreys, *Combustion*, vol. 16, 1944, pp. 53–55.

Contributed by the Heat Transfer Division and presented at the Annual Meeting, New York, N. Y., Nov. 27–Dec. 1, 1944, of THE AMERICAN SOCIETY OF MECHANICAL ENGINEERS.

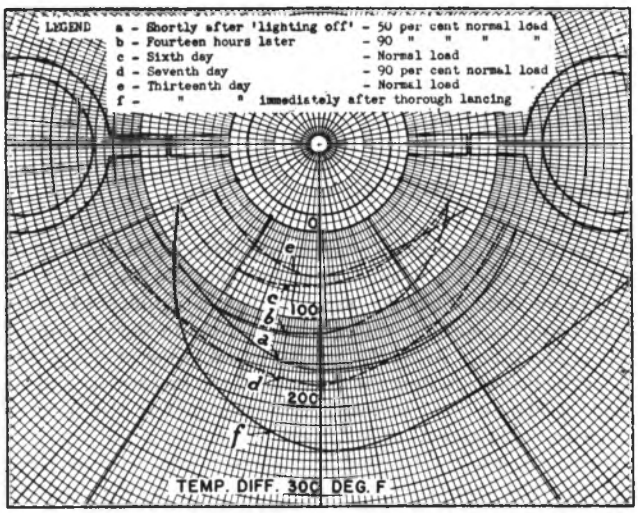

FIG. 2 CURVES SHOWING TEMPERATURE DIFFERENCES BETWEEN TUBE SURFACE AND SATURATION TEMPERATURE AROUND SEMI-CIRCUMFERENCE

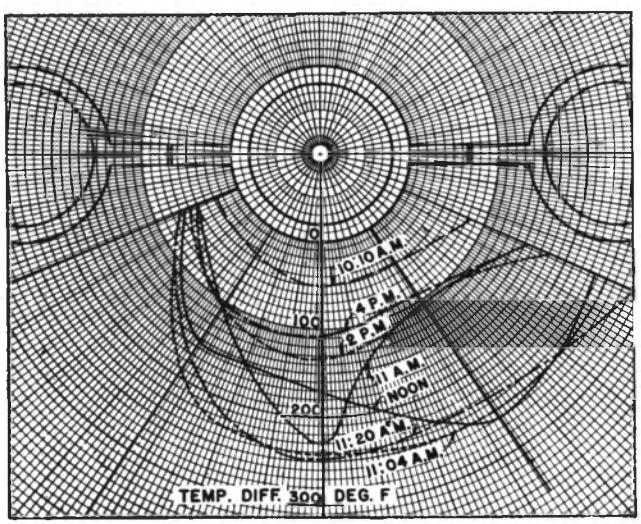

FIG. 3 TEMPERATURE DIFFERENCES FOR PERIOD PRECEDING AND FOLLOWING LANCING OF WALL

ceding and following the lancing of the wall is shown in Fig. 3. The wall in the region of this particular tube was lanced between 11 a.m. and 11:20 a.m. and the changes in heat transfer are indicated by the temperature differences. At 10:10 a.m. before lancing, the average temperature difference was 50 F, being somewhat lower in the left quadrant. At 11 a.m. at the start of lancing, the temperature difference through the tube wall on a normal to the plane of the furnace wall increased to 230 F with lesser increases at other points. If the rate of heat transfer is taken as proportional to the temperature drop, then the rate at the front face of the tube immediately after lancing is 4.7 times that before lancing. At 11:04 a.m. what is indicated as the cleanest condition was reached, and this was practically unchanged at 11:20 a.m. when the lancing had been completed. At noon, 2 p.m., and 4 p.m., the rate of accumulation of the insulating layer of ash is indicated by a decreasing temperature difference. A better appreciation of the changes taking place will be realized by noting the location of this tube in Fig. 1 with relation to the approaching coal stream and the zone of highest heat intensity off the right quadrant and the lance coming from the left.

In Figs. 2 and 3 zero of the temperature scale is at the tube surface. The elevation within the furnace at which these temperatures were taken is in the zone of high heat release and slag deposits and therefore, although these temperatures are not representative of the entire furnace, they do serve as a good indication of the variations which can take place in the zone of intense heat transfer during operation. Conclusive study of the heat-flux pattern in a finned tube would require the collection of field data, not only over a long period in a coal-fired furnace, but over many areas of the furnace in which insulating layers of slag are or are not deposited.

In Fig. 4 are plotted several curves which show the temperature differences which existed at various times on the circumference of the tube and at the extremity of one fin. The temperature scale is the same as used in Figs. 2 and 3. The variations of surface temperature are most pronounced at the tip of the fin and on the tube wall adjacent to the fin. Except for the general rise after 11:30 a.m., the variations in the right quadrant were comparatively small, but in the left quadrant were so great that the most feasible explanation is the dropping off of a fairly dense layer of slag. The method of presentation does not take into consideration the fact that the metal thickness between the measuring point and the internal fluid is greater by 1 in. for the fin-temperature point. If it were certain that the entire fin had been exposed, a heat flux proportional to the tempera-

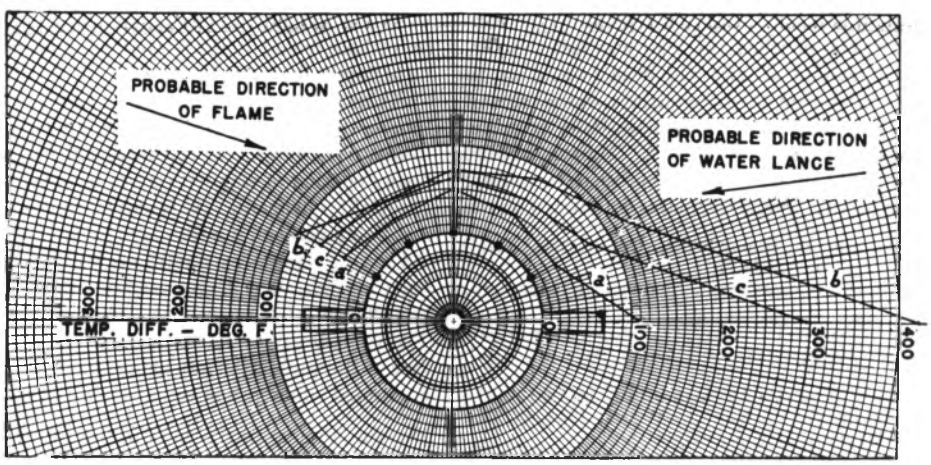

FIG. 4 TEMPERATURE DIFFERENCES AT VARIOUS TIMES ON CIRCUMFERENCE OF TUBE AND AT EXTREMITY OF FIN

ture drop per inch of metal could have been assumed, but with the available data there was no assurance of this, consequently no attempt at correction was made.

Obviously, the variations occurring in this zone of the furnace preclude any short-time study of heat-flux patterns by field measurements in a coal-fired furnace. The opinion should be emphasized that the conditions shown in Figs. 2, 3, and 4 are not representative of the entire furnace, but only of the flowing-slag zone of a slagging-bottom pulverized-coal furnace. The condition at other furnace-wall areas is known to be less variable. Evidence of the variation to be expected in different areas of the furnace has been given by H. Kreisinger and R. C. Patterson.[4] The variable conditions in the slag zone, however, will set the requirements for the testing period because the slag zone is about 10 per cent of the furnace area.

Laboratory Study of Heat-Flux Patterns

The laboratory approach to the problem of heat-flux pattern in finned tubes under radiation permits a determination of temperature drops by analogy and therefore the determination of heat-flux patterns without the interference of ash deposits. Fig. 5 shows a test setup used for the purpose of studying flux patterns with particular emphasis on the flow of heat from the base of the fin through the tube wall. On a sheet of high-resistance alloy

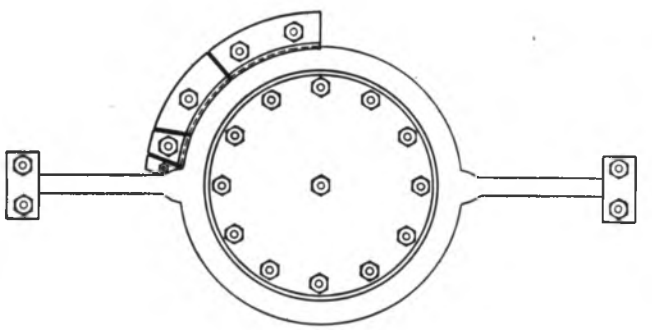

Fig. 5 Diagram of Apparatus for Producing Voltage Drops Across Simulated Finned-Tube Wall

cut in the shape of a section of a finned tube, a number of radial and circumferential lines were machine-scribed. Electric currents were passed through the sheet in such values that were comparable to the heat flow by radiation. By taking voltage drop, amperes, and electrical conductivity as equivalent to temperature drop, quantity of heat per unit of time, and thermal conductivity, respectively, temperature drops could be computed from the electrical measurements. Voltage drops were measured at the intersections of the scribed lines and the analogous temperatures computed.

Fig. 6 shows the calculated temperature distribution at the base of a fin $^1/_4$ in. × 1 in. long on a 4-in. × 0.380-in. tube, and Fig. 7 shows the distribution at the base of a fin $^1/_4$ in. × $^{17}/_{16}$ in. long on the same tube. In each case the current flow was adjusted to be equivalent to a uniform rate of heat transmission for the tube and fin of approximately 50,000 Btu per hr per sq ft. The electrical resistance between the inner face of the tube and the inside contact plate was uniform and corresponded to a thermal conductivity of approximately 3500 Btu per hr per sq ft per deg F temperature difference. Other sources have indicated this to be somewhat low.

The distribution of heat-flux density imposed in the form of

[4] "Heat Transfer of Water-Cooled Furnace Walls," by H. Kreisinger and R. C. Patterson, Trans. A.S.M.E., vol. 66, 1944. Bound at back of volume in pamphlet entitled "Furnace Performance Factors," pp. 71–78.

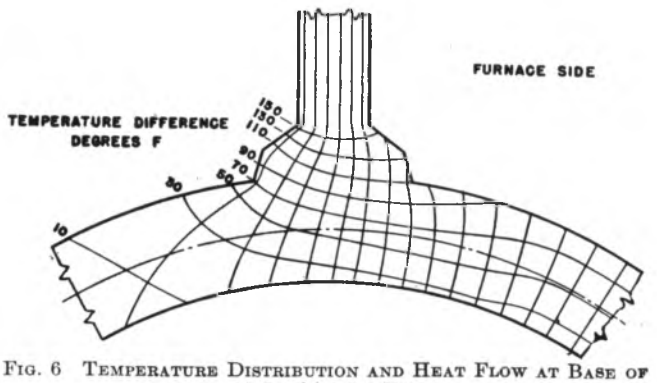

Fig. 6 Temperature Distribution and Heat Flow at Base of $^1/_4$-In. × 1-In. Fin

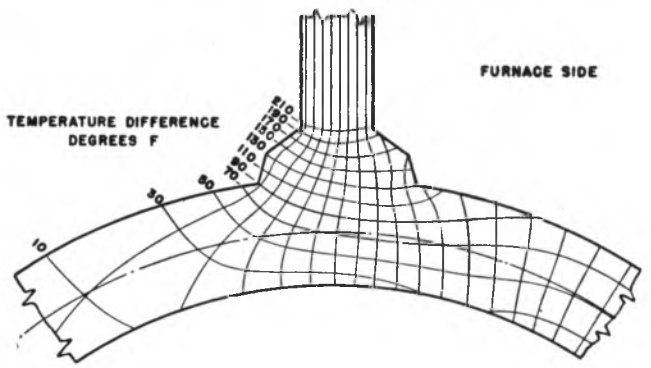

Fig. 7 Temperature Distribution and Heat Flow at Base of $^1/_4$-In. × $^{17}/_{16}$-In. Fin

current flow was uniform on the circumferential part of the tube and the weld of the fin. The heat picked up by the fin was represented by current flow from the end of the fin only. An examination of the two figures makes it quite apparent that the only marked difference in temperature drop occurs in the region of the fin, and the greatest temperature drops occur with the largest fin. The influence of the fin and the heat it picks up is to change the direction of heat flow from radial to a combination of radial and circumferential. The isotherms, instead of being circumferential, dip radially more and more as the circumferential distance increases at or near the fin. Back of the fin, in the region where no heat is being added to the tube, the heat flow extends almost 45 deg but the magnitude is very small after about 15 deg have been passed. The fanning out of the lines of flow of the heat, i.e., normal to the isotherms, is clearly indicated by the movement of the peak of the temperature-difference curves from the line of the fin forward toward the exposure. This forward shift reaches a maximum at the inner face of the tube.

For the experiments uniform radial absorption has been assumed around the semicircumference of the tube. This is seldom realized in actual practice, the rate usually being less near the base of the fin. This factor would tend to reduce the heat concentration ahead of the base of the fin and the temperature difference calculated at that point.

The use of tube-surface-temperature measurements in furnace technique has been discussed elsewhere. It does not seem out of place, however, to indicate that under conditions of parallel radiation at any degree of incidence, a fin tube will have greater exposure than one of a group of tangent tubes because of their spacing, and at some angles the area of the fin will be very important in fixing the heat-flux pattern through the tube because of its proportion to the total.

Heat Transfer and Pressure Drop of Liquids in Double-Pipe Fin-Tube Exchangers

By B. DE LORENZO[1] and E. D. ANDERSON,[2] ELYRIA, OHIO

This paper presents data on the fin side of standard commercial-size longitudinally finned double-pipe exchangers. Three fin-tube sizes were investigated in heating and cooling for both heat transfer and pressure drop. The data indicate that the transition between laminar and turbulent flow begins at R < 400 for both heat transfer and pressure drop, corroborating results reported by previous investigators. Methods of evaluating heat-transfer coefficients and pressure drop for liquids inside tubes are applicable for liquids in the fin side of finned double-pipe exchangers. For values of R up to 4000 (approximately), recommended curves for fin-side heat transfer give higher coefficients than the values obtained, by the procedure outlined by the Tubular Exchanger Manufacturers Association for liquids flowing in tubes. A method is presented for determining the weighted average temperature of the outside surface of the fin tube to be used in evaluating μ_w in the viscosity gradient correction μ/μ_w.

Nomenclature

The following nomenclature is used in this paper:

A = $(A_f + A_t)$ = total fin-side surface area, sq ft
A_e = net free cross-sectional area for flow on fin side, sq ft
A_f = surface area of fins only, sq ft
A_i = inside surface area of tube, sq ft
A_t = outside surface area of tube only, sq ft
b = height of fin (see Fig. 2*e*), ft
c = specific heat of fluid, Btu/(lb)(deg F)
D_e = $4A_e/\psi$ = equivalent hydraulic diameter of fin side, ft
D' = inside fin-tube diameter, in.
f = friction factor in Fanning equation, dimensionless
G = mass velocity of fluid, lb/(sq ft)(hr)
g = acceleration due to gravity = 4.17×10^8 ft/(hr)(hr)
h_d = reciprocal of fouling resistance (see Fig. 4), Btu/(hr)(sq ft)(deg F)
h_f and h_{fd} = fin-side film coefficient based on A, clean and fouled, respectively, Btu/(hr)(sq ft)(deg F)
h_{fi} and h_{fdi} = fin-side film coefficient referred to A_i, corrected for weighted fin effectiveness, clean and fouled, respectively, (see Fig. 4), Btu/(hr)(sq ft)(deg F)
h_i = tube-side film coefficient, based on A_i clean, Btu/(hr)(sq ft)(deg F)
h_t = reciprocal of tube-wall resistance, Btu/(hr)(sq ft)(deg F)
j = $\dfrac{h_f}{cG}\left(\dfrac{c\mu}{k}\right)^{2/3}\left(\dfrac{\mu}{\mu_w}\right)^{-0.14}$ = Colburn's (1)[3] heat transfer factor modified by Sieder and Tate's (2) viscosity correction, dimensionless
k and k_f = thermal conductivity of fin-side fluid and of fin material, respectively, Btu/(hr)(sq ft)(deg F/ft)
L = length of fin section (see Fig. 2), ft
L_e = total equivalent length of fin side (see Fig. 6), ft
Q = total quantity of heat transferred, Btu per hr
Δp = pressure drop of fin-side fluid, psf
$\mathbf{R}$ = D_eG/μ = Reynolds number, dimensionless
t = average temperature of fin-side fluid, deg F
T = average temperature of fluid inside tubes, deg F
T_t = average temperature of tube wall, (see Equation [7]), deg F
T_w = weighted average temperature of fin surface and tube-wall surface, defined by Equation [8], deg F
U_i = over-all heat-transfer coefficient (clean), based on A_i, Btu/(hr)(sq ft)(deg F log MTD)
V = linear velocity of fin-side fluid (at A_e), fph
V' = linear velocity of water inside fin tube, (see Equation [2]), fps
δ = fin thickness (see Fig. 2), ft
η = effectiveness factor of fin surface only (see Fig. 4), dimensionless
η' = total weighted effectiveness of fin and tube surface, (see Fig. 4), dimensionless
μ = viscosity of fin-side fluid, evaluated at t, lb/(ft)(hr)
μ_w = viscosity of fin-side fluid, evaluated at T_w, lb/(ft)(hr)
ψ = total wetted perimeter of fin side (fins plus outside of tube, plus inner surface of shell pipe), ft
ρ = density of fin-side fluid evaluated at t, lb per cu ft
ϕ = viscosity ratio = $(\mu/\mu_w)^{0.25}$ and $(\mu/\mu_w)^{0.14}$ for pressure drop in laminar and turbulent flow, respectively (see Fig. 6), dimensionless

Introduction

Double-pipe heat exchangers, having longitudinal fins attached to the outside of the inner pipe, have come into more and more general use in recent years as the advantages of this type of exchanger have become better known. The most frequently used form of the double-pipe exchanger is the "hairpin" section. This design permits easy connection of the number of sections required to perform the desired heat-transfer duty into a compact bank.

Generally speaking, the best application of the longitudinally finned double-pipe hairpin exchanger is in transferring heat between two fluids having unequal heat-transfer characteristics; the fluid having the higher rate of heat transfer flows through the innermost tube, and the fluid with the lower heat-transfer rate flows through the space between the two tubes, i.e., the fin, or shell side. Fig. 1 illustrates a typical installation of this type of exchanger. The bank consists of 20 hairpin sections arranged 5 in parallel by 4 in series. This unit is used for cooling gasoline. Water, used as the cooling medium, passes through the inner tube, the gasoline flows through the fin side.

Longitudinally finned double-pipe hairpin exchangers have

[1] Manager, Heat Transfer Department, Brown Fintube Company.
[2] Design Engineer, Brown Fintube Company.

Contributed by the Heat Transfer Division and presented at the Annual Meeting, New York, N. Y., Nov. 27-Dec. 1, 1944, of The American Society of Mechanical Engineers.

[3] Numbers in parentheses refer to the Bibliography at the end of the paper.

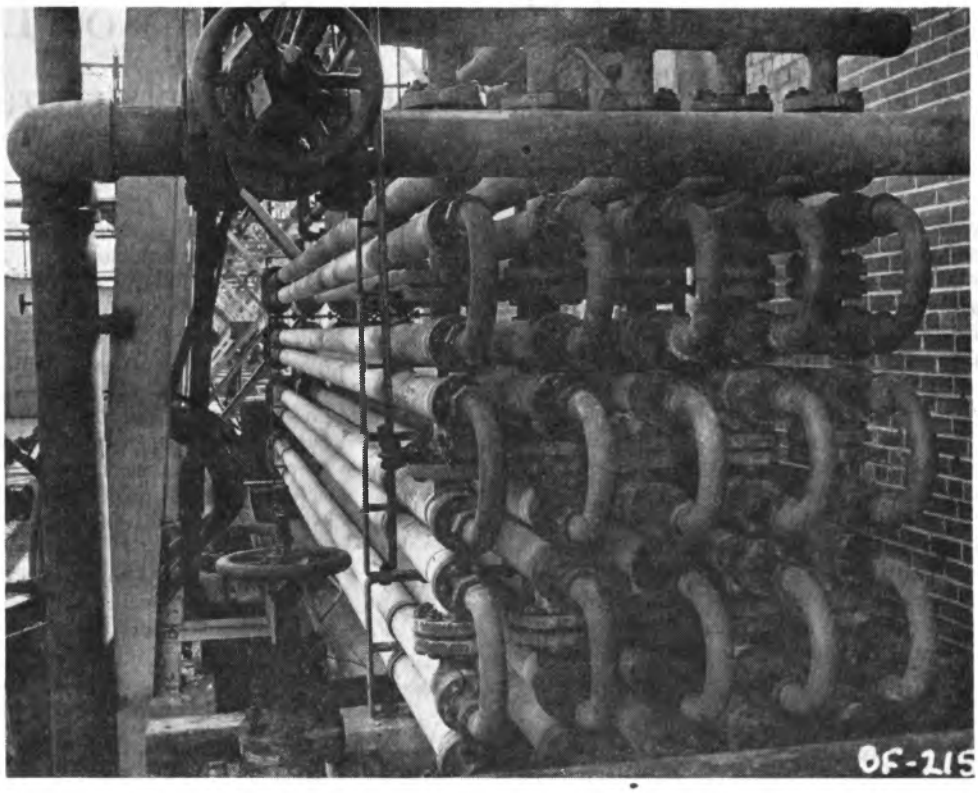

FIG. 1 GASOLINE COOLER CONSISTING OF 20 FINNED HAIRPIN SECTIONS

also been used extensively, and to great advantage, in transferring heat between two fluids having similar heat-transfer characteristics. In these cases the tube-side fluid generally flows at high velocity, utilizing the maximum allowable pressure drop, so as to secure the best coefficient possible, while the fin-side fluid may flow at moderate velocities. Also, in effecting transfers between fluids having unequal transfer characteristics, it is entirely feasible to pass the fluid having the lower heat-transfer properties through the center tube (in cases where the characteristics of the fluid makes this desirable) by using removable turbulence promotors on the inside of the tube. These turbulence promotors increase the tube-side heat-transfer coefficient at the expense of a higher pressure drop (3).

Since the ratio of the total outside fin surface A to the inside tube surface A_i is generally 5 to 1 and greater, the fin-side coefficient may be considerably lower than the tube-side coefficient, yet, when the factor of relative surface area is introduced, the fin-side coefficient, corrected for the weighted fin effectiveness, may amount to a higher value than the value secured on the tube side.

The primary purpose of this paper is to make available to engineers practical proved methods for evaluating the film heat-transfer coefficients and pressure drops of liquids flowing in the fin side of standard commercial-size longitudinally finned double-pipe heat exchangers. With the exception of the excellent pioneer paper by Gunter and Shaw (4), design data on double-pipe fin-tube exchangers are nonexistent. To provide these data a series of tests was made on standard hairpin exchangers manufactured by the authors' company.

It is not the intention of this paper to present a theoretical analysis of the data reported; nor to make comparisons with extended-surface-heat-transfer- and pressure-drop data reported by other investigators. It is, rather, the object of this paper to present the results obtained clearly and concisely for not only experienced design engineers but also for operating personnel.

TEST APPARATUS AND PROCEDURE

The test apparatus consisted of three standard double-pipe hairpin heat exchangers of the type described, and shown in Fig. 2 (*a*). One exchanger was used as a heater and two as coolers, see Fig. 3. The entire equipment including the heater, both coolers, and all connecting piping was covered with 1-in-thick standard insulation to minimize heat loss.

Tests were run on exchangers using three different fin tubes (see Table 1), shown in Fig. 2(*b*), (*c*), and (*d*). Each hairpin consisted of two identical standard Brown resistance-welded fin tubes, taken at random from production runs and having 24, 28, and 36 longitudinal low-carbon-steel fins, $^1/_2$ in. high $\times$ 0.035 in. thick and 20 ft long, integrally bonded by overlapping spot welds, Fig. 2 (*e*). The fin channels were evenly spaced around the perimeter of $1^1/_2$-in. I.P.S. standard-weight seamless steel tubing. These fin tubes were welded to 180-deg steel return bends thus forming hairpins having a total 40-ft of fin length. The shells of the double-pipe heat exchangers consisted of two 3-in. I.P.S. standard-weight steel pipes welded to a housing which encloses the 180-deg return bend of the finned hairpin.

Table 1 gives areas, surface ratios, and other physical data of the three different fin-tube hairpins tested.

The fluids used in the tests were S.A.E. 40 and 50 lube oils and 43 deg API kerosene. These fluids, in all cases, were circulated through the finned or shell side of the exchanger. Saturated steam, at pressures ranging from 10 to 100 psig, was used as the heating medium inside the fin tubes of the heater. City water flowing through the fin tubes countercurrent to the flow of the oil on the fin side was used as the cooling medium in the coolers. Flow rates, of both lube oils and water, were measured with

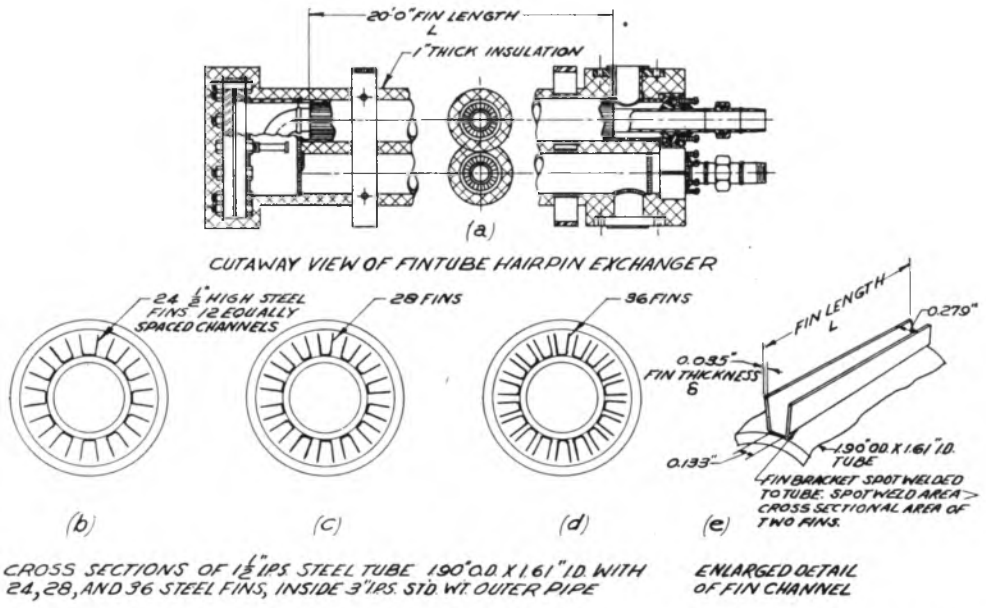

FIG. 2 DETAILS OF DOUBLE-PIPE LONGITUDINALLY FINNED HAIRPIN EXCHANGER AND THREE SIZES OF FIN TUBES TESTED

TABLE 1 PHYSICAL DATA OF FIN-TUBE HAIRPIN SECTIONS TESTED (SEE FIG. 2)

No. of fins	24	28	36
Net free area fin side, A_c, sq ft	0.0285	0.0280	0.0275
Hydraulic diameter, D_e, ft	0.0346	0.0308	0.0251
Ratios:			
Fin length L / Hydraulic diameter, D_e	578	650	797
Fin surface only A_f / Total fin-tube external surface, A	0.800	0.824	0.858
Tube external surface A_t / Total fin-tube external surface, A	0.200	0.176	0.142
Total fin-tube external surface, A / Fin-tube internal surface A_i	5.93	6.72	8.30
Total fin-side surface per hairpin section, sq ft	101	114	141

calibrated displacement-type flowmeters. No flowmeter was used to measure the kerosene, as the kerosene flow rates exceeded the capacity of the meter. It was possible, however, to determine the kerosene flow rate by a heat-and-material balance on the coolers, as a flowmeter was always used to measure the water rate. Temperatures were taken with standard A.S.T.M. mercury-bulb glass thermometers located in thermowells. Check thermowells were installed at several points, and, as a further check, the thermometers were interchanged at intervals. Pressure drops across the heater and each cooler were measured by differential mercury manometers. Pressure taps were located in the inlet and outlet nozzles, thus the pressure drop obtained included end losses. No calming sections were used as all the tests were made with standard commercial-size hairpin sections.

In all runs the oil tested was pumped from the storage tank, through the heater and the two coolers in series, and back to the storage tank, as shown in Fig. 3. Each test run lasted from 15 to 20 min after equilibrium was attained. Readings were taken at 5-min intervals. Flow rates and inlet temperatures of the two lube oils were varied over wide limits to obtain the maximum spread of Reynolds numbers for each oil. Steam temperatures and water flow rates were also varied for a fixed oil-flow rate so that a wider range of film temperatures could be investigated. Heat balances to within 5 per cent were obtained in the different tests.

Of the three fin-tube sizes tested, the Reynolds numbers have the greatest spread on the runs made with the fin tubes having 28 fins. Runs with **R** up to 1000 were made with refined S.A.E. 40 and 50 lube oils and above 1000 with commercial kerosene. The fin tubes with 24 fins were tested in the range from **R** = 20 to 800 using refined S.A.E. 40 lube oil. Only a few runs were made with the tubes having 36 fins, and the same S.A.E. 40 lube oil was used. The heat-transfer and pressure-drop results of all the runs covered by this paper are shown in Figs. 5 and 6, respectively. The range of the Prandtl number was from a minimum of 11.0 to a maximum of 1625. L/D ratios are given in Table 1.

The over-all heat-transfer coefficient was obtained by dividing the total heat transferred by the log MTD and the total inside surface of the fin tubes

$$U_i = \frac{Q}{(\log \text{MTD})(A_i)} \quad [1]$$

For the steam-side coefficient, the value $h_i = 2500$ was used, as this figure was considered to be in line with field operation. For heating lube oil, a maximum deviation of 4 per cent would result by assuming steam-condensing coefficients ranging from

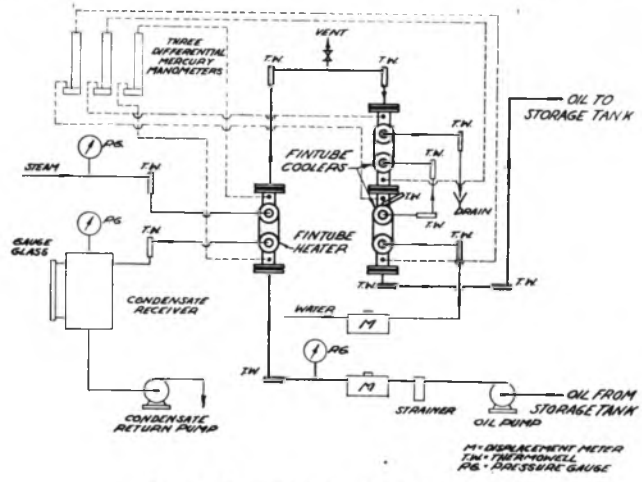

FIG. 3 FLOW DIAGRAM OF TEST UNIT

1500 to 5000 Btu/(hr)(sq ft)(deg F). For heating light fluids such as kerosene, with Reynolds numbers over 1000 where the fin-side coefficient would be higher than that for heating lube oil, the deviation would be greater. The water-side coefficient was calculated by the equation as given by McAdams (5).

$$h_i = \frac{150(1 + 0.011T)(V')^{0.8}}{(D')^{0.2}} \quad [2]$$

The fin-side film coefficient h_{fi} for the three sizes of fin tubes tested was then calculated readily from the equation

$$\frac{1}{U_i} = \frac{1}{h_i} + \frac{1}{h_t} + \frac{1}{h_{fi}} \quad [3]$$

and the curves shown in Fig. 4 which employ the Harper and Brown (6) method of computing fin efficiency.

Evaluation of T_w

The term μ_w as used in this paper to correlate the heat-transfer and pressure-drop data, denotes the viscosity of the fin-side fluid evaluated at the weighted average temperature of the finned surface and the outside bare surface of the tube, herein designated by T_w. No satisfactory method for evaluating T_w for tubes having extended surface could be found in the available literature. Consequently, the method for determining T_w illustrated subsequently and the values obtained by using this method were used in calculating the results reported in this paper.

The derivation of the equation for T_w is based on a heat balance between the fluid inside the tubes and the fluid on the fin side, and the corresponding surfaces. Thus when the hot fluid is inside the fin tubes and the cold fluid in the shell side, the heat transferred per unit area of inside tube surface can be defined by the equation

$$\frac{Q}{A_i} = h_i(T - T_i) \quad [4]$$

also

$$h_i(T - T_i) = h_f\eta'(T_i - t)A/A_i \quad [5]$$

and again

$$h_i(T - T_i) = h_f(T_w - t)A/A_i \quad [6]$$

Solving Equation [5] for T_i

$$T_i = \frac{h_iT + h_f\eta' t\, A/A_i}{h_i + h_f\eta' A/A_i} \quad [7]$$

Substituting the expression for T_i in Equation [6] and solving for T_w it is found that

$$T_w = \frac{\eta' h_i(T - t)}{h_i + h_f\eta' A/A_i} + t \quad [8]$$

When the cold fluid is in the inside of the fin tube and the hot fluid is on the fin side, it is found that Equation [8] is the same and can therefore be used for both heating and cooling.

In the foregoing derivation the assumption is made that there is no temperature gradient across the tube wall of the fin tube. This was a reasonable assumption as the equation for T_w would be more complicated if this assumption were not made and the effect on T_w would be small.

Temperature T_w is evaluated by successive approximations of h_f and finding the corresponding η'. All the other terms in Equation [8] are either known or are previously calculated. Generally, a first approximation suffices, as an error in T_w is greatly reduced when the corresponding μ_w is raised to the fractional power of 0.14 or 0.25.

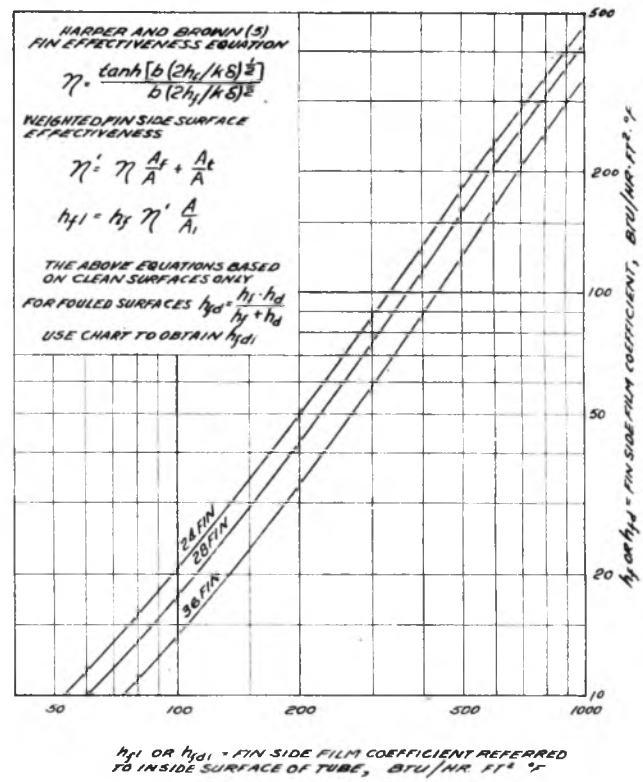

Fig. 4 Fin-Side Film Coefficients Corrected for Fin-Side Surface Effectiveness Referred to Inside Surface of Tube

Heat-Transfer Results

The heat-transfer data were correlated by the Colburn (1) heat-transfer factor j, modified by Sieder and Tate's (2) viscosity correction $(\mu/\mu_w)^{-0.14}$ giving the dimensionless expression

$$j = \frac{h_f}{cG}\left(\frac{c\mu}{k}\right)^{2/3}\left(\frac{\mu}{\mu_w}\right)^{-0.14} \quad [9]$$

The reason for using this method of correlation is that one curve can be used for heating and cooling for each fin-tube size. Also the same method was used by other investigators (4, 7), reporting data on heat transfer for extended surface.

The results for the 24- and 28-fin fin tubes plotted in Fig. 5 show that good agreement is obtained between heating and cooling in the range of R covered, indicating that this method of correlation is valid.

The results of the heat-transfer data obtained for the 36-fin fin tubes are not shown in Fig. 5, since only a few runs were made with this fin-tube size. A sufficient number of tests were made on this fin tube to determine the slope of the curve plotted for these data. The results obtained were in accord with the findings reported for the 24- and 28-fin fin tubes, when allowance was made for the higher L/D_e ratio for the 36-fin fin tube.

Inspection of the plotted results for the 28-fin fin-tube tests shown in Fig. 5 indicates that the transition between laminar and turbulent flow begins between R = 200 to 300. This is also indicated, to a lesser extent, by the results of the 24-fin fin-tube tests also shown in Fig. 5. Additional runs, not reported in this paper, made with other fin-tube sizes also gave similar results; i.e., the transition began at R < 300.

This phenomenon was also observed by Gunter and Shaw (4),

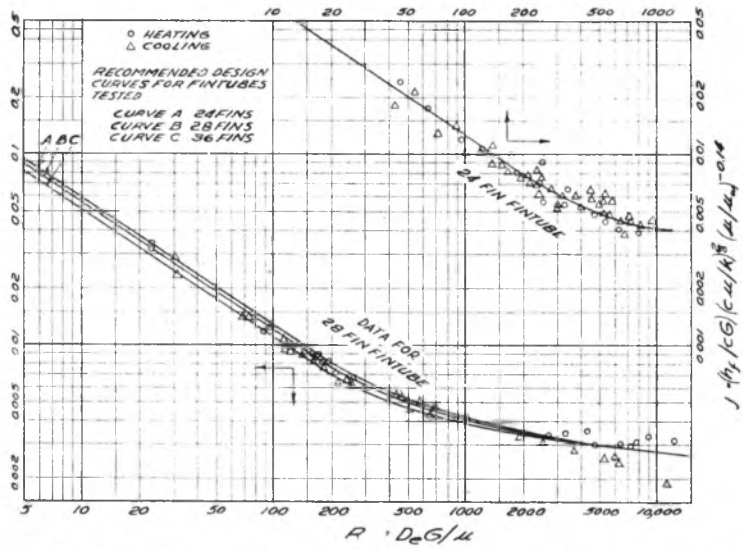

FIG. 5 HEAT TRANSFER ON FIN SIDE OF LONGITUDINALLY FINNED DOUBLE PIPES

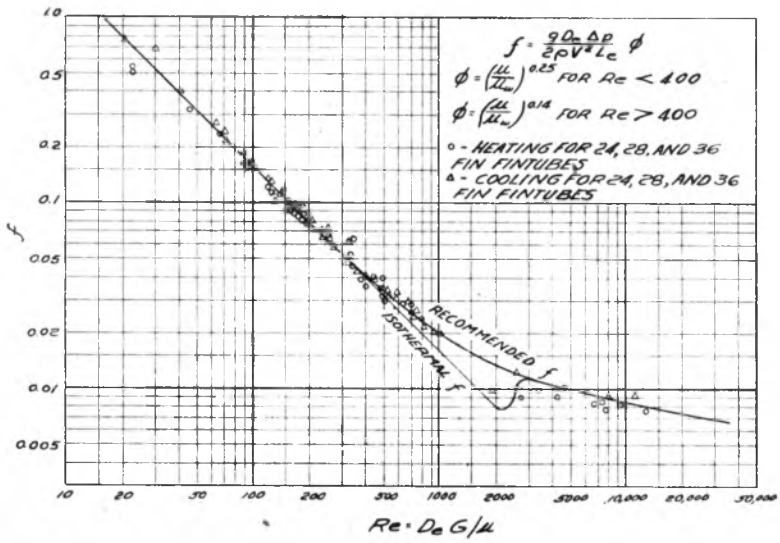

FIG. 6 PRESSURE DROP IN FIN SIDE OF LONGITUDINALLY FINNED DOUBLE PIPES

who reported the results of numerous tests heating oils in a similar double-pipe exchanger, using smaller fin tubes. They point out the analogy that an increase in the friction factor f normally increases the heat-transfer coefficient h. The pressure-drop results reported in this paper (see Fig. 6) show an increase in f over that normally expected for the isothermal f for circular ducts at Reynolds numbers ranging from 400 to 3000. In view of this it is not surprising to expect a break in the heat-transfer curve at around $\mathbf{R} = 300$ to 400.

The data presented here are based on clean surfaces. For design purposes fouling rates as recommended by T.E.M.A. (8) should be used.

PRESSURE-DROP RESULTS

The pressure-drop data obtained were evaluated by the general sothermal Fanning equation, modified by adding the Sieder and Tate (2) function $(\mu/\mu_w)^{0.25}$ in the laminar-flow region and $(\mu/\mu_w)^{0.14}$ in turbulent flow, to make it applicable for both heating and cooling liquids. The pressure-drop results are shown in Fig. 6 for all three sizes of fin tubes tested.

Sieder and Tate (2) found that the friction factor for liquids inside tubes in nonisothermal flow would fall on the isothermal f when multiplied by $1.1(\mu/\mu_w)^{0.25}$ and $1.02(\mu/\mu_w)^{0.14}$ in the laminar- and turbulent-flow regions, respectively. In this paper better correlation was obtained by omitting the constants 1.1 and 1.02.

Since the pressure taps were located in the inlet and outlet nozzles of each hairpin section, Fig. 3, end and return-bend housing losses were included. It was found that these losses could be adjusted by increasing the actual length from 40 to 45 ft equivalent fin length.

Fig. 6 shows excellent agreement between the isothermal line and the plotted results for $\mathbf{R} < 400$. Between $\mathbf{R} = 400$ to 1000 the results obtained are slightly higher than the isothermal curve, indicating that the transition between laminar and turbulent flow may start at $\mathbf{R} = 300$ to 400. At $\mathbf{R}$ between 3000 and 12,000 the data are again in good agreement with the isothermal curve.

Originally the data were plotted using $(\mu/\mu_w)^{0.25}$ and $(\mu/\mu_w)^{0.14}$ for $\mathbf{R} < 2100$ and $\mathbf{R} > 2100$, respectively. It was found, how-

ever, the correlation for heating and cooling was improved by using the factor $(\mu/\mu_w)^{0.14}$ for all values of **R** above 400. This finding provides an additional argument that the transition between a laminar and turbulent flow, for liquids flowing in the fin side, begins at a Reynolds number considerably below 2100. Both the heat-transfer and pressure-drop results substantiate this point.

Conclusions

1 Heat transfer on the fin side of longitudinally finned double-pipe exchangers for both heating and cooling is correlated by the conventional j factor corrected by μ/μ_w for viscosity gradient.

2 Correlation of the pressure drop for three sizes of fin tubes tested in both heating and cooling was in excellent agreement with isothermal pressure drop for values of **R** below 400 and also for **R** above 3000. In the range of **R** between 400 and 3000, pressure drop was greater than that predicted by the conventional Fanning equation.

3 The breaks in both the heat-transfer and pressure-drop curves indicate that transition between laminar and turbulent flow begins at $\mathbf{R} < 400$.

4 It has been found that the usual methods for evaluating heat transfer and pressure drop for liquids inside tubes are applicable for liquids in the fin side of finned double-pipe exchangers. The equivalent diameter used in both cases was the hydraulic diameter, $D_e = 4A_c/\psi$.

BIBLIOGRAPHY

1 "A Method of Correlating Forced-Convection Heat-Transfer Data and a Comparison With Fluid Friction," by A. P. Colburn, Trans. American Institute of Chemical Engineers, vol. 29, 1933, pp. 174–210.

2 "Heat Transfer and Pressure Drop of Liquids in Tubes," by E. N. Sieder and G. E. Tate, *Industrial and Engineering Chemistry*, vol. 28, 1936, pp. 1429–1435.

3 "Heat Transfer and Pressure Drop in Empty, Baffled, and Packed Tubes," Part III—Relationship Between Heat Transfer and Pressure Drop," by A. P. Colburn and W. J. King, Trans. American Institute of Chemical Engineers, vol. 26, 1931, pp. 196–207.

4 "Heat Transfer, Pressure Drop, and Fouling Rates of Liquids for Continuous and Noncontinuous Longitudinal Fins," by A. Y. Gunter and W. A. Shaw, Trans. A.S.M.E., vol. 64, 1942, pp. 795–802.

5 "Heat Transmission," second edition, by W. H. McAdams, McGraw-Hill Book Company, Inc., New York, N. Y., 1942, p. 183.

6 "Mathematical Equations for Heat Conduction in the Fins of Air-Cooled Engines," by D. R. Harper, 3rd, and W. B. Brown, U. S. Technical Report no. 158, National Advisory Committee for Aeronautics, 1922.

7 "Laminar-Flow Heat-Transfer Coefficients for Ducts," by R. H. Norris and D. D. Streid, Trans. A.S.M.E., vol. 62, 1940, pp. 525–533.

8 "Standards of Tubular Exchanger Manufacturers Association," 1941 edition, published by T.E.M.A., Inc., 366 Madison Avenue, New York, N. Y.

Discussion

A. Y. Gunter[4] and W. A. Shaw.[5] The authors are to be complimented on their paper covering double-pipe longitudinal fin-tube heat exchangers.

After accounting for slightly different methods of obtaining T_w and fin effectiveness, their data on heat-transfer and friction factors check very well with the results published in a previous paper by the writers.[6]

It is gratifying to note that these data cover a much wider range than the writers' previously published material and should be of added benefit to design engineers in this field of equipment rating.

It is suggested that a table giving the range of variables covered in their tests be provided so that the extent of accurate application of the data will be made known to all concerned.

Authors' Closure

The table below gives the range of variables covered in the tests reported.

G from 63,800 to 665,000

R from 7.5 to 12,800

$\frac{c\mu}{k}$ from 11.0 to 1625

$\frac{\mu}{\mu_w}$ from 0.274 to 3.45

A statement on the effect of using an assumed value of 2500 Btu/(hr) (sq ft) (deg F) for the condensing steam coefficient has been added to the text of the paper. It must be remembered that the tests reported were made on hairpin sections having 20 ft 0 in. continuous fin. For shorter fin lengths an adjustment must be made for the change in $\frac{L}{D_e}$ ratio.

---

[4] Director of Development, Alco Products Division of the American Locomotive Company, New York, N. Y. Mem. A.S.M.E.

[5] Development Engineer, Alco Products Division of the American Locomotive Company, New York, N. Y. Jun. A.S.M.E.

[6] Refer to authors' bibliography (4).

Numerical Methods for Transient Heat Flow

By G. M. DUSINBERRE,[1] BLACKSBURG, VA.

This paper deals with the application of numerical methods for the solution of heat-conduction problems, their generality being extended in the following ways: (*a*) A modulus is developed by choice of which the worker may proceed most rapidly to a solution, or may proceed more slowly and with greater precision; (*b*) criteria are developed for the choice of modulus to insure convergence. This is most important at a convective surface; (*c*) a method is developed for handling *k* and *c* when these properties vary independently with temperature. A comprehensive Appendix gives the derivations, and the use of equations and charts is demonstrated by typical examples.

Nomenclature

THE following nomenclature is used in the paper:

k = conductivity
c = specific heat
ρ = density
t = time
Δt = a small finite time interval
x, y, z = space co-ordinates
Δx = a small finite distance
T = temperature
T' = temperature after an interval Δt
h = surface coefficient of heat transmission
M = modulus relating Δx and Δt
N = the ratio $h\Delta x/k$
F = a coefficient
C = a temperature change
p = a ratio of specific heats
q = a ratio of conductivities

General

The conventional treatment of heat conduction problems, since the time of Fourier, has been by analytical attack on the general equation

$$\frac{\partial}{\partial x}\ k_x \frac{\partial T}{\partial x} + \frac{\partial}{\partial y}\ k_y \frac{\partial T}{\partial y} + \frac{\partial}{\partial z}\ k_z \frac{\partial T}{\partial z} = c\rho \frac{\partial T}{\partial t} \quad \ldots\ldots [1]$$

This is quite unmanageable as it stands. Fortunately, the variation of k with orientation and temperature, and of c with temperature, are often negligible within the required accuracy of a particular problem, so these properties are taken as constant. It is generally necessary also to impose certain simplifications on the boundary conditions. Under these assumptions a literature has grown up, too extensive and too familiar for detailed reference. Solutions arrived at in this way are known, somewhat strangely, as "exact" solutions.

Recently some attention has been given to numerical and graphical methods. A few of the more accessible references are given in the bibliography (1, 2, 3).[2] These treat generally of the simpler cases. There remains then a wide range of engineering problems for which no analytical solution exists, or for which the analytical solution is intolerably complex. Many of these yield to the method of analogous electrical circuits (4), but the necessary apparatus may not be available when and where needed. Numerical methods can be used by any engineer at any time.

We extend the generality of these methods in the following ways:

(*a*) A modulus is developed, by choice of which the worker may proceed most rapidly to a solution, or may proceed more slowly and with greater precision.

(*b*) Criteria are developed for the choice of modulus to insure convergence. This is most important at a convective surface.

(*c*) A method is developed for handling k and c when these properties vary independently with temperature.

Derivations will be found in the Appendix. The use of the equations and charts will be demonstrated by examples.

Example 1 Illustrating Flexibility of Numerical Method

Example 1 is set up to illustrate the flexibility of the numerical method. A relatively complex situation is analyzed by a combination of simple procedures. The assumptions are to be taken as merely typical and perhaps not the most accurate that might be made.

A large cast-iron slab 1 in. thick lies on a bed of insulating material. Slab and surroundings are at 100 F. A large copper slab 2 in. thick, having been heated uniformly to 400 F, is placed on the iron slab and sprayed with water at 100 F.

Required. The cooling curves at $^1/_2$-in. intervals in the two slabs, down to a surface temperature of 300 F.

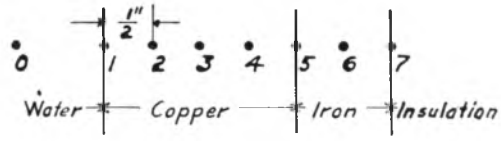

Fig. 1 Reference Points for Example 1

Assumptions. Edge effects may be neglected, making the flow one-dimensional. Surface resistance between the slabs is negligible. Conduction from iron to surroundings is negligible. The following values of metal properties may be assumed as constant: Copper, $k = 218$, $c = 0.094$, $\rho = 556$; Iron, $k = 27$, $c = 0.118$, $\rho = 442$. The surface coefficient h may be assumed 500 at 400 F, 700 at 350 F, and 900 at 300 F.

Solution. Reference points are as designated in Fig. 1. The following preliminary calculations are made, the derivation and significance of which are given in the Appendix:

$$\frac{M_{Cu}}{M_{Fe}} = \frac{0.094 \times 556 \times 27}{0.118 \times 442 \times 218} = 0.124$$

$$N_{max} = \frac{900}{24 \times 218} = 0.172$$

$$2N + 2 = 2.34 < 3$$

[1] Department of Mechanical Engineering, Virginia Polytechnic Institute. Mem. A.S.M.E.

Contributed by the Heat Transfer Division and presented at the Annual Meeting, New York, N. Y., Nov. 27–Dec. 1, 1944, of The American Society of Mechanical Engineers.

[2] Numbers in parentheses refer to the Bibliography at the end of the paper.

Choosing

$$M_{Cu} = 3,\ M_{Fe} = 3/0.124 = 24.2$$

$$\Delta t = \frac{0.094 \times 556}{3 \times 218 \times 24 \times 24} = 0.000139 \text{ hr} = 0.5 \text{ sec}$$

$$\text{Initial } T_5 = \frac{400 \times 0.094 \times 556 + 100 \times 0.118 \times 442}{0.094 \times 556 + 0.118 \times 442} = 250 \text{ F}$$

	Sec.	0	1	2	3	4	5	6	7
	$F_{n-1,n}$		0.064				0.333	0.041	0.082
	$F_{n,n}$		0.269				0.626	0.918	0.918
	$F_{n+1,n}$		0.667				0.041	0.041	—
0	0	100	400	400	400	400	250	100	100
			6A				133	10	8
			107A	1200B	1200B	1050B	156	92	92
			267A				4	4	—
1	0.5	100	380	400	400	350	293	106	100
			6				117	12	9
			102	1180	1150	1043	183	98	92
			267				4	4	—
2	1.0	100	375	393	383	348	304	114	101
	0.089 C		9				116	12	10
	0.244 C		91	1151	1124	1035	190	104	93
	0.667 C		262				5	4	—
3	1.5	D	362	384	375	345	311	120	103

Notes: A. We add $F_{0,1}T_0, F_{1,1}T_1$ and $F_{2,1}T_2$ to get T_1'. The same "weighting" procedure is used at points 5, 6 & 7.
B. We add T_1, T_2 and T_3 and divide by 3 to get T_2'. This "averaging" procedure is used at points 3 & 4.
C. T_1 having reached 375, we change $F_{0,1}$ & $F_{1,1}$.
D. Remaining work omitted, for brevity.

FIG. 2 SAMPLE WORK SHEET FOR EXAMPLE 1

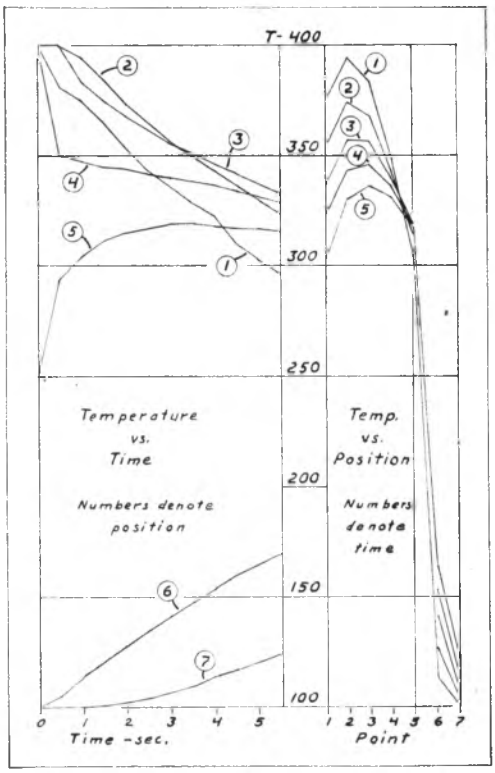

FIG. 3 TEMPERATURE CURVES FOR EXAMPLE 1

An "averaging" procedure is available for points 2, 3, and 4. Coefficients used for other points are calculated and entered on the work sheet, Fig. 2. Additional coefficients for point 1 are given in Table 1.

TABLE 1 COEFFICIENTS FOR EXAMPLE 1

T_1	h	N	F_{01}	F_{11}	F_{21}
400 — 375	500	0.096	0.064	0.269	0.667
375 — 325	700	0.134	0.089	0.244	0.667
325 — 300	900	0.172	0.114	0.218	0.667

The calculations are then performed according to the work sheet. Results are shown graphically in Fig. 3.

EXAMPLE 2, ILLUSTRATING PROCEDURE WHEN k VARIES WITH TEMPERATURE

Example 2 is chosen to illustrate the procedure when k varies with temperature, and because an experimental solution is available for check. This is the subject of a paper by Bradley and Ernst (5).

A furnace is operated cyclically, on 8 hr and off 16 hr. During operation the hot-side temperature is as near 1900 F as possible. The ambient temperature is 100 F. The furnace wall is laid up with a single course of brick, headed to the fire, giving a thickness of 9 in.

Required. The time-temperature curves for the outer surface and three interior points of the wall, and an estimate of the daily heat loss when the furnace has reached an equilibrium cycle.

Assumptions. The T — k relation for the brick is given in Table 2, and $c = 0.23$, constant. Strictly, we should assume the furnace airtight with no heat losses from the interior while secured, or else assume a rate of air leakage. But to permit a closer comparison of results we use the experimentally measured fire-side surface temperatures as "feed-in." The same was done with the electric analyzer, as described in reference (5). A rough steady-state analysis shows that the outer surface temperature will rise less than 100 deg F above the ambient, so the fluctuation here will not be great. We estimate h to be 2.4 and assume that its variation can be neglected.

TABLE 2 SAMPLE CALCULATIONS FOR FIG. 5

T	k*	q	$q\Delta T$	$\sum_{100}^{T} q\Delta T$
100	..	...	...	...
			94	
200	..	...		94
			96	
300	..	...		190
			98	
400	0.99	1.000		288
			101	
500	..	...		389
			104	
600	1.04	1.050		493
			107	
700	..	...		600
			110	
800	1.11	1.121		710
			114	
900	..	...		824
			118	
1000	1.19	1.202		942
			123	
1100	..	...		1065
			127	
1200	1.29	1.303		1192
			135	
1300	..	...		1327
			139	
1400	1.42	1.434		1466
			148	
1500	..	...		1614
			153	
1600	1.56	1.576		1767
			162	
1700	..	...		1929
			170	
1800	1.73	1.747		2099
			179	
1900	..	...		2278
			189	
2000	1.91	1.929		2467

* Conductivity was reported on a "per-inch" basis.

Solution. Δx has been set at $^1/_4$ the length of the brick, 0.1875 ft. We designate reference points as in Fig. 4. Preliminary calculations are as follows:

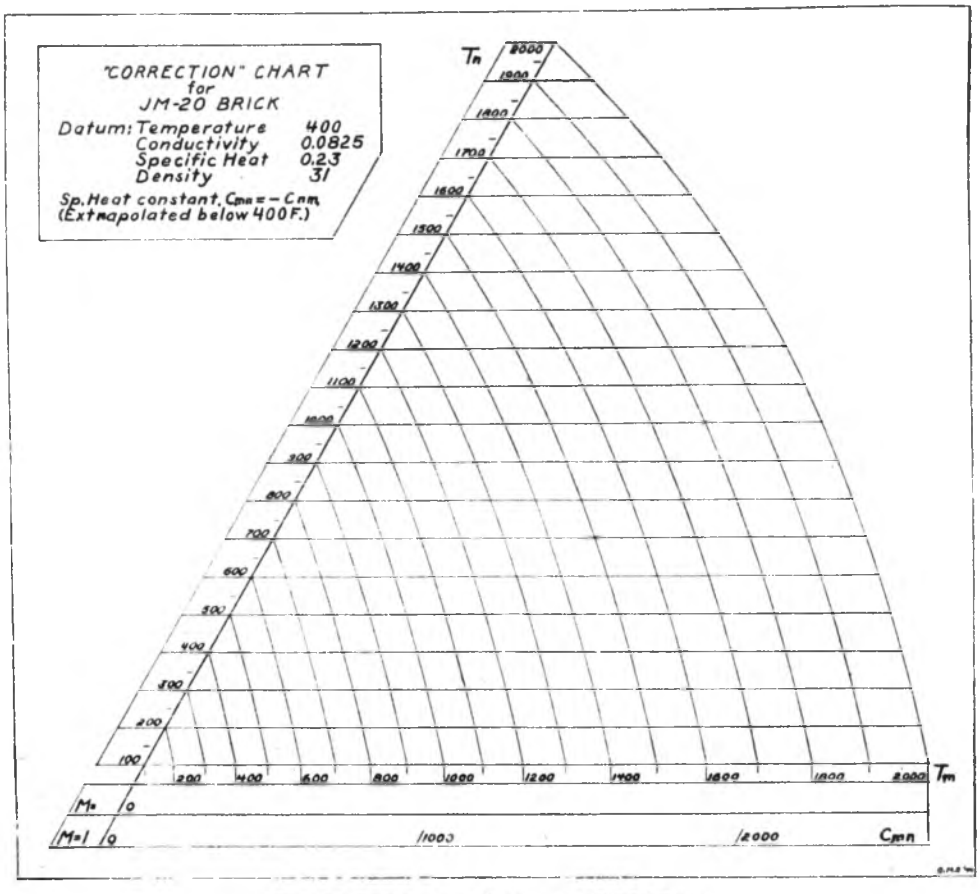

FIG. 5 CORRECTION CHART FOR JM-20 BRICK

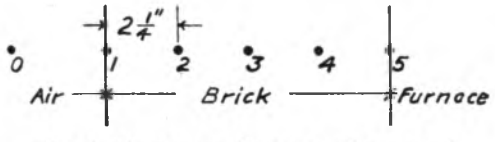

FIG. 4 REFERENCE POINTS FOR EXAMPLE 2

$$q_{mn\ \max} = q_{1,900,100} = 2278/1800 = 1.264$$

$$M \geqq 2 \times 1.264 = 2.53$$

Steady-state analysis shows $T_2 \leqq 800$ F, and

$$q_{21\ \max} = q_{800,100} = 710/700 = 1.014$$

$$M \geqq 3 \times 1.014 = 3.04$$

$$N = \frac{2.4 \times 0.1875}{0.0825} = 5.45$$

$$M \geqq 2(5.45 + 1) = 12.90$$

The conditions are such that we can disregard the last restriction. Choosing $M = 3.04$

$$\Delta t = \frac{0.23 \times 31 \times 0.1875^2}{3.04 \times 0.0825} = 1 \text{ hr}$$

We have a previously prepared "correction" chart for the material, Fig. 5. We convert this to the chosen modulus, drawing the diagonal lines shown in Fig. 6. The chart now shows, for an interior point, the change during Δt due to the temperature at an adjacent point. For the outer surface we calculate the auxiliary diagonal lines at the lower left.

Starting with the initial distribution and taking T_5 from the experimental data, we calculate the succeeding temperatures. The results for three days are shown in Fig. 7. The fourth day was practically a repetition of the third, showing that an equilibrium cycle had been reached.

The complete work sheet is too long for reproduction but we show for example how the temperatures for the 58th hour are obtained. At the 57th hour we have

Point	0	1	2	3	4	5
Temperature	100	175	620	1075	1440	1500

Using Fig. 6 we find the "corrections" for each point

$-C_{01}$	C_{21}	$-C_{12}$	$C_{22} = -C_{23}$	$C_{43} = -C_{34}$	C_{54}
60	65	150	175	160	30

These values are entered directly on the work sheet, Fig. 8.

If we were not using experimental data for point 5 and wished to assume no air leakage, we should use $C_{45} = -2C_{54}$, whence $T_5 = 1440$.

The calculated heat flow for the equilibrium cycle is 3430 Btu per sq ft per day. From the experimental curves the figure is 3350. This agreement should be satisfactory for most purposes.

A slight overshooting can be observed at several points in Fig. 7. This will occur when the temperature changes rapidly, especially with a minimum M. When greater precision is required, the remedy is to use a larger M, and the cost is extra work. In this problem it could be foreseen that the T_4 curve would

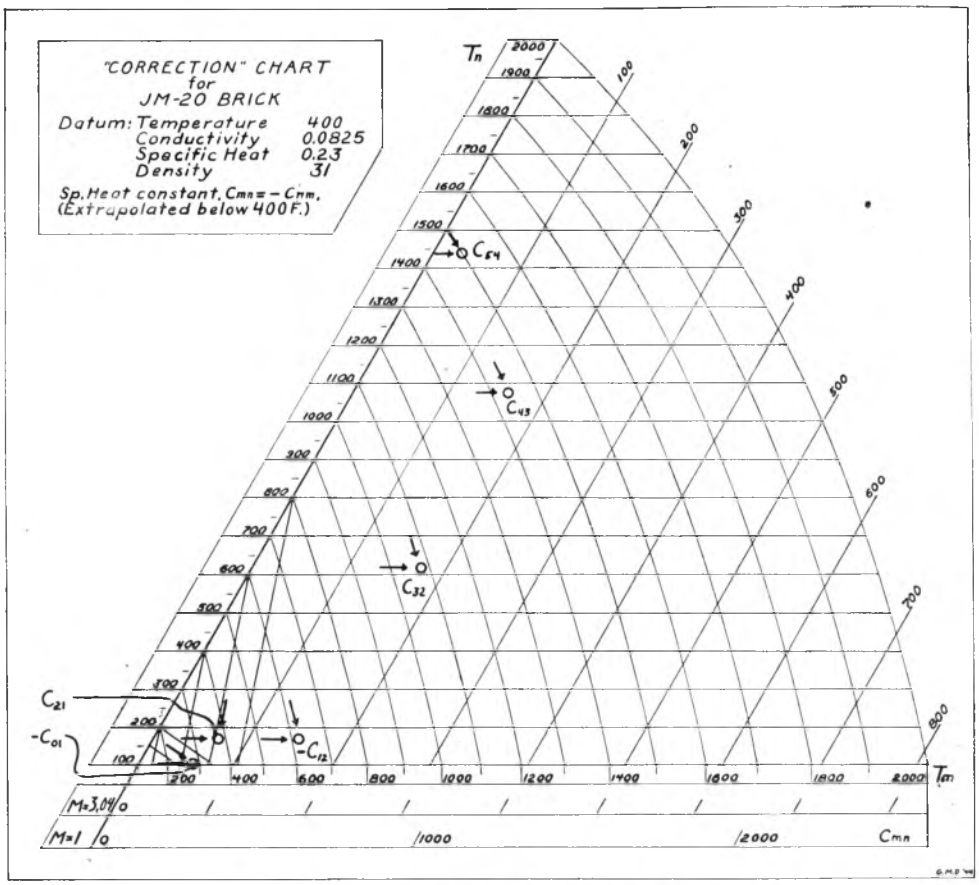

FIG. 6 CORRECTION CHART AS USED FOR EXAMPLE 2

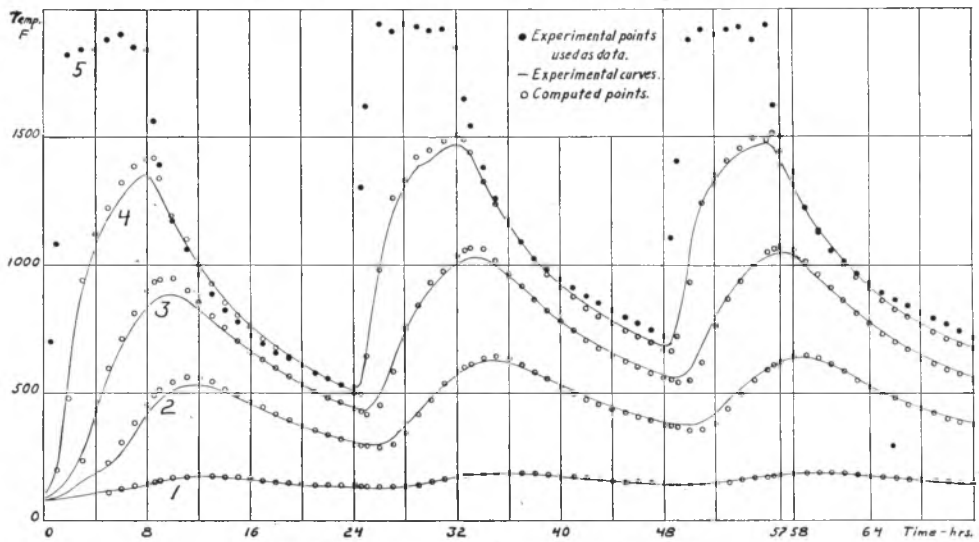

FIG. 7 TEMPERATURE CURVES FOR EXAMPLE 2

Time	Point	0	1	2	3	4	5
57	Temperature	100	175	620	1075	1440	1500
	$C_{n+1,n}$		65	175	160	30	
	$C_{n-1,n}$		-60	-150	-175	-160	
	C_{total}		5	25	-15	-130	
58	Temperature	100	180	645	1060	1310	1360

FIG. 8 SAMPLE WORK SHEET FOR EXAMPLE 2

overshoot at the beginning and end of the heating period, so half-intervals were used as shown in Fig. 7.

CONCLUSION

These examples have shown the use of a number of the procedures outlined in the Appendix. Many other combinations are possible, permitting investigation of a wide range of heat-transfer problems. Applications suggest themselves especially in metal-

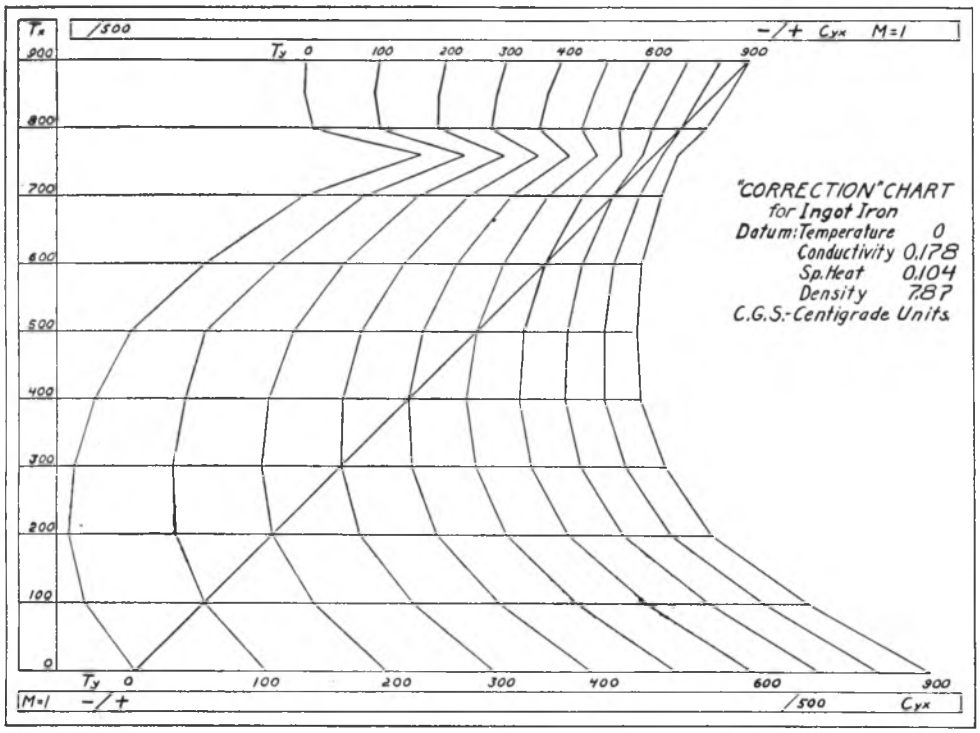

FIG. 9 CORRECTION CHART FOR INGOT IRON

lurgical processes where k, c, and h vary greatly. Fig. 9 is exhibited to show the form the correction chart may take for a metal in which k has a range of about 4:1 and c about 3:1.

ACKNOWLEDGMENTS

The author is grateful to his associates, H. G. Elrod, Jr., and C. M. Fowler for continued interest, criticism, and advice, and to Dr. C. B. Bradley of Johns-Manville Research Laboratory for furnishing the large-scale chart from which Fig. 7 was drawn.

Appendix

1 Regarding k and c as constant for the present, and flow as one-dimensional, we consider Fig. 10 an element of the material centered at 2. The dimension Δx has some small value consistent with the practical requirements of the problem. The element 2 is insulated except where it adjoins element 1, which is no larger than 2. At time t the temperatures are T_1 and T_2 and the gradient is $(T_1 - T_2)/\Delta x$.

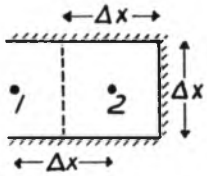

FIG. 10 ONE ADJACENT ELEMENT

We now make three important assumptions:

(*a*) A time interval Δt can be chosen sufficiently small that there is negligible error in using the initial gradient $(T_1 - T_2)/\Delta x$ to compute the heat flow during this interval.

(*b*) Time interval Δt is sufficiently small that there is negligible error in neglecting the effect on 2 of any region beyond 1.

(*c*) Δx is sufficiently small that there is negligible error in using the temperature at point 2 to compute the heat capacity of the element 2.

Under these assumptions we can write the following heat balance

$$k\,\Delta t(T_1 - T_2) = c\rho\,\Delta x^2(T'_2 - T_2) \quad [2]$$

We introduce a modulus defined as

$$M = c\rho\,\Delta x^2/k\,\Delta t \quad [3]$$

Then Equation [2] becomes

$$T_1 - T_2 = M(T'_2 - T_2) \quad [4]$$

Under our assumptions, T'_2 cannot, in any Δt, attain a value more than half way between the initial values T_1 and T_2, that is

$$T'_2 - T_2 \leqq \tfrac{1}{2}(T_1 - T_2) \text{ and } M \geqq 2 \quad [5]$$

This is the first criterion for a valid numerical procedure.

2 Now consider element 2 as lying between two similar elements, Fig. 11. The heat flow from 3 is additive to that from 1, and

$$(T_1 - T_2) + (T_3 - T_2) = M(T'_2 - T_2) \quad [6]$$

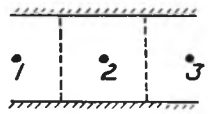

FIG. 11 TWO ADJACENT ELEMENTS

We may put this in three different forms as follows

$$T'_2 = \frac{T_1 + (M-2)T_2 + T_3}{M} \quad [7]$$

This defines what we may call an "averaging" procedure.

It is the quickest and most convenient since it involves only two arithmetical steps for each computed point, namely, one addition and one division.

Or

$$T'_2 = F_{12}T_1 + F_{22}T_2 + F_{32}T_3 \quad [8]$$

in which

$$F_{12} = F_{32} = 1/M \qquad F_{22} = (M-2)/M \qquad \Sigma F = 1 \quad [9]$$

This defines a "weighting" procedure. It involves three multiplications and one addition.

Or

$$T'_2 = T_2 + C_{12} + C_{32} \quad [10]$$

in which

$$C_{12} = (T_1 - T_2)/M \qquad C_{32} = (T_3 - T_2)/M \quad [11]$$

This defines a "correction" procedure. It involves two subtractions, two multiplications, and an algebraic addition. However, the work can be simplified by the use of a chart, and this is our best recourse when thermal properties vary with temperature.

In Equation [7], if we give M its low limiting value of 2, we get the Schmidt[3] formula, $T'_2 = (T_1 + T_3)/2$. This says that the temperature at a point depends upon the previous temperatures at adjacent points but not upon its own previous temperature.[4] Starting with a constant temperature in the material, this method gives rise to a stepwise time-temperature plot, though by "cranking-in" the initial calculation from an analytical solution, this can be avoided (1, 2). The choice of modulus 3 gives $T'_2 = (T_1 + T_2 + T_3)/3$, which is about as convenient as the Schmidt formula and has a number of advantages.

A further justification of Equation [5] can be had from Equation [8]. If $M < 2$, then $F_{22} < 0$, which says that T'_2 depends on T_2 in a negative sense. Intuitively, this seems absurd. No formal proof can be offered here,[5] but it would appear that we may take as a general criterion

$$F_{nn} \geqq 0 \quad [12]$$

3 At a surface where convection occurs, the reference points may be disposed as in Fig. 12 (*a*) or (*b*). Formulas may be developed for (*b*), and these have certain advantages, but as we are generally interested in the surface temperature, we confine attention here to (*a*).

The point 0 in Fig. 13 is taken in the adjacent medium at some distance where the gradient normal to the surface has become negligible. We make use of a surface coefficient h which is to include the effect of convection and radiation. Temperature T_0 and h may vary, so long as they may be regarded constant over any Δt. Under our assumptions the heat balance is

$$k\,\Delta t(T_2 - T_1) + h\,\Delta x\,\Delta t(T_0 - T_1) = c\rho\,\Delta x^2(T'_1 - T_1)/2 \quad [13]$$

We define a "Nusselt number"

$$N = h\Delta x/k \quad [14]$$

Introducing M and N

$$(T_2 - T_1) + N(T_0 - T_1) = \frac{M}{2}(T'_1 - T_1) \quad [15]$$

If $T_0 = T_1$, a very common initial condition, then

$$T'_1 - T_1 \leqq \frac{2}{3}(T_2 - T_1) \text{ and } M \geqq 3 \quad [16]$$

If we write Equation [15] in the form of Equation [8]

$$F_{21} = 2/M, \quad F_{01} = 2N/M, \quad \text{and } F_{11} = (M - 2N - 2)/M \quad [17]$$

Then if we are to meet the condition of Equation [12]

$$M \geqq 2N + 2 \quad [18]$$

In choosing M, we should be guided by whichever of Equations [16] or [18] is more restrictive, using of course the largest N which occurs in the problem.

If N is large, observance of these criteria may be inconvenient. Provided the surface temperature does not fluctuate much from the steady-state value (but not otherwise), a permissible approximation is to jump at once to the steady-state relations (1)

$$F_{21} = 1/(N+1), \quad F_{11} = 0, \quad F_{01} = N/(N+1) \quad [19]$$

At a well-insulated surface h, N, and F_{01} may approximate zero.

4 In a heterogeneous wall, Fig. 14, materials 2 and 4 have different properties. Time interval Δt must be the same for all layers. If it is convenient to choose

$$\Delta x_2/\Delta x_4 = \sqrt{k_2c_4\rho_4/k_4c_2\rho_2}$$

then the same modulus applies in both regions. But Equation [3] allows more freedom in treating such cases. For example, if we wish to keep Δx the same in both regions it is only necessary that

$$M_2/M_4 = c_2\rho_2k_4/c_4\rho_4k_2$$

We choose M for the region in which it is lowest and use an averaging procedure here, and weighting procedures elsewhere. In this case, for point 3, the weighting formulas become

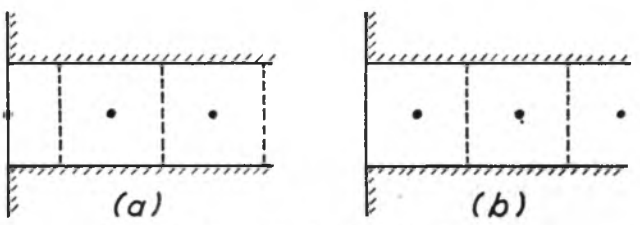

FIG. 12 TWO POSSIBLE REFERENCE SYSTEMS

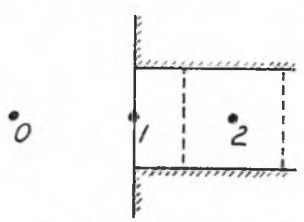

FIG. 13 A CONVECTIVE SURFACE

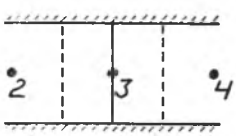

FIG. 14 A HETEROGENEOUS WALL

[3] Max Jakob (Trans. A.S.M.E., vol. 65, 1943, p. 613) states that the method should be credited to L. Binder.

[4] After the calculation is under way, the temperature at a point does depend on the value at the second preceding time interval.

[5] In a paper under preparation, C. M. Fowler undertakes a formal mathematical investigation of the convergence of these methods.

$$F_{22} = 2k_2/(k_2M_2 + k_4M_4), \quad F_{42} = 2k_4/(k_2M_2 + k_4M_4),$$
$$F_{22} = 1 - F_{23} - F_{43} \ldots\ldots [20]$$

If two materials at different temperatures are placed in good thermal contact, the initial T_3 may be taken as a weighted mean with respect to $c\rho\,\Delta x$ in the two regions, by conservation of energy. If there is an appreciable interface resistance, the surfaces are treated under section 3.

A homogeneous material may be treated under varying Δx and M if we wish to study changes more closely in certain regions.

5 Sensible heat may be absorbed within the material by a phase change or chemical reaction and may be produced by these phenomena and by electrical means. In the last case it is only necessary to add, at each point involved, the temperature rise during each Δt, which is the energy supplied divided by the heat capacity of the element.

Where a latent heat exists, temperature changes are delayed. When the calculated temperature at a point passes the phase-change temperature, we subtract the excess, making an account of it, and continue the calculation using the phase-change temperature. When our account of excess degrees reaches the value L/c we discontinue the account and use the computed temperature.

6 Weighting equations are readily derived for the effectively one-dimensional radial flow in a long cylinder, Fig. 15. $M \geqq 4$ and $F_{mn} \neq F_{nm}$, etc. The uniform Δx shown may be preferable to a possible logarithmic spacing when we are interested in gradients near the surface.

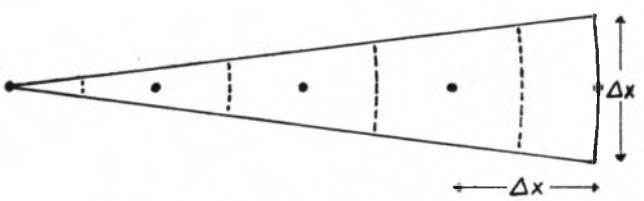

FIG. 15 REFERENCE POINTS IN A CYLINDER

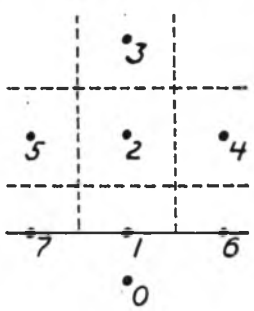

FIG. 16 A TWO-DIMENSIONAL SYSTEM

7 From Fig. 16 we can derive equations for two-dimensional flow. For the interior, $M \geqq 4$ and preferably $M = 5$. There is no great additional difficulty in allowing for a k variable with orientation.

8 We now take up methods useful when k and c vary independently with temperature. Inspection of Equation [1] shows that the concept of diffusivity is not applicable here, which is why we have not introduced it.

In order to continue the use of the modulus already developed, it is convenient to select a datum temperature to which the subscript d refers.

Then

$$M = c_d\rho\,\Delta x^2/k_d\Delta t \quad p_n = c_n/c_d \quad q_n = k_n/k_d \ldots\ldots [21]$$

Referring to Fig. 11, the heat balance is now

$$k_{12}\,\Delta t(T_1 - T_2) + k_{32}\,\Delta t(T_3 - T_2) = c_2\rho\,\Delta x^2(T'_2 - T_2) \ldots [22]$$

Double subscripts here indicate a mean value. Using Equations [21]

$$q_{12}(T_1 - T_2) + q_{32}(T_3 - T_2) = p_2M(T'_2 - T_2) \ldots\ldots [23]$$

If we put this in the form of Equation [10], then, corresponding to Equation [11]

$$C_{12} = q_{12}(T_1 - T_2)/p_2M \text{ and } C_{32} = q_{32}(T_3 - T_2)/p_2M \ldots [24]$$

These formulas are the basis of the "correction" chart. The trouble of computing and plotting this chart may be justified by the fact that it can be used for any problem with the material to which it refers.

Any C_{mn} can be taken as

$$\left[\frac{1}{M}\right] \cdot \left[\frac{1}{p_n}\right] \cdot [q_{mn}(T_m - T_n)]$$

The last factor amounts to

$$\int_n^m \frac{k\,dT}{k_d}$$

If the $T - k$ relation is expressed by a table, we integrate numerically; if by an equation, we can integrate formally. In either case, construct a table of this factor over the required range of T_m, T_n. Introduce the second factor by dividing each entry by p_n. This gives a table of C_{mn} to modulus 1. Plot (a) horizontal straight lines of T_n to a uniform scale, (b) straight lines of C_{mn} to a uniform scale, inclined about 30 deg to the right of the vertical, and (c) curves of T_m inclined to the left and non-uniform. Erase the C_{mn} lines and the chart is like Fig. 5 or 9. It can be converted to any desired modulus by drawing new diagonal lines to the appropriate scale.

Table 2 shows part of the calculations for Fig. 5. The $T - k$ data are from reference (5). In this case c is constant, p drops out, and $C_{nm} = -C_{mn}$, so only half the chart need be drawn.

9 For a convective surface the equations are analogous to those derived in Section 3. We redefine N as $h\,\Delta x/k_d$. As before, we must give attention to the maximum N occurring in the problem, and also to the maximum q/p ratio. Referring to Fig. 13

$$C_{21} = 2q_{21}(T_2 - T_1)/p_1M \quad C_{01} = 2N(T_0 - T_1)/p_1M \ldots [25]$$

C_{21} at a surface is then double the value from the chart.

Criteria corresponding to Equations [16] and [18] are

$$M \geqq 3(q_{21}/p_1) \quad M \geqq 2(N + q_{21})/p_1 \ldots\ldots [26]$$

Steady-state approximations corresponding to Equation [19] are

$$C_{21} = q_{21}(T_2 - T_1)/(N + q_{21}) \quad C_{01} = N(T_0 - T_1)/(N + q_{21}) \ldots [27]$$

If conditions are nearly steady at a surface, we can plot the results as auxiliary lines on the correction chart. Otherwise we must tabulate.

BIBLIOGRAPHY

1 "Heat Transmission," by W. H. McAdams, McGraw-Hill Book Company, Inc., New York, N. Y., 1942, pp. 39–43.

2 "Applied Mathematics in Chemical Engineering," by T. K. Sherwood and C. E. Reed, McGraw-Hill Book Company, Inc., New York, N. Y., 1939, pp. 241–255.

3 "The Numerical Solution of Heat-Conduction Problems," by H. W. Emmons, Trans. A.S.M.E., vol. 65, 1943, pp. 607–615.

4 "A Method for Determining Unsteady-State Heat Transfer by Means of an Electrical Analogy," by V. Paschkis and H. D. Baker, Trans. A.S.M.E., vol. 64, 1942, pp. 105–112.

5 "Analyzing Heat Flow in Cyclic Furnace Operation," by C. B. Bradley and C. E. Ernst, *Mechanical Engineering*, vol. 65, 1943, pp. 125–129 and 527–530.

Discussion

C. M. Fowler.[6] The author's two representative problems seem to dispose of the practical side of the theoretically unsolved cases where both thermal properties and transfer coefficients are functions of temperature.

The writer has had occasion to study heat flow through steel specimens for the purpose of determining hardness distributions throughout specimens after quenching, and to his knowledge, the work done so far on this problem has been confined to cases where transfer coefficients and thermal properties are assumed constant over the quenching range, with no account being taken of heats of phase change in the steel. It is the writer's opinion that the numerical study of the heat flow in, say, a circular cylinder or slab taking into account the variable properties mentioned would be of real value in making more accurate predictions of "after-quench" hardness distributions of these specimens.

In the actual mechanics involved in solving a problem, the author develops a restrictive criterion for the modulus, $M = 2$, Equation [5]. For all practical purposes this is true. However, the assumptions used in deriving this criterion are actually more restrictive than necessary for many problems, and in a paper under preparation the writer has shown that in some cases M may be as low as 1 which, as the author points out, is intuitively absurd. It appears to the writer that most of the criteria developed for both the modulus and the surface transfer coefficient N have been demonstrated under conditions more restricted than those actually called for in the problems under consideration.

The writer would also be very much interested in seeing some problems worked out involving a phase change such as the author suggests in the Appendix, Section 5.

W. A. Hadley.[7] It would appear to the writer that the method described in the paper would be even more useful in evaluating unsteady-state diffusional processes, such as drying, carburization of steel, etc., than heat transfer. In general, most diffusional processes are not steady state and must be analyzed mathematically by making untrue but simplifying assumptions. It would appear that the paper offers every engineer a simple but powerful tool whose use will permit him to analyze closely diffusional processes which he could only approximate before.

Will the author please verify this contention?

Victor Paschkis.[8] The numerical method is a powerful tool and any paper which attempts to make this tool more acceptable is to be welcomed.

In studying the paper the writer notes in particular the following observations of the author:

1 That ". . . under our assumptions T'_2 cannot in any Δt attain a value more than halfway between the initial values T_1 and T_2 . . ." Whereas this statement is certainly correct, it would help the reader unfamiliar with the basis of this method if this point would be clarified.

2 At another point the author states, "intuitively it seems absurd that T'_2 should depend on T_2 in a negative sense." Probably one could establish a reasoning from which such a dependence could be calculated and therefore the formal proof which is forthcoming will be of high interest.

3 In Fig. 3 curve 4 on the left side shows a remarkable discontinuity at approximately 0.8 sec. This discontinuity has either to be attributed to too coarse a lumping or to an error in the procedure. Clarification of this point would be helpful.

The author mentions the electric-analogy method in which the writer is particularly interested. He states, "the necessary apparatus may not be available when and where needed. Numerical methods can be used by any engineer at any time." It is the opinion of the writer that each method (numerical and electric analogy) has its useful applications. The fact that a "heat-and-mass-flow analyzer" is available in only one or two places does not appear to be a legitimate reason against the method. For all cases where the electric method is a more powerful tool it should be applied, and when the numerical method is better, it should be applied. It appears that the refinements presented in the paper make the last part of the author's statement a bit doubtful. The rules and procedure become so complicated that many engineers in the field may not have the time to familiarize themselves with the necessary steps. Moreover, it appears to the writer that the electric-analogy method has unusual educational values in showing the observer, on instruments, what is going on in the pieces subject to heat flow.

Finally it should be noted that the numerical method and the electric-analogy method have in common the necessity of lumping. But the electric method does not in most instances call for any lumping of time, and in those cases where lumping of time is required it is never an entire lumping. The numerical method is of course based entirely upon lumping in time as well as in space, which is obviously a disadvantage as against the analogy method.

In the presentation, the author brought up the problem of constant properties of materials, and in problems dealing with metals, the desirability of working with the actual specific-heat and conductivity curves which show a temperature dependency.

The writer feels that the practicing engineer will by and large make use only of such engineering knowledge as is reduced to charts and graphs or to material available in handbooks. Often he has not the time to work out numerically any type of problem.

Now, if curves with dimensionless parameters should be used, the introduction of changing properties increases the necessary number of charts very considerably. For example, in quenching the introduction of each phase change adds three parameters to those necessary for representation in dimensionless units. The consequence is the necessity of a vast number of charts too unwieldy for use. For many purposes the charts with constant properties, as for example those by Gurney and Lurie, are sufficient.

This of course should not imply that it is not desirable to have methods which permit the solution of problems considering the change of properties, but it is the opinion of the writer that such methods will be more helpful to the research worker than to the practicing engineer and that it is most important to help the latter by development of easily usable curves and charts.

Author's Closure

Lieutenant Fowler's discussion is welcome in supporting the author's opinion that the methods may be of use in metallurgical research. The phase change of principal interest to Lieutenant Fowler, and perhaps to other metallurgists, is that occurring in steel around 723 C. There are many examples of this; for a

[6] Department of Marine Engineering, United States Naval Academy, Annapolis, Md.

[7] Ensign, U.S.N.R., Department of Marine Engineering, United States Naval Academy, Annapolis, Md. Jun. A.S.M.E.

[8] Research Associate, Department of Mechanical Engineering, Columbia University, New York, N. Y.

recent one we may cite a paper by Hess.[9] By the numerical method, good qualitative agreement has been obtained with experimental heating and cooling curves. Better quantitative results depend on better determinations of physical properties. If merely a mean value of specific heat is used, the true shape of the curves is not obtained. When qualitative agreement does not exist, quantitative accuracy can be only accidental.

Where temperature changes are small and the principal phenomenon is freezing, the author recommends the analysis of London and Seban.[10]

Lieutenant Fowler suggests that the criteria for choice of modulus are unduly restrictive, and it is to be hoped that his studies on this subject will be published soon. In the meantime, the author can only say that, in practice, observance of the criteria will avoid divergence and the oscillating type of convergence. The worst one gets is a poor result at the first computed point, such as occurs in Fig. 3 of the paper, at 0.5 sec at point 4. This was noted by Professor Paschkis. If this is not satisfactory for the purpose at hand, the remedy is to use a closer network or a larger modulus.

Mr. Hadley's discussion is welcome, as it brings out the point that these methods may be used for any physical situation which gives rise to the same form of differential equation. The treatment of diffusion, however, involves some features which are worth illustrating by an example.

The problem chosen[11] concerns the drying of clay slabs. We have the following data and notation:

Diffusivity, D	0.4 sq cm per hr
Density (bone dry), ρ	1.55 g per cc
Initial concentration, T_0	0.27 g per g
Drying rate, α	0.20 g per sq cm hr
Half-thickness of slab, L	0.4 cm
Equilibrium concentration, T_{ec}	0.05 g per g

The constant drying rate α will obtain until the surface concentration reaches the equilibrium value. We are required to find the time at which that will occur, and also the average concentration at that time.

We express T_0 and T_{ec} on a volume basis as 0.418 and 0.078 g per cc, respectively. We choose reference point 1 at the surface, 3 at the center line, and 2 halfway between. Then $\Delta x = 0.2$ cm. If $M = 3$, $\Delta t = \Delta x^2/DM = 0.04/0.4 \times 3 = 1/30$ hr. For points 2 and 3 the formulas are: $T_2' = (T_1 + T_2 + T_3)/3$ and $T_3' = (2T_2 + T_3)/3$.

The treatment of the surface point is somewhat different, as we use the ideas of section 5 of the Appendix, rather than section 3. Considering the effect of the interior alone, we would have the formula $T_1' = (T_1 + 2T_2)/3$. We use this, but concurrently we have the effect of the constant drying rate. Applying this to the half-element at the surface, and calling the result ΔT, we have: $\Delta T = \alpha \Delta t/{}^1/_2 \Delta x = 0.2 \times 2/0.2 \times 30 = 0.067$ g per cc.

We are now ready to calculate Table 3 of this closure. In the numerical work, all concentrations are multiplied by 1000 to avoid decimals.

By interpolation, the time of reaching the equilibrium concentration at the surface is $(16 + 7/17)/30 = 0.55$ hr. The solution given in the reference[11] is 0.545 hr.

When $T_1 = 0.078$, $T_2 = 0.153$, and $T_3 = 0.178$. The mean value, $T_c = 0.141$ g per cc = 0.091 g per g. The reference solution is 0.094 g per g.

[9] "Fuel-Fired Techniques and Their Possibilities," by F. O. Hess, *Mechanical Engineering*, vol. 67, 1945, p. 442.

[10] "Rate of Ice Formation," by A. L. London and R. A. Seban, Trans. A.S.M.E., vol. 65, 1943, p. 771.

[11] "Principles of Chemical Engineering," by W. H. Walker, W. K. Lewis, W. H. McAdams, and E. R. Gilliland, McGraw-Hill Book Company, Inc., New York, N. Y., 1937, p. 656.

TABLE 3

Δt	T_1	T_2	T_3	Δt	T_1	T_2	T_3
0	418	418	418	4	289	364	388
					1017	1041	1116
					339		
	67				67		
1	351	418	418	5	272	347	372
(a)	1187	1187			966	991	1066
(b)	396				322		
(c)	67				67		
2	329	396	418	6	255	330	355
	1121	1143	1210				
	374			(d)	170	170	170
	67						
3	307	381	403	16	85	160	185
	1069	1091	1065		405	430	505
	356			(e)	135		
	67				67		
4	289	364	388	17	68	143	168

NOTES: (a) On this line we enter $T_1 + 2T_2$, $T_1 + T_2 + T_3$, and $2T_2 + T_3$.
(b) We divide the entries on line (a) by 3. The result for column 1 is entered on this line. The results for the other columns are final and are entered below.
(c) We subtract 0.067 here, at every time interval.
(d) Here we observe that a parabolic distribution has been established and each T decreases by 0.017 during each time interval. So we can jump to the 16th interval by subtracting 0.170 from each T.
(e) The given equilibrium concentration at the surface is reached between the 16th and 17th intervals.

But now, assuming no vapor forms in the material, suppose we want to go on and find the time required to bring the center-line concentration down to 0.70 g per g = 0.109 g per cc. To do this analytically requires shifting to a new formula. But we can do it numerically merely by continuing the calculation with a fixed value of T_1, as in Table 4. The solution is 22/30 hr.

As a final illustration, suppose the equilibrium concentration is less than 0.078 g per cc, so that it is possible to go below this value. But suppose this figure represents a concentration below which we do not wish to go. Then the lines such as (c) in Table 4 give the drying rates which we must maintain in order to get this result. In other words, the method enables the prediction of a schedule for controlled drying.

TABLE 4

Δt	T_1	T_2	T_3	Δt	T_1	T_2	T_3
16	85	160	185	19	78	120	137
(a)	405	430	505		318	335	377
(b)	135				106		
(c)	57				28		
17	78	143	168	20	78	112	126
	364	389	454		302	316	350
	121				101		
	43				23		
18	78	130	151	21	78	105	117
	338	359	411		288	300	327
	113				96		
	35				18		
19	78	120	137	22	78	100	109

NOTES: (a) and (b). These lines are obtained as before.
(c) The value of T_1 being fixed by equilibrium, we get this line by subtraction. It shows the rate at which drying will actually proceed, under the assumptions.

It adds to the paper to have a discussion by Professor Paschkis who has done so much with the electrical analyzer. In reply to his comments, we note first that if elements 1 and 2 are brought in contact and isolated, the steady-state temperature will be the weighted average of the initial temperatures, and each element can approach this steady-state temperature from only one direction.

As to T'_2 depending on T_2 in a negative sense, this would amount to saying that the hotter a body is at a given instant, the colder it must be at some selected future instant.

The discontinuity in Fig. 3 of the paper has been noted in reply to Lieutenant Fowler's discussion. It is due, not to error in the calculations, which are easily verified, but to the crude "lumping" chosen to make the example simple.

Professor Paschkis states that "lumping in time... is obviously a disadvantage as against the analogy method." The author is unable to agree. If a method can be made "sufficiently" accurate for the engineering purpose at hand, then no further refinement is

necessary or justified. If it cannot be made sufficiently accurate, then it must be discarded upon that ground, and not for any hypothetical reason.

As to what constitutes "sufficient" accuracy, that is a matter of engineering judgment. A good engineer will use all refinements which the job demands and will skip any refinements which the job does not warrant. In fact, many problems in heat conduction are too complicated for any sort of analysis and are best solved by trial-and-error experiment.

Finally, in favor of the numerical method, there is a sort of accuracy not subject to reasoning. This lies simply in human fallibility—the chance of making a mistake. The author finds that in simple arithmetic, which is all that this method demands, it is hard to make a mistake and easy to detect and remedy one when made. The opposite is true when working with parameters which have no obvious physical significance, or with the series which arise in analytical solutions.

An Electrical Geometrical Analogue for Complex Heat Flow

By C. F. KAYAN,[1] NEW YORK, N. Y.

Through the medium of the resistance concept, the general similarity of "contour maps" for heat flow and electrical flow may be visualized. The electrical analogy permits ready study of simple and complex heat-flow conditions which, because of distorted temperature conditions, would defy orthodox mathematical or graphical analysis. Internal-temperature lines (isotherms) obtained by relatively simple equipment with a geometrical type of analyzer are shown for one complex case of flow conditions.

Previous Electrical Analogies

USE of the electrical analogy to study heat flow for different shapes is not new. Herein electrical potential differences (voltages) are equivalent to the thermal (temperatures). Because of ready manipulation and prospect of accurate measurements, the electrical analogy is regarded as a very useful tool. Whereas the electrical-conduction effect is more usually thought of in this connection, still it is not the only electrical effect available; for example, electrical capacity for steady-flow studies has also been used. But the electrical-conduction effect so well parallels the heat-conduction effect that in terms of the so-called resistance concept, inherently involving Ohm's law of electrical flow extended to heat flow, the problem of flow may be readily visualized.

Langmuir, Adams, and Meikle (1)[2] in 1913 described the use of an electrical bath in a shallow tank for model study of different heat-flow shapes, as, for example, a thick corner. Here the inside and outside surfaces of a thick corner in two-dimensional heat flow were represented in the model by metal corners forming the vertical walls of the tank. Beyond the corner for each wall were set up boundary partitions; these and the tank bottom were made of nonconducting material. A conducting liquid electrolyte represented the single isotropic homogeneous material of the heat-flow corner. With an alternating-current electrical potential established between the parallel wall electrodes, the equivalent of steady-state heat-flow conditions between constant-temperature walls was set up. By means of an electrical probe, isopotential lines representing isothermal lines in the solid body could be established. This was truly a geometrical heat-flow analogue. The same type of analysis for two-dimensional flow could be made by replacing the liquid bath by a solid conductor of uniform electrical characteristics, using thin metal or other conductive sheet cut to the pattern desired, with isopotential electrodes connected at the boundary for isothermal conditions. This has been used by many as a simplification of the Langmuir liquid bath. With direct-current electrical flow established between boundary edges, isopotentials could be probed and plotted to represent conditions for a simple homogeneous material between isothermal surfaces.

Another form of electrical analogue, the network analyzer, primarily devised for transient heat flow, was described by Paschkis and Baker (2) in 1942. Here the heat-flow path, whether one-, two-, or three-dimensional, was represented by a number of electrical resistors arranged in the form of built-up network to simulate through the resistance concept the thermal resistance of the original heat-flow form. A direct-current electrical-potential difference established across the boundaries of the network set up the flow conditions equivalent to the heat-flow conditions. The network type of analogue also permitted handling of transient conditions. This was truly the outstanding point basic to the design. Here heat-storage effects of solid-wall structures were simulated by electrical condensers which could be charged or discharged, during a transient process. For steady flow the condensers were not required.

Of additional interest is the electrical analogue as based on conductive sheet. This has been used to some extent for flow analysis by different experimenters, principally foreign. It has received scant attention in the American literature, more in the European literature; particularly recent work by Bruckmayer (3) has come to light and should be cited. Using metallic foil to represent a wall of composite material between isopotential boundaries, Bruckmayer cut the sheet to include straight thin strips of foil to represent a layer of insulating material. This was a step in the right direction, but it obviously had limited application and could handle only simple cases of one-dimensional flow between isothermal faces, without surface-boundary effects, such as due to air "films."

Finally should also be mentioned, in passing, the heat-flow version of the Southwell relaxation method, the numerical procedure of Emmons (4). This is often cited by its proponents as having preferential features over the analogical methods. It is a useful tool. For certain work it has admitted advantages, but since it does not fall into the classification of electrical analogies, it will not be discussed any further here.

The geometrical analogue of the Langmuir type, whether fluid or solid, has the advantage of simplicity in obtaining the direct geometrical patterns occurring in flow; it has certain shortcomings: (*a*) Limitation to a single homogeneous material between the two potential levels; (*b*) requirement of isopotential boundary-surface wall conditions. There are also some practical objections to working with a bath. On the other hand, the network type of analyzer has the advantage of full utilization of the resistance concept with extension to multiple materials in a complex heat-flow path. It is very flexible. It has the advantage of permitting change of physical properties readily, and above all of being able to handle transient conditions, which is its particularly outstanding feature. However, its equipment is admittedly extensive and since it is not a direct geometrical analyzer, the determination of the geometrical pattern of isothermals is not readily made.

Present Geometrical Analyzer

To meet some of these shortcomings, the present electrical "analogger" employing conductive sheet has been devised. It is

[1] Department of Mechanical Engineering, Columbia University. Mem. A.S.M.E.

[2] Numbers in parentheses refer to the Bibliography at the end of the paper.

Contributed by the Heat Transfer Division and presented at the Annual Meeting, New York, N. Y., Nov. 27–Dec. 1, 1944, of The American Society of Mechanical Engineers.

of the geometrical type and primarily for steady-state one- and two-dimensional studies. It permits inclusion of fluid boundary conditions for multiple homogeneous materials in the heat-flow path. Thus it is not limited to isothermal conditions at the boundary walls, and to one single material. Broadly considered, it is founded on the basic principles of the electrical analogy; equivalent temperature conditions for a heat-flow path can be determined through analysis of an electrical flow path in which the component resistances have the same relationship between themselves as the thermal resistances. In both types of flow the potential difference is equal to the product of flow rate and resistance.

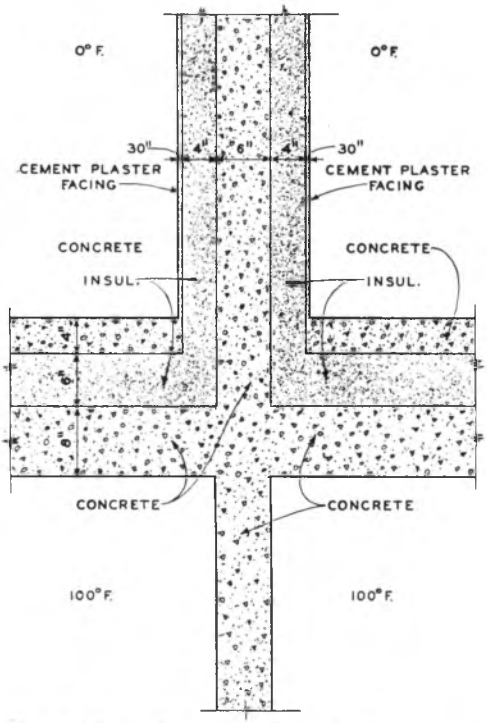

FIG. 1 CROSS SECTION OF BUILDING STRUCTURE

The analogger is best understood by considering a particular case. Fig. 1 represents conditions for a given building structure. One set of rooms is at 0 F, another at 100 F, with a concrete floor between the two temperature zones, and a concrete wall between the adjoining rooms at one given temperature. The floor and the cold wall in addition carry insulation as indicated, with concrete surface added for physical protection. Dimensions are indicated in the figure. Since opposite conditions are similar (mirrored), only one side need be analyzed as set up by the center line. (This is equivalent to considering perfect insulation at the center-line boundary.) It is desired to obtain the steady-state internal-temperature lines, as well as the underside floor and wall-surface temperatures in the 100 F room, to study possible condensation under humid conditions.

The boundary condition produced by the still air in both rooms is readily interpreted through the "film" concept of heat transfer, added and coupled to the resistance concept. Considering resistances on the unit-area basis, the air boundary resistance R_a, deg F/[Btu/(ft²)(hr)], may be defined as

$$R_a = \frac{1}{h_a} \quad \ldots\ldots [1]$$

where h_a = air-side surface conductance, Btu/(ft²)(hr)(deg F). The resistance R_w, deg F/[Btu/(ft²)(hr)], of the wall material is

$$R_w = \frac{L_w}{k_w} \quad \ldots\ldots [2]$$

where

L_w = thickness of wall material, ft
k_w = thermal conductivity of wall material, Btu/(ft²)(hr)(deg F/ft)

Thus for a given value of h_a there is a corresponding value of resistance R_a. For a given conductivity of wall material, there is some equivalent length or thickness L_e of material that would give the same resistance R_e to heat transfer as the air boundary

$$R_a = \frac{1}{h_a} = R_e = \frac{L_e}{k_w} \quad \ldots\ldots [3]$$

thus

$$L_e = \frac{k_w}{h_a} \text{ ft} \quad \ldots\ldots [4]$$

Hence if there were involved only an air boundary and a wall thickness, the equivalent electrical resistances to represent the conditions would be proportional to L_e and L_w. For conductive sheet of uniform unit resistance therefore these resistances could be represented by proportional lengths directly on the sheet. This takes care of the fluid boundary conditions, in terms of equivalent length of solid material to produce the same resistance effect. (Though not so apparent, the same general result would be produced by direct consideration in terms of the resistance concept.)

The next point to be considered is the problem of insulation, or of different materials in the heat-flow path. Considering the solid wall as the basic material in the problem, lengths of the actual heat-flow path are directly represented on the conductive sheet. However, insulation in the geometrical electrical analogy requires increased unit resistance in the sheet material to represent increased thermal resistance: this is brought about by modifying the electrical characteristics of the sheet.

The effective electrical unit resistance of a given section may readily be altered by cutting the sheet carefully into a mesh pattern (perforating). This alteration may be made in progressive steps during an investigation, thus covering different values of equivalent thermal resistance in insulation, and enabling progressive study as well as interpolation for exact value. One type of mesh that may readily be used is the square mesh shown in Fig. 2 with progressive alteration. The transverse (edge-to-edge) resistance of mesh sheet as compared with equivalent solid sheet increases as the amount of cutout area increases. The resistance characteristics may be determined by direct comparative electrical measurements. (For a 1-in. nominal mesh, 0.80-in-square holes and 0.20-in. web, the resistance ratio was measured and averaged about 4.6.) Of course it is essential that one continuous sheet be used and that the webs of the mesh be in no way cut through. It is further to be noted that the mesh may be adjusted to handle material with differing conductivities depending on the direction of heat flow, as, for example, in wood with-the-grain vs. across-the-grain conductivity.

DETAILS OF CONSTRUCTION FOR MODEL

Based on the principles outlined, a geometrical model representing the insulated structure in Fig. 1 has been constructed and is shown in Fig. 3, with its electrical connections for the one-half section of the symmetrical layout. In accordance with the geometrical-model requirements, the proportions are to scale; as a matter of fact the model is full size and of the actual structure dimensions. It is made from one large continuous sheet of metallized paper.

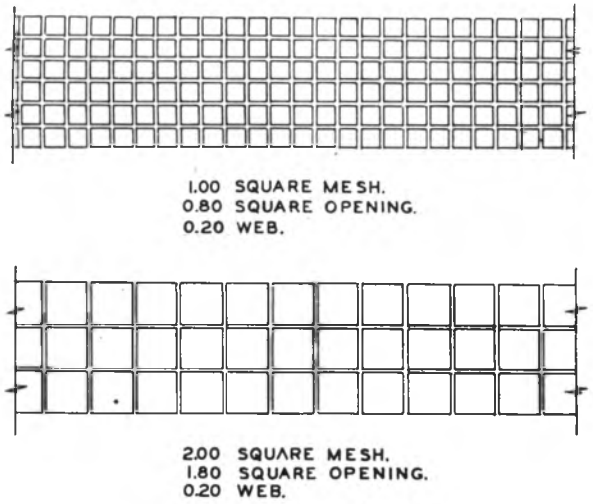

FIG. 2 TYPES OF MESH

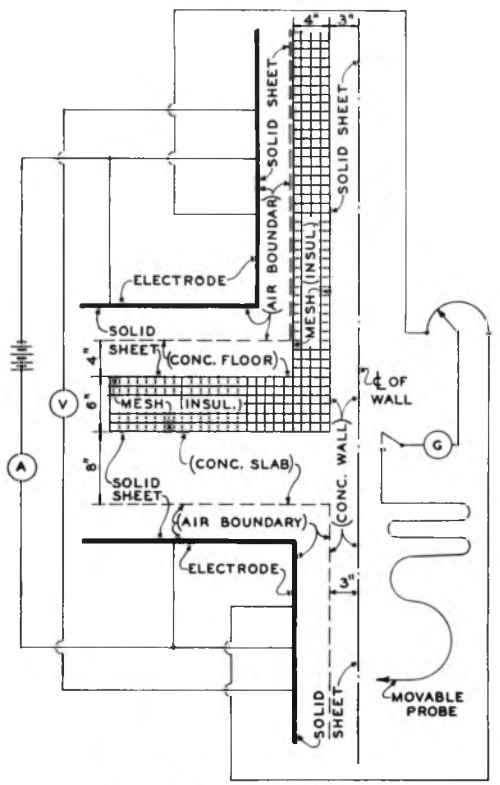

FIG. 3 EXPERIMENTAL SETUP

In addition to the dimensions shown in Fig. 1, the following basic data have been assumed for the problem: h_a, representing still air, has been taken at 1.65 Btu/(ft²)(hr)(deg F) for all of the air boundaries. This could readily be varied for different conditions. The conductivity of the concrete floor and wall, taken as equal, has been assumed as 0.50 Btu/(ft²)(hr)(deg F/ft). Thus

$$L_e = \frac{k_w}{h_a} = \frac{0.50}{1.65} = 0.303 \text{ ft} = 3.63 \text{ in.}$$

Using continuous metallized conductive sheet for the geometrical model, one edge of the conductive sheet is assumed to represent the center line of the wall, Fig. 3. The wall proper as the basic material is represented by a 3-in. width on the sheet as measured from the center-line edge. As shown at the bottom, an additional 3.63 in. represents the air-boundary effect on the bare concrete wall. The 4 in. of interposed insulation on the upper wall are represented by a 4-in. strip of modified sheet as produced by cutting a mesh pattern in the original sheet. To account for the 0.30 in. of concrete facing as well as the air boundary, the additional solid material beyond the insulation on the upper wall is 3.93 in. Similar treatment is arranged for the floor conditions, 6 in. of insulation being represented by 6 in. of modified sheet, the floor slab and air boundary together represented by 7.63 in. of solid sheet. The treatment for the different parts is clearly shown in the diagram. An electrode making good line contact with the sheet is fastened down at the limiting positions as shown. Thus isopotential conditions are established for the air. Electrical connections are made according to the diagram. Direct current from a storage battery supplies the electrical needs, the voltage required being relatively small, a matter of a few volts. Proportional electrical potentials over the entire field are obtained using the slide wire, a detecting galvanometer for balance, and a probe for point contact at different locations.

The results are best illustrated by a "contour map" of relative electrical potentials with equivalent temperatures shown. Thus the 90 per cent isopotential line (0.900) is equivalent, for an overall value of $\Delta t = 100$ F to $100 \times 0.900 = 90$ F. Fig. 4 represents such a contour map for the 1-in. mesh, that is, for insulation having a resistance ratio of about 4.6, i.e., $k_{ins} = 0.109$ Btu/(ft²)(hr)(deg F/ft).

It must be pointed out that the method is dependent on the uniformity of the sheet electrical conductivity in all directions. This has been a problem and various materials have been studied from this point of view. In addition, an analysis by this method can be no better than the original assumed data and physical properties. Also receiving further consideration is the requirement that the resistance ratio for mesh in all directions should be the same. This is somewhat dependent upon the accuracy of cutting and duplicating the mesh. Present investigations show

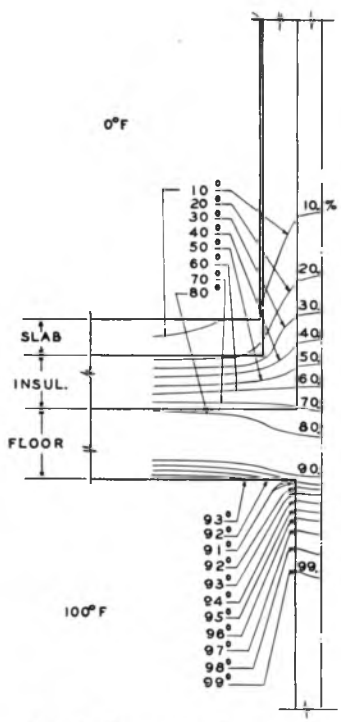

FIG. 4 STRUCTURE ISOTHERMS

an apparent deviation of less than 5 per cent. It should further be noted that the model for multiple thermal conditions may also be built up by using different component materials such as sheet of different unit resistance, with or without mesh. Experimental studies are also being continued, for comparative purposes, on the application of the fluid model to this type of problem.

Multiple Materials by Tank Method

The extension of the geometrical analogy in steady-state flow, to cover fluid boundary resistances as well as multiple materials of different relative conductivity, has been undertaken for the tank (electrolyte) method and will be reported on in detail at another time. Here the solid boundaries of the structure are associated with a thermal-film resistance. This is represented by tank-wall electrodes, having electrical resistances interposed between them and the electrical potentials representing the fluid temperature levels.

The problem of altering the electrical resistance of the liquid bath according to the fixed pattern of the actual structure is quite important and accordingly has been studied in detail. The liquid bath, it must be remembered, is conductive by virtue of its behavior as an electrolyte. Salt solutions such as NaCl, etc., take care of this requirement. But for different unit resistances in different parts of the tank, in effect a different material must be present. This can be realized to some measure by using sand or other porous material for the more resistive sections of a structure, the electrolyte penetrating the porous material in its fixed location.

More promising results have been obtained in another manner. The goal in the ideal is to have material combinations whose proportional resistances can be adjusted at will, to cover different physical characteristics of structural materials. The use of a solidified-jelly bath (about 1 in. deep) with different amounts of dissolved salt is proposed for this purpose. The jelly is liquid at temperatures somewhat above atmospheric, and different amounts of salt may be dissolved in it while it is in the liquid form.

As a practical operation, different material combinations may readily be made up by using plain salt solution against a solid-jelly mass. Different shape configurations may be cut out of the solidified-jelly mass to conform to the actual structure shapes. The jelly, a semirigid solid mass, is still soft enough to permit the penetration of an exploring potential probe.

Fig. 5 shows alternating-current results (potential versus length of path) for a test cell originally containing one solid-jelly mass between its end electrodes, as well as the results with the middle-third solid section cut out and replaced by a liquid electrolyte of different conductivity from the solid. The sharp change of slope clearly shows the differing possibilities in the analysis of complex flow systems.

The present method offers possibility in handling numerous complex flow problems in different fields of stable flow on a simple basis. One problem of interest in this connection is that of extended surface.

Another is that of diffusion. Still another is involved in some aspects of fluid flow. The equipment required is not complex, and the general advantage of geometrical similarity to actual configurations makes it an attractive working tool.

Acknowledgments

Acknowledgment is hereby made to different associates of the author who have so generously co-operated on various aspects of the problem; to Prof. J. A. Balmford of the Electrical Engineering Department at Columbia University for his continued advice and co-operation on electrical details; and to Mr. Harvey W. Bell, Consulting Engineer, Yonkers, N. Y., for his help in preparing the mesh patterns in the test sheet.

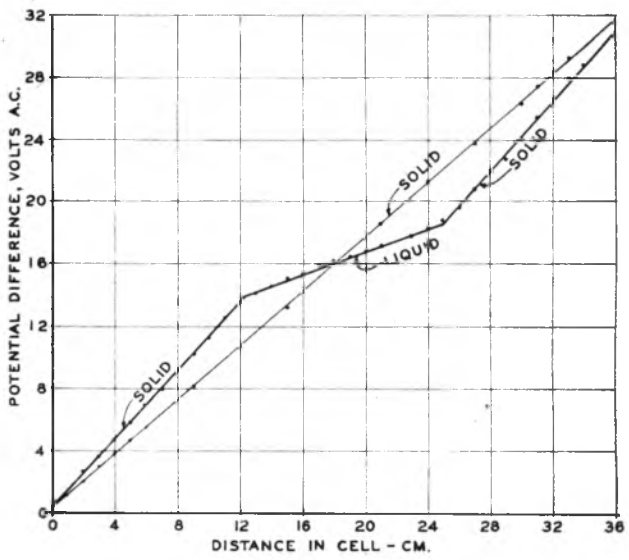

Fig. 5 Potential Difference Versus Length for All-Solid and Solid-Liquid System

BIBLIOGRAPHY

1 "Flow of Heat Through Furnace Walls," by I. Langmuir, E. Q. Adams, and F. S. Meikle, Trans. American Electrochemical Society, vol. 24, 1913, pp. 53–84.

2 "A Method for Determining Unsteady State Heat Transfer by Means of an Electrical Analogy," by V. Paschkis and H. D. Baker, Trans. A.S.M.E., vol. 64, 1942, pp. 105–110.

3 "Elektrische Modellversuche zür Lösung wärmetechnischer Aufgaben," by F. Bruckmayer, *Archiv für Wärmewirtschaft und Dampfkesselwesen*, vol. 20, 1939, pp. 23–25.

4 "The Numerical Solutions of Heat Conduction Problems," by H. W. Emmons, Trans. A.S.M.E., vol. 65, 1943, pp. 607–615.

Discussion

G. M. Dusinberre.[3] The writer has favored the "relaxation" method for solution of most steady-state heat-conduction problems. But where the geometry is complex, a close network is needed and the work becomes rather tedious. Also, if a plot of the isotherms is required, we must interpolate over the network. Though this last step is not difficult, the electrical analogue avoids the necessity for it. Thus the ingenious methods developed by the author have certain definite advantages in this field of application.

One may question the accuracy of the use of a thick layer of isotropic conducting material to represent the effect of a convective air film. The model permits a heat transfer parallel to the surface, equally with the normal direction, and this would not appear to be correct for the actual film.

Max Jakob.[4] The paper under discussion shows that the possibilities to develop or modify analogy methods for heat-flow determination are not exhausted as yet. However, the author

[3] Department of Mechanical Engineering, Virginia Polytechnic Institute, Blacksburg, Va. Now on duty at U. S. Naval Academy, Annapolis, Md. Mem. A.S.M.E.

[4] Consultant in Heat Research, Armour Research Foundation, and Research Professor of Mechanical Engineering, Illinois Institute of Technology, Chicago, Ill.; Nonresident Research Professor of Heat Transfer, Purdue University, Lafayette, Ind. Mem. A.S.M.E.

seems to have overlooked that Awberry and Schofield[5, 6, 7] have previously used the electric resistance of a thin metal sheet, cut geometrically similar to the cross-sectional area of a wall, to find the thermal resistance of that wall. An ingenious modification of this method is also due to Schofield.[6, 7] Since the flow and equipotential lines cross each other perpendicularly, he measured the electrical resistance of the model in the direction of the equipotential lines of the original in cases where the resistance along the flow lines of the original was much smaller than perpendicular to them and would have been difficult to measure exactly.

In general, the writer would prefer continuous sheets of different thickness to mesh sheets. An advantage of the model method with solid sheets, compared to the relaxation method, is the perfect geometrical similarity between object and model, whereas a web approaches geometrical similarity less well than the ideal web used in the relaxation method. However, if local differences in the thermal resistance of a wall are to be imitated, this may be done efficiently by punching holes of appropriate size at corresponding places of the model. A wall built up from hollow bricks would be such a case although the merit of the method should be greatest when irregular and singular differences in the resistance are to be imitated. The change of thermal conductivity of the material of a wall with temperature through the wall may also be dealt with in this way.

In addition to the previous electrical analogies quoted in the paper, the writer would like to mention that he used a magnetic analogue[8] as early as 1914. An electromagnet was made having a core of sheets which were cut to size so that the poles imitated the shape of the surface of the object. Cardboard, cut geometrically similar to the cross-sectional area of the object, was placed between the magnet poles and covered with iron filings. The magnetic-force lines formed by the iron filings, after excitation of the magnet, imitated the thermal flow lines and were used to determine the heat conduction.

Victor Paschkis.[9] The author should be commended for bringing into literature a tool which is so frequently used today but of which little has been written in American literature.

The use of electrical analogy between heat flow and electric current for the analysis of steady-state problems, based on a geometrically similar model, has undergone a long development between its inception by Langmuir and the present status. It may be of interest to review briefly some of the intermediate steps. In so doing it should be kept in mind that the analogy holds for any field to which the Laplace equation may be applied.

In 1922 N. N. Pavlovski (Leningrad) applied this method to a study of the flow of water under hydraulic constructions. Also in 1922 Puppini (Bologna) used electric models for the same purpose.[10]

In 1933, C. B. Biezeno and J. J. Koch described the application of the geometric analogue to stress analysis.[11] This method was again described by H. Meyer and F. Tank.[12] In 1937, B. Finzi-Contini (Milan) published an article on the application of this method to heat flow.[13]

In the same year C. L. Beuken (Maastricht, Netherlands) published some work on development based on Langmuir's tank method.[14] Finzi-Contini and Beuken, apparently working independently of each other, developed a method allowing the introduction of boundary conductance. The continuous electrode as applied by Langmuir is replaced by a number of individual electrodes, each connected with a resistor which may be equal if the boundary conductance is to be assumed constant or can by the trial-and-error method be adjusted to the potential at the electrode; it then simulates a temperature dependency of the boundary conductance. It should be noted that Finzi-Contini mentions work with India ink, with mixtures of carbon and graphite, and with a gelatin containing electrically conducting powders. Without giving details, he states that these methods did not give so good a result. He also tried to reproduce different conductivities by applying tanks of different depths but found that if the depths were too different the analogy to heat flow was no longer close enough; or to be more precise, replacing change of conductivity by change of cross section is permissible only within limits.

The author mentions meshing in order to represent a higher thermal resistivity. His method is a definite improvement as against Bruckmayer. From Bruckmayer's paper it would appear that the conductivity perpendicular and parallel to the direction of main heat flow are not the same, at least in the "cork part." Kayan's method provides for equal conductivity in both directions of flow. Bruckmayer's method may be simpler and may be acceptable if conductivity in one direction can be neglected. Otherwise Kayan's method seems preferable. Bruckmayer uses copper connectors for introducing the current to the tinfoil and places the tinfoil and the copper connectors on linoleum, and finally the entire assembly on a board. By bolting the metal to the board he claims to get intimate contact between copper and tin.

It may be of interest to note that Bruckmayer[15] recently described the application of his method for a problem quite closely related to that dealt with in the paper, namely, the investigation of thermal short circuits in refrigerated spaces.

The author points out two dangers inherent in the geometric-analogy method. One is the possibility of uneven thickness of resistivity of the metallized paper. It is mentioned that the resistivity across the paper was measured in length and width and that the difference was 5 per cent. If irregularities do occur, it is not sufficient to measure over-all resistance in two or three directions, because a local change in thickness at critical points may spoil the entire measurements. The other is the necessity of cutting the perforations very accurately. In the example mentioned, the web was 0.2 in. wide; a change in thickness of 0.02 in., which certainly is within possibility, would cause an error of 10 per cent. It appears dangerous to represent high resistivity by a material of low resistivity using very small cross sections.

The author of the present paper mentions also the "heat and

[5] "Effect of Shape on Heat-Loss Through Insulation," by J. H. Awberry and F. H. Schofield, 5th International Congress on Refrigeration, 1928.

[6] "The Heat-Loss From a Plate Embedded in an Insulating Wall," by F. H. Schofield, *Philosophical Magazine*, series 7, vol. 10, 1930, pp. 480–500.

[7] "The Heat-Loss From a Cylinder Embedded in an Insulating Wall," by F. H. Schofield, *Philosophical Magazine*, series 7, vol. 12, 1931, p. 329.

[8] "American Heat Flow Measurements Using the Twin-Plate Method," by Max Jakob, *Zeitschrift für die gesamte Kälte-Industrie*, vol. 29, 1922, pp. 83–87.

[9] Research Associate, Department of Mechanical Engineering, Columbia University, New York, N. Y.

[10] "Modelli Elettrici per lo Studio Della Acqua Filtranti," by Puppini, Bologna, *Monitore Tecnico*, vol. 28, 1922, p. 209.

[11] Über einige beispiele zur elektrischen Spannunggsbestimmung," by C. B. Biezeno and J. J. Koch, *Ingenieur Archiv.*, vol. 4, 1933, pp. 384–393.

[12] "Über ein verbessertes elektrisches Verfahren zur Auswertung der Gleichung $\Delta \phi = o$ und Seine Anwendung Bei Photoelastischen Untersuchungen," by H. Meyer and F. Tank, *Helvetica Physica. Acta*, vol. 8, 1935, pp. 315–317.

[13] "Un modello elettrico," by B. Finzi-Contini, Milan, *Il Politecnico*, vol. 85, Sept., 1937, pp. 291–298.

[14] "Die Wärmeströmung durch die Ecken von Ofenwandungen," by C. L. Beuken, *Wärme- und Kältetechnik*, vol. 39, 1937, issue 7, p. 1.

[15] "Elektrisches Modellmessverfahren zur Wärmebrückes im Kühlraumbau," by F. Bruckmayer, *Zeitschrift des Vereines deutscher Ingenieure*, vol. 88, May 13, 1944, pp. 270–272.

mass flow analyzer" at Columbia University and gives a brief description of it. The network analyzer and the geometric analyzer both have their useful fields of application. For investigations of one single problem probably the use of the geometric analyzer is less expensive, provided the necessary measuring equipment is available and provided the afore-mentioned difficulties can be overcome. If, however, a series of investigations has to be carried out with only minor changes either in properties or in geometry, then the circuit set up on the network analyzer (heat and mass flow analyzer) remains almost the same and the only necessary changes are settings of the resistors. In that case work on this type of equipment would appear preferable because the actual measurements are at least as fast on the network analyzer as on the geometric analyzer and the change of setting of resistors is certainly faster than the preparing of new geometric analogues.

In comparing the two methods of electrical analogy it should be kept in mind that the accuracy of the elements of the circuit in the case of the lumped (network) method is easily measurable and not subject to change from one experiment to the next, whereas in the geometric-analogy method the accuracy (even thickness and precise cutting) has to be ascertained in every case anew.

R. G. Vanderweil.[16] We made a thorough investigation as to the behavior of building structures heated by tubes (panel heating); and the time required for building and testing the panels would have been reduced to a fraction if the panels could have been "cut out of paper," and the readings taken in volts. There is one point, however, the writer would like to note. The boundary layer in this system is replaced by a layer of "building material" of constant thickness (author's equation)

$$L_e = k_w/h_a \quad [4]$$

Now, we have found in tests that the equivalent thickness of the actual boundary layer does not only vary with the average surface conductance of the film h_a, but also with the direction of the heat flow near the surface of the slab. Wherever the heat flow at the slab surface is essentially perpendicular to this surface Equation [4] of the paper is in excellent agreement with panel test results, but at points where the heat-flow lines within the panel intersect the slab surface under an angle much smaller than 90 deg, the actual equivalent thickness of the boundary layer seems to be smaller than the computed thickness L_e. Applied to Fig. 3 of the paper, this would indicate that all readings along the center part of ceiling and floor will be in good agreement with actual conditions but readings taken near the intersection of ceiling and wall as well as floor and wall may be off for 10 per cent or more. By comparing the measurements on the actual slab and on the electrical analogue it may be possible to compensate for this inaccuracy by changing the thickness L_e near the corner.

[16] Office of Consulting Engineer, Chase Brass & Copper Company, Waterbury, Conn.

Author's Closure

The author wishes to acknowledge, with appreciation, the contributions of the discussers, particularly those of Dr. Max Jakob and Dr. V. Paschkis in providing the additional citations for amplification of the brief list of fundamental references given in the paper. They round out the history of the electrical analogy for the American literature.

As pointed out directly at the beginning of the author's paper, the general method is not new and stems from the Langmuir development cited. However, the additional references, dealing in the main with relatively simple cases, serve to emphasize the point brought out in the paper that the present treatment was particularly devised to meet some of the shortcomings of earlier electrical analogies, i.e., to permit "geometrical" analysis of complex cases involving multiple materials and also boundary conditions.

Commander Dusinberre properly brings up a point on which the author gave some considerable thought, having been of the same opinion as to the possibility of crossflow in the boundary material, particularly at the corners. Nevertheless, upon slitting the conductive sheet at the corners after the final experiments, no perceptible changes in values could be detected, with the conclusion therefore that whereas the possibility of crossflow still exists, no ultimately great error need be expected.

Likewise the point of Mr. Vanderweil, with respect to the nonuniform character of the film conductance h_a, has merit. In the paper the value was assumed constant over the surface, and through the use of a constant value for L_e a fixed distance was assigned as the corresponding value of wall resistance. It is suggested that if more specific information is available for the variation of h_a over the surface, the variation may be handled by using the correspondingly varying value of L_e along the surface.

Finally, the author has pointed out the need for care in dealing with the conductive sheet method. Dr. Paschkis's observations, in concurring with the author's viewpoint, serve to emphasize the need for diligent procedure in using the described analogue.